NRRI Technical Report - July 2017

# The MnDRIVE Transdisciplinary Project Implementation of Smart Bioremediation Technology to Reduce Sulfate Concentrations in NE Minnesota Watersheds


Submitted by:
George Hudak, Lisa Estepp, and Patrick Schoff



Date: July 14, 2017

Report Number:
NRRI/TR-2017/17



Collaborators:
J. Hanson[1], B. Hanson[1], S. Hanson[1], M. Sadowsky, R. Hicks, D. Jones, T. Löesekann, S. Huang, W. Scherkenbach, T. Ferguson, M. Haynes, G. Chiodi Grensing, T. Eisenbacher, A. Burke, K. Haedtke, and O. Kolomitsyna



Funder:
University of Minnesota/MnDRIVE Program



Natural Resources Research Institute
University of Minnesota Duluth
Driven to Discover

Duluth Laboratories & Administration
5013 Miller Trunk Highway
Duluth, Minnesota 55811

Coleraine Laboratories
One Gayley Avenue
P.O. Box 188
Coleraine, Minnesota 55722

[1]Clearwater Layline, LLC

This publication is accessible from the Natural Resources Research Institute's website (https://www.nrri.umn.edu/publications) as a PDF file readable with Adobe Acrobat.

*Date of release: July 2017*

Natural Resources Research Institute
University of Minnesota, Duluth
5013 Miller Trunk Highway
Duluth, MN 55811-1442
Telephone: 218.788.2694
e-mail: nrri-m3pubs@umn.edu

Web site: http://www.nrri.umn.edu/egg

# Contents

# List of Tables

# List of Figures

# Preface

This report opens with an Executive Summary, which briefly describes the project's major accomplishments to date. The body of the report is constructed in sections focused on five related project efforts: 1) Bioreactor Design, Operation, and Performance, 2) Power Management, 3) Microbiology, 4) Chemical Treatments, and 5) Economic Aspects of Sulfate Reduction. Each of these sections, in turn, starts with a brief summary, which is followed by a detailed report. Additional materials concerning bioreactor design, construction, and operation, as well as experimental design, rationale, methods, and data are included in appendices. In addition, the MnDRIVE Project Accountability metrics, which contain a breakdown of particular project tasks, are included as appendices.

This MnDRIVE-supported project continues a long-running set of experiments jointly conducted by the Natural Resources Research Institute (University of Minnesota Duluth), researchers from the University of Minnesota Twin Cities and the University of Minnesota Duluth, and several public agencies and private corporations to address issues associated with mining-impacted waters. These experiments were originally scheduled for completion by mid-2016, but we have extended the data-collection portion of the projects into fall 2016.

*A note about this document*: This report is organized into major sections, including: I. Introduction and Background; II. Design, Engineering, and Operation; III. Energy and Control Systems; IV. Microbiology; V. Chemical Treatment for Sulfide Precipitation; and VI. The Case for Sulfate Reduction Technology. Additional detailed information is also available in a series of appendices, including: 1. Bioreactor Construction, Flow, and Operation, 2. Chemical Analysis of Bioreactor Ballast Materials, 3. Chemical Treatments for Sulfide Precipitation. 4. MnDRIVE Project Accountability – Year 1, and 5. MnDRIVE Project Accountability – Year 2. A reader can jump between any of the listed topics or sections by using the Bookmarks embedded in this document.

Because of the length and complexity of this report, each section is treated independently, with each containing its own sequence of figures, tables, and references. Footnotes, however, are numbered continuously throughout the document.

# Project participants

**Project Management**

George Hudak, UMD, Natural Resources Research Institute – PI
Lisa Estepp, UMD, Natural Resources Research Institute
Patrick Schoff, UMD, Natural Resources Research Institute

**Engineering and Operation**

Jeff Hanson, Clearwater Layline, LLC – Co-PI
Brandon Hanson, Clearwater Layline, LLC
Stephanie Hanson, Clearwater Layline, LLC

**Microbiology**

Michael Sadowsky, UMTC, Biotechnology Institute – Co PI
Randall Hicks, UMD, Biology – Co-PI
Daniel Jones, UMTC, Biotechnology Institute
Tina Löesekann, UMTC, Biotechnology Institute
Siqian Huang, UMD, Biology
Whitney Scherkenbach, UMD, Biology

**Energy and Control Systems**

Thomas Ferguson, UMD, Electrical Engineering – Co-PI

**Economic Analysis**

Monica Haynes, UMD, Labovitz School of Business and Economics – Co PI
Gina Chiodi Grensing, UMD, Labovitz School of Business and Economics
Travis Eisenbacher, UMD, Labovitz School of Business and Economics
Andrew Burke, UMD, Labovitz School of Business and Economics
Karen Haedtke, UMD, Labovitz School of Business and Economics

**Chemistry**

Oksana Kolomitsyna, UMD, Natural Resources Research Institute

**Acknowledgements.** Portions of this project were funded by the IRRRB via the East Range Joint Powers Board, the University of Minnesota via MnDRIVE, and NRRI internal funding mechanisms. Generous in-kind support was provided by PolyMet Mining, Inc. (Kevin Pylka), Cliffs Erie, LLC (Scott Gischia), and Clearwater Layline, LLC (Jeff Hanson).

# Executive Summary

Surface water, including lakes, rivers, wetlands, and all of their connecting waterways, can collect sulfate through geological weathering of local rock, atmospheric deposition from local and distant coal-burning power plants, and from activities that disturb and expose sulfur-bearing rock, like mining and roadbuilding. Many northeastern Minnesota water bodies contain sulfate concentrations that exceed current regulatory levels, and the removal of excess sulfate and remediation of those sites remains a paramount concern in the state. While sulfate and other contaminants can be effectively removed from water by municipal or industrial waste water treatment plants, these systems are technologically complex, require high capital and operational costs, and demand continuous energy supplies. Notably, many of these waste treatment schemes include biological components, which use microbial metabolism to lower the concentrations of specific contaminants, like phosphates, nitrates, or sulfates. Bioremediation, referring to treatment processes that depend primarily on biological metabolism, can offer advantages over mechanical or chemical systems in terms of capital and operational costs, energy demands, and maintenance requirements, and thus they can offer an attractive alternative or supplement to conventional water treatment processes for addressing water quality problems in small water bodies or those in remote areas.

The objectives of the MnDRIVE Transdisciplinary project, "Implementation of Smart Bioremediation Technology to Reduce Sulfate Concentrations in NE Minnesota Watersheds," were to design, build, and operate bioremediation platforms that could be used to decrease aqueous sulfate concentrations at remote sites, to evaluate their functional and economic efficiency, and to determine whether and how they might be used in their current or modified form. Essentially, these bioremediation platforms were continuous-flow systems that brought high-sulfate water into contact with bacteria that converted sulfate into reactive hydrogen sulfide, which was then chemically treated to form insoluble iron sulfide precipitates that could be removed from the system. Outflow water was returned to the source, but the platforms were designed so that the outflow could be directed offsite or to secondary treatment processes.

The bioremediation platforms were built around a series of modular bioreactors, which were essentially sealed containers filled with a matrix that served as microbial habitat. The bioreactors were designed to float in the water body with slight positive buoyancy, allowing the bulk of the complex to be submerged, which provided a protected environment for both biological and mechanical systems. Sets of bioreactors operating in parallel were joined to other modules containing carbon substrates that bacteria use as food sources, other nutrients, pumps, monitoring equipment, and other mechanical systems, into platforms referred to herein as rafts. The rafts also contained independent hydraulic, monitoring, and power systems, which consisted of propane-fueled generators with solar photovoltaic panel backup, or, in advanced tests, exclusively solar photovoltaics. Physico-chemical, hydraulic, and electrical parameters were monitored at multiple points throughout the process, and the rafts were designed and fitted for remote monitoring and control.

Early phases of the project, which included small and mid-scale bench testing and full-scale prototype testing, established the proof-of-concept that the system could operate and function effectively in the pit lake throughout the year. In the current phase, we concentrated on characterizing the sulfate-reducing microbial communities and studying their metabolic behavior and patterns over time, monitoring bioreactor activity and production over an annual cycle, optimizing microbial growth and

metabolism by manipulating culture conditions, and developing effective and efficient chemical methods to precipitate various sulfur species. In addition, energy-efficient power management and remote/robotic control schemes were developed and tested, and final specifications for a fully operational system were determined.

Highlights of our results include:

- The bioreactor sulfate-reducing bacterial community, which came from sediments collected in the pit outflow, was capable of converting more than 90% of the pit water sulfate into hydrogen sulfide and achieved rates of sulfate reduction over the winter ranging from 60-100%. [Sec. II, Sec. IV]
  - These conversion rates were achieved using a flow rate of about 0.6 gallons/minute/ bioreactor, which resulted in a four-day hydraulic retention time. Lab and field experiments indicated that high rates of sulfate reduction are possible at increased flow rates and substantially shorter residence times.
  - Prokaryotic cell concentrations in the bioreactor water ranged from approximately 0.5 to 4.5 x $10^7$ cells/ml, and, as expected, growth was sensitive to ambient temperature.
  - Bioreactors were dominated by a diverse anaerobic microbial community including multiple types of sulfate-reducing bacteria, fermenters, and methanogens. Major genera of SRB in the reactors include *Desulfovibrio*, *Desulfobacter* and *Desulfobulbus*.
- The modular design provides a replicated platform for rigorous scientific inquiry, robust operation, and the ability to actively monitor and adjust bioreactor components. [Sec. II]
- Field tests validated the concept and utility of separating the sulfate reduction and sulfide precipitation steps, and showed that sulfate reduction could proceed in the presence of elevated sulfide if certain nutrient and pH conditions were met. [Sec. II, Sec. V]
- Sulfate-reducing bacteria are known to methylate mercury during ordinary metabolism, and our analysis showed methylmercury production to varying degrees in each of the rafts. Notably:
  - Methylmercury concentration in bioreactor effluents was not elevated above the levels found in ambient waters in the area [Sec. II]; and
  - No changes in carbon substrates, nutrients, or flow rates were associated with changes in methylmercury production, indicating that our experimental manipulations did not alter this aspect of sulfate-reducing bacterial metabolism.
- Energy for powering the pumps, sensors, and electronics for one independently operating set of bioreactors was completely supplied by a solar-based renewable energy system, with availability approaching 100%. [Sec. III]
- Preliminary designs for a control system that would provide remote monitoring, control, alarming, and autonomous operation in subsequent bioremediation systems were produced. [Sec. III]
- Lab experiments showed that conditions for optimal removal of sulfur species from bioreactor effluents include pH adjustment using formic acid, oxidation using hydrogen peroxide, and, finally, flocculation and precipitation using aluminum sulfate. [Sec. V]
- Based on lab experiments, estimated costs for reagents needed to chemically remove sulfide from SRB bioreactor effluents system were $12.50/1,000 gallons of bioreactor effluent. [Sec V]
- Economic modeling shows that the mining industry currently directly employs more than 2,500 workers, and contributes nearly $2 billion in industry sales. [Sec. VI]

- Reductions or termination of the iron mining industry due to failure to achieve sulfate standards could eliminate between 6,000 and 10,000 jobs in the northeast region of the state, resulting in losses between $430 and $750 million, respectively, in wages and benefits, and GRP would decline by $1 to $2 billion. Overall, the region could see a total decline in output of between $2.6 and $4.4 billion annually if mining operations were to cease. [Sec VI]

Results of this project to date show both promise and challenges for floating sulfate-reducing bacterial bioreactors as they are currently configured. Functional tests show that the bioremediation process can substantially decrease aqueous sulfate concentrations in water. These results suggest that the bioreactor platform could be useful as a preliminary stage to reduce sulfate concentrations in water prior to treatment by conventional energy- and material-intensive methods, such as reverse osmosis or ion exchange. The bacterially mediated reduction in sulfate could substantially decrease the burden on those more expensive systems, which both have limited efficiency in high-sulfate environments, and thus increase the cost-effectiveness of the remediation system as a whole.

While this project was not intended to produce a final design for a stand-alone bioremediation system, the results of our trials and experimental manipulations provide some general and specific insights that can be considered in future projects.

- The *in situ*, floating/neutrally-buoyant design provided a stable platform that was fully functional throughout all seasons and during all weather conditions. However, our data clearly showed seasonal fluctuations in biological activity corresponding to water temperature, which could negatively affect the overall efficiency of the platform in this region. The design also proved to be robust, and the monitoring and sampling devices were accessible throughout the year, but the fact that the bulk of the bioreactors were submerged presented some challenges that could be exacerbated in long-term operations.
- Differences in functional performance among different bioreactors and rafts suggest that each bioreactor had developed a slightly different sulfate-reducing bacterial community, even though they were seeded with the same inoculum. While this sort of biological variation is not surprising, the corresponding differences in sulfate-reducing performance indicate that community structure should be viewed as a vital operating parameter and thus needs additional characterization prior to further *in situ* testing.
- The current bioremediation platform was designed to address a single contaminant issue, sulfur, but many, if not all, contaminated source waters have multiple impairments, and comprehensive remediation is the ultimate goal. Opportunities to add processes that address other common water discharge quality standards such as alkalinity and hardness also exist but were beyond the scope of this project.
- All bioremediation schemes produce their own physico-chemical outputs, including in this case, sulfide, methylmercury, and increases in dissolved organic materials. Chemical treatments of the bioreactor effluent reduced or eliminated sulfide but increased concentrations of a variety of other elements in the final effluent. While these excesses were the result of experimental manipulation, and thus were of very small volume, they may be more consequential in larger, longer-term operations.
- Precipitation of iron sulfides or elemental sulfur *in situ* appeared to be feasible, but the associated processes, including sequential chemical addition and mixing, characterization of

reaction products, and techniques for collecting slurries, sludge, or precipitated materials, need further development before the methods could be incorporated into large-scale operations.

# I. Introduction and Background

The MnDRIVE Transdisciplinary project, "Implementation of Smart Bioremediation Technology to Reduce Sulfate Concentrations in NE Minnesota Watersheds," is part of a continuing research program designed to use natural processes to address long-standing problems associated with the release of sulfur into the aqueous environment. Sulfur is an abundant element that is naturally widely distributed over the Earth due to geological weathering and volcanoes, and, to some extent, biological activity. It reacts with many other elements and can be found in a host of minerals, including metal sulfides and sulfates that sometimes occur in concentrations high enough to be efficiently mined as ores. Sulfur is also an essential constituent of virtually all biological matter, functioning specifically as metal sulfides or organosulfides in enzyme reaction centers, as sulfhydryls in reducing agents like glutathione, and as crosslinking components in proteins like keratin, a primary constituent of vertebrate hair, feathers, scales, and skin.

Given its reactivity, sulfur will rapidly participate in a variety of chemical reactions, depending on physico-chemical conditions like the presence of air (oxygen), water, and metals, and, as suggested above, it is an active agent in the metabolism and structural biology of organisms ranging from bacteria to vertebrates. Therefore, it is not surprising that natural sulfur cycling through abiotic and biotic realms is usually environmentally benign and that a variety of stable ecosystems thrive in a wide range of sulfate levels, usually reflecting the underlying geology of the region. However, large releases of sulfur into the air through fossil fuel combustion, or into air or water from mining, road-building, and other processes that involve geological disturbance, can present a hazard. For example, when sulfur is exposed to air and water, sulfuric acid ($H_2SO_4$) will form to some degree, which can reduce the pH of the terrestrial or aquatic matrix. Small amounts of acid produced by natural weathering are often neutralized by basic soil components or diluted by precipitation, and some fortunate regions, like northeast Minnesota, have sufficient geologic buffering capacity to eliminate most sulfate acidification. But in other areas, exposure of large quantities and/or high concentration of sulfur to air and water can generate sulfuric acid concentrations in precipitation and runoff that exceed natural buffering or dilution capacity. Acidified precipitation originating from coal-fired power plants and runoff from newly exposed rocks in mining operations has caused severe disruptions in sensitive aquatic and terrestrial ecosystems that have limited natural buffering capacity.

Situations where sulfur is involved in direct toxicity are less common but have been documented in specific cases. When exposed to oxygen, sulfur quickly oxidizes to form sulfate anions ($SO_4^{2-}$), which can then combine with calcium or magnesium to form highly soluble salts that can enter surface waters through precipitation runoff. Fortunately, most of these sulfates are not toxic to humans and other vertebrates, even at moderate-to-high concentrations. In fact, surface water sulfate limits are more often regulated on aesthetic grounds (i.e., odor) than by toxicity. But Minnesota's 10 mg/L sulfate standard is an exception. It was established in 1973 specifically to protect native wild rice, *Zizania palustris*, which, according to census surveys, grows well in water containing sulfate at concentrations at or below 10 mg/L but is relatively sparse in waters containing sulfate at 50 mg/L or more. Given the historical, cultural, and spiritual importance of wild rice to the Native American citizens in the region, as well as its value as a subsistence and commercial crop, the state instituted a sulfate limit of 10 mg/L for any water flowing into designated wild-rice-producing areas. Recent studies designed to determine the toxicity of sulfate to wild rice throughout its life cycle and to establish a mechanistic rationale for a

possible revision of the standard largely confirmed the toxic effects of sulfur on long-term wild rice survival. But these studies also revealed that sulfide ($S^{2-}$), the chemically reduced form that is typically generated under anoxic conditions in sediments, is the toxic agent affecting wild rice growth and survival. However, these studies also add complexity to the regulatory situation by showing that other compounds that can interact with sulfide in sediments such as dissolved organic carbon and iron can modify sulfide toxicity levels, and thus might need to be considered in rulemaking.

These uncertainties notwithstanding, it is clear from numerous surveys that sulfate remediation will be necessary for water from many sources in northern Minnesota in order to meet the current standard or the variants proposed thus far. Well-established technological processes like reverse osmosis (RO), in which contaminated water is forced through a semi-permeable membrane that essentially filters the contaminants out, and ion exchange, which operates much like home water softeners but on an industrial scale, are highly effective at removing sulfate from water. These processes yield very pure water, and thus are considered the premium in remediation technologies, but their efficacy comes at a cost. Water treatment plants based on RO or ion exchange are very expensive to build and operate, with capital and operating costs, high energy demands, and substantial maintenance and replacement requirements. In addition, both processes produce a considerable amount of brines and solid waste that contain sulfates, salts, and other contaminants that often must be treated as hazardous waste.

Numerous other sulfate remediation processes have been developed for municipal and industrial water treatment, many of which incorporate biological components. These processes, termed bioremediation, use microbial metabolism to transform or remove contaminants from water and are often used in one or more stages of complex treatment schemes. In the current project, which is aimed at reducing sulfate concentrations in mine pit waters, we exploit the ability of naturally occurring microbes to metabolically convert sulfate to sulfide, which can then be precipitated in a solid, non-reactive form by thermodynamically favorable chemical reactions.

Sulfur-reducing microbes are ubiquitous in nature and are most abundant in aqueous environments with high sulfur and low oxygen concentrations, conditions commonly found in the sediments of rivers, lakes, and wetlands in northern Minnesota. Under specific controlled conditions, like those that can be created and maintained inside a bioreactor vessel by restricting oxygen and providing carbon substrates and nutrients, these microbes can efficiently convert sulfate to sulfide, which can either exit the system as a gas ($H_2S$), or, as in our system, be subjected to chemical conditions in which solid, non-toxic precipitates form. The potential advantages of this bioremediation system include low-power demand that can be satisfied by on-site solar photovoltaic panels, year-round operation with minimal need for human intervention, reasonable capital costs and low operating costs, and minimal waste production. In addition, the bioreactors used in this study are extremely flexible and adaptable; they have been designed as interchangeable modules that can operate in series or in parallel and will accommodate changes in flow rate. These properties provide advantages over mechanical systems in smaller or more remote remediation targets, particularly those not served by the electrical grid.

Bioremediation also comes with some challenges, starting with the fact that the process depends on the ongoing culture of living organisms, which are known to change constitutionally (i.e., microbial communities are dynamic) and functionally over time, which could lead to changes in efficiency. These systems also operate at considerably lower flow rates than those achievable in mechanical systems, which could limit their use to smaller, more remote water bodies. Finally, microbial-driven systems are

typically less effective at removing contaminants than RO or ion exchange, so may not achieve remediation to criteria levels. This limitation may be especially pertinent in cases where multiple water quality parameters must be addressed. For instance, passage through a bioreactor may decrease aqueous sulfate by 90% but have no effect whatsoever on phosphorus, pH, or other potential targets.

Considering the overall advantages and limitations of bioremediation systems, a reasonable goal is to develop a system that could operate either as a "stand-alone" unit that could be set up in remote areas and be operated with minimal human intervention or as a stage in more extensive remediation processes in which the bioremediation outflow would receive further treatment. In the latter case, a relatively low-cost bioremediation step could serve to reduce the burden on the downstream technological processes, thus reducing overall costs. Thus, the overall goals for semi-passive bioremediation designed specifically for mining-affected waters in northeast Minnesota include effective and efficient sulfate reduction and ultimate removal of sulfur species, low energy demand, minimal maintenance, and the capacity for remote or independent operation. Our MnDRIVE Smart Bioremediation project, "Implementation of Smart Bioremediation to Reduce Sulfate Concentrations in NE Minnesota Watersheds," is the latest phase of a program that started in 2010 as a bench-scale bioreactor that employed native sulfate reducing microbes to convert mining-generated sulfates to sulfide. Success in these "proof-of-concept" bioreactors provided the conceptual and scientific background for construction of pilot-scale floating bioreactors in a raft placed in a small pit lake that contained elevated sulfate concentrations.[1] Water from this pit lake, which was part of a former mining operation conducted by LTV Mining Corporation near Hoyt Lakes, Minnesota (St. Louis Co.), drains into Spring Mine Creek, which flows for about five miles into the Embarrass River, which eventually joins the St. Louis River. The Minnesota Pollution Control Agency (MPCA) has designated or proposed portions of the Embarrass and St. Louis rivers as wild rice waters, making them subject to the 10 mg/L sulfate criteria. The overall goals of these initial trials included the manufacture and operation of multiple, 4,000-gallon bioreactors capable of converting sulfate to hydrogen sulfide and subsequently precipitating solid sulfur species by chemical reactions in separate settling tanks.

By 2014, the project had successfully operated multiple bioreactors in the pit lake over an entire year. The bioreactor microbial community effectively converted sulfate to sulfide, and tests of chemical methods to precipitate sulfides were initiated and showed some promise. At that point, the project managers applied for and received MnDRIVE Transdisciplinary Research funding to advance the project, with objectives that included:

1) Demonstrate that the smart technology platforms can be controlled and operated independently using a combination of in-situ communication transmitters, computer modules, embedded temperature and flow sensors, pumps, flow valves, and nutrient feed columns, all powered by solar panels which charge battery packs powering this array of controls;

[1]The pit lake is located on a former LTV Mining Corporation mining site, currently owned by Cliffs/Erie LLC. Funding and in-kind support for the initial phase of the project (2012-2013) were provided by the IRRRB via the East Range Joint Powers Board, the University of Minnesota via NRRI, Clearwater Layline, LLC, Cliffs/Erie, LLC, and PolyMet Mining Corporation.

2) Demonstrate that the sulfate reduction bioremediation technology can be operated and controlled effectively in remote locations similar to those that might impact natural wild rice beds, and where access to roads and power lines is nonexistent; and

3) Optimize the bacterial activity in system modules and expand the scale of the technology to treat increased water flows in the individual modular bioremediation systems to most efficiently reduce sulfate concentrations to help meet regulatory limits set for discharges from existing and future mining operations, municipal wastewater treatment plants, and various industrial businesses operating in northeastern Minnesota.

These objectives were approached as a series of Project Tasks (Appendixes 4 and 5) that focused on building and operating refined bioreactors and precipitation tanks, characterizing the sulfate-reducing bacterial communities and their metabolic behavior and patterns, monitoring bioreactor activity and production over an annual cycle, optimizing microbial growth and metabolism by manipulating culture conditions, and developing effective and efficient chemical methods to precipitate various sulfur species. In addition, energy-efficient power management and remote/robotic control schemes were developed and tested, and final specifications for a fully operational system were determined.

## II.A. Design, Engineering, and Operations - Summary

Floating sulfate-reducing bacteria bioreactors have been designed to provide an effective, efficient, and economical system for decreasing sulfate concentrations in impacted waters. The results of the project to date show that bioreactors inoculated with indigenous sulfate-reducing bacterial communities can significantly decrease sulfate concentrations in mine pit water, converting the sulfate primarily to hydrogen sulfide. Pit water sulfate concentrations decreased by an average of 60 – 70% in the two bioreactor rafts that had operated for 24 months, and tests indicated a nearly stoichiometric conversion to sulfide. A third raft, which was inoculated during the winter and operated for only seven months, did not achieve full bacterial activity by the end of the project and was considerably less efficient. A variety of methods designed to chemically precipitate and remove sulfides from SRB bioreactor effluents (bio-effluents) have been tested. Furthermore, the floating raft design has proven to be robust and efficient, operating continuously for over two years using power generated primarily by on-board solar panels and at flow rates that would support large-scale operations.

## II.B. Design, Engineering, and Operations

### Introduction

Bench-scale sulfate-reducing bacteria (SRB) bioreactors were tested in 2011, followed by a pilot-scale trial that was conducted in a mine pit lake (Area 5 Pit NE-center), managed by Cliffs Erie, LLC and Poly Met Mining, Inc., starting in 2013. These proof-of-concept tests demonstrated the utility of the floating bioreactor design (see below and Appendix 1 for design details) and confirmed the ability of native bacterial communities to substantially decrease sulfate concentration in mine pit water (Hendrickson and Hanson, 2015)[2]. The pilot tests were followed by a larger trial in which 14 SRB bioreactors organized in two rafts (A & B) were used to evaluate chemical and metabolic flux through the system and to perform initial evaluations of the microbiological communities as they formed and evolved through seasonal cycles. In this stage we also developed and performed initial tests on multi-stage effluent treatment processes designed to precipitate sulfides, and developed and tested an autonomous solar-panel-based power system.

MnDRIVE funding provided support to build and operate seven additional bioreactors and two additional settling/precipitation tanks (Raft C) that incorporated design improvements and to test performance at multiple flow rates (hydraulic retention times), and to facilitate testing variations in sulfide precipitation regimes. A brief description of the floating bioreactor design and construction is provided below, and a detailed account is included in Appendix 1. Bioreactor and precipitation tank performance are addressed below and in more detail in Section IV. Microbiology, Section V. Chemical treatments, and Appendix 3. Chemical treatments – details.

[2]Hendrickson D, Hanson J. 2015. Smart bioremediation technology to achieve high sulfate reduction in mining waters of NE Minnesota: Natural Resources Research Institute Technical Report NRRI/TR-2015/07, 58 p.

## Bioreactor raft design and operation overview

Full-scale, 7’ X 7’ X 11’ deep cuboid bioreactor tanks were made of impermeable high-density polyethylene sheets and were filled with a non-biodegradable polypropylene substrate that provided a substrate for bacterial biofilm formation. The bioreactors were designed to operate almost entirely submerged, with only the upper 12 inches of floatation material forming a solid surface in contact with the water. Although designed to be buoyant, the tanks were kept nearly submerged using ballast. Keeping the bulk of the tanks and all water intakes, outlets, and liquid handling lines underwater provided numerous advantages including moderation of summer and winter temperatures, reduced energy requirements for pumping water, due to low head pressures, and protection from extreme weather events and ordinary environmental stressors (see Appendix 2 for a detailed chemical analysis of the ballast material). This design provided the basis for developing the low oxygen environment needed to support sulfate-reducing bacterial communities. Rafts were formed by joining seven bioreactors, along with two additional tanks of the same dimension that were used for nutrient inputs and as precipitation/settling tanks, respectively. The bioreactors were inoculated with sediment from the pit outflow stream, which had been shown in preliminary tests to contain native sulfate-reducing bacteria. The bioreactors were supplied with carbon substrates (ethanol, lactic acid, or sodium lactate) and nitrogen and phosphorus amendments as well as sulfate-containing pit water. Over time, robust microbial populations of sulfate-reducing bacteria were detectable in the bioreactor water and in biofilms on the fiber matrix.

Anoxic water from deep within the pit lake was pumped to each raft, combined with substrates and nutrients, and split among the individual bioreactors, where it was distributed over the upper fiber surface. As the pit water percolated down through the fibers, sulfate-reducing bacteria metabolically converted the sulfate to chemically reactive hydrogen sulfide. The seven bioreactors in a given raft operated in parallel, and their individual effluents were pumped into a common chamber where the combined effluent was mixed with chemicals that initiated reactions intended to form insoluble sulfur compounds and, finally, pumped into the precipitation/settling tank. After reaction and settling of sulfur-containing precipitates, effluent water was returned to the pit. The settling tanks were designed to be emptied at the base via a port that could be manually opened and closed from the surface, thus allowing the precipitated material to empty into the pit. However, at this early stage of project development and analysis, no materials were released into the pit. Instead, precipitated materials, which had been sampled and chemically analyzed, were pumped out to the tanks at the end of the project and disposed of in an appropriate landfill.

Additional water and material samples (e.g., fiber, biofilm) were collected at various points during the project and analyzed for physical and biological characteristics (see below and Appendix 1 for a list of sampling sites, materials, and analyses).

See Panel II-1 and Figures II-1 – II-4 in this section and Appendix 1 for further details on raft design and operation.

## Operation and performance

**Raft operation and sampling.** Rafts A, B, and C were each built with seven independent bioreactors operating in parallel, plus one (Rafts A and B) or two (Raft C) precipitation/settling tanks, which received the bioreactor effluent and discharged the final effluent back into the pit (Figs. II-1 and II-2). Operating three independent rafts allowed a limited degree of replication and redundancy as well as the flexibility to compare the performance of different designs, carbon substrates, hydraulic retention time (flow rate) and sulfide precipitation regimes. As described in more detail below and in Appendix 1, the long-term performance of Rafts A and B were comparable, confirming the functionality and reliability of the overall design. In addition, operating and testing the system continuously for over two years allowed us to implement and test numerous modifications in the bioreactors and in the solar power system, which acted as a supplemental power source for Rafts A and B and was the sole power source for Raft C. These modifications have resulted in easier and more efficient construction, more reliable operation, better performance, and lower overall costs.

The individual bioreactors were designed and constructed as replicates and performed similarly throughout the project, but each raft had a dedicated intake line, drawing water from similar but not identical sources, and the bioreactors in each raft acted in parallel to supply their dedicated precipitation/settling tanks. Thus, each raft was operated and sampled independently. Rafts A and B operated for a total of 27 months, from June 2014 through August 2016. A monthly sampling schedule was maintained throughout that period, but some adjustments were made over the course of the project.[3] Raft C was put into operation during the final year of the project (Dec. 2015 – June 2016) and had not established sufficient SRB activity to generate comparative data by the end of the project. However, Raft C was designed and used as a platform for tests of hydraulic retention time, power management, and automation and incorporated numerous design and flow modifications that improved overall performance.

Samples were taken from influent water, effluents from combined bioreactor flows, and precipitation/ settling tanks at least monthly by staff from Northeast Technical Services, Inc. (NTS, Virginia, MN), Clearwater Layline, LLC and the University of Minnesota. Bioreactor matrix (fiber) material and precipitation tank liquids and suspended solid materials were sampled periodically, as required for particular experimental protocols. Operational data such as flow rates, pH, and oxidation-reduction potential (ORP) for individual and combined bioreactor effluents, and precipitation/settling tank effluents were monitored by Clearwater Layline staff at least weekly. In addition, physico-chemical analyses including sulfate and sulfide concentration were performed monthly on influent water and combined bioreactor effluent and precipitation/settling tank effluent water by NTS and Pace Analytical Services, Inc. (Virginia, MN). Total and dissolved mercury and methylmercury in influent and effluent waters were analyzed by North Shore Analytical, Inc. (Duluth, MN) using USEPA-standard sampling, processing, and analytical techniques.

The bioreactors were inoculated with sediment collected from Spring Mine Creek, which receives discharge water from several Area 5 pit lakes that include our site (Area 5NE-center; see Hendrickson and Hanson, 2015) and was known to contain active sulfate-reducing microbial communities. Ethanol,

[3]For example, Raft A influent water was analyzed throughout the entire project, June 2014 – August 2016, n = 27 months; Raft B influent, December 2015 – August 2016, n = 9 months; Raft C influent, December 2015 – June 2016, n = 7 months. Additional details regarding individual rafts can be found in Appendix 1.

lactic acid, and sodium lactate were used as carbon substrates, and nitrogen and phosphorus were added to the influent water in the form of monoammonium phosphate and urea. For more details on individual bioreactor design, raft configuration, flow diagrams, materials list, and flow schematics for each raft, see Appendix 1.

Rafts A and B began operating in May 2014, and the first full data set was collected in June 2014. Both rafts operated nearly continuously until August 2016, resulting in 27 monthly data collections. Data is reported herein from the last 24 months, reflecting two complete years of operation. However, some continuity gaps exist due to occasional shutdown for repairs, missing or unreliable samples, and changes in experimental protocols. Exceptions are noted within the narrative and in the tables and graphs.

**Sulfate and sulfide concentrations.** Pit water influent sulfate concentrations averaged around 1,000 mg/L over a 24-month reporting period (Table II-1). After passage through the SRB bioreactors, sulfate concentrations decreased around 60 – 70% (Table II-1, Rafts A and B), indicating sulfate-reducing bacterial metabolism. After leaving the bioreactors the effluents were further processed in precipitation tanks, but these were not intended to support additional bacterial metabolism and, as expected, sulfate concentrations did not substantially change (Table II-1). See Section IV. Microbiology for details about microbial metabolism of sulfur compounds.

While pit water contained high sulfate concentrations, its sulfide concentration was negligible. But after passage through the bioreactors, average sulfide concentrations rose to 178 ± 63 mg/L and 170 ± 97 mg/L from Rafts A and B, respectively (Table II-1), as a product of microbial sulfate reduction. Bioreactor effluent sulfide concentrations generally increased as the sulfate-reducing bacterial communities matured after inoculation, presumably reflecting changes in composition and/or metabolism (see Section IV for further details). Notably, the aqueous hydrogen sulfide concentrations measured in the bioreactor effluents were close to stoichiometric balance with the decrease in influent water sulfate, confirming that the majority of hydrogen sulfide remained dissolved in the water and did not escape as gas.[4,5] Note also that Raft C, which was inoculated in December 2015 and operated for only seven months before the end of the project, did not establish a vigorous sulfate-reducing bacterial community and thus produced very little change in sulfate concentrations (Table II-1).

Sulfide concentrations in the precipitation tank effluents varied (Table II-1), reflecting experimental attempts to precipitate sulfur species using various chemical treatments. These experiments are addressed briefly in the next section and in more detail in Section V. Chemical Treatment. Although a mass balance analysis for sulfur in its oxidized and reduced forms was not conducted, it is important to note that very little gas-phase hydrogen sulfide escaped from the bioreactors and that the aqueous hydrogen sulfide that was returned to the upper, well-oxygenated levels of the pit water in the precipitation tank effluent would have been rapidly oxidized back to sulfate. By removing and disposing

[4]Calculations for the maximum sulfide concentrations in bioreactor effluents resulting from sulfate-reducing bacteria metabolism calculations were based on the following formula: [sulfide] = [sulfate] x (32/96); sulfate ($SO_4^{2-}$) MW = 96, sulfide ($S^{2-}$) MW = 32.

[5]In September 2015 we added the capability to monitor sulfate, hydrogen sulfide, and other parameters including chloride, phosphate, temperature, pH, oxidation-reduction potential (ORP), and alkalinity on a weekly basis for all bioreactors to further enhance operational control and monitoring. Gas phase hydrogen sulfide was also monitored in all bioreactors and precipitation tanks as warranted.

of the sulfur-containing sludge and other precipitated materials at the end of the experiment, this project resulted in a net-removal of sulfur from this small pit lake.

**Sulfide precipitation.** Each raft contained a precipitation tank designed to receive the bioreactor effluents, mix them with chemical precipitating agents, and allow the resulting solids to settle before discharging the aqueous portion back to the pit lake. Raft A bioreactor effluent hydrogen sulfide was initially treated with ferric hydroxide to form an iron sulfide precipitate. Although amorphous insoluble sulfide compounds formed as anticipated, the method proved to be inconsistent and ineffective, primarily because of problems in adequately mixing ferric hydroxide with the bioreactor effluent and channeled flow inside the mixing chamber. In addition, an analysis of the process as it took place in the precipitation tank indicated that it would require much larger quantities of ferric hydroxide than had been anticipated and that the resultant costs would make this technique impractical. Therefore, ferric hydroxide treatment was suspended in January 2015.

Precipitation tests using ferric chloride were performed in Raft B during 2015 and resulted in decreases in final effluent sulfide concentrations (Table II-1). Analysis of the precipitated material indicated that it consisted of an amorphous iron-sulfide matrix, containing some euhedral iron sulfides with an elevated S:Fe ratio, compared to the matrix. This material was considered likely to be a crystalline phase that may have formed in the precipitation tank or, possibly, during prolonged storage in the refrigerator prior to processing. Lab experiments aimed at optimizing sulfide precipitation using $Fe(OH)_3$ or $FeCl_3$, as well as in forming elemental sulfur precipitates by methods that do not require the addition of iron or chloride, are reported in detail in Section V. Chemical treatment.

**Oxidation reduction potential.** Pit water oxidation reduction potential (ORP) was generally positive (188 ± 179 mV, Raft A[5], n = 24 months; Table II-1) but was highly variable, possibly reflecting a seasonal shift towards neutral or slightly negative conditions. Bioreactor effluent ORP was more uniformly negative (Raft A -169 ± 26 mV, n = 24; Raft B -172 ± 22 mV, n = 24), indicating that the bioreactor biota had established and maintained the reducing environment required to support their own growth and metabolism. ORP values changed little in the precipitation tanks but did reflect the various chemical addition experiments that were periodically administered.

**pH.** System pH was monitored at multiple points several times each week by Clearwater Layline staff using an Orion portable pH meter as well as in monthly analyses performed by contract laboratories. Pit water influent pH ranged between 7.3 and 8.2, averaging 7.7 ± 0.2 (Raft A, n = 24 months, Table II-1). Although the sulfate reduction process normally raises pH, this effect was not evident in the bioreactor or precipitation tank effluents. Raft B precipitation tank effluent pH decreased when $FeCl_3$ dosing was tested but returned to values > 6.0 after dosing was reconfigured and adjusted in September 2015. The decrease in pH associated with $FeCl_3$ treatment would be expected due to the dissociation of $FeCl_3$ into $Fe^{3+}$ and $Cl^-$ ions. The $Cl^-$ ions would form HCl (hydrochloric acid) and lower the pH.

**Hardness, total dissolved solids, conductivity, alkalinity, and specific conductance.** Comparison of pit water, bioreactor effluents, and precipitation tank effluents showed no substantial changes in hardness, total dissolved solids, and specific conductance (Table II-1). However, alkalinity increased in the bioreactor effluents by about three-fold, probably due to microbial metabolic conversion of pit water $H_2SO_4$ to $H_2S$, resulting in a concomitant increase in the available buffering capacity of the bioreactor effluent. We tested several methods designed to precipitate bioreactor-generated $H_2S$ in Raft B, which should also have decreased alkalinity. While these efforts were nominally successful, producing some

sulfide precipitates, problems with incomplete mixing and channeling of bioreactor effluents water with our chemical additives prior to entering the precipitation tank prevented large-scale reactions, and substantial decreases in sulfide or alkalinity were observed. These mixing issues were addressed in the design of Raft C, but limitations of time and resources prevented full-scale testing of the modified Raft C precipitation regimes. Laboratory studies aimed at optimizing sulfide precipitation and developing methods to chemically reduce hydrogen sulfide to elemental sulfur, which should substantially decrease effluent alkalinity, are reported in Section V. Chemistry.

**Other operational parameters.** Additional water quality indicators including chloride, iron, sodium, nitrogen, phosphorus, chemical oxygen demand (COD), and dissolved organic carbon (DOC) were monitored throughout the project (Table II-1). Changes in each of these parameters from influent to effluent waters corresponded to additions (chloride, sodium, nitrogen, phosphorus) or biological activities (COD, DOC) as the water proceeded through the bioreactors and precipitation tanks.

**Mercury and methylmercury – general summary.** Mercury is a common constituent of Upper Midwest landscapes and is often detected in soils, sediments, and water, including lakes, rivers, rain, and snow. Recent studies[6] have reported mercury concentrations in the Embarrass River, which receives our pit outflow water via Spring Mine Creek, of 3 – 5 ng/L, and we measured mercury at 0.7 – 1.4 ng/L in the pit water itself (Table II.2). Since our bioreactor system recycled pit water (i.e., neither adding nor subtracting from the original water volume and adding no extraneous mercury), we anticipated that the flux of mercury from the pit to the receiving waters would be unchanged. However, sulfate-reducing bacteria can convert mercury into organic forms, like methylmercury, so it was possible that our bioreactor effluents might contain slightly higher methylmercury concentrations than the pit water influent, which is indeed evident in our data (Table II-2). Thus, it was important to estimate the total flux of mercury and methylmercury through our system and to put these estimates into a landscape context by comparing them to the known mercury flux in the Embarrass River.

To calculate the maximum mercury and methylmercury flux through our system, we used the highest mercury and methylmercury concentrations measured in any sampled component (see Table II-2), the highest flow rate used at any point in the study, and longest period that any bioreactor operated. The resulting estimate of mercury flux is conservative (i.e., represent the highest possible value), because the rafts did not always operate at maximum flow nor did they operate at maximum metabolic activity, which would theoretically produce the highest methylmercury concentrations. For calculations of mercury flux, the permitted flow rate through the combined rafts was 18 gallons/minute (68.1 liters/minute); the maximum possible operating period for the three rafts was 27 months[7] ($1.2 \times 10^6$ minutes); and the highest average mercury measurement found in any effluent flow was 1.4 ng/L (Raft B, precipitation tank effluent, n = 19 months, Table II-2). The maximum amount of mercury that might have passed through the system would have been about 0.11 grams, which converts to 0.000134 grams/day for the total period of operation. To put this quantity into a landscape or watershed

[6]Berndt D, Bavin TK. 2012. Environmental Pollution 161:321-327; Final Environmental Impact Statement (FEIS) NorthMet Mining Project and Land Exchange; Table 4.2.2-4; http://www.dnr.state.mn.us/input/environmentalreview/polymet/feis-toc.html.

[7]The longest operating bioreactors ran for 27 months; full analytical characterization was conducted for 26 months for Rafts A and B; different rafts have different monthly totals because of downtime for repairs, switching substrates, or other interruptions; see Table 2 for specific sample quantities.

perspective, mercury concentrations in the Embarrass River have been reported in several studies as averaging 3.4 ng/L (n = 5 monthly samples; Berndt and Bavin 2012[7]) and 4.3 – 5.1 ng/L (n = 23 and 28 samples, respectively, MnDNR[7]). If we use an average annual flow for the Embarrass River of 64 $ft^3$/second[8] (1,812 liters/second), we calculate that these receiving waters carry an average of about 0.54 – 0.80 g of mercury per day, or about 4,000 – 6,000-fold more than the hypothetical maximum daily flow through our system.

Methylmercury was also recorded in pit influent water, and, as expected, concentrations generally increased after passage through the sulfate-reducing bacterial bioreactors, but these measurements were quite variable, fluctuating as a result of changes in bacterial metabolism. However, using the flow and time conditions specified above, the highest methylmercury concentration recorded for any bioreactor component (0.38 ng/L, Raft C Bioreactor Effluent, n = 6 monthly samples, Table II-2), and the reported average Embarrass River methylmercury concentration of 0.19 – 0.51 ng/L (Berndt and Bavin 2012; MnDNR[7]), we find that the Embarrass River receiving waters carry between 800 – 2,200-fold higher daily loads of methylmercury than the hypothetical flux through our system.

Our measurements clearly indicate that our experiment had very little material effect on the existing landscape flux of mercury or methylmercury.

**Mercury and methylmercury - Detailed description and discussion**. Total and dissolved mercury (Hg) and methylmercury (MeHg, $CH_3Hg^+$) measurements were performed by North Shore Analytical, Inc. (NSA, Duluth, MN) using EPA Methods 1631 and 1630, respectively. Monthly samples of Raft A influent (i.e., pit water), combined bioreactor effluent water, and precipitation tank effluent water were analyzed for 21 months (Dec. 2014 – Aug. 2016). Raft B influent water was analyzed for 9 months (Dec. 2015 – Aug. 2016), and both combined bioreactor and precipitation tank effluent samples were analyzed for 21 months (as in Raft A). Raft C operated for 7 months (Dec. 2015 – Jun. 2016), with influent and both effluent samples analyzed for each of these. Hg and MeHg data were reported by NSA as either below the practical quantitation limit (> PQL)[9] or quantitatively as ng/L. The PQL for total and dissolved (the aqueous portion after filtering) mercury was 0.5 ng/L and for MeHg and dissolved MeHg, PQL = 0.05 ng/L. Data is reported herein and in Table II-2 as the mean ± standard deviation, along with the total sample number (n) and n ≥ PQL, which allows some additional context to interpret the respective Hg and MeHg concentrations found in pit water and in effluents from the bioreactors and precipitation tanks.

*Pit water influent.* (Note – Refer to Table II-2 for all mercury data). In the 21 months between Dec. 2014 and Aug. 2016, Hg above the PQL was detected in Raft A influent only once (0.668 ng/L), and then only in the total mercury assay, while MeHg (PQL = 0.05 ng/L) was reported in 10 of 20 samples, averaging 0.124 ± 0.082 ng/L. Of the methylmercury total, about 60% (0.073 ± 0.0212 ng/L) was detected in the dissolved fraction.

Raft B influent water, which was drawn from a source that was near, but independent of, the Raft A influent source, was analyzed for the nine months between Dec. 2015 – Aug. 2016. During that period,

[8]Annual average flow data from the Embarrass River at Embarrass, MN; referenced in the MnDNR NorthMet FEIS, Table 4.2.2-27; http://www.dnr.state.mn.us/input/environmentalreview/polymet/feis-toc.html.
[9]The practical quantitation limit (PQL; also sometimes referred to as the reporting limit) is calculated, by convention, as 5X the laboratory's method limit of detection (MDL).

no Hg samples exceeded the PQL, while three monthly samples with MeHg concentrations ≥ PQL were reported (0.051 ± 0.083 ng/L), with only one dissolved MeHg sample recorded at the reporting limit (0.05 ng/L). These Raft B influent results correspond well with the data from Raft A influent, but since they were collected at the same time from nearly the same place, they should be considered replicates and not independent samples.

*SRB bioreactor effluents.* Mercury concentrations above the PQL (0.5 ng/L) were reported in the majority of monthly bioreactor effluent samples from all three rafts (Raft A, in 17/21 samples; Raft B, 16/21 samples; Raft C, 6/7 samples), with mean concentrations ranging between 0.9 – 1.0 ng/L. Notably, almost all Hg detections were reported from unfiltered (Hg - total) samples, with only one dissolved (aqueous) fraction registered above the PQL, suggesting that the majority of mercury flowing out of the bioreactor was retained in the particulate fraction.

Methylmercury concentrations above the PQL (0.05 ng/L) were also detected in the majority of bioreactor effluent samples (Raft A, 11/20 samples; Raft B, 12/20 samples; Raft C, 6/7 samples), with mean concentrations ranging between 0.11 and 0.36 ng/L. MeHg ≥ PQL was found in 16 of 47 dissolved fractions. In Raft B samples, mean MeHg concentration in the dissolved fraction (0.243 ± 0.152 ng/L) was greater than the total MeHg concentration (0.112 ± 0.069 ng/L), and this paradoxical reversal occurred in five of six monthly samples. This unexplained situation occurred two other times in the other 115 pairwise comparisons between total and dissolved Hg and MeHg, both times in Raft C, and in both cases the values for total and dissolved Hg concentration were much closer.

*Precipitation tank effluents*. Since the precipitation tanks, which received bioreactor effluents, were not designed to support a microbial community, little change in mercury or further metabolic production of methylmercury was expected, and virtually none was found.

*Mercury in Pit 5NE-c and the surrounding watersheds.* Mercury deposition, sequestration, and release have been monitored in the watersheds immediately surrounding our study site (Berndt and Bavin 2012; PolyMet FEIS)[10], and the primary role of wetlands in accumulating and periodically releasing inorganic- and methyl-mercury has been well established. In drier, sparsely vegetated landscapes, aerially deposited mercury is often rapidly transported through the watershed via precipitation runoff, but in wetlands mercury accumulates and concentrates via wet/dry cycling, often for years. Thus, wetland-rich areas generally contain higher overall mercury concentrations, and these landscapes can act as mercury sources, releasing accumulated mercury during heavy rainfall or flooding events.

Berndt and Bavin (2012) used this capture/release dynamic to explain the relatively lower mercury concentrations found in northern St. Louis River tributary watersheds that drain mined areas, compared with higher concentrations in the more southern watersheds, which usually contain more wetlands. Our study site sits nearly at the height of land between the Embarrass and Partridge River watersheds and thus is not expected to receive input other than from precipitation and runoff from the former mine land immediately surrounding it. The pit lake is part of a complex that drains into Spring Mine Creek, which flows north for about five miles and drains into the Embarrass River. The majority of the mercury in our influent and effluent water samples (> 0.5 – 1.4 ng/L) was probably transported in runoff from the relatively small, sparsely vegetated area surrounding the pit. But downstream mercury concentrations

[10]Berndt D, Bavin TK. 2012. Environmental Pollution 161:321-327;
PolyMet FEIS: http://www.dnr.state.mn.us/input/environmentalreview/polymet/feis-toc.html

are much higher. At the confluence of Spring Mine Creek and the Embarrass River, mercury was reported at about 5 ng/L (Berndt and Bavin 2012; PolyMet FEIS, Table 4.2.2-32) under high-flow conditions, probably reflecting transport in runoff from a much larger and wetter area that contained much more accumulated mercury.

The proportion of Hg present as MeHg is an important metric, because organic forms of mercury are more toxic and bioaccumulative than elemental or other inorganic forms. Methylmercury has been reported in the Embarrass River by both Berndt and Bavin (2012[7]) in 2008 and in the PolyMet FEIS[7] (Table 4.2.2-32) in multiple samples taken between 2004 and 2013. Methylmercury fractions were calculated as between 7.1% – 10.4% in surface water samples from regional rivers, suggesting that microbial metabolism had contributed to the methylmercury content.

As expected, when both total mercury and methylmercury were reported in the bioreactor effluents (n = 36/119 pairwise comparisons for all effluents, all rafts), methylmercury fractions were relatively high, ranging between 4.2 – 94.9%. Given the low mercury concentration in the pit water and the low flow rate of our system, our rafts contributed a very small amount of additional methylmercury to the pit water, even at the moderate to high methylation efficiencies reported. That said, methylmercury production in larger scale operations and/or influent water containing higher mercury concentrations could be a concern, and should be considered in future applications of this technology.

*Open questions and caveats.* An apparent discrepancy between the mercury concentrations reported in the pit water influent (often below the PQL) and the higher concentrations (usually greater than the PQL) reported in the bioreactor and precipitation tank effluents is unexplained at this time.

**Power supply and rationalization.** The long-term objectives of the bioremediation program include continued development and refinement of independent, low power systems that could be efficiently operated on a continual basis using self-contained renewable energy sources. The pumps, valves, and sensors on Rafts A and B, which operated for over 27 consecutive months, were powered by electricity provided by a propane-fueled generator and supplemented with solar photovoltaic panels. Raft C, built in the current phase of the project using refinements and modifications based on the earlier rafts, was entirely powered using solar photovoltaics, which energized marine batteries that maintained operations at night and on overcast days. Refinements in the raft design reduced energy demand to that the solar panels provided sufficient power to fully activate Raft C through the short days during the winter months.

See Section III. Energy and Control Systems for a full description of Raft C power design and function.

**Biological profiling and analysis.** Bench and pilot testing verified the presence of sulfide-reducing bacteria in the sediments used for inoculating the bioreactors, and early *in situ* tests showed that the bacterial communities remained active throughout an annual cycle.

Long-term, continuous operation of the rafts during the current study allowed assessment of microbial population density in water and on matrix fibers over extended periods covering a complete annual cycle. As expected, prokaryotic population numbers were sensitive to temperature and to the supplied carbon substrate.

Identifying individual genera or species of the microbial consortium is an important step in determining how the bioreactors operate under varying conditions and how their communities might evolve over

time. Initial tests indicate that the sulfate-reducing bacteria made up about 10-30% of the microbial community in bioreactor water and fibers, with the most abundant genera including *Desulfovibrio*, *Desulfobacter* and *Desulfobulbus***.**

See Section IV. Microbiology for a detailed analysis and description of microbiological characteristics.

**Table II-1.** Characteristics of pit water influents, bioreactor effluents, and precipitation/settling tank effluents.

| | Raft A Influent | | | | | Raft A Bioreactor Effluent | | | | | Raft A Final (Iron ppt.) Effluent | | | | |
|---|---|---|---|---|---|---|---|---|---|---|---|---|---|---|---|
| **RAFT A** | **Mean ± SD** | **Low** | **High** | **n** | **n ≥ PQL** | **Mean ± SD** | **Low** | **High** | **n** | **n ≥ PQL** | **Mean ± SD** | **Low** | **High** | **n** | **n ≥ PQL** |
| Sulfate (mg/L) | 1001 ± 155 | 838 | 1680 | 24 | 24 | 319 ± 138 | 45.9 | 572 | 24 | 24 | 301 ± 162 | 28 | 666 | 21 | 21 |
| Sulfide (mg/L) | 4.2 ± 2.5 | <2 | 6 | 24 | 2 | 178 ± 63 | 17 | 274 | 23 | 23 | 156 ± 83 | 10 | 274 | 21 | 21 |
| ORP (mV) | 188 ± 179 | -105 | 468 | 24 | 24 | -169 ± 26 | -207 | -73 | 24 | 24 | -123 ± 142 | -181 | 492 | 21 | 21 |
| pH | 7.7 ± 0.3 | 7.33 | 8.23 | 24 | 24 | 7.2 ± 0.3 | 6.2 | 8.2 | 24 | 24 | 7.1 ± 0.4 | 5.87 | 7.51 | 21 | 21 |
| Alkalinity, total as $CaCO_3$ (mg/l) | 302 ± 17.6 | 259 | 328 | 24 | 24 | 810 ± 207 | 77.5 | 1060 | 24 | 24 | 861 ± 246 | 331 | 1570 | 21 | 21 |
| Total hardness (mg/l) | 1099 ± 70 | 932 | 1200 | 23 | 23 | 1100 ± 67 | 981 | 1220 | 23 | 23 | 1094 ± 64 | 990 | 1240 | 21 | 21 |
| Total dissolved solids (mg/l) | 1586 ± 75 | 1430 | 1740 | 24 | 24 | 1444 ± 180 | 801 | 1700 | 24 | 24 | 1481 ± 169 | 1160 | 1850 | 21 | 21 |
| Specific conductance (µS/cm) | 2055 ± 83 | 1924 | 2209 | 24 | 24 | 2149 ± 107 | 1947 | 2357 | 24 | 24 | 2180 ± 118 | 1972 | 2404 | 21 | 21 |
| Chloride (mg/l) | 3.1 ± 1.8 | <1.0 | 6.7 | 24 | 11 | 3.8 ± 2.5 | <1.0 | 7.7 | 24 | 7 | 18.3 ± 16.8 | <1.0 | 69.1 | 21 | 14 |
| Iron (µg/l) | 418 ± 458 | <100 | 1600 | 24 | 9 | 324 ± 379 | <100 | 1480 | 24 | 12 | 1994 ± 2340 | <100 | 7730 | 21 | 17 |
| Iron, dissolved (µg/l) | 292 ± 250 | <100 | 826 | 24 | 7 | 148 | <100 | 300 | 24 | 2 | 116 | <100 | 116 | 21 | 1 |
| Sodium (mg/L) | 67.4 ± 3.6 | 60.6 | 76.1 | 24 | 24 | 67.0 ± 3.6 | 61.6 | 75 | 24 | 24 | 75.0 ± 11.0 | 65.3 | 108 | 21 | 21 |
| Nitrogen, ammonia (mg/l) | 0.24 ± 0.10 | <0.5 | 0.58 | 24 | 10 | 5.6 ± 4.5 | <0.5 | 18.2 | 24 | 12 | 9.5 ± 11.8 | <0.5 | 44.3 | 21 | 12 |
| Nitrogen, Kjeldahl, total (mg/l) | 0.7 | <0.5 | 0.69 | 16 | 1 | 8.5 ± 11.6 | 2.0 | 52.3 | 17 | 17 | 6.7 ± 2.8 | 2.2 | 10.8 | 13 | 13 |
| Phosphorus (mg/l) | 0.07 ± 0.03 | <0.08 | 0.12 | 24 | 12 | 3.8 ± 6.8 | 0.098 | 30.8 | 24 | 24 | 4.9 ± 7.7 | <0.08 | 32.8 | 21 | 20 |
| COD (mg/l) | 17.4 ± 7.8 | <10 | 34.4 | 23 | 9 | 610 ± 385 | 170 | 1970 | 23 | 23 | 662 ± 427 | 260 | 2190 | 20 | 20 |
| DOC (mg/l) | 1.4 ± 0.2 | <1 | 2 | 24 | 23 | 168 ± 121 | 44 | 614 | 24 | 24 | 173 ± 129 | 54 | 655 | 21 | 21 |

| | Raft B Influent | | | | | Raft B Bioreactor Effluent | | | | | Raft B Final (Iron ppt.) Effluent | | | | |
|---|---|---|---|---|---|---|---|---|---|---|---|---|---|---|---|
| **RAFT B** | **Mean ± SD** | **Low** | **High** | **n** | **n ≥ PQL** | **Mean ± SD** | **Low** | **High** | **n** | **n ≥ PQL** | **Mean ± SD** | **Low** | **High** | **n** | **n ≥ PQL** |
| Sulfate (mg/L) | 975 ± 31 | 928 | 1040 | 9 | 9 | 360 ± 198 | 26.2 | 736 | 24 | 24 | 320 ± 180 | 62.6 | 607 | 23 | 23 |
| Sulfide (mg/L) | - | <2 | <2 | 9 | 0 | 170 ± 97 | 17.4 | 459 | 24 | 24 | 122 ± 71 | 2.2 | 270 | 23 | 23 |
| ORP (mV) | -30.0 ± 58 | -85 | 109 | 9 | 9 | -172 ± 22 | -218 | -125 | 24 | 24 | -132 ± 77 | -189 | 191 | 23 | 23 |
| pH | 7.7 ± 0.2 | 7.4 | 8.0 | 9 | 9 | 7.3 ± 0.4 | 6.6 | 8.4 | 24 | 24 | 7.0 ± 0.7 | 5.8 | 8 | 23 | 23 |
| Alkalinity, total as $CaCO_3$ (mg/l) | 303 ± 18 | 279 | 331 | 9 | 9 | 896 ± 216 | 509 | 1450 | 24 | 24 | 761 ± 276 | 63.3 | 1080 | 23 | 23 |
| Total hardness (mg/l) | 1124 ± 56 | 1030 | 1190 | 8 | 8 | 1155 ± 69 | 992 | 1260 | 23 | 23 | 1142 ± 73 | 970 | 1250 | 22 | 22 |
| Total dissolved solids (mg/l) | 1611 ± 65 | 1520 | 1710 | 9 | 9 | 1545 ± 156 | 1320 | 1860 | 24 | 24 | 1577 ± 180 | 1300 | 2140 | 23 | 23 |
| Specific conductance (µS/cm) | 2065 ± 68 | 1951 | 2154 | 9 | 9 | 2322 ± 249 | 1967 | 2943 | 24 | 24 | 2440 ± 338 | 2001 | 3483 | 23 | 23 |
| Chloride (mg/l) | - | <1.0 | <1.0 | 9 | 0 | 2.4 ± 1.5 | <1.0 | 6 | 24 | 11 | 205 ± 295 | <1.0 | 1330 | 23 | 20 |
| Iron (µg/l) | 227 ± 109 | <100 | 398 | 9 | 5 | 123 ± 44 | <100 | 196 | 24 | 5 | 35066 ± 68125 | <100 | 258000 | 23 | 14 |
| Iron, dissolved (µg/l) | 196 ± 85 | <100 | 327 | 9 | 5 | - | <100 | <100 | 24 | 0 | 27537 | <100 | 244000 | 23 | 9 |
| Sodium (mg/L) | 66.8 ± 2.0 | 64.6 | 70.3 | 9 | 9 | 95.3 ± 54.1 | 62.5 | 252 | 24 | 24 | 94.0 ± 46.8 | 63.3 | 220 | 23 | 23 |
| Nitrogen, ammonia (mg/l) | 0.17 ± 0.1 | <0.5 | 0.2 | 9 | 3 | 6.6 ± 7.1 | ND | 27.9 | 24 | 12 | 8.0 ± 10.7 | <0.5 | 35.5 | 23 | 14 |
| Nitrogen, Kjeldahl, total (mg/l) | - | <0.5 | <0.5 | 9 | 0 | 8.0 ± 9.8 | 2.6 | 44.8 | 17 | 17 | 5.2 ± 2.3 | 1.9 | 9.4 | 15 | 15 |
| Phosphorus (mg/l) | - | <0.08 | <0.08 | 9 | 0 | 3.89 ± 6.33 | <0.08 | 25.9 | 24 | 23 | 4.14 ± 7.18 | 0.039 | 28.5 | 23 | 23 |
| COD (mg/l) | 14.2 ± 2.1 | <10 | 15.6 | 9 | 2 | 426 ± 269 | 82.1 | 1160 | 23 | 23 | 381 ± 275 | 35 | 1120 | 22 | 22 |
| DOC (mg/l) | 1.4 ± 0.3 | 1.1 | 1.8 | 9 | 9 | 97.8 ± 91.7 | 6.9 | 359 | 24 | 24 | 95.2 ± 89.2 | 7.2 | 345 | 23 | 23 |

**Table II-1 (continued).**

| | Raft C Influent | | | | | Raft C Bioreactor Effluent | | | | |
|---|---|---|---|---|---|---|---|---|---|---|
| **RAFT C** | **Mean ± SD** | **Low** | **High** | **n** | **n ≥ PQL** | **Mean ± SD** | **Low** | **High** | **n** | **n ≥ PQL** |
| Sulfate (mg/L) | 981 ± 35 | 924 | 1040 | 7 | 7 | 916 ± 55 | 836 | 990 | 7 | 7 |
| Sulfide (mg/L) | - | <2 | <2 | 7 | 0 | 24.3 ± 22.5 | 4.0 | 58.0 | 7 | 7 |
| ORP (mV) | -9.9 ± 84 | -74 | 170 | 7 | 7 | -100 ± 48 | -157 | -15 | 7 | 7 |
| pH | 7.7 ± 0.2 | 7.3 | 8.0 | 7 | 7 | 7.0 ± 0.3 | 6.6 | 7.4 | 7 | 7 |
| Alkalinity, total as $CaCO_3$ (mg/l) | 306 ± 22 | 283 | 284 | 7 | 7 | 379 ± 134 | 278 | 666 | 7 | 7 |
| Total hardness (mg/l) | 1133 ± 41 | 1100 | 1210 | 6 | 6 | 1125 ± 46 | 1060 | 1200 | 6 | 6 |
| Total dissolved solids (mg/l) | 1617 ± 57 | 1560 | 1680 | 7 | 7 | 1666 ± 164 | 1560 | 2030 | 7 | 7 |
| Specific conductance (µS/cm) | 2072 ± 102 | 1941 | 2254 | 7 | 7 | 2129 ± 159 | 1959 | 2449 | 7 | 7 |
| Chloride (mg/l) | - | <1.0 | <1.0 | 7 | 0 | - | <1.0 | <1.0 | 7 | 0 |
| Iron (µg/l) | 173 ± 14 | <100 | 157 | 7 | 3 | 182 ± 47 | <100 | 206 | 7 | 4 |
| Iron, dissolved (µg/l) | 158 ± 32 | 137 | 194 | 7 | 3 | 176 ± 36 | <100 | 217 | 7 | 3 |
| Sodium (mg/L) | 67.2 ± 2.7 | 64.1 | 71.9 | 7 | 7 | 87.4 ± 56.3 | 64.3 | 215 | 7 | 7 |
| Nitrogen, ammonia (mg/l) | 0.13 ± 0.3 | 0.10 | 0.17 | 7 | 4 | 1.26 ± 1.08 | <0.5 | 3 | 7 | 4 |
| Nitrogen, Kjeldahl, total (mg/l) | - | <0.5 | <0.5 | 7 | 0 | 2.6 ± 1.6 | <0.5 | 5 | 7 | 6 |
| Phosphorus (mg/l) | - | <0.08 | <0.08 | 7 | 0 | 0.3 ± 0.1 | <0.08 | 0 | 7 | 5 |
| COD (mg/l) | 17.2 | <10 | 17.2 | 7 | 1 | 270 ± 212 | <10 | 658 | 7 | 6 |
| DOC (mg/l) | 1.4 ± 0.3 | 1.0 | 1.9 | 7 | 7 | 75.4 ± 72.2 | 2.4 | 214 | 7 | 7 |

Mean and standard deviation were calculated from monthly samples that registered at or above the practical quantitation limit (PQL), or reporting limit, which is established by convention as five times the method limit of detection, as reported by the analytical lab. Values with below than (<) notations indicate detection below the stated PQL value. (n) indicates the total number of monthly samples, and n ≥ PQL indicates the number of those samples above the reporting limit. (-) indicates no samples at or above the PQL.

**Table II-2.** Mercury and methylmercury in Rafts A, B, and C influents and effluents.

| Source | Mean ± SD (ng/L)[A] | Range | | n | |
|---|---|---|---|---|---|
| | | Low | High | Total | ≥ PQL[B] |
| **Raft A Influent** | | | | | |
| Mercury - total (ng/l) | 0.668 | <0.500 | 0.668 | 21 | 1 |
| Mercury - dissolved (ng/l) | <PQL | <0.500 | <0.500 | 21 | 0 |
| Methylmercury - total (ng/l) | 0.124 ± 0.082 | <0.050 | 0.136 | 20 | 10 |
| Methylmercury - dissolved (ng/l) | 0.075 ± 0.021 | <0.050 | 0.108 | 20 | 9 |
| **Raft A Bioreactor Effluent** | | | | | |
| Mercury - total (ng/l) | 0.931 ± 0.330 | <0.500 | 1.79 | 21 | 17 |
| Mercury - dissolved (ng/l) | <PQL | <0.500 | <0.500 | 21 | 0 |
| Methylmercury - total (ng/l) | 0.158 ± 0.061 | <0.050 | 0.217 | 20 | 11 |
| Methylmercury - dissolved (ng/l) | 0.134 ± 0.058 | <0.050 | 0.190 | 20 | 6 |
| **Raft A Final (Iron ppt.) Effluent** | | | | | |
| Mercury - total (ng/l) | 1.022 ± 0.641 | 0.514 | 2.86 | 18 | 15 |
| Mercury - dissolved (ng/l) | 0.514 | <0.500 | 0.514 | 18 | 1 |
| Methylmercury - total (ng/l) | 0.193 ± 0.125 | <0.050 | 0.397 | 17 | 9 |
| Methylmercury - dissolved (ng/l) | 0.151 ± 0.104 | <0.050 | 0.293 | 17 | 4 |
| **Raft B Influent** | | | | | |
| Mercury - total (ng/l) | <PQL | <0.500 | <0.500 | 9 | 0 |
| Mercury - dissolved (ng/l) | <PQL | <0.500 | <0.500 | 9 | 0 |
| Methylmercury - total (ng/l) | 0.151 ± 0.083 | <0.050 | <0.050 | 9 | 3 |
| Methylmercury - dissolved (ng/l) | 0.050 | <0.050 | <0.050 | 9 | 1 |
| **Raft B Bioreactor Effluent** | | | | | |
| Mercury - total (ng/l) | 1.032 ± 0.366 | 0.548 | 1.82 | 21 | 16 |
| Mercury - dissolved (ng/l) | 0.570 | <0.500 | <0.500 | 21 | 1 |
| Methylmercury - total (ng/l) | 0.112 ± 0.069 | <0.050 | 0.248 | 20 | 12 |
| Methylmercury - dissolved (ng/l) | 0.243 ± 0.152 | <0.050 | 0.520 | 20 | 6 |
| **Raft B Final (Iron ppt.) Effluent** | | | | | |
| Mercury - total (ng/l) | 1.359 ± 0.767 | <0.500 | 3.25 | 20 | 17 |
| Mercury - dissolved (ng/l) | <PQL | <0.500 | <0.500 | 20 | 0 |
| Methylmercury - total (ng/l) | 0.153 ± 0.041 | <0.050 | 0.195 | 19 | 6 |
| Methylmercury - dissolved (ng/l) | 0.083 ± 0.018 | <0.050 | 0.099 | 13 | 3 |

**Table II-2 (continued).**

| Source | Mean ± SD (ng/L)[A] | Range | | n | |
|---|---|---|---|---|---|
| | | Low | High | Total | ≥ PQL[B] |
| **Raft C Influent** | | | | | |
| Mercury - total (ng/l) | <PQL | <0.500 | <0.500 | 7 | 0 |
| Mercury - dissolved (ng/l) | <PQL | <0.500 | <0.500 | 7 | 0 |
| Methylmercury - total (ng/l) | 0.056 ± 0.007 | <0.050 | <0.050 | 7 | 2 |
| Methylmercury - dissolved (ng/l) | <PQL | <0.050 | <0.050 | 7 | 0 |
| **Raft C Bioreactor Effluent** | | | | | |
| Mercury - total (ng/l) | 1.044 ± 0.572 | <0.500 | 0.758 | 7 | 6 |
| Mercury - dissolved (ng/l) | <PQL | <0.500 | <0.500 | 7 | 0 |
| Methylmercury - total (ng/l) | 0.375 ± 0.336 | 0.118 | 0.778 | 7 | 6 |
| Methylmercury - dissolved (ng/l) | 0.274 ± 0.162 | <0.050 | 0.376 | 7 | 4 |

A. Total mercury and methylmercury were analyzed by North Shore Analytical, Inc. (Duluth, MN) using EPA methods 1631 and 1630, respectively.

B. PQL = practical quantitative limit (5X method limit of detection); for total mercury, PQL = 0.5 ng/L, for methylmercury, PQL = 0.05 ng/L.

**Panel II-1 – SRB Bioreactor general design and operational parameters.**

Floating SRB bioreactors were designed to provide the following characteristics:

- A replicable, modular design that allows:
    - Flexibility in handling different flow rates, and
    - Monitoring of influents, amendments, and effluents to gauge individual bioreactor performance.
- A 2-stage system with a first stage that biologically converts sulfate to hydrogen sulfide, and a second stage that chemically converts and precipitates sulfur for removal from the water flow (Fig. II-1). This 2-stage system avoids premature plugging of the bioreactors by keeping the sulfur precipitates separate from the bioreactors (Fig. II-2).
- Each 1st stage bioreactor uses a non-biodegradable, fibrous growth substrate for SRB attachment and biofilm development. This substrate is not consumed by the SRB, providing for a long life system without the need for substrate replacement.
- A vertical downflow system with buoyant substrate that provided good flow distribution and minimized growth substrate packing (Fig. II-2).
- Carbon substrates and nutrient amendments for feeding the SRB are supplied as a liquid feed that can be accurately controlled and monitored while allowing for variations in nutrient feed to optimize performance.
- Carbon substrates and nutrient amendments are introduced directly into the top of each bioreactor where they mix for the first time with the sulfate laden mine pit water. This minimizes biomass growth and accumulation in the influent system (Fig. II-2).
- The 2nd stage effluent treatment systems provide for separate settling tanks for each phase of treatment allowing for monitoring of each phase and type of effluent treatment. Separate settling tanks provide containment of precipitate materials for posterior analysis, collection, and disposal.
- All bioreactors and settling tanks are suspended and floating in a mine pit lake with all active, flowing components kept underwater to allow for year-around operation without freezing or over-heating (Figs. II-3 and II-4).
- Basic water flows and amendment additions are monitored remotely and controlled to assure accurate flow and feed rates to achieve maximum performance.
- Influent water is drawn from deep in the mine pit lake to minimize dissolved oxygen in the influent. This influent water is never exposed to the ambient air to keep oxygen levels low, as oxygen is detrimental to the SRB (Fig. II-2).
- Water flow is never raised above pit lake levels to minimize energy requirements.

A conceptual flow pattern and system schematic are illustrated in Figures II-1 and II-2. Individual bioreactors (Fig. II-3) were joined together to form independent rafts, which were further coupled to form a single unit (Fig. II-4). This configuration facilitated operations, stability, and safety.

**Figure II-1. Flow diagram.**

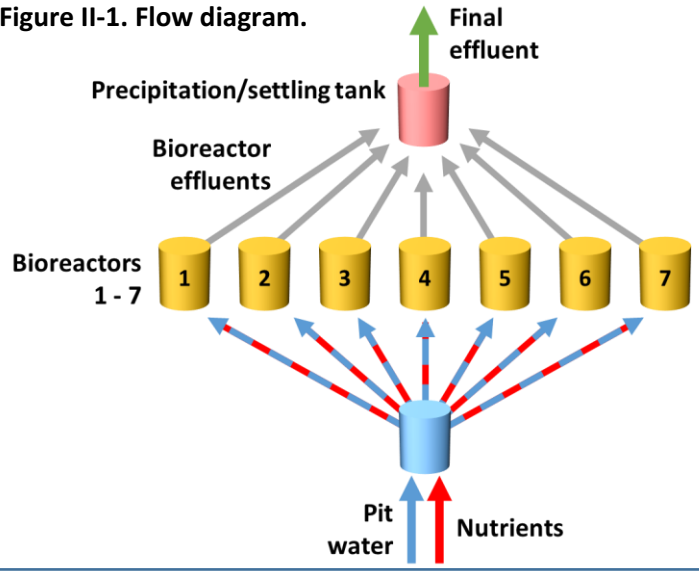


Conceptual flow pattern for bioreactor/precipitation tanks. Influent pit water is drawn from a depth of about 20 feet and distributed, along with carbon substrates and nutrients, to seven bioreactors. After passage through the bioreactors, the composite effluent is collected in a central tank for treatment to remove the hydrogen sulfide; for instance, by adding iron compounds to create insoluble precipitates. Flow rates, which determine hydraulic retention times, can be controlled by influent and effluent pumping.

**Figure II-2. Basic bioreactor design.**

Basic bioreactor and precipitation tank design and flow schematic (Raft A). Each 4,000-gallon bioreactor (left) is filled from a common pit water intake source, with flow rates controlled by a pump. Carbon substrates and nutrient amendments are added. After passage through the bioreactors, combined effluent water is pumped into a precipitation tank (right), where it is chemically treated and solids are allowed to precipitate. Raft A was supplied with ethanol; Raft B bioreactors were supplied with lactic acid or sodium lactate. Raft C incorporated a few modifications to this basic design (see Appendix 1, Figure 7) and was supplied with lactic acid.

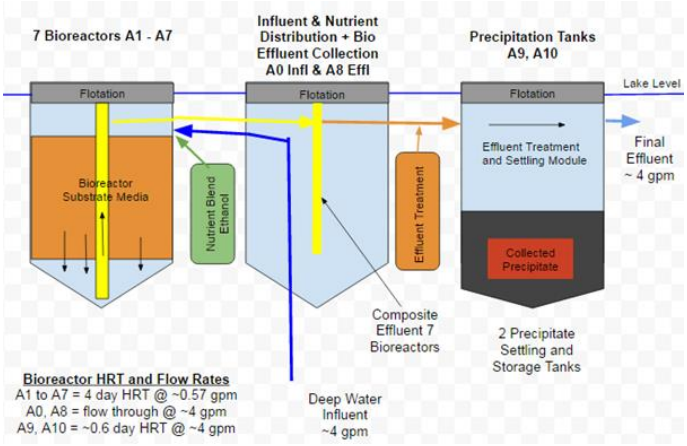


**Figure II-4. Bioreactor module.**

Full-scale bioreactor prior to placement in the water. Bioreactors were partially constructed on land.

**Figure II-3. SRB bioreactor rafts.**

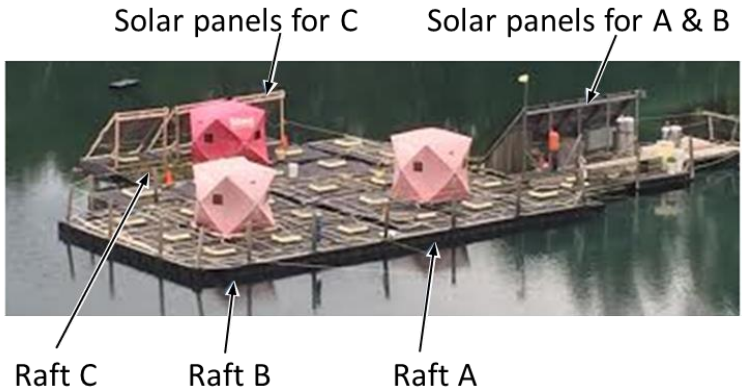


Rafts A, B, and C. For scale, note the technician standing near the Raft A/B solar panels. Tents were placed over the central module, which housed influent and effluent sampling access tubes.

## III.A. Energy and Control Systems – Summary

The primary efforts with respect to the electrical engineering aspects of the treatment system were twofold: to use a form of renewable energy technology to power the treatment system and to develop a specification for remote monitoring and control of the system.

The remote location of the pit lake near Hoyt Lakes, Minnesota is similar to many closed mining operations globally in that the electrical infrastructure has been removed as part of restoration efforts. Therefore, it was mandatory that the treatment system at the Cliffs/Erie-PolyMet site use standalone renewable energy technology to power the system's pumps, sensors, and communications equipment. Accordingly, an optimum combination of solar photovoltaic (PV) panels and batteries were specified so that the system would operate with sufficient energy even during a worst-case, sunlight-scarce winter month in northern Minnesota. The design was arrived at using solar data from the National Renewable Energy Laboratory (NREL) as input to an hour-by-hour simulation of the energy produced by the solar panels, as well as the hourly behavior of batteries and electrical loads, to ensure that the treatment system would be powered with an availability approaching 100%. Additionally, to minimize the variation in flow rates due to fluctuations in power that are common to isolated renewable energy-powered systems, a dual-voltage power supply design was adopted. Such a design also reduces the life-cycle cost of the system by extending the life of the storage batteries and stabilizes the rate at which water is treated by the bioremediation system.

Constructed rafts were equipped with a number of basic sensors that measure various flow rates and other parameters. The data from these sensors continue to be remotely available to the project team via cellular radio and a web-based portal and are critical to assessing the daily operation of the system and in corroborating the results from the hourly solar energy simulations. A next-generation design would include both remote monitoring and control of the treatment system from a central control location as well as alarming and autonomous operations at the treatment site. A specification for this type of control system has been developed to assist with the design of future bioremediation treatment systems.

## III.B. Specification for Energy and Control Systems for Floating SRB Bioreactors

### 1. Functional Description of SRB System

The sulfate-reducing bacterial bioreactor (SRB) system is a modular system designed to reduce sulfate concentrations in iron ore mine pit lakes. Bioreactor modules have equivalent sizes so that increasing the number of modules increases the volume of water treated per unit time. This modular system utilizes natural populations of sulfur-reducing bacteria sampled from the pit discharge stream sediment to convert sulfate concentrations to hydrogen sulfide in a floating bioreactor where the bacteria grow on specialized inert media inside the bioreactor. The bioreactor discharge water, high in hydrogen sulfide, is then passed into a second floating precipitation tank where the hydrogen sulfide is converted to metal sulfides or elemental sulfur. After a period of time, these particles settle and can be discharged to the pit bottom or removed from the tank. The design of this system is patterned after natural

processes occurring in lake or stream sediment, where sulfate can be chemically reduced and converted into solid precipitates in the sediment.

The SRB system requires various pumps, sensors, and communications and control equipment, all of which require electrical energy. Since there is no access to the electric grid at the remote pit lake site, the SRB system must be completely powered by on-site renewable energy sources. Candidate sources are wind and solar photovoltaic (solar PV). Solar is the technology-of-choice for the initial SRB system.

To achieve sulfate reduction targets, the SRB system must have an availability approaching 100%. Forced outages of the various pumps in the system due to a shortage of electrical energy may result in plugged hydraulic lines. Therefore, the energy system requires adequate peak capacity and adequate energy storage to serve the SRB system's electrical loads during the longest historical periods of low solar insolation. This document provides a functional and design specification for both autonomous and remote control of the bioremediation system to serve as a template for future operations.

## 2. SRB System Operating Environment

### 2.1 Location

The SRB system shall reside on a floating raft with a fixed proximity on a closed mine pit lake. The system shall be adjacent to shoreline to facilitate system operations and maintenance. The pit lake is surrounded on most sides by coarse rock piles in excess of 50 feet in height.

### 2.2 Climate

#### 2.2.1 Temperature

The SRB system shall be designed to operate with 100% availability, exclusive of planned maintenance outages, in the climate of northern Minnesota, with ambient air temperatures ranging from 100 °F to minus 60 °F. Sol-air, or effective summer temperatures during high levels of solar insolation, may reach 140 °F.

#### 2.2.2 Weather

System design shall anticipate the presence of heavy rain, freezing rain, sleet, hail, winds in excess of 70 mph. Wave action may be present on the pit lake. All cabling and SRB system fluid lines shall be capable of withstanding half-inch radial ice with 70 mph wind.

#### 2.2.3 Lightning

The SRB system design shall assume and address the presence of lightning storms. The SRB system's electrical system shall be designed in accordance with National Electrical Code Article 690 to ensure adequate grounding. The SRB raft's master ground bar shall connect, with the shortest conductor possible, to a shoreline grounding point having a grounding resistance (mat to ground) of 1 Ω or less.

## 2.3 Dust Environment

The SRB system will be located in a former mining site consisting of coarse rock piles and sparse-to-moderate amounts of brush and small trees. Relatively little airborne dust and coarse particulates are anticipated.

## 2.4 Access to Electrical Grid

The SRB system shall be designed to operate independent of the electrical grid. The system's location is assumed to be dozens of miles from the nearest 60 Hz feeder and would, therefore, be uneconomic to serve from the grid.

## 2.5 Personnel Issues

### 2.5.1 Access to SRB System

Access to the SRB system site shall be restricted to authorized personnel. The raft shall be designed to allow unimpeded access to all systems and subsystems on the raft, from the shoreline to the raft and on the raft itself.

### 2.5.2 Personnel Safety

#### 2.5.2.1 Authorized Personnel

Personnel shall be deemed to be Authorized Personnel if: 1) they are required by their employer to be on site; 2) they have received permission to enter the site from mine operators as well as SRB system operators; 3) they are current on all employer-provided safety training, including, but not limited to, CPR/first aid, personal protective equipment, confined space, and blood-borne pathogens; and 4) they are current on MSHA training; or 5) they are emergency responders.

#### 2.5.2.2 Site Communications

All authorized personnel shall be equipped with cell phones compatible with a local cellular provider and that are capable of sending and receiving calls from the SRB system location. If such access is not deemed sufficient, authorized personnel shall carry a satellite phone to the site.

#### 2.5.2.3 Posted Emergency Information

The SRB system site shall post emergency information, both on the shoreline where the raft attaches to land and on the raft itself, to facilitate an efficient response to any emergency that may arise on-site. Such information shall include but is not limited to: 1) the name of the site and the name of the mine owners/operators; 2) the latitude and longitude of the site, as well as the county and township; 3) the names, addresses, and phone numbers of the nearest fire, police, and sheriff's department, and hospital or emergency medical service; and 4) the name and phone number of the mine operator.

#### 2.5.2.4 Hazardous Materials

Material Safety Data Sheets (MSDS) shall be available at the site for ready access by authorized personnel. Additionally, a list of any hazardous materials located on-site shall be attached to the Posted Emergency Information described in Section 2.5.2.3.

#### 2.5.2.5 Applicable Codes

Since the SRB system installation is a floating "watercraft" with no AC power, it is specifically excluded from coverage under NEC code per Section 90.2.B1.

## 3. Energy Supply System

### 3.1 Determination of System Capacity

The quantity of solar panels and batteries shall be determined by the following:

a) 100% availability of the energy system across a worst-month test period;
b) The latitude of the mine site;
c) NREL Redbook data for solar insolation for the nearest location;
d) The rated power of each load in the system and associated duty cycles, with a margin for new loads of at least 10%; and
e) The setpoint of the low voltage disconnect (LVD) function within the charge controller.

### 3.2 SRB Design Values for Capacity and Energy

Solar panel and battery selection shall be based on a total connected load of 87W, with an annual energy consumption of 584 kWh (resulting in a capacity factor of 77%). The SRB system is energy constrained.

### 3.3 Solar Photovoltaic Panels

Based on the requirements in 3.1, the quantity of solar panels shall be six. The system shall utilize Silicon Energy Model SiE-V-275 panels, each with 60 monocrystalline silicon cells. These panels exhibit, at STC (Standard Test Conditions), an open-circuit voltage of 39.4 vdc, a short-circuit current of 9.58 amps, and a maximum output of 275 W with a MPP (maximum power point) of 31.0 volts and 8.94 amps.

#### 3.3.1 Panel Mounting

The panels shall be mounted vertically, with three panels in the lower row and three panels in the upper row, to form an array. The panels shall be oriented to be permanently positioned with a due-south heading, with an elevation or tilt angle from horizontal of 47 degrees. It shall be acceptable to mount the array at 45 degrees alternatively.

### 3.3.2 Panel Wiring

#### 3.3.2.1 Array Wiring Configuration

Panels shall be connected in a 2X3 series-parallel configuration, where each of three pairs of panels are connected in series to double the available voltage, and where the three pairs of panels are then connected in parallel to triple the available current.

#### 3.3.2.2 Conductor Sizing

Conductors between the solar panels and a NEMA combiner box shall be #10 AWG. Conductors from the NEMA combiner box to the Flexmax controller shall be #6 AWG.

#### 3.3.2.3 Panel Grounding

A #10 AWG ground wire shall connect the panels to SRB system's master ground bar (MGB).

## 3.4 Battery Energy Storage (Batteries)

Based on the requirements in 3.1, the quantity of batteries shall be nine. The system shall utilize Sun XTender Model PVX-840T AGM (Absorbed Glass Mat) Deep-cycle batteries with a 24-hour discharge rating of 84 amp-hours at 25°C. This rating shall constitute the battery capacity from a terminal voltage of 2.25 volts per cell (13.5 volts for six cells) to 1.75 volts per cell (10.5 volts for six cells).

The discharge algorithm used in the sizing model shall, under normal operating conditions, respect the minimum battery terminal voltage of 11.5 volts by specifying the Low Voltage Disconnect value at this level. Under emergency conditions the battery may be discharged to a terminal voltage of 10.5 v, recognizing that some loss of battery life may occur.

## 3.5 Charge Controller

A charge controller shall be employed to coordinate energy flow between the solar panels, the batteries, and the electrical loads. A Flexmax 60 controller shall be used. The controller shall be capable of supplying 80 amps of direct current continuously at ambient temperatures of at least 40°C. The controller shall support nominal battery voltages of 12, 24, 36, 48, and 60 volts DC. The controller shall have the ability to accumulate, or log, at least 120 days of operating data and shall be equipped with an RJ45 modular connector to facilitate interrogation. The controller shall draw no more than 1 watt for its internal operation.

## 3.6 DC System Voltage

The SRB system shall employ a primary DC bus voltage of 36 v nominally. In this instance, the term "primary" denotes the "high side" of a two-voltage system. This arrangement requires that batteries be connected with three in series. Increasing the number of batteries beyond three is unacceptable due to uneven cell charging and loss of battery life that may result.

## 3.7 DC to DC Converter

A DC-to-DC Converter shall be employed to convert the primary DC bus voltage of 36 v to a "secondary" bus voltage of 12.5 v. The term "secondary" denotes the "low side" of a two-voltage

system, which is the voltage at which all loads on the SRB system platform will be served. The Converter shall regulate the secondary voltage within a tolerance of ± 0.2 vdc. A Samlex IDC-200C-12 Converter shall be used.

3.8 Equipment Enclosures

Enclosures used for the solar panel combiner box and the charge controller with associated equipment shall be NEMA Type 4X.

## 4. SRB Control System

4.1 Control System Energy Requirement

Minimization of energy consumption is a key requirement for all systems comprising the SRB system. The control system shall be designed to perform all specified functions with the least amount of electrical energy usage.

The annual energy consumption for all non-pumping SRB system loads shall be limited to 150 kWh. Affected loads include: a) the on-board data logger; b) all sensors and wireless transceivers; c) the cellular communications equipment; and d) a DC-to-AC inverter in stand-by mode.

4.2 Status, Analog, and Alarm Points

The control system shall monitor the following points in each SRB system subsystem:

4.2.1 Energy Supply

This subsystem consists of the solar PV panels, batteries, charge controller, and DC/DC converter. Alarms shall be generated by the control system for any values tagged with an ABNORMAL quality code. All alarms shall be time- and date-stamped when first reported. A point that changes from ABNORMAL to NORMAL shall also result in the issuance of an alarm (time- and date-stamped) that indicates that the point has returned to its normal state. All times shall be reported in Universal Time Coordinated (UTC).

4.2.1.2 Charge Controller Points

Status

The control system shall report the functional status of the charge controller, consistent with available outputs on the unit, to indicate either an ON or OFF status.

Analog

The control system shall monitor the PV +/- and BAT +/- analog values at the charge controller terminal strip.

Alarms

The control system shall use the presence or absence of voltage at the PV and BAT terminals to indicate ENERGIZED or DEENERGIZED states for these terminal points. The control system

shall also return the analog values measured at these terminals, as indicated above, with a NORMAL quality code tagged to values within ±10% of nominal, and an ABNORNAL quality code tagged to values outside of this range.

Data

The control system shall interface with the charge controller through the Flexmax Hub Mate RJ45 interface to allow for interrogation of a variety of status, analog, and historic operating values.

4.2.1.3 DC/DC Converter Points

Status

The control system shall report the functional status of the DC/DC converter, consistent with available outputs on the unit, to indicate either an ON or OFF status.

Analog

The control system shall monitor the output voltage of the converter at its outpu, and report the analog value as requested.

Alarms

The control system shall use the presence or absence of voltage at the Converter's low-voltage terminals as an ENERGIZED/DEENGERGIZED alarm. Also, the control system shall use this voltage to indicate NORMAL operation (voltage between 12.0 and 13.0 vdc) or ABNORMAL (for voltages outside of the NORMAL range).

4.2.2 Ancillary Raft Electronics

4.2.2.1 Data Logger

Status

The control system shall report the functional status of the data logger, consistent with available outputs on the data logger, to indicate either an ON or OFF status.

Data

The control system shall interface with the charge controller to allow for interrogation of a variety of status, analog, and historic operating values.

4.2.2.2 GPS Unit

Status

The control system shall report the functional status of the GPS Unit, consistent with available outputs on the unit, to indicate either an ON or OFF status.

Data

The control system shall interconnect with an on-board GPS receiver and shall ingest the following data from the GPS unit: latitude, longitude, date, and time. The GPS shall be configured to report time in Universal Time Coordinated (UTC). The primary purpose of the GPS unit is to facilitate accurate time stamping of alarms and control actions.

4.2.2.3 Cellular Phone Transceiver

Status

The control system shall report the functional status of the Cellular Transceiver, consistent with available outputs on the unit, to indicate either an ON or OFF status.

4.2.2.4 Pyranometer (optional)

Analog

The control system shall monitor the output voltage of the pyranometer at its output and report the analog value as requested.

4.2.2.5 Weather Station (optional)

Status

The control system shall report the functional status of the Weather Station, consistent with available outputs on the unit, to indicate either an ON or OFF status.

Data

The control system shall interface with the weather station and ingest the following quantities: wind direction, wind speed, air temperature, humidity, barometric pressure, and precipitation. The control system shall also allow interrogation of any historic operating data stored within the weather station.

4.2.2.6 Pit Lake/Stream Water Temperature (optional)

Data

The control system shall interface with a submersed digital thermometer and ingest the temperature value.

4.2.3 Effluent/Influent Hydraulic System

The control system shall monitor the status of hydraulic flows within the SRB system. The objectives of such monitoring are: 1) sensing flow rates to assess treatment adequacy; 2) sensing flow rates to determine if hydraulic lines are abnormally constricted; and 3) sensing flow rates to assist in SRB system start-up and shut-down sequences.

Analog

The following flow rate analog points shall be monitored:

4.2.3.1 Influent Pump Output

4.2.3.1 Effluent Pump Output

Alarms

For each pump monitored in Section 4.2.3, the control system shall use an algorithm that compares: 1) power or current input to pump, to 2) flow rate exiting pump. Such comparison shall be for the purpose of determining whether a "locked rotor"-type situation exists, indicative of a plugged or constricted hydraulic line. The control system shall provide configurable ranges for the input power-to-flow output ratio, indicative of either NORMAL flow rates or ABNORMAL flow rates.

4.3 Control Points

The control system shall be capable of controlling each of the following specified systems and subsystems in the SRB design. The type of control interface shall be consistent with the equipment under control and may include the following: 1) dry relay contacts; 2) 4-20 mA control loop; and 3) digital data transmission to and from equipment.

The following systems and subsystems shall be controllable:

4.3.1 Effluent Pump (if utilized; a gravity/hydraulic pressure system may eliminate this pump)

4.3.2 Influent Pump

4.3.3 Data Logger (reset function)

4.3.4 Weather Station (reset function)

4.4 GPS Unit

The control system shall interconnect with an on-board GPS receiver and shall ingest the following data from the GPS unit: latitude, longitude, date, and time. The GPS shall be configured to report time in Universal Time Coordinated (UTC). The primary purpose of the GPS unit is to facilitate accurate time stamping of monitored data and control events.

4.5 Real-time Concentration and Quality Monitors (optional)

The control system shall interface with any devices that monitor the concentration of sulfides and sulfates at various stages of treatment, as well any devices that monitor water quality parameters at various points such as hardness, pH, and any other parameters as later specified.

4.6 Control System Operational Regimes

The control system shall be capable of operating in three primary operating regimes: system startup, normal operations, and system shutdown.

During the startup regime, the control system shall be configured to verify proper operational status of all devices before taking further action. Once such verification is established, the control system shall properly sequence the energization of pumps and activation of valves to ensure an orderly startup.

During the shutdown regime, the control system shall properly sequence the de-energization of pumps and activation of valves to ensure that the treatment system returns to a state capable of restarting. Shutdown shall initiate either: 1) by command received from operators at a remote location; or 2) as a result of the control system at the treatment site taking action in response to a major alarm at the treatment site.

## 5. Human-Machine Interface (HMI)

The control system shall include an HMI consisting of the equipment and software necessary to allow human operators, at a location distant from the SRB system site and presumably in a control center, to monitor and control the SRB system. The HMI screens or pages shall allow operators to use cursor and mouse control to interface with the SRB Control System. The HMI shall include the following types of screens or pages:

### 5.1 One-line Diagrams

The HMI shall present several one-line diagrams to the operator, displayed uniquely on dedicated monitors or in a multiple-page format on a single monitor. The following one-line diagrams shall be provided, at a minimum:

#### 5.1.1 SRB Treatment System One-line

This diagram shall depict the treatment process including influent and effluent flow rates, volume remaining of SRB treatment chemicals as well as percentage remaining, concentrations of sulfide and sulfate at various stages, flow rates, status of precipitation tank, and any other such quantities necessary to monitor the operation of the System.

This diagram shall also depict the operational status of all pumps, valves, and gates.

Each device depicted on this one-line shall have a data set displayed adjacent to the device that indicates the operational status in a color-coded manner, to indicate whether or not the device is in its NORMAL or ABNORMAL state. The adjacent data set shall also indicate if communication with the point is intact. The status shall flash if any aspect of the device's operation is out-of-limits.

The HMI shall allow the operator to select the device with a right-mouse-click to display detailed information about the device such as make and model number, ratings, date of installation, and history of alarms and maintenance.

The HMI shall allow the operator to select a controllable device with a right-mouse-click to display a control action window that allows the operator to stop or start the device, to vary its output or input, or to change the limits of its NORMAL and ABNORMAL limit ranges.

5.1.2 SRB system Energy Supply One-line Diagram

This diagram shall depict the entire energy supply system, with real-time operating data, that includes the operational status of solar panels, charge controller, DC/DC converter, batteries, and any other related devices. The one-line shall depict the voltage and current generated by each photovoltaic solar panel in the array of panels, the output voltage of the charge controller, the state of charge controller (e.g., equalize, float, trickle), the output voltage of the DC/DC converter, and the terminal voltage of each battery.

Each device depicted on this one-line shall have a data set displayed adjacent to the device that indicates the operational status in a color-coded manner, to indicate whether or not the device is in its NORMAL or ABNORMAL state. The adjacent data set shall also indicate if communication with the point is intact. The status shall flash if any aspect of the device's operation is out-of-limits.

The HMI shall allow the operator to select the device with a right-mouse-click to display detailed information about the device, such as make and model number, ratings, date of installation, and history of alarms and maintenance.

The HMI shall allow the operator to change the low-voltage disconnect (LVD) setpoint within the charge controller. The HMI shall allow the operator to change the limits of any device's NORMAL and ABNORMAL limit ranges.

This diagram shall display the calculated angle of solar radiation to the solar panel array's normal vector as well as the intensity of solar insolation in watts per square meter. The diagram shall display a calculated ratio of expected solar insolation (using the radiation angle-to-normal vector value) to actual solar insolation (using solar panel efficiency, temperature correction factors, and measured panel voltage and current) to determine if the solar panel glass cover requires maintenance.

5.1.3 SRB System Ancillary Equipment One-line Diagram

This diagram shall depict the operational status of all other equipment at the SRB system site that is not part of the treatment system or energy supply system, such as the weather station.

Each device depicted on this one-line shall have a data set displayed adjacent to the device that indicates the operational status in a color-coded manner, to indicate whether or not the device is in its NORMAL or ABNORMAL state. The adjacent data set shall also indicate if communication with the point is intact. The status shall flash if any aspect of the device's operation is out-of-limits.

The HMI shall allow the operator to select the device with a right-mouse-click to display detailed information about the device such as make and model number, ratings, date of installation, and history of alarms and maintenance.

5.2 Alarm Pages

The HMI shall include one monitor dedicated to system alarms. The display shall be a scrolling-type, with the most recent alarms listed at the top. A single line on a given page shall be dedicated to a

single alarm. Each alarm displayed shall consist of the following parameters: the serial number of the alarm; the date; the time in a HH:MM:SS.SSS format in both local daylight savings time-adjusted time and in UTC; the name of the system from which the alarm originated (e.g., SRB Treatment or Energy Supply); the name of the device in alarm; and the alarm status (e.g., “in alarm” or “returned to normal”).

Alarms shall be issued and displayed for any monitored point that is out-of-limits, and an alarm listed shall also be issued when the device returns to normal.

The alarms database shall be fully searchable by any of the aforementioned parameters.

## 6. Software

The supplier shall provide a functional description of all software applications as well as detailed descriptions of algorithms used within various applications. The supplier shall provide updates to provided software for a period of twenty (20) years.

## 7. Control System Spare Parts

Minimizing outages or failures of the SRB system control system is a primary design objective for the SRB system. Part of the strategy for minimizing such outages is an inventory of spare parts that facilitate the rapid restoration of operational status. The following spare parts shall be provided for the control system:

7.1 Central Monitoring Site

Qty 1 Fully functional workstation with software

Qty 1 Mass storage device; this spare shall be networked with the primary mass storage device and shall receive all updates that the primary storage device receives.

7.2 SRB System Site

The following equipment may be stored either at the treatment site or at a location accessible to the technicians that will be servicing the SRB system site:

Qty 1 Charge Controller

Qty 1 DC/DC Converter

Qty 1 Cellular Radio System with Antenna and Transmission Line

Qty 1 GPS Unit

## 8. Documentation

The supplier shall provide all hardware and software documentation required to operate and maintain the control system. A total of four (4) sets of documentation shall be provided, one of which shall reside at the treatment site.

The supplier shall provide all updates to such documentation for a period of twenty (20) years.

## 9. System Development and Training

The supplier shall provide resources necessary to work cooperatively with the owner/operator of the SRB system during the development of the control and energy systems. The final design shall be a joint design effort. The development project team may consist of representatives from the supplier, owner/operator, academia, and regulatory agencies.

Prior to control system acceptance testing, the supplier shall provide a comprehensive training program for operators and hardware and software engineers of the owner/operator responsible for maintaining the system.

# IV.A. Microbiology Summary

The overarching objectives of the microbiology group were to evaluate and improve sulfate-reducing bioreactor performance by determining the nutrient conditions, physical and geochemical parameters, and microbial communities that would produce optimal sulfate reduction. Experiments using two continuous-flow bench-scale bioreactors reactors provided data for establishing initial conditions in the floating bioreactors, where microbial communities and sulfate-reducing performance were monitored under various nutrients blend and flow rate regimes. Two carbon sources, ethanol ($C_2H_6O$) and lactate ($C_3H_5O_3^-$), were equally effective at supporting sulfate-reducing bacterial communities, which were capable of reducing over 90% of the pit water sulfate during our standard four-day hydraulic retention time (flow rate). SRB populations were sensitive to temperature, and bioreactor performance diminished during the colder winter months, but overall sulfate reduction was consistently greater than 60% throughout the year. Bioreactors were dominated by a diverse anaerobic microbial community that included multiple types of sulfate-reducing bacteria, fermenters, and methanogens. Sulfate-reducing bacteria generally made up to 10 – 30% of the microbial community, with the most abundant genera including *Desulfovibrio*, *Desulfobacter,* and *Desulfobulbus*. Experiments designed to test the effects of hydraulic retention time were inconclusive, probably because the tested bioreactors were relatively new and had yet to reach full activity. However, data from the lab bench-scale bioreactors and data from the field bioreactors suggest that high rates of sulfate reduction are possible at substantially higher flow rates and shorter residence times.

# IV.B. Microbiology

## 1. Bioreactor performance

Data from the full-scale bioreactors showed that the nutrient feed was optimized at a molar C:N:P ratio of 1080:49:1. Two carbon substrates, ethanol ($C_2H_6O$) and lactate ($C_3H_5O_3^-$), as lactic acid ($C_3H_6O_3$) and sodium lactate ($C_3H_5NaO_3$), were tested as microbial food sources. Both Raft A and B were fed ethanol at the start of the experiment and achieved consistently high rates (>80%) of sulfate reduction (Fig. IV-1). Raft B was switched to lactic acid after several months and decreased in conversion efficiency before recovering at about <50%. Subsequent replacement of lactic acid with sodium lactate in Raft B resulted in efficiency rates comparable to the ethanol-fed bioreactors (Fig. IV-1).

**Figure IV-1.** Total dissolved sulfide in bioreactors from Rafts A, B, and C.

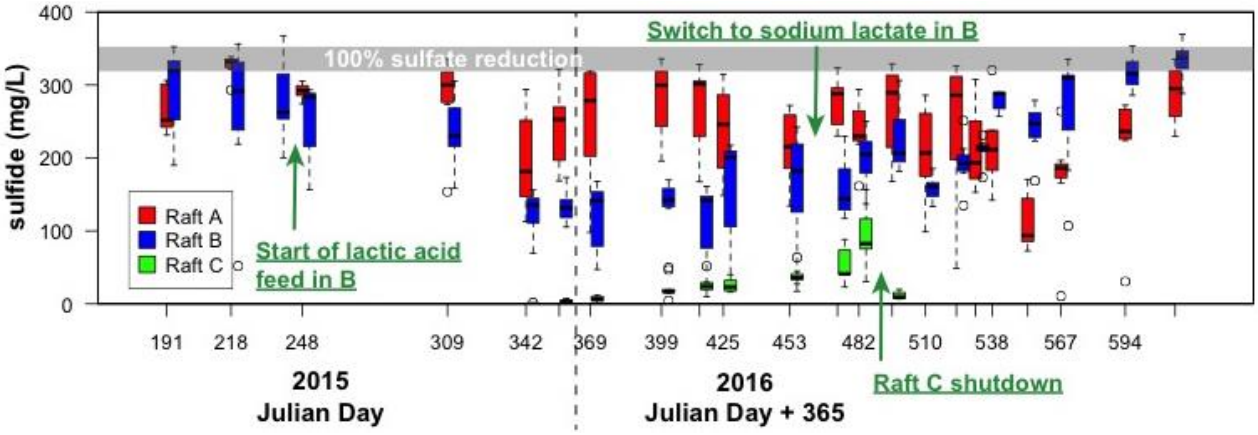


**Fig. IV-1.** Total dissolved sulfide in representative bioreactors over the course of the project. Box and whisker plots showing the range in total dissolved sulfide concentrations in the seven individual reactor module effluents over 14 months (July 9, 2015 to September 7, 2016). In the box and whisker plots, the middle thick line is the median, the box represents the 1st and 3rd quartiles, the whiskers are the outer quartiles, and the circles are outliers (1.5x the interquartile range from the box). The average influent sulfate concentration during this period was 975 mg/L. Raft A was supplied with ethanol throughout the experiment; Raft B was first supplied with ethanol, then switched to lactic acid prior to Julian Day 248, then to sodium lactate prior to Julian Day 473; Raft C started operations on Julian Day 345 and fed with lactic acid, which was ended prior to Julian Day 496. 100% sulfate reduction refers to the complete conversion of influent sulfate to sulfide in the bioreactor. Complete reduction of 975 mg/L sulfate would yield 325 mg/L sulfide, according to the equation [sulfide] = [sulfate] x (32/96) in which 32 and 96 are the molecular weights of sulfide and sulfate, respectively.

## 2. Microbial populations and communities[11]

Total prokaryotic cell numbers, including both sulfate-reducing bacteria (SRB) and non-SRB forms, were fairly uniform over several months of the experiment in water and fiber within the floating bioreactors.

Total Prokaryotic Cell Abundance in Water and Fiber from Bioreactors

Direct microscopic counts of DAPI-stained cells were used to estimate the abundance of prokaryotic cells in flowing bioreactor water and fiber sampled from representative units (Figs. IV-2 – IV-5) at discrete depths using sampling tubes. Prokaryotic cell concentrations in bioreactor water ranged from approximately 0.5 x $10^7$ to 6.1 x $10^8$ cells/ml (Fig. IV-2A). Prokaryote cell densities fluctuated in the warmer months (April through July 2016), particularly in Raft B (sodium lactate substrate), and cell numbers increased rapidly in both Raft A (ethanol substrate) and Raft B between August and September 2016. Raft C water samples contained about half the prokaryote abundance as seen in Rafts A and B samples, most likely because the microbial community was relatively young (inoculated in November 2015), and biofilms had not fully developed. Notably, the spike in Raft B, August 2016, 0.5 m prokaryotic

[11]See Section IV.B.3. Bioreactor Biological Sampling and Analysis Methods for all experimental design, sampling devices, and methods.

cell count corresponded to the development of robust biofilm that formed in the top 0.5 m of these bioreactors during that highly productive period.

**Figure IV-2.** Prokaryotic cell abundance in water and fiber from bioreactors in Rafts A, B, and C.

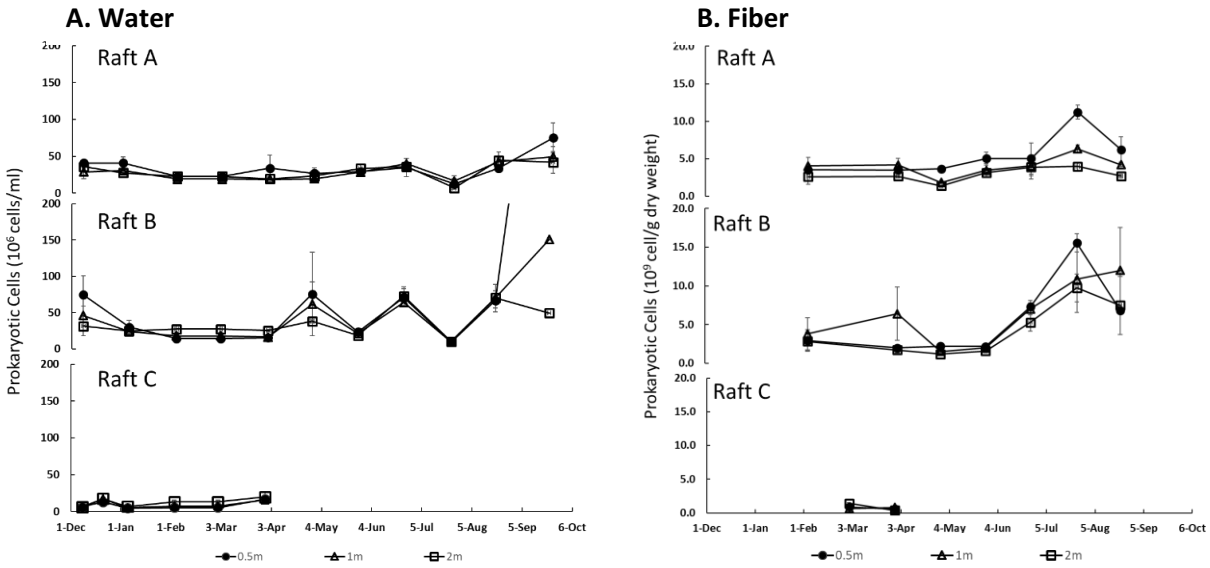


**Fig. 2. A.** Prokaryotic cells in water were counted monthly from December 2015 to September 2016 at three depths (0.5, 1. and 2 m) in replicate bioreactors (n=3) in Rafts A (ethanol substrate), B (lactic acid substrate), and C (lactic acid substrate). The average cell count and standard error are plotted for each depth. The upper panel shows results from Raft A bioreactors, the middle panel, Raft B, and the lower panel, Raft C bioreactors. Water in all bioreactors shown had about a four-day hydraulic retention time. **B.** Bioreactor fibers were collected monthly (February 2016 to August 2016) at three depths (0.5, 1, and 2 m) in replicate bioreactors (n=2) in Rafts A (ethanol substrate), B (lactic acid substrate), and C (lactic acid substrate). Prokaryotic cell count (mean ± standard error) is plotted for each depth. The upper panel shows results from Raft A bioreactors, the middle panel, Raft B, and the lower panel, Raft C. Hydraulic retention time was approximately four days for all bioreactors.

* Raft B, Aug. 2016 water sample = 6 X $10^9$ cells/ml

** Fibers were sampled only twice because Raft C operations were terminated at the end of March 2016.

Microbial growth on the bioreactor fiber matrix was assessed in samples that were collected using devices made from 1" diameter PVC pipes that held fiber-filled mesh bags (see Microbiology Methods) attached at 0.5, 1.0, and 2 meter depths which were inserted vertically into the bioreactor matrix at the start of the experiment and pulled out on the specified sampling dates. Prokaryotic cell concentrations in the bioreactor fiber matrix ranged from approximately 0.4 – 16 x $10^9$ cells/g dry fiber weight (Fig. IV-2B). Fiber from Raft A (ethanol substrate) and Raft B (lactic acid substrate) showed similar cell count trends throughout the sampling period. The cell numbers on fiber from Rafts A and B were relatively low and stable until June and July 2016, when counts increased substantially. Note that only two fiber samples were taken from each Raft C bioreactor before sampling of these bioreactors was terminated at the end of March 2016.

Raft C was designed to facilitate tests of hydraulic retention times (HRT; flow rates, but HRT between one and four days appeared to have little effect on prokaryotic cell number in water (Fig. IV-3A) and fiber (Fig. IV-3B). Vertical profiles of prokaryote abundance in water from depths between 0.5 and 3.0 meters also showed little variation with substrate or hydraulic retention time (Figs. IV-4A and IV-B). Cell counts generally ranged between 1-3 X $10^7$ cells/ml, with the exception of one sample (Bioreactor B2 at 3 m depth, ethanol substrate), that had counts over 10-fold higher than that average. Whether this is an outlier or a genuine proliferation is currently unknown; however, the metabolic performance of Raft B, as indicated by the conversion of sulfate to sulfide, did not reflect a similar departure from normal, suggesting that the high cell count may have been a true outlier.

**Figure IV-3.** Effect of hydraulic retention time on prokaryotic cell abundance in water and fiber.

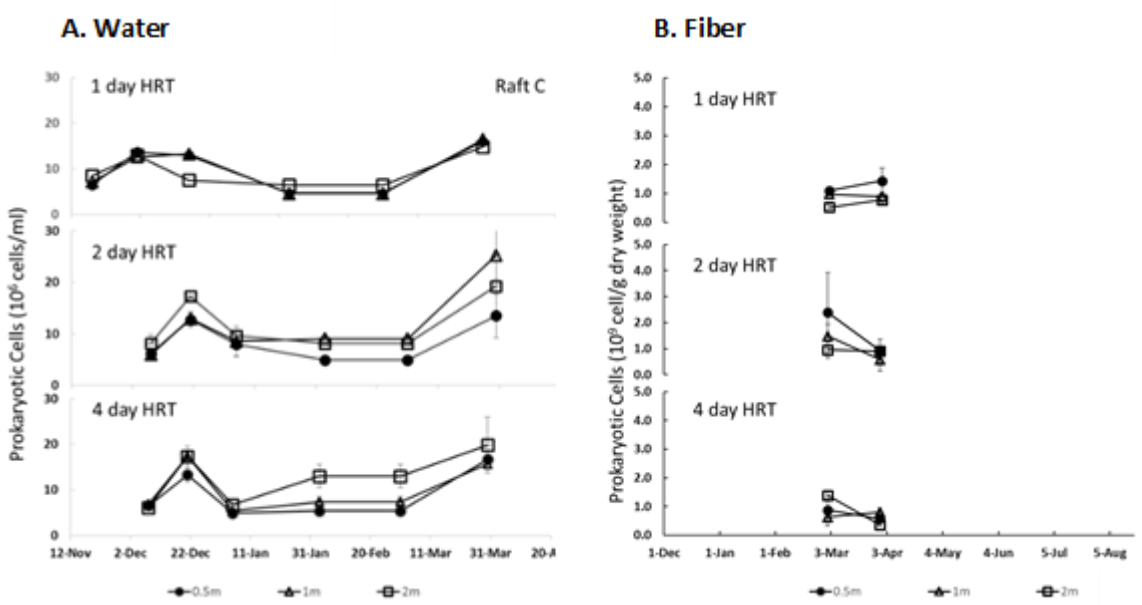


**Figure IV-3. A.** Prokaryotic cell abundance (mean ± standard error) are reported for water from replicate Raft C bioreactors (lactic acid substrate) from December 2015 to March 2016 at three depths (0.5, 1. and 2 m), under three different hydraulic retention time (HRT) regimes (1, 2, and 4 days). Raft C was inoculated five days prior to the first sampling date (Dec 8, 2015). The upper panel shows results for 1-day HRT (n=2 bioreactors; C1 and C7). The middle panel shown results for the 2-day HRT (n=2; C2 and C6). The lower panel shows results for the 4-day HRT (n=3; C3, C4, and C6). **B.** Prokaryotic cell abundance (mean ± standard error) on fibers from Raft C (lactic acid substrate) bioreactors is reported for two sampling events, February and March 2016*, at three depths (0.5, 1. and 2 m) in replicate bioreactors under different HRT regimes. The upper panel shows results for 1-day HRT (n=2 bioreactors; C1 and C7). The middle panel shown results for the 2-day HRT (n=2; C2 and C6). The lower panel shows results for the 4-day HRT (n=2; C4, C5).
*Fibers were sampled only twice because Raft C operations were terminated at the end of March 2016.

**Figure IV-4.** Prokaryotic cell abundance depth profiles in water from bioreactors supplied with different organic substrates.

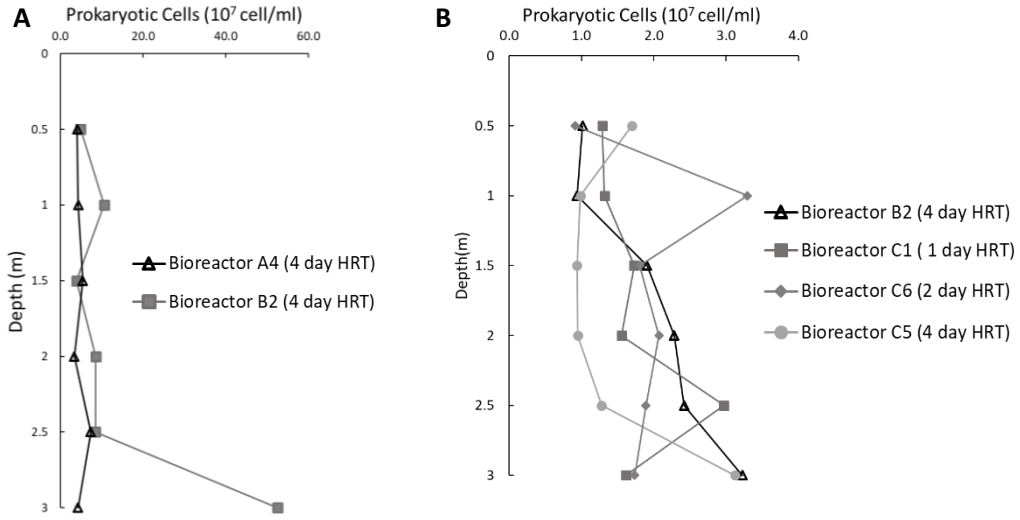


**Fig. IV-4. A.** Vertical profiles of prokaryotic cell abundance in water from bioreactor A4 (ethanol substrate) and B2 (lactic acid substrate) operating on a four-day hydraulic retention time regime. Samples were taken on August 16, 2016. **B.** Vertical profiles of prokaryotic cell abundance in water from bioreactors in Rafts B and C (both lactic acid substrate) operating under a variety of hydraulic retention time regimes. Samples were taken on March 30, 2016.

In the fiber matrix, prokaryotic cells counts decreased with depth in bioreactors from both Rafts A (ethanol substrate) and Raft B (lactic acid substrate) but were consistently higher with the lactate substrate (Fig. IV-5A). Comparisons of the effects of hydraulic retention time on fiber cell counts in bioreactors from Rafts B and C, both using lactic acid as a substrate, were inconsistent. Prokaryotic cell counts decreased slightly with depth on fiber from bioreactors B4 (four-day HRT) and C1 (one-day HRT), while little change with depth was noted in bioreactors C5 (four-day HRT) and C6 (two-day HRT) (Fig. IV-5B).

When prokaryotic cell abundances measured in water or on fiber from all bioreactors, regardless of treatment type, were considered, significant but weak correlations were detected between cell abundance and various physical and chemical parameter measured in bioreactor water (Table IV-1).

**Figure IV-5.** Prokaryotic cell abundance depth profiles on fiber from bioreactors supplied with different organic substrates.

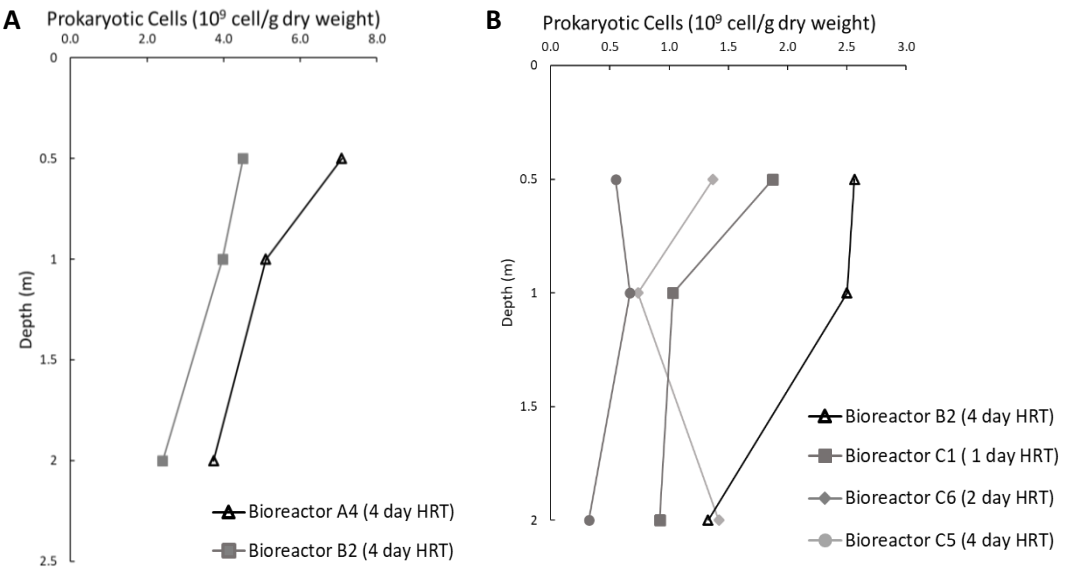


**Fig. IV-5. A.** Vertical profiles of prokaryotic cell abundance on fiber material from bioreactors A4 (ethanol substrate) and B4 (sodium lactate substrate) on August 16, 2016. **B.** Vertical profiles of prokaryotic cell abundances on March 30, 2016 on material from fiber bags in bioreactors fed the lactic acid but with different hydraulic retention times. Representative bioreactors from Raft B (B4; four-day HRT) and Raft C (C1, one-day HRT; C5, four-day HRT; C6, two-day HRT) were sampled for a comparison of fiber cell abundance.

**Table IV-1.** Adjusted R-squared values for correlations between prokaryotic counts in water or fiber from all bioreactors regardless of treatment type and various physical and chemical parameters measured in the water of all bioreactors. All correlations were weak but significant (all p's <0.05, N's >60).

| Sample Type | Temp | pH | ORP | $H_2S$ | $SO_4$ |
|---|---|---|---|---|---|
| **Water** | 0.098 | 0.016 | 0.078 | 0.080 | 0.108 |
| **Fiber** | 0.087 | 0.108 | 0.136 | 0.123 | 0.226 |

Sulfate-Reducing Bacterial Abundances in Bioreactor Water and Fiber

Sulfate-reducing bacteria (SRB) abundance was estimated by measuring the concentration of the diagnostic gene *dsr*A (dissimilatory sulfite reductase) in water and fiber samples taken from different depths of selected bioreactors using quantitative polymerase chain reaction (qPCR). Provisional results on *dsrA* gene abundance are presented in this report.

An evaluation of the vertical distribution of *dsr*A gene concentrations in water from two Raft A bioreactors (ethanol substrate) revealed different SRB population densities are various depths (Fig. IV-6A and IV-6B), as well as expected seasonal changes (Fig. IV-6A, IV-6B, and IV-6C). These data indicate that SRB abundance typically increased during the spring and summer when bioreactor water

temperatures increased. Further comparisons of *dsr*A gene concentrations in bioreactors from Raft A (ethanol substrate) and Raft B (lactic acid substrate) indicated that SRB populations were stable or increasing over time (Fig. IV-7), as the microbial communities reacted to changing environmental conditions. SRB abundances ranged from approximately 0.5 to 4 x $10^6$ dsrA gene copies/ml water in bioreactors in both treatments. SRB abundance increased slightly with depth in Raft B bioreactors but not in Raft A bioreactors.

Raft C was designed to facilitate within-raft comparisons of hydraulic retention time. Figure IV-8 displays *dsr*A abundance data from such a test, using multiple bioreactors under one-, two-, and four-day HRT regimes. SRB abundance ranged from near zero to 0.4 x $10^6$ *dsr*A gene copies/ml water in Raft C bioreactors over a four-month period, starting from the point of inoculation. These relatively low abundance figures, less than half those typical from Raft A and B, were not unexpected considering that Raft C was relatively new, so biofilm had probably not developed into the robust form seen in Rafts A and B, which were inoculated approximately 1.5 years before the start of this experiment. When Raft C was shut down at the end of March 2015, there were no apparent differences in SRB abundances with depth or HRT.

Bacterial Diversity in Bioreactor Water and Fiber Samples

16S rRNA gene sequencing of bioreactor water and fiber samples allowed us to synthesize the microbial data in the context of nutrient feeding and sulfur geochemistry, resulting in a recommendation for the nutrient feed and microbial community composition (both in terms of sulfate reducer biomass and different sulfate-reducing bacterial groups) to achieve the highest sulfate reduction rate.

The reactors were populated by diverse communities that contain sulfate reducers, methanogens, and fermenters. The most abundant microbial taxa in the libraries are likely fermenters. Notably, the genus *Pelosinus* were especially abundant in the lactate-fed Rafts B and C (sometimes >50% of sequences) and the genus *Alkalibacter* was especially abundant in the ethanol-fed Raft A (sometimes >50% of sequences). Sulfate reducers were generally between 10 – 30% of the libraries and methanogens were between 0 – 5% (Fig. IV-9). Major families of sulfate reducers in the reactors include *Desulfobacteraceae, Desulfobulbulbaceae, Desulfovibrioceae*, and *Desulfomicrobiaceae*. Sulfur-oxidizing bacteria occurred in the reactors, especially near the surface of Raft B and in Raft C (Fig. IV-9). The abundance of sulfur-oxidizing populations in Raft C (between 10 – 30% of sequences) was likely caused by the slow sulfate reduction (Fig. IV-10) in this raft, which allowed micro-oxic conditions or other oxidants to persist at depth.

Overall, sulfate reducers abundance changed little with depth, but we did observe trends in specific groups of sulfate-reducing bacteria (Fig IV-10). In Raft A, “complete oxidizers” in the family *Desulfobacteraceae* that use acetate as a substrate increased with depth. In contrast, *Desulfobulbaceae*, which are likely “incomplete oxidizers” that oxidize lactate or ethanol to acetate, were most abundant at the surface. These observations are consistent with a two-step ethanol or lactate oxidation process, although we note that other families that are typically associated with incomplete oxidation increased in abundance at depth, or show little trend.

**Figure IV-6.** Sulfate-reducing bacteria abundance in water from Raft A bioreactors during 2014-2015.

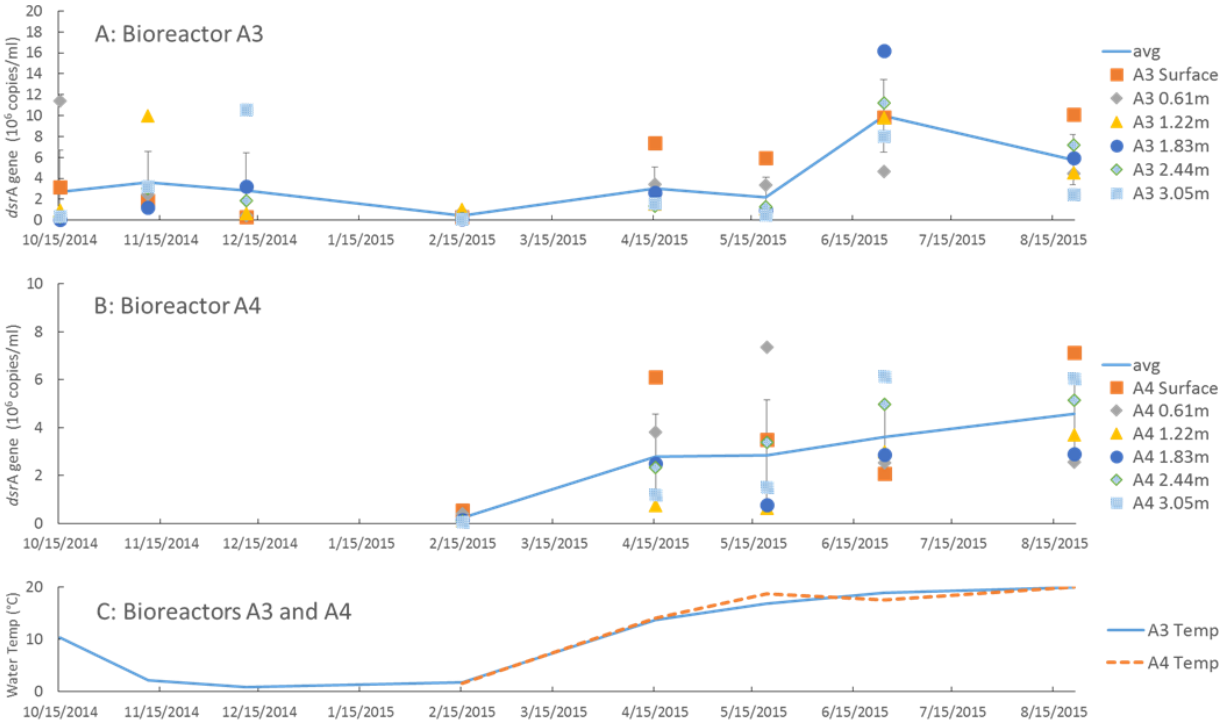


**Fig. IV-6.** Dissimilatory sulfite reductase (*dsr*A) gene concentrations were used to estimate the abundance of sulfate-reducing bacteria in water in bioreactors A3 and A4 from Raft A (both ethanol substrate) from October 2014 to August 2015. Concentration data are shown for each depth sampled (surface to 3.05 m) in these bioreactors and the average *dsr*A abundance for all depths is plotted as a line. Panels A and B show *dsr*A gene copy numbers in water collected from the surface to 3.05 m in bioreactors A3 and A4. Panel C shows the average water temperature throughout each bioreactor (average of temperature measurements at six depths).

**Figure IV-7.** Sulfate-reducing bacteria abundance in water from bioreactors in Rafts A and B during 2016.

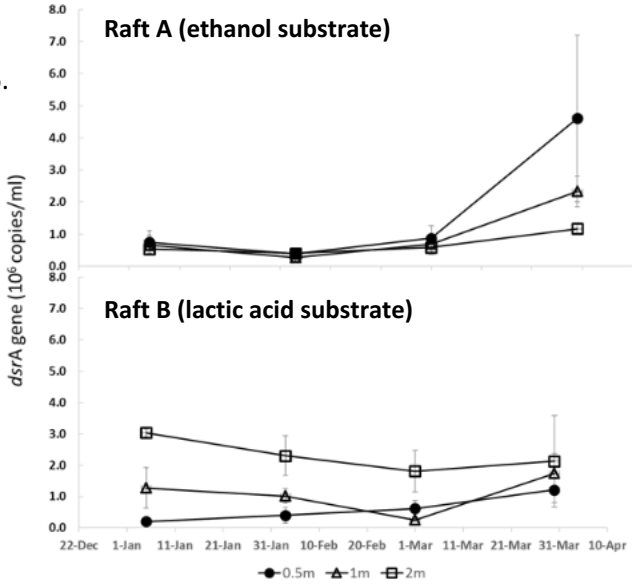


**Fig. IV-7.** The abundance of the dissimilatory sulfite reductase (*dsr*A) gene was measured in water to estimate SRB abundance from early January to late March 2016 at three depths (0.5, 1, and 2 m) in replicate bioreactors within Raft A (ethanol substrate; upper panel) and Raft B (lactic acid substrate; lower panel). Mean values for replicate measurements are plotted with standard errors. Both Rafts A and B had approximately four-day hydraulic retention times.

**Figure IV-8.** Sulfate-reducing bacteria abundance in water from Raft C bioreactors with different hydraulic retention times.

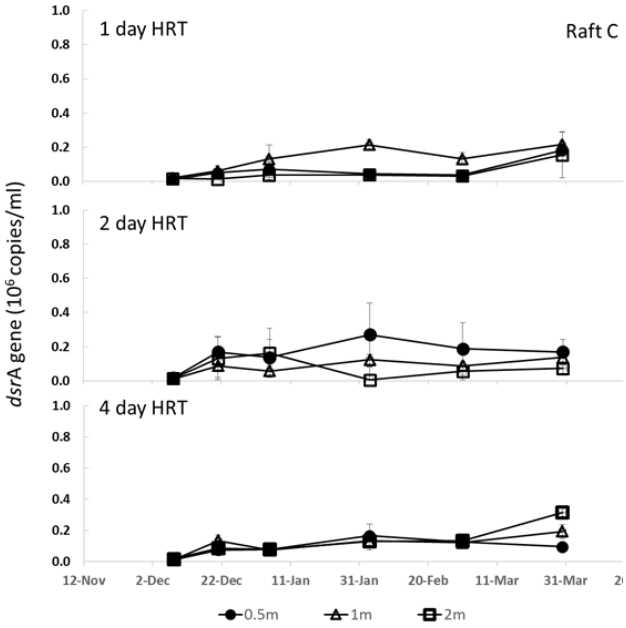


**Fig. IV-8.** The abundance of the dissimilatory sulfite reductase (dsrA) gene was measured in water from early December 2015 to late March 2016 at three depths (0.5, 1, and 2 m) in replicate bioreactors within Raft C (lactic acid substrate). Mean values for replicate measurements are plotted with standard errors. Raft C was inoculated five days prior to the first sampling date (Dec 8, 2015). Different bioreactors had different hydraulic retention times (HRT) of one, two, and four days. The upper panel shows results for 1-day HRT (n=2; C1 and C7). The middle panel shown results for the 2-day HRT (n=2; C2 and C6). The lower panel shows results for the four-day HRT (n=3; C3, C4, and C6).

**Figure IV-9.** Trends in sulfate-reducing, sulfur-oxidizing, and methanogens with depth in Rafts A, B, and C.

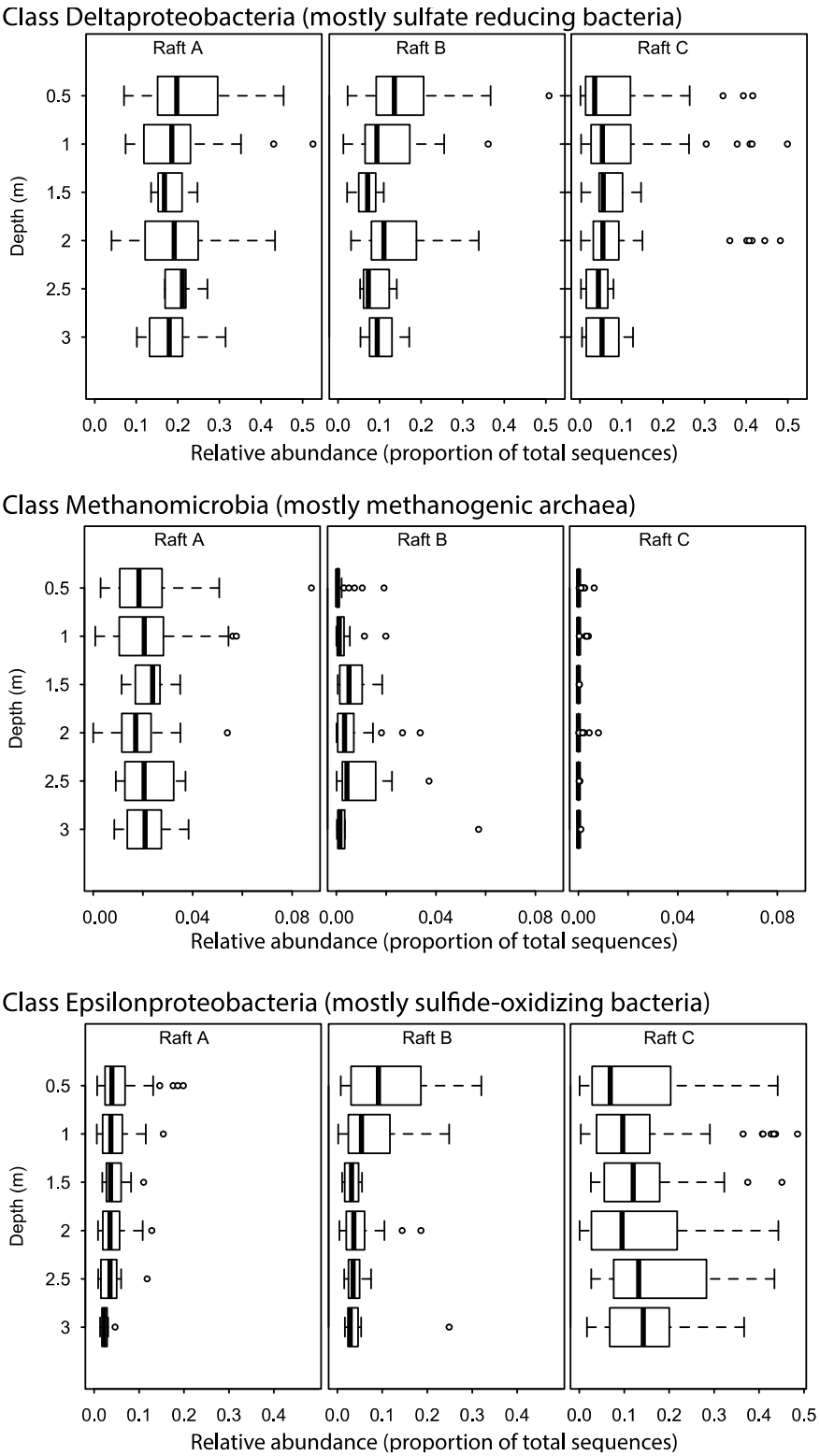


**Fig. IV-9.** Trends in sulfate-reducing bacteria (class *Deltaproteobacteria*), sulfur-oxidizing bacteria (class *Epsilonproteobacteria*), and methanogens (class *Methanomicrobia*) with depth in Rafts A, B, and C.

**Figure IV-10.** Depth profiles of abundant families of sulfate-reducing bacteria in Rafts A and B.

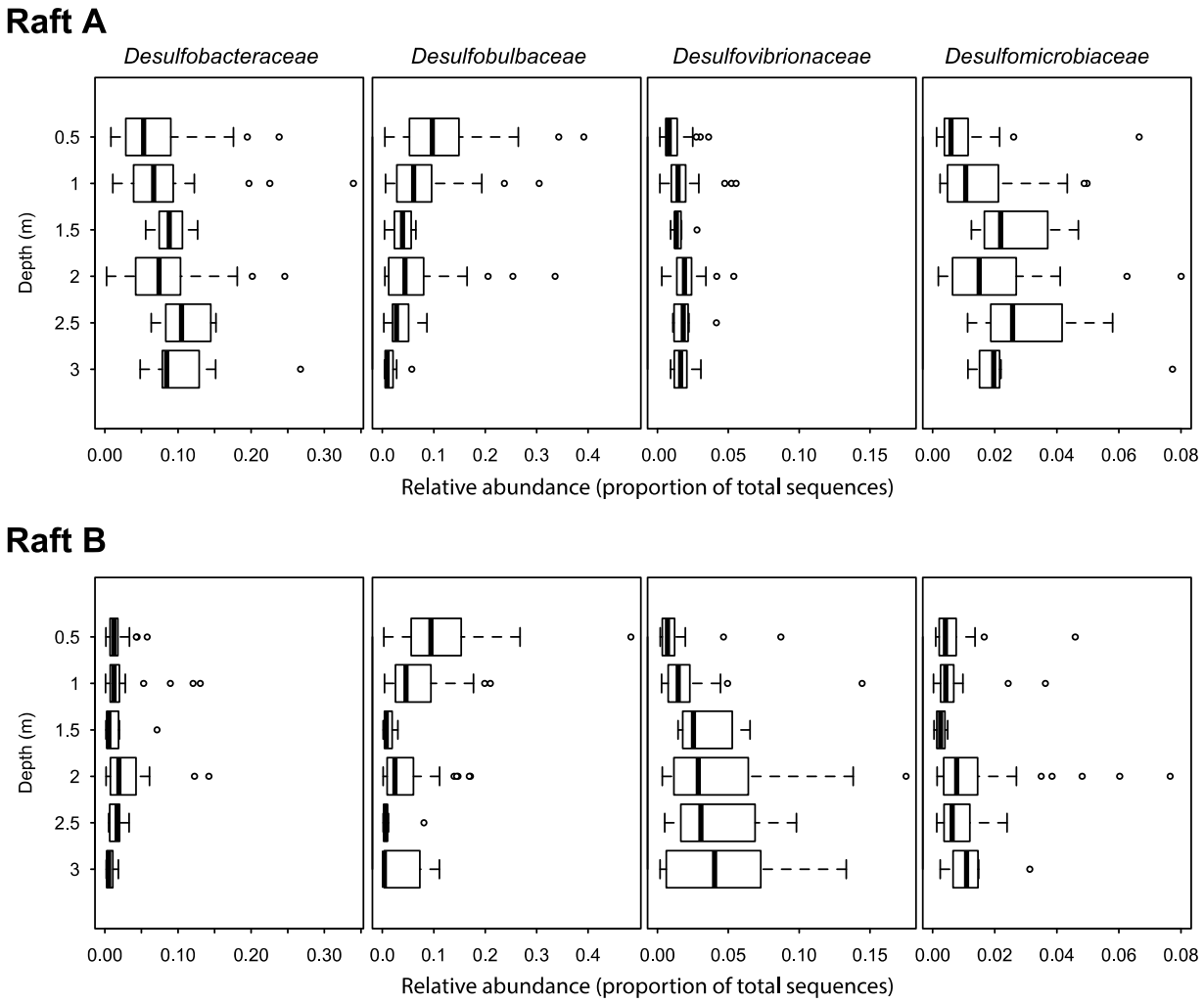


**Fig. IV-10.** Depth profiles of abundant families of sulfate-reducing bacteria in Rafts A and B. Most members of family *Desulfobacteraceae* are "complete oxidizers" that use acetate as a substrate and oxidize it completely, while families *Desulfobulbaceae*, *Desulfovibrionaceae*, and *Desulfomicrobiaceae* are primarily "incomplete oxidizers" that oxidize more complex organic carbon substrates (like ethanol and lactate) to acetate. Note that communities of sulfate-reducing bacteria in ethanol- versus lactate-fed rafts are reflected in differences at the family level. Box and whiskers descriptions as in Fig. IV-1.

Microbial communities in Rafts A, B, and C could be separated by non-metric multidimensional scaling (NMS) ordination analyses based a progression over time and the type of organic feed source (Fig. IV-11A and IV-11B). Microbial assemblages of water and fiber bag samples showed similarities but were not identical (Fig. IV-12A and IV-12B). Overall, fiber-associated communities corresponded slightly stronger to high sulfate reduction rates than planktonic communities. When reactors were performing best in terms of total sulfate reduction, they were populated by diverse communities that contained specific methanogens and fermenters. Those communities, however, were likely taking advantage of low sulfate conditions in most of the reactor to ferment lactate, oxidize acetate, and use other residual organic substrates, and probably did not contribute to reactor performance. Despite differences in families of sulfate reducers among the two Rafts (Fig. IV-10), the sulfate-reducing populations that were specifically associated with optimal reactor performance were often members of the *Desulfobulbaceae*, although additional work will be required to confirm that association. It seems noteworthy, however, that *Desulfobulbaceae* were also the most abundant group of sulfate reducers in the laboratory reactors that were achieving more than 90% sulfate reduction with short residence times.

**Figure IV-11.** Non-metric multidimensional scaling ordinations of all water and fiber bag samples.

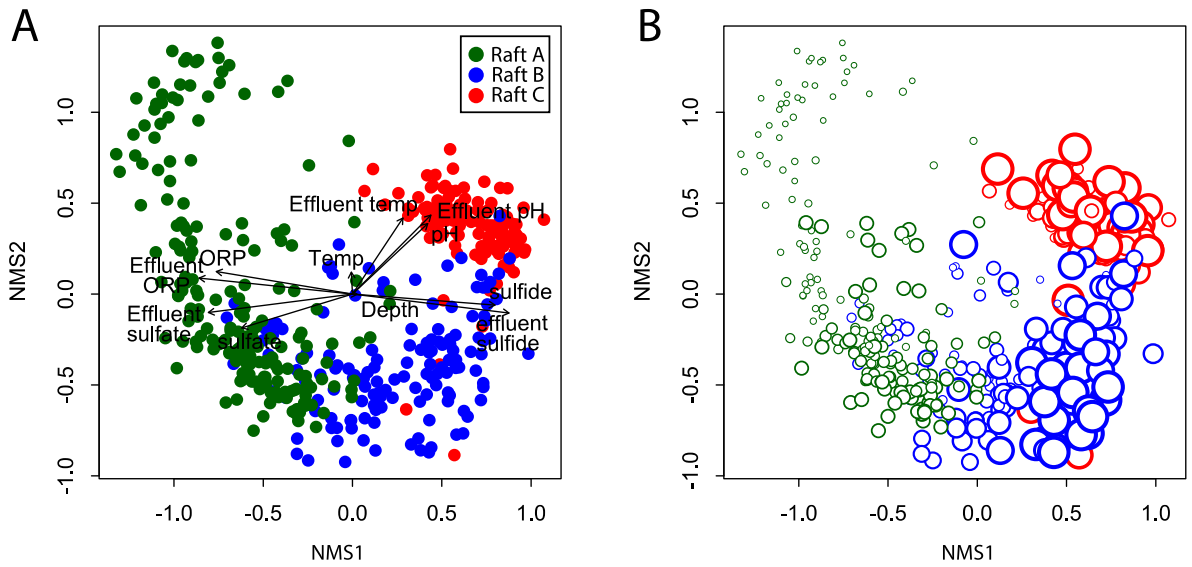


**Fig. IV-11.** Non-metric multidimensional scaling (NMS) ordinations of all water and fiber bag samples. Points are colored by raft. The environmental overlay in ordination (A) shows that major geochemical variables trend with the first ordination axis. All variables are significantly correlated with the ordination axes ($p < 0.001$), except for depth and temperature. Effluent variables are from the bioreactor effluents and other variables are from the same depth as the sample (for example, "sulfide" is the concentration of sulfide from which the sample was collected, while "effluent sulfide" is the sulfide concentration from the effluent for that bioreactor at the time the sample was collected). The ordination in (B) contains the same data as in panel (A), except that points are scaled by time so that earlier samples are smaller circles and later samples are larger circles. With time, communities in Raft C appear to converge toward those in Raft B (but note that Raft B ran for several months longer than Raft C). Communities in Raft A were similar over the year of sampling. The first NMS axis appears to correspond to community progression during reactor startup, and the second axis corresponds with differences between lactate and ethanol feeds.

**Figure IV-12.** Microbial assemblages of water and fiber bag samples, Rafts A and B.

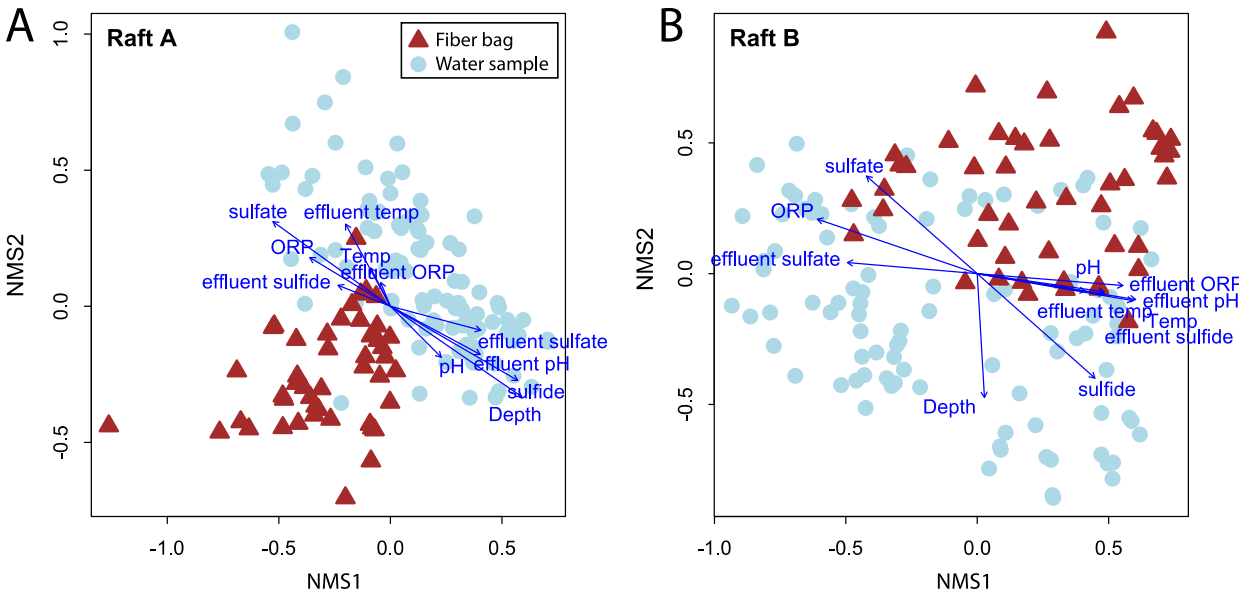


**Fig. IV-12.** Non-metric multidimensional scaling ordinations of samples from Raft A (panel A) and Raft B (panel B), with environmental overlays of the geochemical variables described in Figure IV-11 and points colored to indicate libraries from fiber bag versus water samples.

**Figure IV-12.** Microbial assemblages of water and fiber bag samples, Rafts C.

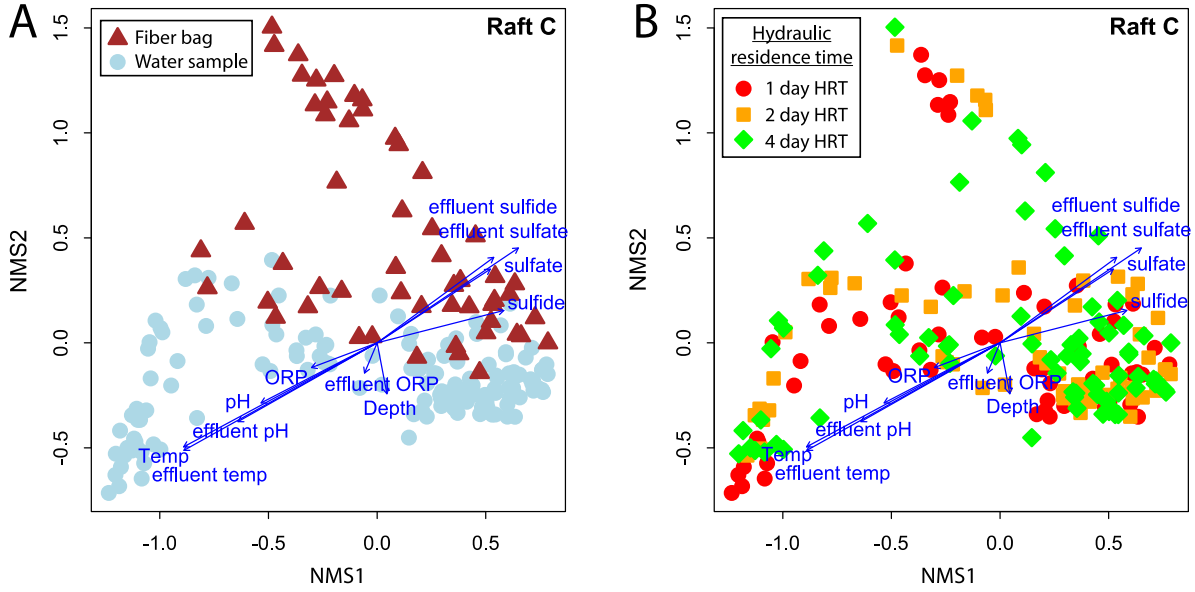


**Fig. IV-13.** Non-metric multidimensional scaling ordinations of samples from Raft C, with environmental overlays of the geochemical variables described in Figure IV-11. The data in the ordinations in (A) and (B) are equivalent, with points in (A) colored to indicate libraries from fiber bag versus water samples and points in (B) are colored to indicate libraries from reactor modules with different hydraulic residence times. Hydraulic residence time does not appear to have had a substantial impact on microbial community structure while this raft was running.

Insights from laboratory bioreactors

Experiments performed with the bench-scale bioreactors showed that a continuously fed sodium lactate blend (pH 7.5 – 8) can achieve >90% sulfate reduction with 36 hours residence time. It seems likely that residence time in the system could be substantially decreased to reduce more sulfate per unit time. Experimentally manipulating residence time bench-scale bioreactors indicated that even shorter residence times of 18 hours may lead to enhanced sulfate reduction (greater than 1.5x higher sulfate reduced per unit time). Indeed, dissolved sulfide and sulfate profiles in the field bioreactors suggest that most of the reduction happens in the top meter (Fig. IV-15), confirming that residence time might be shortened in a full-scale system.

The prevalence of fermentative and methanogenic populations further indicates that sulfate reduction is not optimized in the system and that shortening residence time or adjusting feed ratios might better select for sulfate reducers and/or more sulfate reducer biomass. Moreover, changes in feed concentration in the bench-scale bioreactors showed that the microbial communities are resilient and recover quickly as indicated by high sulfate reduction rates (Fig. IV-14A). During low-feed conditions, the laboratory bioreactors became micro-oxic, promoting the growth of *Pseudomonas* and *Polaromonas* species.

After re-establishment of the original feed, the community shifted back to be dominated by sulfate reducers, in particular *Desulfobulbaceae*. Interestingly, sulfate-reducing populations represented a larger portion of the community in the laboratory reactors that operated on shorter residence times. Residence time experiments in the floating bioreactors were inconclusive because the microbial communities in Raft C bioreactors had not yet been fully established before shutdown of this raft, but the available geochemical and microbial data do not suggest that shorter residence times were detrimental to performance (Figs. IV-1, IV-3B, IV-4B, IV-5B, IV-8, and IV-13). In the laboratory reactors, the communities in the 36- and 18-hour residence time reactors were very similar (Fig. IV-14B).

**Figure IV-14.** Non-metric multidimensional scaling ordinations of bench-scale lab bioreactor samples.

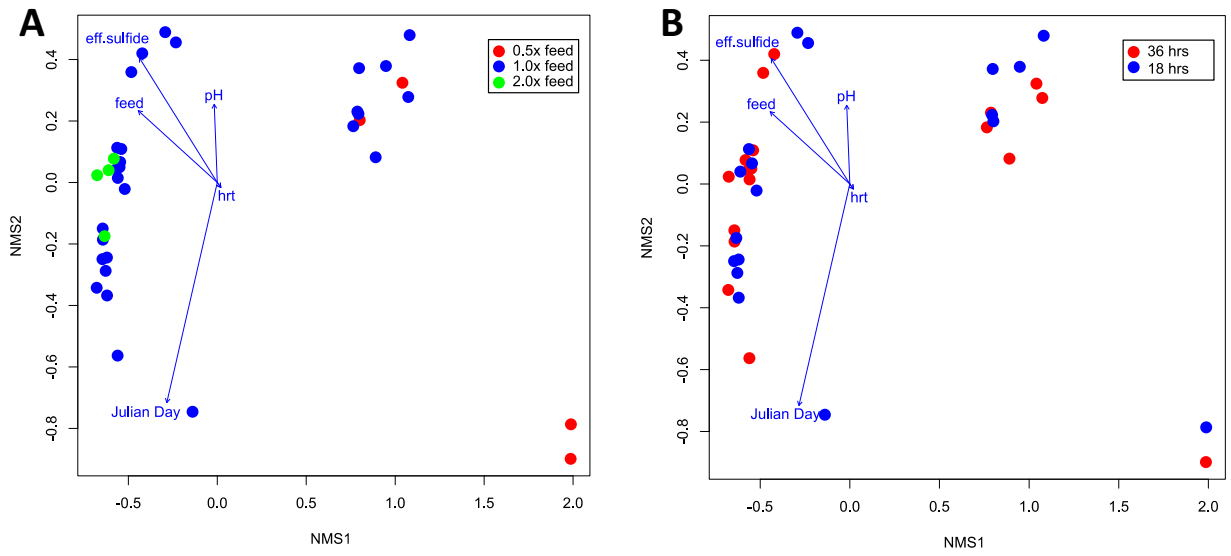


**Fig. IV-14.** Non-metric multidimensional scaling (NMS) ordinations of bench-scale lab bioreactor samples. The environmental overlay shows that major geochemical variables trend with the second ordination axis. In panel A, points are colored by nutrient feed concentration. A higher nutrient load than used for the floating field bioreactors did not result in higher sulfate reduction efficiency. After disturbance with lower feed concentrations, the microbial community recovered quickly. The ordination in panel B contains the same data as in panel A except that colors indicate hydraulic retention times. In general, parallel samples that differed only in hydraulic retention time clustered together, indicating that other variables than hydraulic retention time correspond to most of the variance in the dataset.

**Figure IV-15.** Sulfide concentration by depth in Raft A bioreactors.

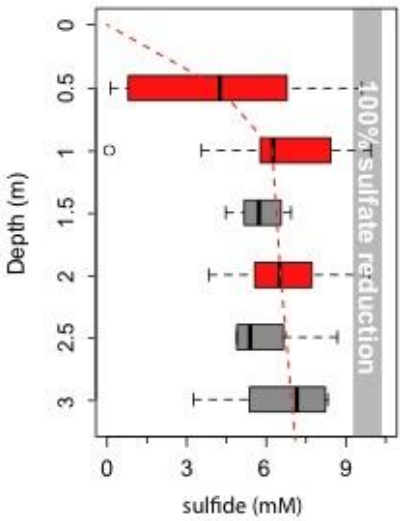


**Fig. IV-15.** Sulfide concentration with depth in Raft A bioreactors. Data from December 2015 to April 2016. Most sulfate reduction occurs in the top 0.5 to 1 meter. Red data are averaged from three bioreactor modules; gray data is from a single module that was sampled at higher depth resolution.

## 3. Bioreactor Biological Sampling and Analysis Methods

### Experimental Design and Treatments

Experimental treatments were devised to evaluate the effects of organic carbon substrates for microbial growth, ethanol and lactate (as lactic acid and sodium lactate), and hydraulic retention time (HRT, flow rate) on the conversion of sulfate in mine pit waters to sulfide in the bioreactors (Table IV-2). Lactate was first added as lactic acid at the beginning of the experiment in December 2015, due to its low freezing point, and continued until it was determined that this form of lactate depressed the bioreactor pH enough to be near the margin of the pH range optimal for sulfate-reducing bacterial (SRB) growth. After April 2016, lactate was added to the bioreactors as sodium lactate. These two organic substrates were chosen based on previous studies of SRB bioreactors (Liamleam and Annachhatre 2007; Muyzer and Stams 2008). Three hydraulic retention times were evaluated: the base rate, four-day HRT, as well as one- and two-day HRTs. Three replicate bioreactors each in Rafts A, B, and C with four-day hydraulic retention times were chosen to evaluate the effect of organic substrate on prokaryotic community abundance and diversity. Bioreactors in Raft C were newly constructed in summer 2016 and inoculated and fed the lactate substrate starting on December 3, 2015, while Raft B bioreactors were constructed and inoculated in summer 2014 and fed ethanol until fall 2015 when they were switched to the lactate organic substrate. The inflow of four additional bioreactors in Raft C were adjusted to yield one- and two-day hydraulic retention times. The duplicated bioreactors with one- and two-day HRT were compared with the triplicate bioreactors in Raft C with four-day HRT to evaluate the influence of hydraulic retention time on sulfate reduction rates as well as microbial community abundance and diversity.

**Table IV-2.** Experimental treatments in bioreactors on different rafts.

| Raft | Organic Substrate | Hydraulic Retention Time (days) | Number of Replicate Bioreactors |
|---|---|---|---|
| A | Ethanol | 4 | 3 |
| B | Lactate | 4 | 3 |
| C | Lactate | 4 | 3 |
| C | Lactate | 2 | 2 |
| C | Lactate | 1 | 2 |

### Water and Fiber Sampling Devices

Unique water- and fiber-sampling devices were constructed for these experiments. Water samplers consisted of three or six ½" PVC pipes cut to lengths appropriate for sampling bioreactor water at depths of 0.5, 1, 1.5, 2, 2.5, and 3 m. One replicate bioreactor in each raft was fitted with a full profile sampler, while the remaining replicates were fitted with partial profile samplers consisting of 0.5, 1, and 2 m pipes (Fig. IV-16). The PVC pipes were secured in a PVC plate at the bioreactor surface, where they were inserted into push-in fittings to ensure a tight seal during sampling. Sampling was conducted using an electric water pump to draw water through the appropriate pipe into sample bottles.

**Figure IV-16.** Bioreactor water sampling device.

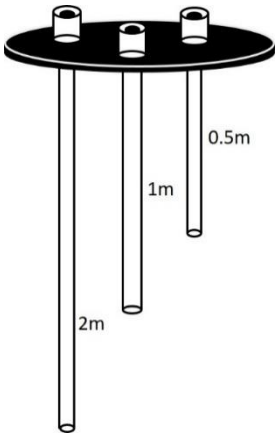


**Fig. 16.** Water sampling device developed for experiment. A similar device was installed in bioreactors where full water profiles were samples, but those sampling devices included three extra sampling tubes of 1.5-, 2.5-, and 3-meter lengths.

Bioreactor matrix fibers were sampled using collection devices built from ½" PVC pipes that were capped at both ends to prevent creation of a preferential flow path. Holes were drilled completely through the pipes at appropriate depths to sample at 0.5, 1, and 2 m. Fiber bags were constructed from lengths of Drain-Sleeve® fabric (Carriff Engineered Fabrics, North Carolina) that were pulled through the hole in the PVC pipe and were filled with the shredded polypropylene fiber material used for the bioreactor matrix (Fig. IV-17). The drain sleeve material was cut long enough to hold a golf ball sized (~ 7.62 x 7.62 cm) portion of fiber to create fiber bags that were attached at each depth on the PVC holder pipe. The fiber bags were secured to the pipe by placing cable ties around the fabric on both sides of the pipe. After the bag was filled with fiber, the open end was also closed using a cable tie (Fig. IV-17).

Fiber bag sampling pipes were installed in two of the three replicate bioreactors of each experimental treatment, with eight fiber sampling pipes in each bioreactor. Both the water and fiber bag sampling devices were tied to the opening of the bioreactor using synthetic rope for additional security.

## Water and Fiber Sampling Procedures

Water was sampled and fiber bags were removed approximately monthly from replicate bioreactors of each experimental treatment starting on December 8, 2016. Bioreactors in Rafts A were sampled until August 2016. Bioreactors in Raft B were sampled until June 2016, when the available sodium lactate substrate was consumed. Sampling and measurements in Raft C were suspended after April 26, 2016 because of a lack of funds to operate this raft of bioreactors.

Water samples were obtained from three depths (0.5, 1, and 2 meters) in duplicate bioreactors and from six depths (0.5, 1, 1.5, and 2, 2.5, and 3 m) from a third replicate bioreactor from each treatment. Water samples were pumped through clear vinyl tubing attached to the push-in fittings of the water sampling pipe. Samples were captured in a 1 L Erlenmeyer flask between the sampling device and the water pump. Two full flasks of water were drawn and discarded to flushed the system before a third full flask was collected and used to rinse and fill a 500 ml plastic bottle.

**Figure IV-17.** Bioreactor fiber sampling device.

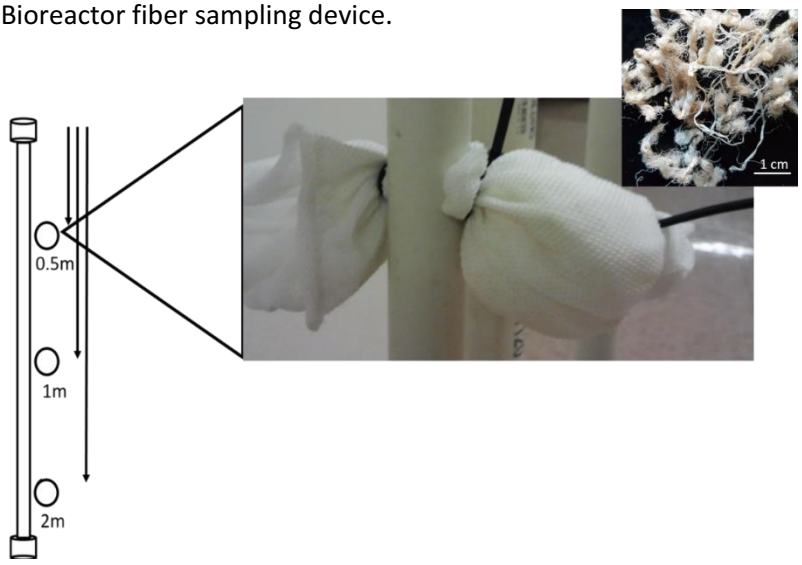


**Fig. IV-17.** Fiber sampling device developed for the experiment. Eight identical pipes with fiber bags were placed in duplicate bioreactors of each experimental treatment. Pipes were periodically removed to collect fiber bags for analysis. The circle represents locations for fiber bag placement at different depths. The photo on the right shows a fiber bag attached to the PVC holder pipe with cable ties prior to being placed in a bioreactor (picture courtesy of Dr. Chanlan Chun). The photomicrograph inset on the upper right shows the variety of lengths and widths of carpet fibers which were used to fill all of the bioreactors and fiber bags samplers.

Each bottle was capped and placed in a cooler with ice and transported within a few hours to the University of Minnesota Duluth. After returning to the lab, the cooler was stored in a cold room until the samples were filtered, usually within 24 hours of sampling.

Fiber sampling bags containing the polypropylene matrix material used in the bioreactors were placed in the bioreactors in October 2015 at three depths (0.5, 1, and 2 m). Water samples were collected prior to removing fiber bags to prevent mixing in the bioreactor. Fiber bags were then collected by removing the entire pipe from bioreactor. As soon as the first fiber bag reached the surface, it was cut free (Fig. IV-18) close to the pipe to minimize disturbance to the fiber contents and placed in a Whirl-Pak® bag for transport.

**Figure IV-18.** Fiber sampling bag and water sampling ports.

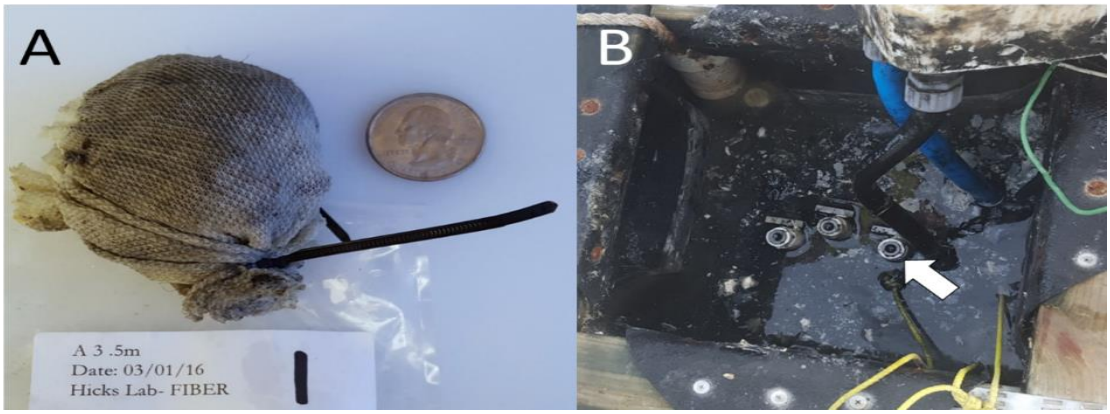


**Fig. IV-18.** A) Fiber bag collected from bioreactor A3 compared to a U.S. quarter. The dark color on the outside was associated with microbial growth. B) Image showing the top openings to the water sampling tubes in a bioreactor. Note the arm of the valve at the top of each sampling pipe that allowed controlled access.

## Preparation of Water and Fiber Samples from Bioreactors

One portion (several hundred milliliters) of each water sample was filtered within two days after collection through a 47 mm Duropore membrane filter (0.22 µm-pore; Millipore Corporation) to capture microorganisms. Filters were folded in half, placed in Whirl-Pak® bags, and frozen at -80°C until DNA extraction. DNA was extracted with a PowerSoil DNA Isolation kit (Mo Bio Laboratories, Solana Beach, CA) and suspended in 50 µl of sterile water, following the provided instructions. Total DNA was quantified (ng/µl) using a ThermoScientific Nanodrop spectrophotometer, labeled, and frozen (-80°C) until DNA further analyses.

Another water subsample was preserved for prokaryotic cell counts that were performed within two weeks after preserving the samples. Immediately after returning to the laboratory, a 10 ml subsample was preserved using 37% formaldehyde (1.8% final concentration) and refrigerated at 4°C until filters were prepared for cell counting. A subsample (~0.2 to 0.5 ml) of each preserved sample was diluted to 2 ml with 0.2 µm-filtered Milli-Q water, stained with DAPI (Porter and Feig 1980), and concentrated by filtering through a black 25 mm (0.22µm-pore) Nuclepore Track-Etch Membrane filter (Whatman). Prokaryotic cells on these filters were counted using a Nikon epifluorescence microscope with 100x oil immersion objective. An average prokaryotic cell count was determined using measurements from replicate bioreactors (Porter and Feig 1980).

Four subsamples of each fiber sample were used for extracting DNA, counting prokaryotic cells, calculating wet:dry weight ratios, and for ESEM examination of biofilm. First, DNA was extracted using a PowerSoil DNA Isolation Kit (Mo Bio Laboratories, Solana Beach, CA). Due to the size of the tubes, only about 50 mg of fiber material could be processed within a single tube. Like DNA extracted from water samples, the resulting DNA was suspended in 50 µl of sterile water and quantified (ng/µl) using a ThermoScientific Nanodrop spectrophotometer. Each DNA sample was labeled and frozen (-80°C) until used for DNA analyses.

A second fiber subsample (~1 g) was preserved by adding 19 ml of sterile water and 1 ml of 37% formaldehyde to a scintillation vial. These subsamples were stored at 4°C until staining with DAPI and counting prokaryotic cells, as done with the water samples. In order to calculate the number of prokaryotic cells per g of dry fiber, a third subsample of fiber material (1 g) was weighed, dried at 60°C, and then reweighed to obtain a dry weight to calculate the wet:dry weight ratio for each sample. Finally, a fourth, unpreserved portion of fiber was placed into a conical vial and refrigerated for later analysis using a Hitachi Environmental Scanning Electron Microscope (ESEM). Any remaining fiber from each sample was frozen (-80°C) for future DNA extractions or other analyses.

## Microbial genetic analysis

**Sequencing of 16S rRNA genes to evaluate bacterial diversity of water and fiber microbial communities.** Samples were analyzed with computational methods as outlined in Jones et al. (in press). Briefly, for quality trimming and filtering, assembly, and OTU calling, sequences were filtered and trimmed with Sickle (https://github.com/najoshi/sickle), residual adapters trimmed with cutadapt (Martin 2011), R1 and R2 sequences assembled with PEAR (Zhang et al. 2014), and primers were removed with prinseq v.0.20.4 (Schmieder and Edwards 2011). OTU calling (97% similarity) and chimera removal were performed with USEARCH (USEARCH v.8.0; [Edgar 2013]) and VSEARCH v.1.9.5 (Rognes et al. 2016) and the taxonomic classifications performed with mother v.1.3.2 using the Silva database v.123 (Pruesse et al. 2007). Multivariate analyses were performed with libraries generated from bioreactor water and fiber bag samples. To account for uneven library sizes, data were first converted to proportional values by dividing by the number of sequences in each library. Similarities and trends in community composition were determined using non-metric multidimensional scaling and other multivariate techniques using the vegan package in R. Specific associations between reactor performance and microbial populations were determined using canonical correspondence analysis. Environmental overlays were created with the envfit() function in vegan, which computes a multiple alignment of environmental variables against the ordination axes.

**Quantitative Polymerase Chain Reaction (qPCR) Analyses for Sulfate-Reducing Bacteria.** The relative abundance of sulfate-reducing bacteria was estimated by measuring the copies of the dissimilatory sulfite reductase (*dsr*A) gene using a procedure modified from Schippers and Neretin (2006) and Kondo et al. (2008). Each 25 µl reaction consisted of 12.5 µl of Brilliant II SYBR Green Master Mix (Agilent Technologies), 1.0 µl of 10 µM forward and reverse PCR primers (Table IV-3), 2.0 µl of 10 mg/ml bovine serum albumin, and 3.0 µl nuclease-free water. A standard curve was constructed using *Desulfovibrio vulgaris* subsp. *vulgaris* genomic DNA (ATCC 29579D-5) by amplifying it with the DSR1F+ and DSR-R primer set. qPCR reactions were performed using a Rotor-Gene 3000 (Corbett Life Science) qPCR thermal cycler.

**Table IV-3.** PCR primers for quantitative PCR analyses to estimate the abundance of sulfate-reducing bacteria.

| Target | Primer | Sequence (5' – 3') | Program | Reference |
|---|---|---|---|---|
| Sulfate-reducing Bacteria *dsr*A | DSR1F+ | ACS CAC TGG AAG CAC GGC GG | 15 sec, 95ºC<br>60 sec, 60ºC<br>15 sec, 85ºC* | (Kondo et al. 2004) |
| | DSR-R | GTG GMR CCG TGC AKR TTG G | | |

* Data acquisition

The PCR program was preceded by a 10-minute hold at 95°C for initial denaturation and enzyme activation. Following 35 qPCR cycles, a melt-curve analysis was performed in which there was a gradual increase in temperature from 72°C to 95°C by 1° steps to detect primer dimers and other non-specific binding.

## References


Edgar, R.C. 2013. UPARSE: highly accurate OTU sequences from microbial amplicon reads. Nat Methods 10:996–998.

Jones, D.S., K.A. Lapakko, Z.J. Wenz, M.C.Olson, E.W. Roepke, M.J. Sadowsky, P.J. Novak, J.V. Bailey. in press. Novel Microbial Assemblages Dominate Weathered Sulfide-Bearing Rock from Copper-Nickel Deposits in the Duluth Complex, Minnesota, USA. DOI:10.1128/AEM.00909-17.

Kondo, R., D.B. Nedwell, K.J. Purdy, and S. de Queiroz Silva. 2004. Detection and enumeration of sulphate-reducing bacteria in estuarine sediments by competitive PCR. Geomicrobiol. J. 21:145–157.

Kondo, R., K. Shigematsu, and J. Butani. 2008. Rapid enumeration of sulphate-reducing bacteria from aquatic environments using real-time PCR. Plankton Benthos Res. 3(3):180–183.

Liamleam, W., and A.P. Annachhatre. 2007. Electron donors for biological sulfate reduction. Biotechnol. Adv. 25:452–463.

Martin, M. 2011. Cutadapt removes adapter sequences from high-throughput sequencing reads. EMBnet J 17:10–12.

Muyzer, G., and A.J.M. Stams. 2008. The ecology and biotechnology of sulphate-reducing bacteria. Nature Reviews Microbiology 6:441-454.

Porter, K.G., and Y.S. Feig. 1980. The use of DAPI for identifying aquatic microfloral. Limnol. Oceanogr. 25:943–948.

Pruesse E., C. Quast, K. Knittel, B.M. Fuchs, W. Ludwig, J. Peplies, and F.O. Glöckner. 2007. SILVA: a comprehensive online resource for quality checked and aligned ribosomal RNA sequence data compatible with ARB. Nucleic Acids Res 35:7188–7196.

Rognes T., T. Flouri, B. Nichols, C. Quince, and F. Mahé. 2016. VSEARCH: a versatile open source tool for metagenomics. PeerJ 4:e2584

Schippers, A., and L.N. Neretin. 2006. Quantification of microbial communities in near surface and deeply buried marine sediments on the Peru continental margin using real-time PCR. Environ. Microbiol. 8:1251–1260.

Schmieder R., and R. Edwards. 2011. Quality control and preprocessing of metagenomic datasets. Bioinformatics 27:863–864.

Zhang J., K. Kobert, T. Flouri, and A. Stamatakis. 2014. PEAR: a fast and accurate Illumina Paired-End reAd mergeR. Bioinformatics 30:614–620.

## V.A. Chemical Treatment for Sulfide Precipitation - Summary

Methods to decrease aqueous sulfate concentrations focus on neutralization, stabilization, and removal through physical, chemical, and biological processes. Bioremediation, which exploits naturally occurring biological processes, can convey advantages due to lower capital and operational costs. This project employs sulfate-reducing bacteria (SRB) to metabolically convert pit water sulfates to sulfide ($H_2S$), which can then be eliminated by chemical precipitation in subsequent treatment steps. The objectives of the work reported in this section were to evaluate available sulfide precipitation and elimination treatments and to develop feasible and effective protocols that are suitable for conditions found in northeastern Minnesota.

The experiments reported herein address the physicochemical conditions necessary to achieve the maximum removal of sulfur species from SRB bioreactor effluents. Tested parameters include: starting pH, acidifiers, oxidative agents, flocculents, reagent concentrations, ratios and loading sequence of oxidizers and sulfide, oxidation temperature and time, and elemental sulfur precipitation time. Bench-scale models designed to produce sulfide oxidation and sulfur precipitation were used to define optimal conditions, and these parameters are currently being tested in the bioreactor raft system.

Conditions for maximum conversion of sulfide to precipitated sulfur and minimum conversion to sulfate in the bench-scale models include: pH 6.3 – 6.5, adjusted using formic acid, temperatures between -10°C and +25°CC, oxidation using hydrogen peroxide ($H_2O_2$), and final flocculation and coagulation using aluminum sulfate ($Al_2(SO_4)_3$). Ratios and flow rates of chemical components can be adjusted, depending on bioreactor effluent sulfide concentration, to achieve total conversion of sulfide to elemental sulfur. This scheme is illustrated Figure V-1 (also Fig. V-2, in Section V.B., below).

**Figure V-1.** Sulfide precipitation flow chart.

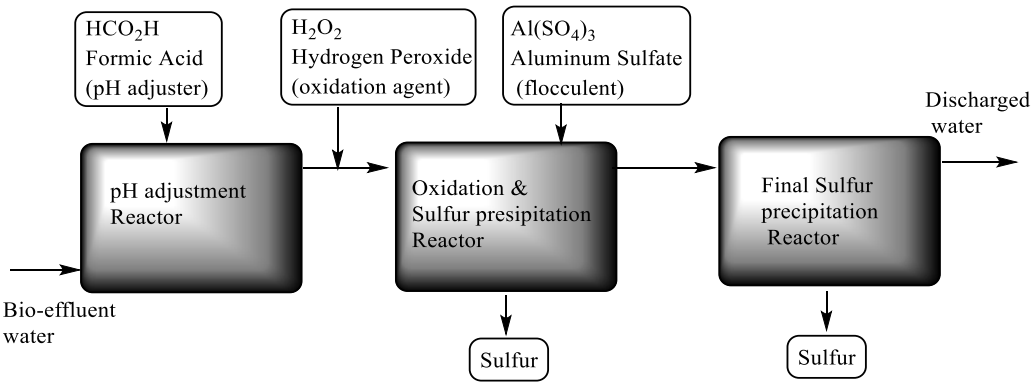


Based on lab tests, the estimated reagent costs for treatment of bioreactor effluent containing sulfide at 333 mg/L, at a flow rate of 10 gallons/minute would be approximately is $12.50/1,000 gal ($69,493/ year; see Table V-4).

# V.B. Chemical treatments for sulfide precipitation

## 1. Introduction

Treatments designed to remove aqueous sulfate typically focus on pH neutralization, followed by stabilization and removal through various physical, chemical, and/or biological processes. Bioremediation, in which naturally occurring biological processes are used to reduce or eliminate contaminants, can offer advantages over conventional physical/chemical remediation systems because they typically require lower capital, operational, maintenance, and disposal costs. In this project, sulfate-reducing bacteria (SRB) were used to metabolically convert mine pit water sulfate ($SO_4^-$) to sulfide ($H_2S$), which can subsequently be eliminated by simple chemical reactions to precipitate elemental sulfur or sulfur compounds. The aims of the work reported here were to evaluate the feasibility of various sulfide elimination treatments (Fig. V-2) and to develop effective chemical precipitation processes that would be suitable for mine water remediation programs in northeastern Minnesota.

**Figure V-2.** Different approaches to reduce $H_2S$ concentration in water.

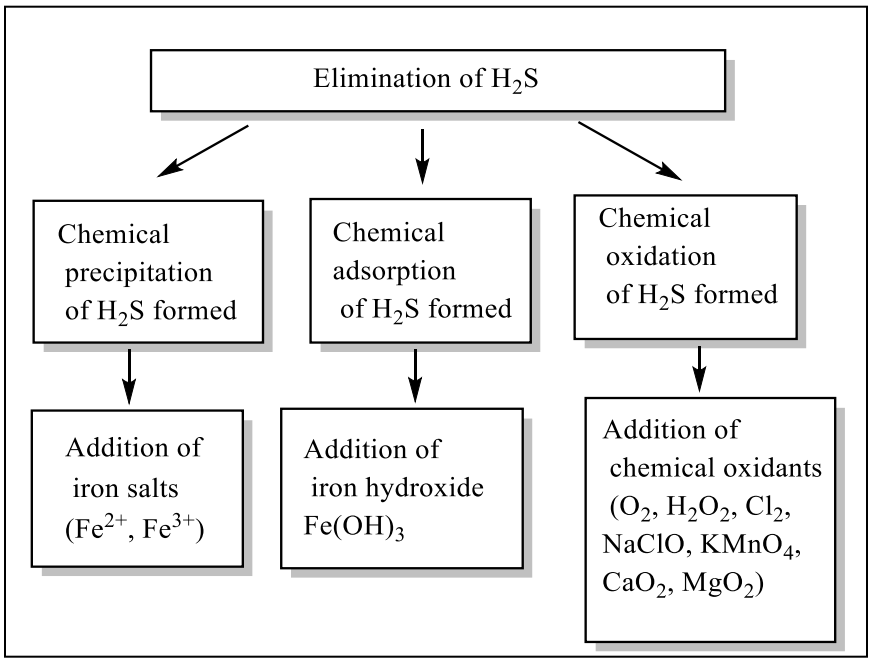


**Fig V-2.** A variety of chemical approaches to reduce aqueous $H_2S$ concentrations have been reported in the literature (citations available upon request).

## 2. Treatment methods for removal of $H_2S$ from bio-effluents.

SRB bioreactor effluents contain sulfides (as $H_2S$) in concentrations that depend, in part, on the pit water sulfate concentration (Table V-1; see Section IIB. Engineering and Operations for typical pit water sulfate content.). Various chemical methods designed to remove $H_2S$ from water have been tested in lab and field trials in this study (Fig. V-1; Table V-2) and are summarized below and discussed in detail in Appendix 3.

**Table V-1.** Hypothetical maximum sulfide concentrations in bioreactor effluents resulting from sulfate-reducing bacteria metabolism in a typical range of sulfate concentrations. Bioeffluent sulfide concentration (mg/L) calculations were based on the following formula: [sulfide] = (([sulfate] – 200)/96) X 32. For this hypothetical example[12], 200 mg/L sulfate is considered the minimum concentration necessary to support metabolism in sulfate-reducing bacteria, so that concentration is subtracted from the pit water total to yield the excess sulfate that could be reduced to sulfide; sulfate ($SO_4^{2-}$) MW = 96, sulfide ($S^{2-}$) MW = 32, so [sulfate]/3 yields the theoretical maximum [sulfide].

| Pit water $SO_4^{2-}$, mg/L | Bioeffluent $S^{2-}$, mg/L |
|---|---|
| **600** | 133 |
| **800** | 200 |
| **1000** | 267 |
| **1200** | 333 |

A variety of methods designed to precipitate sulfides were tested in both lab and field applications. These included precipitation with iron salts ($FeCl_2$ and $FeCl_3$), iron hydroxide ($Fe(OH)_3$, and hydrogen peroxide ($H_2O_2$) alone and with additional flocculating agents. While each of these treatments were effective, each came with specific constraints or disadvantages, including cost, complexity, and the production of unwanted byproducts, that might limit their utility in a final design (see Appendix 3).

In brief, sulfide precipitation using ferrous (Fe(II)) or ferric (Fe(III)) chloride resulted in an unacceptably high concentration of chloride anions in the final effluent, and there was no practical way to economically remove it before release. Precipitation of sulfide using granular ferric hydroxide is a surface reaction, and therefore can be highly inefficient, as the majority of the iron remains unreacted. This, along with the production of large quantities of waste materials, proved to be prohibitively expensive.

Sulfide precipitation via oxidation was tested using chlorine, potassium permanganate, and hydrogen peroxide, which was selected for further study and optimization because it produced no unwanted byproducts, was quite efficient, and could be conducted at a moderate cost. In addition to determining optimal oxidizer:bioeffluent ratios, temperatures, and reaction times, other refinements to increase the overall process efficiency of $H_2O_2$-based sulfide precipitation included adjusting bioeffluent pH to 6.3 – 6.5 using formic acid, and adding aluminum sulfate ($Al_2(SO_4)_3$, alum) as a coagulant (see Appendix 3 for experimental details).

## 3. Experiments

See Appendix 3. Experimental Details and Data, for detailed descriptions of objectives, experimental design, and data.

[12] Hypothetical minimum sulfate substrate concentrations were used only for calculation and modeling purposes.

## 4. Experimental summary and conclusions

- Maximum conversion of sulfide to sulfur and minimum conversion to sulfate was obtained at pH 6.3 – 6.5.
- Formic acid was best pH adjuster for bio-effluent.
- Reaction time for pH adjustment ranges between 1 and 5 minutes.
- Treatment can be successful at temperatures between -10°C and +25°C.
- Oxidation of sulfides to sulfur using hydrogen peroxide is complete between 0.5 – 2 hours.
- The reaction time for a final coagulation using aluminum sulfate ranges between 6 – 10 hours.
- Any concentration of hydrogen peroxide can be used to oxidize sulfide in the bio-effluent.
- The proper proportion of 34% $H_2O_2$ bio-effluent containing sulfide between 200 – 272 mg/L is 1 – 1.4 ml/L for 100% conversion of sulfides.

### 4.1. Recommendations for continuous flow reactors

Our new technology is a combination treatment that integrates aluminum sulfate (alum) which serves as a flocculent and hydrogen peroxide ($H_2O_2$) in a synergistic fashion.

For optimal activity, reagents should be added in order, allowing time for reactions between each addition. The steps include (see Fig. V-3):

1) Addition of formic acid;
2) Allow 3 – 5 minutes for pH to be adjusted;
3) Addition of hydrogen peroxide;
4) Allow 30 minutes to 2 hours for oxidation reaction to be completed;
5) Addition of aluminum sulfate; and
6) Allow 6 – 12 hours for coagulation and precipitation of colloidal sulfur to be completed.

**Figure V-3.** Flow chart for reagent addition to bio-effluent.

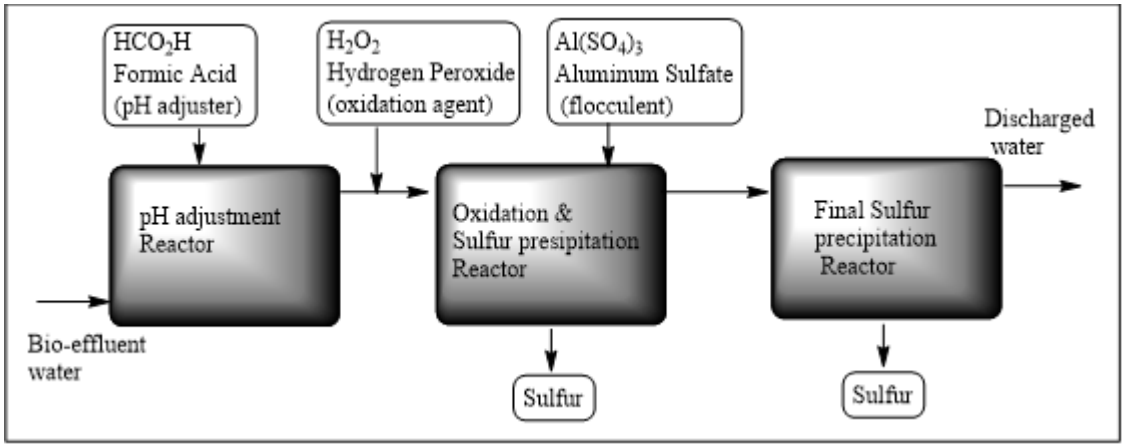


The flow rate of hydrogen peroxide depends on the concentration of sulfide anion in the bio-effluent.

Table V-2 shows the flow rate of a 34% hydrogen peroxide solution that needed to treat bio-effluents containing various sulfide concentrations, flowing at 4.5 gal/min.

**Table V-2.** Loading of hydrogen peroxide.

| Flow rate Raft A, Gal/min | Flow rate Raft A, L/min | $S^{-2}$ mg/L | Flow rate 30% Formic acid, ml/min | Flow rate 34% $H_2O_2$, ml/min | Flow rate 48.5% $Al_2(SO_4)_3$, ml/min |
|---|---|---|---|---|---|
| 4.5 | 17 | 208 | 15 – 17 | 17.5 | 0.88 |
| 4.5 | 17 | 252 | 15 – 17 | 19 | 0.88 |
| 4.5 | 17 | 262 | 15 – 17 | 19.5 | 0.88 |
| 4.5 | 17 | 272 | 15 – 17 | 20 | 0.88 |
| 4.5 | 17 | 288 | 15 – 17 | 20.5 | 0.88 |
| 4.5 | 17 | 333 | 15 – 17 | 23.8 | 0.88 |

Overall, these experimental results indicate that using hydrogen peroxide as an oxidant is a feasible and effective method for treatment of bio-effluent containing the high sulfide concentrations.

## 5. Cost of proposed treatments.

Based on our lab experimental results to date, as well as field conditions, we calculate that chemical treatment of bioreactor effluent containing about 333 mg/L sulfide (resulting from SRB conversion of about 1,200 mg/L sulfate, which reflects the upper range found in our pit water; see Table V-1), and a flow rate of 10 gallons/minute, a hydrogen peroxide-based precipitation system to completely convert sulfide to elemental sulfur would cost about $0.0032/L or $12.52/1,000 gallons (3785 L) of bioeffluent water (Table V-4).

**Table V-3.** Estimated volumes and costs of reagents used for oxidation of sulfides to elemental sulfur, with bioeffluent sulfide input set at 333 mg/L over various periods.

| Bioeffluent Flow rate (L/min)[A] | Period | Bioeffluent Volume (L) | HCOOH (30%) Volume (L) | HCOOH (30%) Cost[B] | $H_2O_2$ (34%) Volume (L) | $H_2O_2$ (34%) Cost[B] | $Al_2(SO_4)_3$ (48.5%) Volume (L) | $Al_2(SO_4)_3$ (48.5%) Cost[B] | Total Cost ($) |
|---|---|---|---|---|---|---|---|---|---|
| | | 1 | 0.001 | $0.0012 | 0.0014 | $0.0020 | 0.00006 | $0.000050 | $0.0032 |
| 17 | day | 24,480 | 24 | $28 | 34 | $49 | 1.5 | $1.2 | $79 |
| | month | 744,600 | 745 | $863 | 1,042 | $1,504 | 45 | $37 | $2,404 |
| | year | 8,935,200 | 8,935 | $10,361 | 12,509 | $18,042 | 536 | $448 | $28,852 |
| 38 | day | 54,720 | 55 | $63 | 77 | $110 | 3.3 | $2.7 | $177 |
| | month | 1,664,400 | 1,664 | $1,930 | 2,330 | $3,361 | 100 | $84 | $5,374 |
| | year | 19,972,800 | 19,973 | $23,161 | 27,962 | $40,330 | 1,198 | $1,002 | $64,493 |

A. The combined flow for Rafts A and B was about 17 L (4.5 gal)/min., while the overall flow rate for Raft C, in which three different flow rates were tested, nearly equaled that volume, so 17 L/min was chosen as representing a, fully-functioning raft. 38 L/min. equals about 10 gallons/min., and was chosen as a convenient metric.

B. See Table V-4. Costs are estimates only and totals could vary with bioreactor efficiency and bulk chemical pricing.

**Table V-4.** Reagent costs.[A]

| | Cost | |
|---|---|---|
| **Reagent** | **208 L** | **1 L** |
| Formic acid | $241.20 | $1.16 |
| Hydrogen peroxide | $300.00 | $1.44 |
| Aluminum sulfate | $174.00 | $0.84 |

A. Hawkins Water Treatment Group, Superior, WI; quotes were for bulk quantities (55 gal/208 L) as of June 2016.

## VI.A. The case for sulfate reduction technology: The regional economic contribution of taconite mining on the State of Minnesota – Summary

As part of the MnDRIVE project, "Implementation of Smart Bioremediation Technology to Reduce Sulfate Concentrations in NE Minnesota Watersheds," the Bureau of Business and Economic Research (BBER) at the University of Minnesota's Duluth's Labovitz School of Business and Economics evaluated the potential economic impacts of a cost-effective bioremediation sulfate-reduction technology for water. Specifically, this study estimates the potential economic impacts to the region if the taconite mining industry was unable to meet sulfate standards imposed by the Minnesota Pollution Control Agency (MPCA), as measured by the industry's economic contribution. The results highlight the need for a cost-effective sulfate reduction technology that will allow iron mines to reduce sulfate levels to the required standard.

The economic modeling software used was IMPLAN. This study models the impacts of the industry using a sensitivity analysis, since this allowed for a range of impacts using multiple scenarios. Data used was the most recent IMPLAN data, which is for year 2014. Results of modeling are reflected in 2016 dollars.

Two scenarios were developed for the sensitivity analysis. Scenario I used 2014 IMPLAN data as the direct input for the model, representing normal production levels for the industry. Scenario II shows the economic contribution of the current state of the industry (using secondary data sources from 2015 and 2016).

According to the results of this analysis, it is estimated that the loss of the iron mining industry would represent a loss of between 6,000 and 10,000 jobs in the northeast region of the state.

Without these jobs, the region would lose almost $430 and $750 million, respectively, in wages and benefits. The forgone contribution to gross regional product (GRP) for scenario I would be more than $2 billion, while the figure would be slightly more than $1 billion for scenario 2. Lastly, the region could see an overall decline in output of almost $2.6 and $4.4 billion per scenario annually if mining operations were to cease.

The results from the state impact analysis yield slightly larger values because the state has increased spending from supporting industries (such as electric power transmission and distribution, wholesale trade, oil and gas operations, and others) that have a larger presence beyond the Arrowhead region. In total, the state of Minnesota could experience a decline in output of almost $4.8 and $2.9 billion per scenario annually if mining operations were to cease.

These results highlight the importance of the iron mining industry on the Arrowhead Region and the State of Minnesota. At the current production levels, the industry directly employs more than 2,500 workers and contributes nearly $2 billion in industry sales. The additional impacts to the region are even greater, supporting jobs in related industries ranging from wholesale trade, restaurants, hospitals, and real estate, among many others. However, the importance of the environmental standards should not be ignored. That is why it is critically important that the iron mines have resources to meet the standards set by the MPCA through technologies like the one currently being researched by the NRRI.

VI.B. The case for sulfate reduction technology: The regional economic contribution of taconite mining on the State of Minnesota

May 27, 2016

Research Report

# The Case for Sulfate Reduction Technology:

# The Regional Economic Contribution of Taconite Mining on the State of Minnesota

For the
Natural Resources Research Institute

Bureau of Business and Economic Research

Labovitz School of Business and Economics

University of Minnesota Duluth

Driven to Discover

## Research Team

**UMD Labovitz School of Business and Economics**
**Bureau of Business and Economic Research**

Monica Haynes, Director
Gina Chiodi Grensing, Editor/Writer
Travis Eisenbacher, Undergraduate Research Assistant
Andrew Burke, Undergraduate Research Assistant
Karen Haedtke, Executive Administrative Specialist
Bureau of Business and Economic Research
11 East Superior Street, Suite 210
Duluth, MN 55802
(218) 726-7895
https://lsbe.d.umn.edu/centers-outreach/centers/bber

**Project Contact**

George J. Hudak, Ph.D., P.G., P.Geo.
Director, Minerals-Metallurgy-Mining Initiative
Associate Director, Precambrian Research Center
Natural Resources Research Institute
University of Minnesota Duluth
5013 Miller Trunk Highway
Duluth, MN 55811
(218) 788-2739
ghudak@nrri.umn.edu

## Table of Contents

## Table of Tables



## Table of Figures

# The potential economic impact of Smart Bioremediation Technology on Minnesota with special focus on the northeast region

## 1. Project Description

This project serves as part of the MnDRIVE-supported project, “Implementation of Smart Bioremediation Technology to Reduce Sulfate Concentrations in NE Minnesota Watersheds” which seeks to develop a commercially viable, remotely operated bioremediation system that will reduce sulfate concentrations in wild rice waters of Minnesota. Sulfate concentrations in natural waters may be increased as a result of chemical weathering of sulfide and/or sulfate minerals that naturally occur in rocks in the region, including iron formations and associated iron ores, as well as in rocks that contain anomalous concentrations of elements such as, but not limited to, copper, nickel, platinum, palladium, zinc and gold. As well, high sulfate concentrations can often be found in water that has been used in the extraction or beneficiation process, and in precipitation runoff from waste rock piles, lean ore stockpiles, or tailings ponds. When sulfur bearing minerals, including sulfide and sulfate minerals, are exposed to air and water, they chemically weather to produce aqueous sulfate. The reduction-oxidation cycle continues as waterborne sulfates enter stream or lake sediments, where sulfates can be chemically transformed to sulfides and vice-versa, depending on local conditions.

Although sulfates generally have low toxicity to plants and animals, natural wild rice, which has significant economic and cultural importance to Native American tribes in the region, appears to be particularly sensitive to fairly low concentrations. In 1973, Minnesota adopted a sulfate standard of 10 mg/L, protecting ”water used for production of wild rice during periods when the rice may be susceptible to damage by high sulfate levels” (Agency n.d.). This standard, as well as the site-specific criteria currently under consideration by the Minnesota Pollution Control Agency (MPCA), may require treatment of mining-affected waters before they can be released into the watershed.

A variety of methods exist for decreasing sulfate concentrations in mining-affected waters, but most are expensive, energy-intensive, and mechanistically complex. The objective of the current MnDRIVE project is to develop a reliable, inexpensive alternative, based on the metabolic activities of naturally occurring microorganisms and relatively simple chemical processes. The Natural Resources Research Institute (NRRI), the project’s primary investigator, contracted the Bureau of Business and Economic Research (BBER) at the University of Minnesota Duluth’s Labovitz School of Business and Economics to study the potential economic impacts of sulfate reducing technologies. Specifically, the study estimates the potential economic impacts to the state of Minnesota and the northeast region were the taconite industry to cease operations due to its inability to meet required sulfate standards.

## 2. Scope of Work

The BBER studied and estimated the regional economic contribution of the taconite industry on the State of Minnesota, with a special focus on the northeast region of the state. The purpose of this analysis was to demonstrate the impacts that the region could experience if the taconite industry were unable to meet sulfate standards and be forced to shut down the industry. This analysis indicates a worst-case scenario to illustrate the importance of developing technology that can reduce sulfate concentrations in wild rice waters.

The consulting objectives of the study include the following:

- To investigate new MPCA sulfate standards for wild rice waters and describe possible effects that implementation of the new standard could have on the taconite mining and mineral processing industry
- To estimate the potential economic impacts to the region if the taconite mining industry was unable to meet sulfate standards, as measured by the industry's economic contribution.
- To provide a range of economic impacts (i.e., sensitivity analysis), based on peak (2014) and current (2016) production levels.

## 3. Study Area

The geographic scope for this economic impact analysis focused primarily on the Northeast region of the state of Minnesota, specifically the counties of Minnesota's Arrowhead region (Aitkin, Carlton, Cook, Itasca, Koochiching, Lake, and St. Louis) and Douglas County, Wisconsin. For further comparison and context, statewide impacts were also modeled, which included all counties within the state of Minnesota as well as Douglas County, WI.

**Figure VI-1.** Designated Wild Rice Waters in Minnesota's Arrowhead Region.

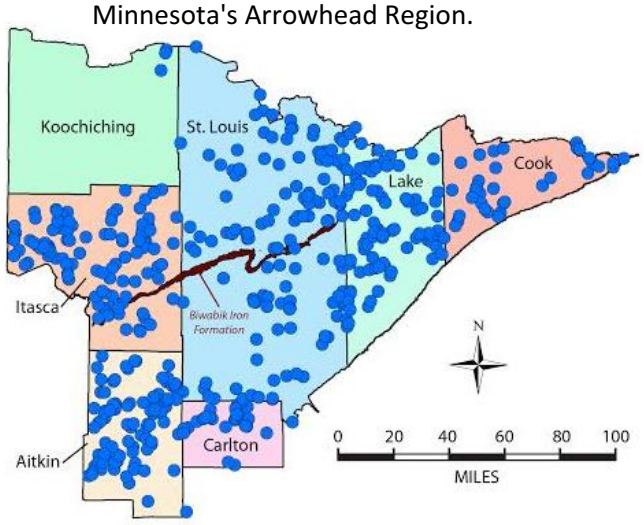


The Arrowhead Region was chosen as the focus of this report's analysis for two primary reasons. First, the region is the center of mining activity within the state. Minnesota's Mesabi Iron Range is currently the state's only actively mined deposit of iron ore and is located primarily within the counties of Itasca and St. Louis (see Figure VI-6 in Appendix VI-A for a map of Minnesota's iron ranges).

In addition to being the center for iron mining in the state, the Arrowhead region is home to a large share of the state's wild rice waters (See Figure VI-1). Therefore, the sulfate standards have the potential to have a very large impact on the Arrowhead region and the mining industry in particular[13].

## 4. Input-Output Modeling

This study uses the IMPLAN[14] Group's input-output modeling data and software (IMPLAN version 3.1). The IMPLAN database contains county, state, zip code, and federal economic statistics, which are specialized by region, not estimated from national averages. Using classic input-output analysis in combination with region-specific Social Accounting Matrices and Multiplier Models, IMPLAN provides a

[13]Although the Minnesota iron mining industry is located primarily within the Arrowhead, its reach extends beyond the borders of that region, so a statewide study area was also modeled.
[14]www.implan.com

highly accurate and adaptable model for its users. IMPLAN data files use the following federal government data sources:

- U.S. Bureau of Economic Analysis Benchmark Input-Output Accounts of the U.S.
- U.S. Bureau of Economic Analysis Output Estimates
- U.S. Bureau of Economic Analysis Regional Economic Information Systems (REIS) Program
- U.S. Bureau of Labor Statistics Covered Employment and Wages (CEW) Program
- U.S. Bureau of Labor Statistics Consumer Expenditure Survey
- U.S. Census Bureau County Business Patterns
- U.S. Census Bureau Decennial Census and Population Surveys
- U.S. Census Bureau Economic Censuses and Surveys
- U.S. Department of Agriculture Census

IMPLAN data files consist of the following components: employment, industry output, value added, institutional demands, national structural matrices, and inter-institutional transfers. Economic impacts are made up of direct, indirect, and induced impacts. The data used was the most recent IMPLAN data available, which is for the year 2014. All data are reported in 2016 dollars.

Some limitations of the modeling and impact results should be mentioned. First, IMPLAN is a fixed-price model. This means that the modeling software assumes no price adjustment in response to supply constraints or other factors. The iron mining industry has experienced a drastic reduction in the price of iron ore in the years between 2011 and 2015. While there are obvious limitations associated with using 2014 prices during this period of fluctuation, there are also problems that come with attempting to adjust for current prices. For instance, adjusting the value of output using current prices would also reduce the amount of intermediate expenditures and value added payments made by the iron industry, without any compensatory price adjustments in other industries. Since there is no way to account economy-wide for price changes and potential input changes across all sectors since 2014, this analysis uses IMPLAN's most current (2014) prices to estimate the economic effects of the iron mining industry's contribution.

More details on the assumptions and limitations of these models can be found in Appendix VI-C, IMPLAN Assumptions.

## 5. Background

Wild rice has a long economic, cultural, and even spiritual history in Minnesota. Native American tribes have harvested wild rice for sustenance over many generations, and some tribes, like the Ojibwa, consider natural wild rice to be a sacred resource. It is estimated that between 4,000 and 5,000 tribal and nontribal people participate in harvesting wild rice each year (Minnesota Department of Natural Resources 2008). Aside from its subsistence and cultural value, wild rice is also important for the regional and statewide economy. Minnesota currently produces between four and eight million pounds of wild rice annually, which represents about 40% of global production, second only to California (University of Minnesota Horticulture 2015). And although cultivated production dominates the production numbers, hand harvested natural wild rice still remains an important component of tribal and local economies in Minnesota. In 2007, nearly 300,000 pounds of unprocessed wild rice were purchased from licensed tribal producers (Minnesota Department of Natural Resources 2008).

However, in recent decades, there has been a dramatic decrease in the number of wild rice licenses sold in Minnesota, from 16,000 in 1968 to only 1,500 in 2006 (Minnesota Department of Natural Resources 2008). This decline prompted the MNDNR to examine why wild rice stands were disappearing, and in 2008, they reported that key threats include the loss of genetic integrity, invasive species, and climate change, and that high sulfate concentration in wild rice waters influenced by mining is a potential threat to the plant's successful natural growth and cultivation (Minnesota Department of Natural Resources 2008). Studies conducted in the 1940s indicated that wild rice did not grow in waters containing elevated sulfate ($SO_4^{2-}$) concentrations, and recent research has shown that it is sulfate's naturally occurring chemically reduced form, sulfide ($S^{2-}$), that is particularly damaging to the plant (Minnesota Pollution Control Agency 2015a,b). Low levels of sulfates are common in water throughout the region, but these concentrations can increase dramatically when sulfur-containing minerals are weathered by exposure to air and water, dissolving the minerals and allowing them to enter the surrounding watershed through precipitation runoff (Minnesota Pollution Control Agency 1999). These dissolved sulfates can then be converted to sulfides by specific forms of sulfur metabolizing bacteria that commonly live in river, lake, and wetland sediments. This combination of exposure, weathering, and microbiological activity can produce increased concentrations of both sulfates and sulfides downstream from mining operations.

In 1973, Minnesota established a specific standard of 10 mg/L sulfate for waters designated as wild rice production areas. Proposed mining operations must prove that they can meet this standard in order to obtain an MPCA permit, but the regulations are currently under a state-mandated review, and the 10 mg/L standard has been stayed for ongoing mining operations until a revised rule is established. In 2010, the USEPA stated that Minnesota regulators must ensure that PolyMet Mining's proposed copper-nickel mine meets the state's sulfate standard (Dunbar 2015a,b).

In response to the increased scrutiny of the mining industry's potential impact on wild rice, Governor Mark Dayton directed the MPCA to conduct research on wild rice-designated lakes in Minnesota (MPCA Minnesota Pollution Control Agency 2015), with the objective of ensuring that the state's sulfate standards protect natural wild rice stands. Based on this research, the MPCA made draft recommendations that limited sulfide, which is the chemically reduced form of sulfate and the suspected toxic agent to wild rice, in sediment porewaters to 0.165 milligrams per liter (mg/L) as protective of wild rice. In addition, because the conversion of aqueous sulfate in a surface water body to porewater sulfide is related to the concentrations of both organic carbon and iron in the associated sediments, the MPCA proposed that a protective sulfate concentration for a water body be calculated by the following equation:

$$\text{Sulfate} = 0.0000136 \times \text{Organic Carbon}^{-1.410} \times \text{Iron}^{1.956}$$

The MPCA's proposal, which takes into account both chemical and biological components of a site on a site-specific basis, indicates that no single level of sulfate in a surface water body can be protective of wild rice in all water bodies (Minnesota Pollution Control Agency 2015a,b). Therefore, the MPCA proposes that surface water sulfate concentrations for a water body be calculated based on measurements of the organic carbon and iron contents of sediments associated with that water body using the equation above.

As the MPCA continues to study the effects of sulfate and sulfide on wild rice, it faces immense pressure by environmentalists, Native American tribes, and mining companies (Matuszak 2016). The EPA,

supported by the tribes and environmentalist groups, is requesting that the MPCA follow protocol and renew permits for mining facilities that respect the sulfate standard. On the other hand, mining companies contend that the current standard is too strict, as many existing operations would not be able to meet the current standard without investing in complex water treatment and pollution control technologies, which can add tremendous costs (Myers 2015). For example, capital costs for a water treatment plant using reverse osmosis, which is a process that separates pollutants by filtering highly pressurized water through a semi-permeable membrane, are estimated to be roughly $43.9 million for a one-million-gallon-per-day (gpd) system, with operational/maintenance costs estimated at $3.3 million annually for the same system (CH2MHill 2010).[15] For reference, the USGS reported there are concerns that meeting the sulfate standard might leave mining companies unprofitable, in which case they may cease operations or not open in the first place, leaving a severely weakened northeastern Minnesota economy.

Thus, there are compelling reasons for developing alternative methods for decreasing sulfate and sulfide concentrations in mining-affected waters and associated sediments. The MnDRIVE bioremediation program referred to herein is designing and testing technologies that can decrease sulfate concentrations in legacy mine pits. As these and other innovative methods evolve and become commercially viable, they can be incorporated by the industry to potentially more affordably meet water quality standards.

## 6. Inputs

The purpose of this analysis is to determine the economic contribution that the iron mining industry has on the study area and the potential negative impacts to the region if the industry were forced to reduce or cease operations as a result of the industry's inability to reduce aqueous sulfate concentrations to the required levels. This section summarizes the data and inputs required for modeling the impacts of the iron mining industry on the Arrowhead region, Douglas County, Wisconsin, and the state of Minnesota.

In recent years, the mining industry has undergone a dramatic downturn as a result of declining iron ore prices and declining production levels nationally (World Bank 2016). While it is commonly thought that this shift is temporary, the current dynamics affecting the industry present a unique challenge to accurately model the impacts of iron mining in the region.

As mentioned previously, the economic modeling data and software used for modeling is IMPLAN[16] version 3.1., and the most recent IMPLAN data available is for the year 2014. Unfortunately, much of the decline in iron ore prices and mining production has occurred since 2014, and thus, modeling the impacts of the industry using 2014 prices and production levels would dramatically overstate the current economic impacts of the industry. However, there are signals that the current mining downturn is reversing course. On June 9, 2016, it was announced that Cliffs Natural Resources United Taconite Mine and Forbes taconite pellet plant would open sooner than originally predicted due to increased demand

[15]Estimates were updated to reflect 2016 USD using the Bureau of Labor Statistics CPI Inflation Calculator http://www.bls.gov/data/inflation_calculator.htm

[16] IMPLAN Group LLC, IMPLAN System (data and software), IMPLAN Group LLC, 16740 Birkdale Commons Pkwy, Suite 212, Huntersville, NC 28078. www.implan.com

for pellets (Burnes 2016). If this upward trend continues, using current production levels would likely understate the importance of the industry.

Therefore, this study models the impacts of the industry using a sensitivity analysis, which provides a range of impacts under multiple scenarios. Two scenarios were modeled. The first estimates the economic contribution of the iron mining industry using 2014 prices, production levels, and employment (i.e., normal production and employment levels). The alternate scenario models the industry's contribution using current levels (i.e., reduced production and employment based on 2016 levels).

Scenario I uses the 2014 IMPLAN data as the direct inputs for the model. These inputs include employment levels, wages, and output (i.e., value of production). Inputs for Scenario II were estimated by gathering data from secondary sources and then comparing the levels reported in 2014 to the most recent data available. The final results are ratios of employment, wages, and output that can be used to adjust the 2014 IMPLAN data to current, 2016, levels. The results of this process are described in this section followed by a summary of the inputs used for modeling both scenarios.

**Table VI-1.** Description of Modeling Scenarios.

| | *Scenario I* | *Scenario II* |
|---|---|---|
| Description | Contribution of iron mining industry at normal production and employment levels | Contribution of iron mining industry at reduced production and employment levels |
| Data Sources | 2014 IMPLAN estimates for employment, wages, and output | Secondary sources, including Minnesota Department of Revenue, Quarterly Census of Employment and Wages (QCEW), and World Bank |

*SOURCE: BBER*

Each of the major iron ore mining facilities in Minnesota can be found in Table IV-2, sorted according to current operational status. The values shown in Table VI-2 were used to calculate employment and production levels for Scenario II. Of the eleven facilities featured in the table, only four are fully operational as of the time of writing. The remainder of the facilities are currently idled, shuttered, or otherwise out of service.

Assuming that all the production at the idled facilities has been suspended, the current utilization of capacity in iron mining would be roughly 61% of the normal production level, a significant drop from previous years. As shown in Table VI-2, the current state of employment is also fairly similar (again, with the assumption that all employees at the idled facilities have been terminated), down to 59% employment relative to normal, or 2014, employment levels. These ratios were the basis for determining the current, 2016, input levels required for modeling Scenario II.

Figure VI-2 shows the change in the annual production of iron (in millions of dry metric tons, or DMTs) in Minnesota over the last twenty years, compared with the global price of iron ore (in U.S. dollars per DMT) during the same time period. As can be seen from the graph, there has been relatively little variation in production levels and only a slight downward trend. Although data for 2015 iron production

is not yet available, a decline in total output for the year is likely, based on the lack of production attributable to those mines that have been idled (see Table VI-2).

The most drastic change among all of the mining related factors can be seen in the sustained slide in global iron ore prices across the past five years. As seen in Figure VI-2, iron ore approached historic highs of nearly $200 per dry metric ton (DMT) in 2007 and again in 2011 (World Bank 2016). Since then the trend has been downward. Most recently, the price per DMT has fallen from $128.12 at the beginning of 2014 down to just $47 as of February 2016. Global prices haven't been as low since 2004.[17]

The effect of this recent decline (since 2014) for Minnesota's iron mining industry has been stark: effectively, every single unit of production is currently worth less than 37% of what it was just over a year ago. The implication of this is that the total normal productive capacity of Minnesota's mines (from Table VI-2) of about 40 million tons per year (Minnesota Department of Revenue 2015), which would have had an estimated value of over $5.3 billion at January 2014 prices, would now be valued at just $1.9 billion. Considering the relatively fixed costs per unit of production that the mining companies face, such a drastic price decline has meant it is simply no longer profitable for many of Minnesota's mines to continue operations. This can be seen in the list of idled facilities in Table VI-2.

**Table IV-2.** Summary Information of MN Mining Facilities According to Current Operational Status.

| *Mining Facility* | *2016 Status* | *2014 Production (millions of tons/year)* | *2014 Employment (number of jobs)* |
|---|---|---|---|
| U.S. Steel - MinnTac | Operational | 14.3 | 1,448 |
| Hibbing Taconite | Operational | 7.4 | 789 |
| ArcelorMittal Minorca | Operational | 2.7 | 354 |
| Magnetation Plant 4 | Operational | 0.6 | 80 |
| Total (Operational Facilities) | | 24.9 | 2,671 |
| | | | |
| NorthShore Mining | Idled | 5.1 | 576 |
| United Taconite | Idled | 4.8 | 535 |
| U.S. Steel - Keetac | Idled | 5.2 | 420 |
| Magnetation Plant 2 | Idled | 0.3 | 81 |
| Mining Resources | Idled | 0.3 | 80 |
| Mesabi Nugget | Idled | 0.2 | 143 |
| Magnetation Plant 1 | Idled | 0.1 | 24 |
| Total (Idled Facilities) | | 16.2 | 1,859 |
| | | | |
| Total (All Facilities) | | 41.0 | 4,530 |
| Current (2016) Utilization | | 60.6% | 59.0% |

*SOURCE: MN DEPARTMENT OF REVENUE*[18]

[17]For an historic presentation of iron ore prices (1960-Present) see Figure VI-7, Appendix VI-A.

[18]Employment and production levels were collected from Figure 20, "Employment and Mine Value by Mine," on page 28 of the Minnesota Department of Revenue 2015 Mining Tax Guide.

Figure VI-2 also highlights the inelastic nature of the iron mining industry. While it might be expected that the mines would react to increased prices (for example, during the period of 2004 to 2008) by increasing their output to increase their revenues and that output should decline when prices decline, this is not the relationship shown in reality. In fact, the mines' output has typically remained at or near their potential full-utilization capacity regardless of exogenous price changes, with the obvious exception of the systemic impact of the Great Recession.[19] In light of this, it is clear that iron mining is highly inelastic to all but the most drastic price changes.

**Figure VI-2.** MN Annual Iron Production (DMT) and Global Price ($/DMT), 1994 – Present.

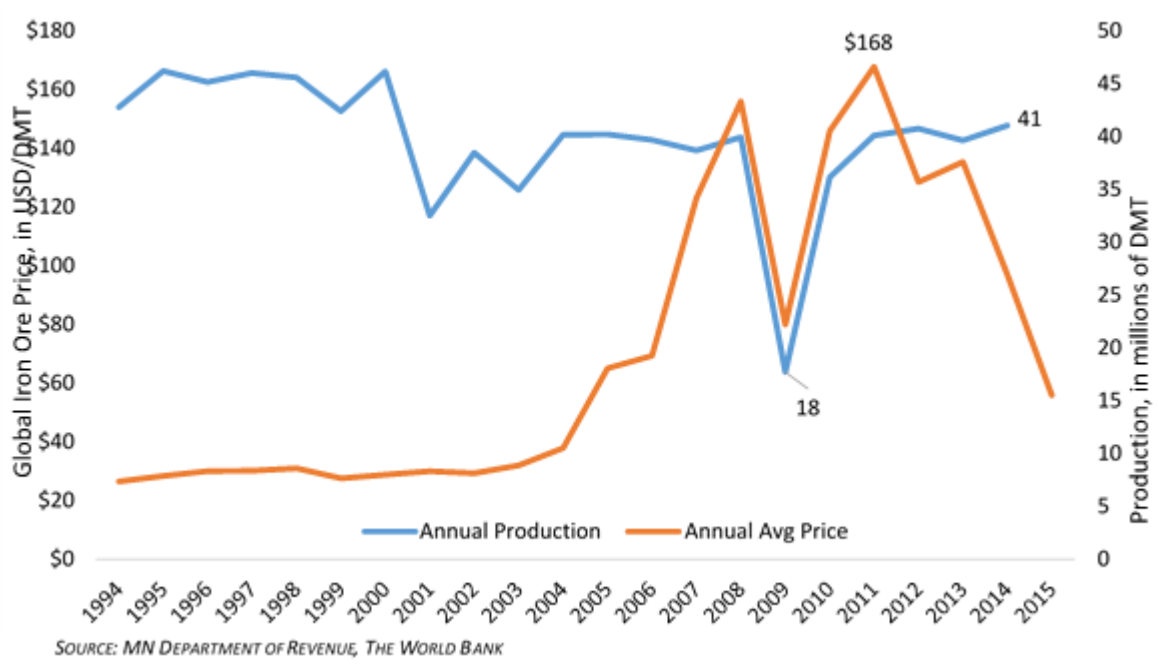

SOURCE: MN DEPARTMENT OF REVENUE, THE WORLD BANK

Figure VI-3 shows monthly employment in the Iron Mining and Support Activities for Metal Mining sectors from January 2012 to September 2015. In 2015 alone, the two combined industries experienced a net loss of nearly 700 jobs[20]. Using the average employment levels in 2014 as a baseline, compared with the most recent data from 2015 (Q3), employment in the two sectors has fallen by about 14%. And, due to the delay in data reporting, it is assumed that the decline has been even greater since Q3 2015, as shown from the estimated employment loss in Table VI-2, in which seven mines had been idled for a combined employment loss of nearly 1,900 workers.

[19]This is likely controlled by the availability of blast furnaces to process the pellets into steel, as well as the rate at which the blast furnaces can convert the pellets into steel. There are only a limited number of blast furnaces available to process the pellets.

[20]For a more detailed breakout of employment loss within each industry, and its relationship with the decline in the price of iron ore, see Figure VI-8 and Figure VI-9 in Appendix VI-A.

**Figure VI-3.** Employment Change in Iron Mining, Support Services for Mining (2012-2015).

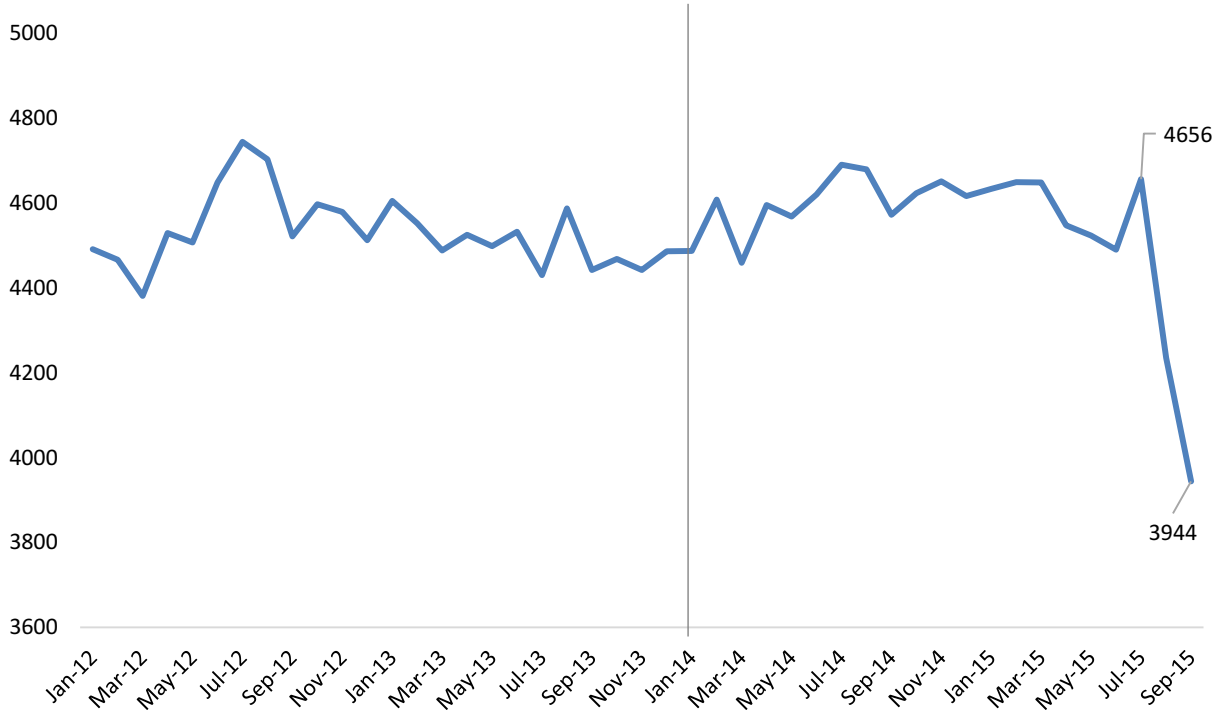


*SOURCE: MN DEED, QUARTERLY CENSUS OF EMPLOYMENT AND WAGES (QCEW)*

Considering each of the factors and assumptions discussed, Table VI-3 provides an estimate of employment, wages, and output from mining in Scenarios I (2014) and II (2016). 2014 estimates for the Iron Ore Mining sector were gathered from IMPLAN's database, and inputs for Scenario II were calculated based on the estimated percentage change in employment and production from 2014 levels to the most recent available.

Industry sales for Scenario II are based on 2016 production levels but utilize 2014 prices. While this likely results in an overestimate of true sales, based on what we know about the current price of iron ore, IMPLAN's model assumes fixed prices and production patterns. This means that even in cases where the value of production declines, the model assumes the same quantity of intermediate expenditures and employment are needed.[21] For that reason, 2014 prices are used throughout the report.

[21]Even with data on the changes that have occurred in the iron mining industry, data would also have to be collected for every other industry in order to develop a truly current model within IMPLAN that would reflect all the current impacts and effects. This was beyond the scope of the analysis.

**Table VI-3.** Direct Inputs Used in Modeling Scenarios I (2014) and II (2016).

| | *Sector* | *Employment* | *Annual Wages (millions)*[22] | *Industry Sales (millions)* |
|---|---|---|---|---|
| Scenario I (2014 contribution) | Iron Ore Mining | 4,383 | $483.8 | $3,125.5 |
| | Support Activities for Mining | 165 | $12.4 | $19.3 |
| Scenario II (2016 contribution)[23] | Iron Ore Mining | 2,583 | $265.6 | $1.895.1 |
| | Support Activities for Mining | 104 | $7.8 | $11.7 |

Source: MN DEED, MN Department of Revenue, IMPLAN, Mining facility websites

These direct inputs represent a range of employment, wages, and sales for the iron mining industry, based on normal (2014) and reduced (2016) production levels. The inputs were used as the basis for the sensitivity analysis, the results of which are described in the following section.

## 7. Findings

### 7.1. Arrowhead and Douglas County, WI Impacts

This section includes the results of the economic contribution sensitivity analysis. These results not only represent the iron mining industry's economic contribution to the region but also the potential economic loss that would be felt were the industry to cease operations.

Table  shows the results of the sensitivity analysis, summarized by each scenario's total effects on the Arrowhead/Douglas County study area. Scenario I used 2014 IMPLAN data as the direct input for the model, representing normal production levels for the industry. Scenario II shows the economic contribution of the current state of the industry (using secondary data sources from 2015 and 2016). The left-most column of Table VI-4, labeled Employment, indicates the number of jobs that the industry contributes to the region, directly and indirectly. Employment estimates are in terms of jobs, not in terms of full-time equivalent employees. According to the results of this analysis, it is estimated that the loss of the iron mining industry would represent a loss of almost 6,000 and 10,000 jobs per scenario in the northeast region of the state.

[22]Annual Wages are based on a per employee estimate of annual wages calculated as the annual average total wages in iron ore mining divided by the annual average total number of employees in the industry. This amount was then multiplied by the number in "Employment." Wage estimates are based on IMPLAN averages for the industry. For a visual presentation of quarterly wages from the Bureau of Labor Statistics (2010-2015 Q3), see Figure VI-10 in Appendix VI-A.

[23]The values shown for Scenario II are based on the assumption that all of the employees and production related to the Idled status facilities (see Table VI-2) have been laid off and has ceased, respectively.

**Table VI-4.** Iron Mining Contribution Sensitivity Analysis; Total Effect on Arrowhead (Millions of Dollars).

| *Impact Type* | *Employment* | *Labor Income* | *Value Added* | *Output* |
|---|---|---|---|---|
| Scenario I | 10,031 | $741.2 | $2,098.1 | $4,416.9 |
| Scenario II | 5,985 | $439.1 | $1,260.7 | $2,672.6 |

*SOURCE: IMPLAN, 2016*

The second column, Labor Income, is an estimate of all employee compensation, including wages, benefits, and proprietor income. It is estimated that, if the iron mining industry did not exist, the region could suffer almost $430 and $750 million annually per scenario in lost employee wages and benefits. Column three, labeled Value Added, shows the economic contribution of the expenditures that the iron mining industry put specifically towards wages, rents, interest, and profits related to its operations. Value Added represents the contribution to gross regional product (GRP) made by an individual producer, industry, or sector. The iron mining industry as a whole was estimated to have a total Value Added impact of more than $2 billion in the study area in 2014 and slightly more than $1 billion in 2016. The last column, Output, is the value of all local production required to sustain activities. Based on 2014 levels of production and employment, it is estimated that the iron mining industry saw more than $3 billion in industry sales in 2014 (see Direct Effect, Table VI-5), leading to a total output impact of $4.4 billion regionally, in combined direct, indirect, and induced spending effects. Were the iron mining industry to cease operations, the region could see an overall decline in output of $2.6 and $4.4 billion annually per scenario.

Further details of the iron mining industry's economic contribution are shown in Table VI-5 and Table VI-6. In these tables, the economic contribution of the iron mining industry (Scenarios I and II) are broken out by impact type: Direct, Indirect, and Induced Effect. Direct employment and expenditures for Scenario I were based on 2014 employment and output levels.[24] Direct inputs for Scenario II were calculated based on the estimated decline in the industry since that time.[25] The results suggest that the iron mining industry directly employed 4,500 workers in 2014. That number has since dropped to roughly 2,680. In addition, the industry's direct contribution to the gross regional product has fluctuated from $1.6 billion in 2014 to approximately $1.0 billion today.

[24] Based on IMPLAN's 2014 datasets.

[25] Data were collected from the most recent available secondary sources, including BLS QCEW monthly employment estimates, IMPLAN wage estimates, and Minnesota Department of Revenue production tax receipts.

**Table VI-5.** Scenario I Impact Detail - Iron Mining's Normal Contribution to Arrowhead (in Millions of Dollars).

| *Impact Type* | *Employment* | *Labor Income* | *Value Added* | *Output* |
|---|---|---|---|---|
| Direct Effect | 4,505 | $479.4 | $1,677.7 | $3,144.7 |
| Indirect Effect | 2,296 | $141.0 | $208.6 | $863.8 |
| Induced Effect | 3,231 | $120.6 | $211.8 | $408.5 |
| Total Effect | 10,031 | $741.2 | $2,098.1 | $4,416.9 |

*SOURCE: IMPLAN 2016*

**Table VI-6.** Scenario II Impact Detail - Iron Mining's Reduced Contribution to Arrowhead (in Millions of Dollars).

| *Impact Type* | *Employment* | *Labor Income* | *Value Added* | *Output* |
|---|---|---|---|---|
| Direct Effect | 2,679 | $282.1 | $1,008.7 | $1,906.8 |
| Indirect Effect | 1,392 | $85.5 | $126.5 | $523.8 |
| Induced Effect | 1,914 | $71.5 | $125.5 | $242.0 |
| Total Effect | 5,985 | $439.1 | $1,260.7 | $2,672.6 |

*SOURCE: IMPLAN, 2016*

Indirect Effects show the measurement of increased spending between commercial, government, and service industries as a result of the direct effects. In this case, it is estimated that between $523 and $863 million in decreased industry spending would occur were the iron mining industry to cease operations.

Finally, Induced Effects measure the amount of increased spending by residential households as a result of the direct effects. These results suggest, if the iron mining industry were to cease operations, the region would see a decline in household spending of $242.0 and $408.5 million per scenario, the result fewer workers employed by the mining industry and related sectors.

Total Effect is the sum of Direct, Indirect, and Induced Effects.

Figure VI-4 shows the estimated employment impacts in the top twenty most impacted sectors. All 4,500 employees (See Direct Effect Table VI-5) employed in the Iron Mining industry in 2014 were classified in the Iron Ore Mining sector, and clearly that is the sector with the largest employment. That particular sector is not shown to scale on the graph, as none of the other details would be visible otherwise. Other impacted sectors are Wholesale Trade, Management of Companies and Enterprises, Full-service Restaurants, and Hospitals.

**Figure VI-4.** Top 20 Industries Impacted by Iron Mining, Employment (Scenario I).

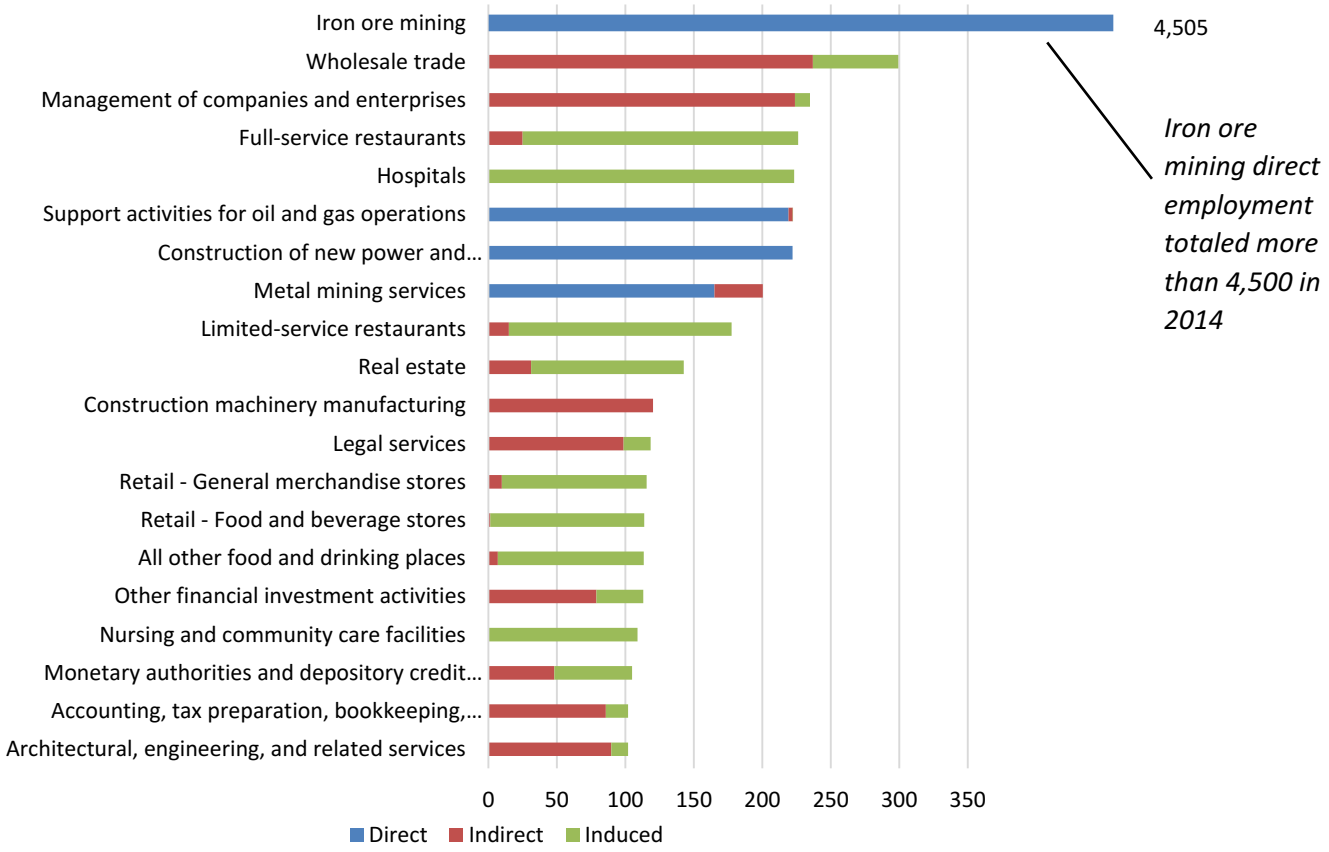


*SOURCE: IMPLAN, 2016*

Figure VI-5 shows the estimated value added impacts in the top twenty most impacted sectors. Value Added represents the amount by which the regional economy (or GRP) increases as a result of the direct spending. Again, the Iron Ore Mining sector sees the largest impacts and is not shown to scale on the graph so that the detail for the other impacted sectors is visible. Other impacted industries include Owner-Occupied Dwellings, Electric Power Transmission and Distribution, Wholesale Trade, and Support Activities for Oil and Gas Operations.

**Figure VI-5.** Top 20 Industries Impacted by Iron Mining, Value Added (Scenario I).

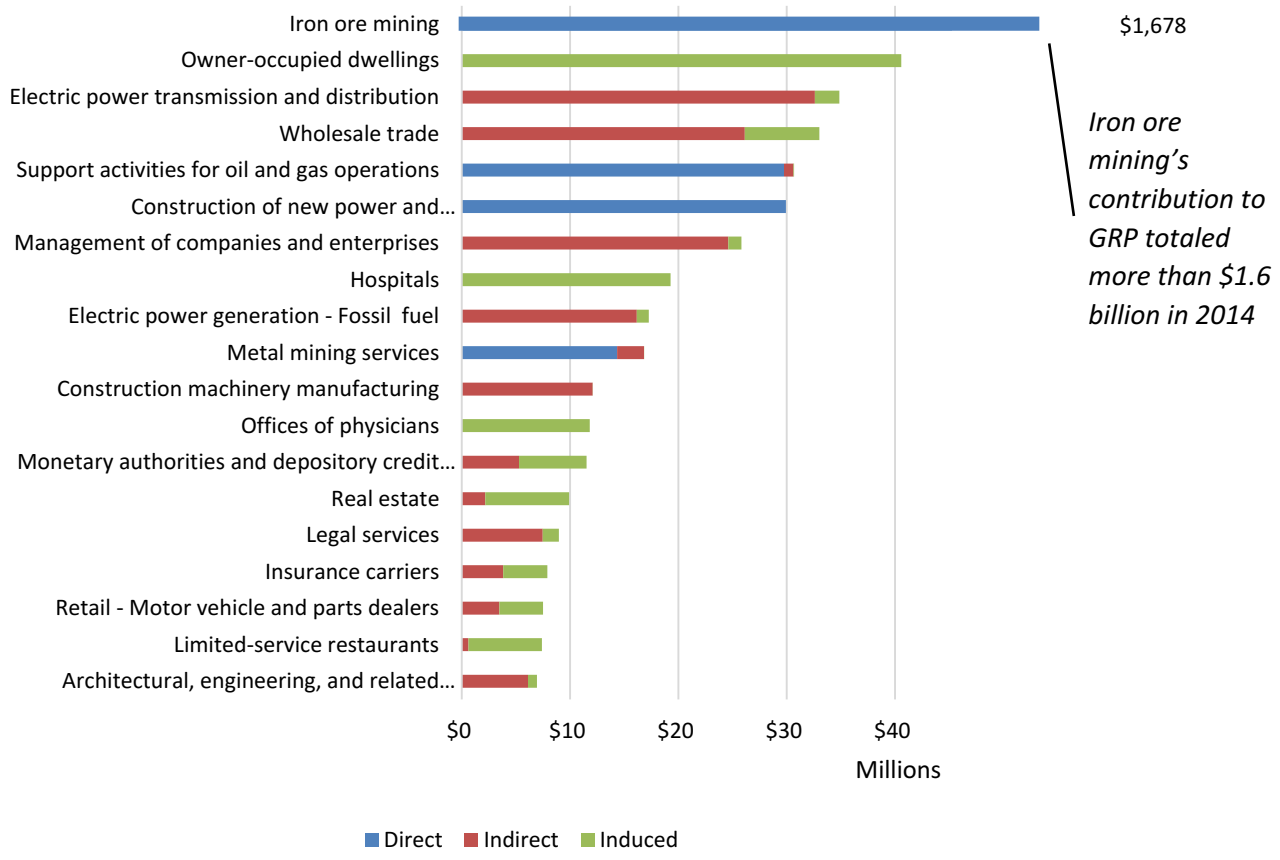


*SOURCE: IMPLAN, 2016*

## 7.2. Statewide Impacts

The following section shows the results of the modeling on the state of Minnesota. Table VI-7 through Table VI-9 summarize the total effects from the two scenarios as well as detailed results of each. It is worth noting that, while the results are slightly larger for the state of Minnesota, the impacts are very similar, as the iron mining industry is fully located within the Arrowhead region. The difference between the two models is due to increased spending from supporting industries (such as electric power transmission and distribution, wholesale trade, oil and gas operations, and others) that have a larger presence beyond the Arrowhead region.

The results of this report highlight the importance of developing cost effective bioremediation sulfate reduction technologies for water. The potential negative economic consequences of not being able to meet the required sulfate levels in water could result in a decline of more than $4 billion in output within the Arrowhead region of Minnesota, and a decline nearly $5 billion statewide, were the taconite industry to cease operations.

**Table VI-7.** Iron Mining Contribution Sensitivity Analysis, by Total Effect on State (in Millions of Dollars).

| *Impact Type* | *Employment* | *Labor Income* | *Value Added* | *Output* |
|---|---|---|---|---|
| Scenario I | 12,091 | $952.2 | $2,462.7 | $4,849.9 |
| Scenario II | 7,209 | $567.4 | $1,481.9 | $2,934.4 |

*SOURCE: IMPLAN, 2016*

**Table VI-8.** Scenario I Impact Detail - Iron Mining's Normal Contribution to State (in Millions of Dollars).

| *Impact Type* | *Employment* | *Labor Income* | *Value Added* | *Output* |
|---|---|---|---|---|
| Direct Effect | 4,546 | $478.1 | $1,671.4 | $3,144.7 |
| Indirect Effect | 3,204 | $269.6 | $445.0 | $1,089.0 |
| Induced Effect | 4,342 | $204.4 | $346.3 | $616.3 |
| Total Effect | 12,091 | $952.2 | $2,462.7 | $4,849.9 |

*SOURCE: IMPLAN, 2016*

**Table VI-9.** Scenario II Impact Detail - Iron Mining's Reduced Contribution to State (in Millions of Dollars).

| *Impact Type* | *Employment* | *Labor Income* | *Value Added* | *Output* |
|---|---|---|---|---|
| Direct Effect | 2,679 | $282.1 | $1,005.7 | $1,906.8 |
| Indirect Effect | 1,943 | $163.5 | $269.8 | $660.3 |
| Induced Effect | 2,587 | $121.8 | $206.4 | $367.3 |
| Total Effect | 7,209 | $567.4 | $1,481.9 | $2,934.4 |

*SOURCE: IMPLAN, 2016*

While this study did not include the economic impacts of the non-ferrous mining industry, the inability to meet sulfate standards could negatively impact that industry as well. Previous research conducted by the Bureau of Business and Economic Research (Skurla 2012) found that the economic impacts of non-ferrous mining on the state (based on 2010 operations estimates and proposed new projects) would add more than $300 million (2012 USD) in value added spending to the state's economy and more than $400 million in total output.

NOTE - Readers are also encouraged to remember the UMD Labovitz School's BBER was asked to supply an economic impact analysis only. Any subsequent policy recommendations should be based on the "big picture" of total impact.

## References


Agency, Minnesota Pollution Control. n.d. *Wild rice study and process of revising standard.* Accessed June 14, 2016. https://www.pca.state.mn.us/water/wild-rice-study-and-process-revising-standard.

Burnes, Jerry. 2016. *United Taconite Restart Moved to August.* June 9. Accessed June 14, 2016. http://www.virginiamn.com/news/local/united-taconite-restart-moved-to-august/article_42aeb086-2e53-11e6-85e1-375c42fbc1d0.html.

CH2MHill. 2010. "Review of Available Technologies for the Removal of Selenium from Water."

Dunbar, Elizabeth. 2015a. *MPR News.* March 25. Accessed May 27, 2016. https://www.mprnews.org/story/2015/03/25/timeline-wild-rice-regulations-in-minnesota.

—. 2015b. *MPR News.* March 25. Accessed May 27, 2016. https://www.mprnews.org/story/2015/03/25/mpca-wild-rice.

Matuszak, Sascha. 2016. *Roads & Kingdoms.* Accessed May 27, 2016. http://roadsandkingdoms.com/2016/the-sacred-grain-of-the-northwoods/.

Minnesota Department of Natural Resources. 2008. "Natural Wild Rice In Minnesota."

Minnesota Department of Revenue. 2015. "2015 Mining Tax Guide." Accessed June 14, 2016. http://www.revenue.state.mn.us/businesses/mineral/Documents/2015_mining_guide.pdf.

Minnesota Pollution Control Agency. 2015a. "Proposal Protecting wild rice from excess sulfate." https://www.pca.state.mn.us/sites/default/files/wq-s6-43k.pdf.

—. 2015b. *Protecting wild rice from too much sulfate: Maps and infographics.* Accessed May 2016. https://www.pca.state.mn.us/sites/default/files/wq-s6-43m.pdf.

Minnesota Pollution Control Agency. 1999. "Sulfate in Minnesota's Ground Water." Saint Paul, MN.

Myers, John. 2015. *Duluth News Tribune.* March 24. Accessed May 2016. http://www.duluthnewstribune.com/news/3707071-mpca-wants-individual-sulfate-limits-wild-rice-waters.

Skurla, Jim. 2012. "The Economic Impact of Ferrous and Non-Ferrous Mining on the State of Minnesota and the Arrowhead Region, including Douglas County, Wisconsin." Duluth, MN.

University of Minnesota Horticulture. 2015. *Zizania aquatica L., Wild Rice; An Evaluation of Cultivation, Domestication, and Production For Use in the United States.* University of Minnesota Horticulture.

World Bank. 2016. "World Bank." *World Bank Commodities Price Data (The Pink Sheet).* February 2. Accessed June 2, 2016. http://pubdocs.worldbank.org/pubdocs/publicdoc/2016/5/391451463000429478/CMO-2016-February-prices.pdf.

## Appendix VI-A. Supporting Figures and Tables

**Figure VI-6.** Minnesota's Iron Ranges.


*SOURCE: MINING HISTORY ASSOCIATION*

**Figure VI-7.** Historical Iron Ore Prices ($/DMT), Annual Averages from 1960 to 2015.

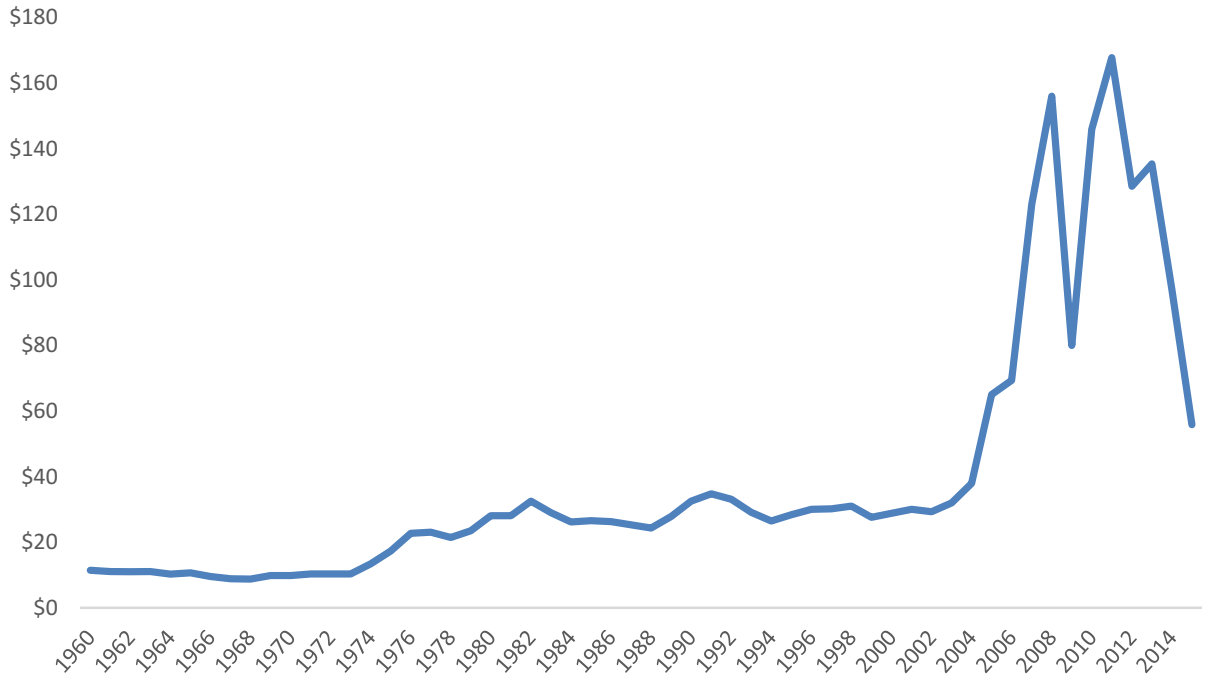


*SOURCE: WORLD BANK*

**Figure VI-8.** Monthly Employment in Iron Mining and Monthly Iron Ore Price ($/DMT).

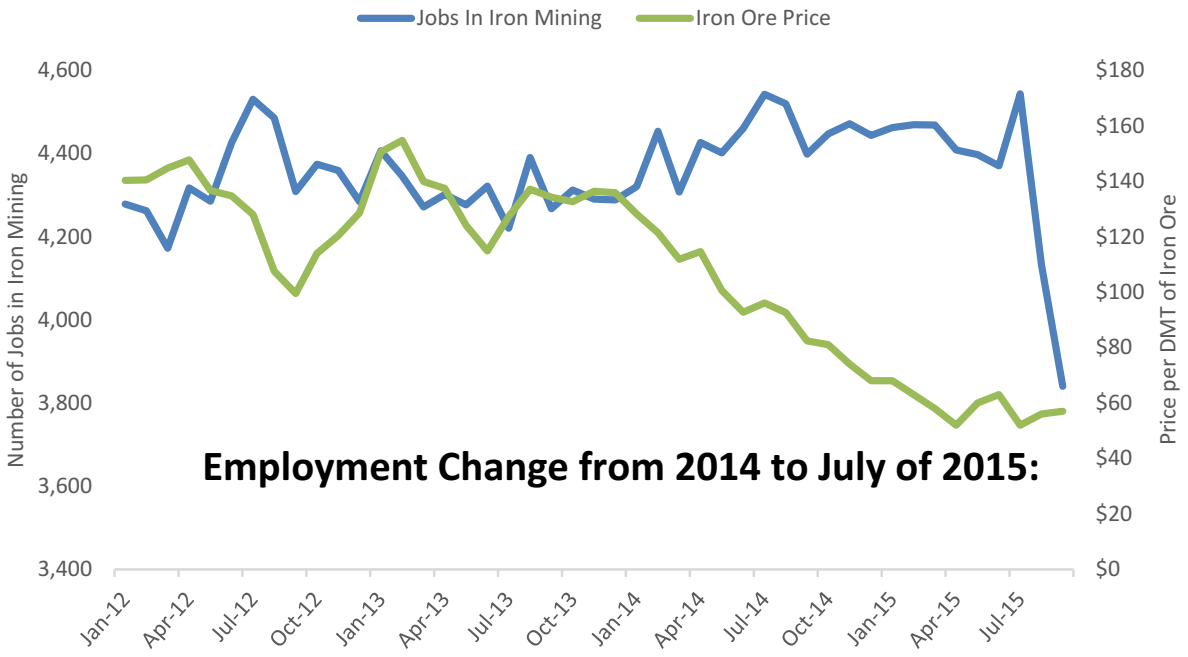


*SOURCE: MN DEED QCEW, THE WORLD BANK*

**Figure VI-9.** Monthly Employment in Support Services for Mining and Monthly Iron Ore Spot Price ($/DMT).

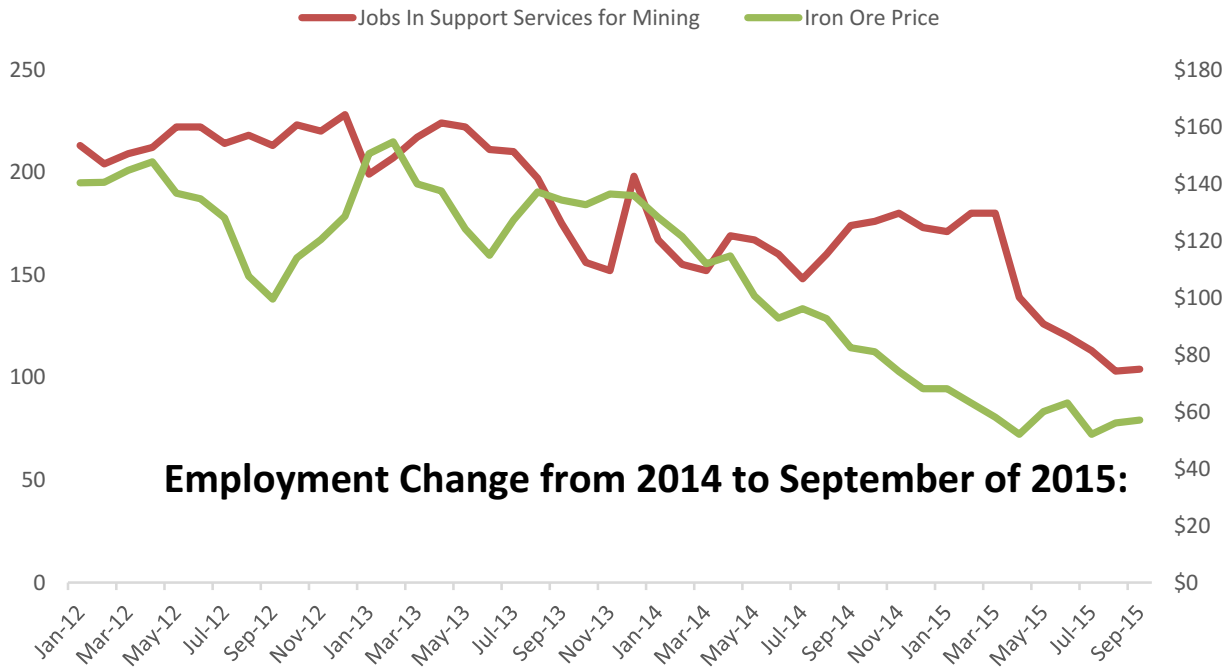


*SOURCE: MN DEED QCEW, THE WORLD BANK*

**Figure VI-10.** Quarterly Wages in Iron Mining and Support Activities for Metal Mining, Total.

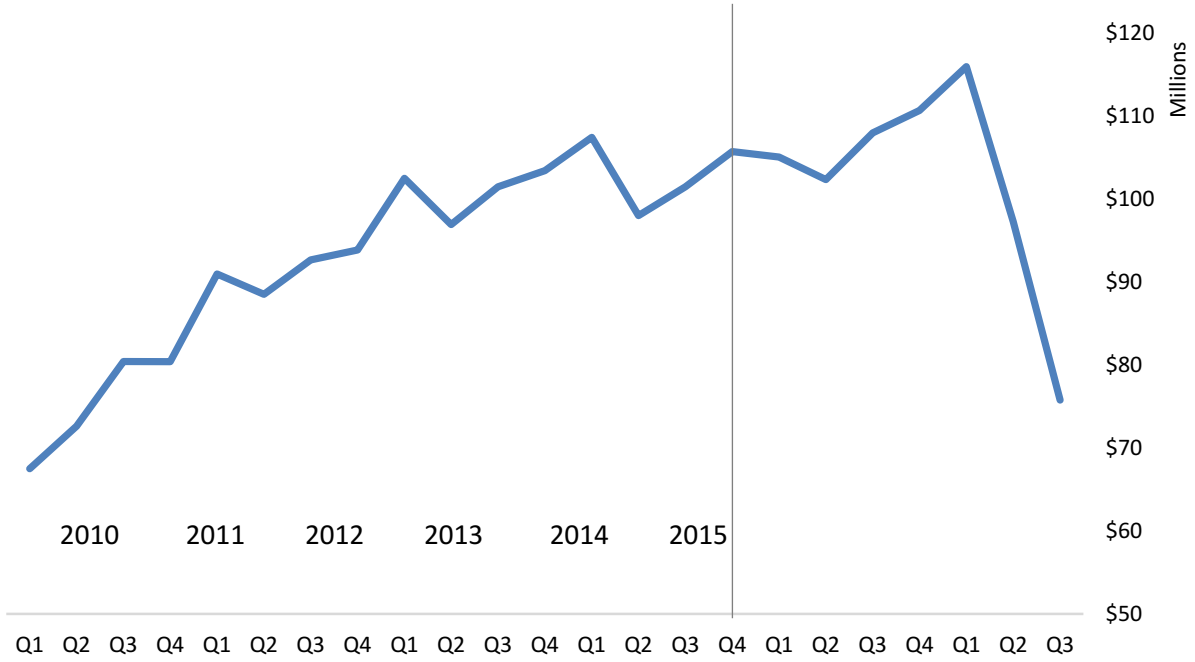


*SOURCE: MN DEED, QUARTERLY CENSUS OF EMPLOYMENT AND WAGES (QCEW)*

## Appendix VI-B. Definitions Used in This Report

**Backward Linkages**: The interconnection of an industry to other industries from which it purchases its inputs in order to produce its output. It is measured as the proportion of intermediate consumption to the total output of the sector (direct backward linkage) or to the total output multiplier (total backward linkage). An industry has significant backward linkages when its production of output requires substantial intermediate inputs from many other industries[26].

**Direct Effect**: Initial new spending in the study area resulting from the project.

**Employment**: Estimates (from U.S. Department of Commerce secondary data) are in terms of jobs, not in terms of full-time equivalent employees. Therefore, these jobs may be temporary, part-time, or short-term.

**Gross Output**: The value of local production required to sustain activities.

**Indirect Effect**: The additional inter-industry spending from the direct impact.

**Induced Effect**: The impact of additional household expenditures resulting from the direct and indirect impact.

**Labor Income**: All forms of employment income, including employee compensation (wages and benefits) and proprietor income.

**Leakages**: Any payments made to imports or value added sectors that do not in turn re-spend the dollars within the region.

**Multipliers:** Total production requirements within the Study Area for every unit of production sold to Final Demand. Total production will vary depending on whether Induced Effects are included and the method of inclusion. Multipliers may be constructed for output, employment, and every component of Value Added.

**Sulfate:** A salt or ester of sulfuric acid. Currently regulated at 10 parts per million in designated wild rice waters.

**Sulfide:** An inorganic anion of sulfur. Sulfides exposed by mining operations or produced by transformation of sulfates by sulfur-reducing bacteria can react with air and water to make sulfuric acid, which is harmful to aquatic ecosystems. Sulfide is also toxic to wild rice at low concentrations.

**Value Added**: A measure of the impacting industry's contribution to the local community; it includes wages, rents, interest, and profits.

[26]IMPLAN, 2015

## Appendix VI-C. IMPLAN Assumptions

The following are suggested assumptions for accepting the impact model:[27]

The following section shows the results of the modeling on the state of Minnesota. Table VI-7 through Table VI-9 summarize the total effects from the two scenarios as well as detailed results of each. It is worth noting that, while the results are slightly larger for the state of Minnesota, the impacts are very similar, as the iron mining industry is fully located within the Arrowhead region. The difference between the two models is due to increased spending from supporting industries (such as electric power transmission and distribution, wholesale trade, oil and gas operations, and others) that have a larger presence beyond the Arrowhead region.

The results of this report highlight the importance of developing cost effective bioremediation sulfate reduction technologies for water. The potential negative economic consequences of not being able to meet the required sulfate levels in water could result in a decline of more than $4 billion in output within the Arrowhead region of Minnesota, and a decline nearly $5 billion statewide, were the taconite industry to cease operations.

[27]Bureau of Economic Analysis https://www.bea.gov/papers/pdf/WP_IOMIA_RIMSII_020612.pdf

# Appendix 1. Bioreactor Construction, Flow, and Operation

The first section of Appendix 1 reviews the overall functional design and operation of the rafts and proceeds with details about how the individual components were built, connected, and operated. The second section briefly describes the overall experimental objectives addressed in each raft.

## Bioreactor and precipitation module construction[28]

Bioreactor skins (7' X 7' X 12'; Fig. 1A, B; Fig. 2A) were made from single 60 mil high density polyethylene (HDPE) pond liner sheets (Industrial & Environmental Concepts, Inc., Lakeville, MN) joined together by a plastic-welded seam. The top 12 inches of each side was folded inward to form 90° flaps (Fig. 1C, 1D), which were plastic welded to the adjacent flaps and formed part of the top surface of the bioreactor. To form the pyramidal base the angled HDPE sheets were welded together, leaving a 1' X 1' opening in the center which was covered by an HDPE sheet containing a 4" diameter circular cutout in the center that served as a discharge port. The 1-ft$^2$ base was stabilized by plastic welding a ½" thick HDPE plate of corresponding dimensions to the inside surface, forming a rigid plate that could accept the press-fitted PVC standpipe and serve as a port for the rubber plug that sealed the module (see detailed descriptions below).

At the top of the bioreactor, a rigid surface was formed by four HDPE dock floats (3' X 4' X 1' thick, foam-filled; ~600 lbs. buoyancy, each; Premier Materials Technology, Minneapolis, MN; Fig. 3A), which were positioned in a staggered array (Fig. 1A, 1C; 2B), so that a 1' X 1' opening was formed in the center. The dock floats were attached to each other (see details below) and the assembly was inserted into the open top of the bioreactor skin (Fig. 1C; 2B) so that the top 12 inches of each side sheet, which had been folded over and plastic welded to the adjoining flap at the factory, laid on the top surface of the floats (Fig. 1C, 1D; 2B). The float assembly was overlaid and sealed with a single HDPE sheet welded around the edges to the bioreactor skin (Rafts A & B) or with layers of ½" marine plywood, HDPE, and a rough-surfaced HDPE (Raft C) to provide additional stability and safety (Fig. 1D; 3B, 1C). The dock float assembly was attached to the overlying HDPE sheets, plywood, and deck boards (see details below), using bolts and screws (Fig. 3). The 1' X 1' central opening at the top the bioreactor was framed with untreated 2" X 4" X 15½" construction lumber, which was joined together by connecting plates and attached to the dock floats with 3/8" hex bolts (Fig. 1D; 2C; 3B, 3C). Treated decking boards (5/4" X 6" X 6') were similarly attached near the periphery of the bioreactor to provide additional strength and stability (Fig. 1D; 2C), and ½" eye bolts were attached to the dock floats at the four corners of the module for lifting and manipulating the unit during construction. Figure 2C shows the top of a completed, sealed bioreactor.

Vertical structural support was established by securing a 12 ft. long PVC standpipe to the top and bottom of the bioreactor (Fig. 4). The standpipe, consisting of a 2" ID X 2' long upper section and a 4" ID X 10' long lower section (Fig. 1A, D), which could be sealed with a rubber plug assembly (Fig. 5). Near the bottom of the standpipe, twelve 12" X ¼" milled slots (Fig. 4A, 4C) allowed water that had flowed down through the bioreactor to return to the top. The returning (effluent) water exited the standpipe through a tee-fitting in the upper 2" ID pipe (Fig. 4A, 4B) that was connected to the effluent pump (see

[28] See Appendix 1.A and 1.B for detailed information about materials and supplies, including source, model numbers, and dimensions, where applicable.

details below) by a reinforced ½" ID PVC effluent hose running through ½" NPT polypropylene bulkhead fittings on the side of the bioreactor. At the top of the bioreactor the standpipe was inserted into a 2" PVC cap (Fig. 4A), which was secured to one corner of the central opening frame or, in later versions to the plywood cover.

The plug assembly (Fig. 5) that sealed the bottom of the standpipe and discharge port was held in place by a rope that ran inside the standpipe to the top, where it passed under the PVC cap and was secured with a cleat or friction fitting on the 2" X 4" wood frame. The bottom (outside) of the plug assembly was similarly attached to a rope that was secured to the top of the bioreactor. The discharge port was designed to be opened by releasing the inner plug rope and pulling on the outside rope, and closed by reversing this sequence. The plug assembly for Raft C (Fig. 4C; 5B) was slightly modified but operated similarly.

Approximately 2,200 lbs. of shredded polypropylene fiber, which provided about 200 lbs. of buoyancy, was inserted into each bioreactor through the central access hole. The bioreactors were stabilized by placing about 100 lbs. of taconite pellets into the base of the module through a temporary standpipe inserted through central opening. Bioreactor weight and buoyancy were balanced to provide just enough floatation so that the bottom surface of the dock float assembly (and thus the upper surface of the fiber material) was always under water. This arrangement minimized air contact at the water surface, maintaining conditions necessary to support anaerobic bacterial growth. Moreover, keeping the bioreactor fibers and the incoming and outgoing liquid lines under the waterline helped ensure stable operating conditions throughout the year, and prevented the bioreactors from freezing in the winter. Additional modules designed for sulfur precipitation and settling (see below), or for nutrient and amendment storage and distribution (see below), were constructed following the same design as the bioreactors, except that they were not filled with polypropylene fiber.

## Flow and operation[29]

**General operational concept** (See detailed descriptions below and in Figures 1-6; see the following section, Bioreactor flow, monitoring, and sampling for details about individual rafts). Seven bioreactor modules, along with additional modules designed for sulfur species precipitation and settling or for material storage, were tied together to form a stable raft (see Fig. 6 for raft variations). Sulfate-containing pit water was pumped into an intake manifold, where it was split and evenly distributed to the bioreactors. Carbon-containing substrates (ethanol, lactic acid, or sodium lactate) and nitrogen supplements (urea and monoammonium phosphate), were added to the influent water at each bioreactor, and the mixture was allowed to percolate down through the polypropylene fibers, which housed biofilms containing native sulfate reducing bacteria that could convert sulfates into hydrogen sulfide. After passing downward through the bioreactor matrix (2-4 days, depending on experimental conditions, see below), the sulfide-containing water entered the standpipe through slots cut in the bottom and flowed back up and out through an effluent hose attached to a tee fitting near the top. Effluent water was collected from each bioreactor, combined, mixed with various chemicals designed to react with sulfides and form insoluble sulfur precipitates, and pumped into a precipitation module. The precipitates settled to the base of the tank, which could be emptied by pumping or by pulling the plug in

[29] Figures 7, 8, and 9 illustrate flow schematics for Rafts A, B, and C, respectively.

the discharge port. Over the life of the project, three rafts (A, B, and C; Fig. 6) were constructed. These were tied together, along with support structures and solar panels, to form a single unit (Fig. 2G).

**Influent system details**. Oxygen-poor pit water was drawn to the raft complex through a 1½" ID PVC hose fitted with a filter screen from a depth of 30 feet, at a point about 100 feet from the rafts, using a 12 VDC variable speed pump, which was suspended under water inside the storage module (Fig. 6, Modules A0, B0, and C8). For Rafts A and B, influent water entered a submerged plenum consisting of a 4" X 3' PVC tube with a 1½" inlet on one end, a removal inspection cap at the other end, and seven, ½"outlets with barbed fittings around the circumference to attach hoses that supplied influent water to each bioreactor. For Raft C, influent water was pumped into a vertical plenum consisting of a 2" X 12' PVC tube with a 1½" inlet on the bottom, a removal inspection cap on the top, and seven ¾" hose outlets around the circumference to supply each bioreactor.

This pressurized system provided equal influent flows to each bioreactor through ½" (Rafts A & B) or ¾" (Raft C) ID PVC or neoprene hoses, which were connected via barbed or Qwik-Lok™ fittings to bulkhead fittings in the HDPE skins, positioned below the waterline at the interface of the dock floats and fiber mass. Before entering the bioreactor, influent water passed through a ½" ID Hall Effect flow meter that generated a pulse signal, which was used to monitor flow on a continuous basis, and through a standard ½" PVC ball valve (Rafts A & B) or a ¾" pinch valve (Raft C ) for controlling flow. Inside the bioreactor, influent water was distributed across the shredded fiber surface through an "H" shaped distribution system of ½" PVC hose with terminal T fittings (Fig. 4C).

**Nutrient pump and system details**. Metabolic substrates and nutrient amendments were provided to the bioreactors in amounts and rates that varied according to experimental protocols. Carbon substrates (ethanol, Chippewa Valley Ethanol, Benson, MN, lactic acid, or sodium lactate, Hawkins, Inc. Roseville, MN) and a mix of nutrient amendments (nitrogen as urea, phosphorus as mono-ammonium phosphate (MAP), Fertamix, Jordan, MN) were stored as solutions in pillow bladder tanks (Aero Tec Laboratories, Ramsey, NJ) that were submerged inside the storage module (Fig. 6, Modules A8, B8, and C8) and individual components were supplied to the bioreactors on schedules that varied according to the specific experimental protocols. Substrates and amendments were delivered to the bioreactors using a 12 VDC pump (Clark Solutions, Hudson, MA), controlled by a programmable 12 VDC timer (YANP, Yueqing City, Zhejiang Province Yipan Industrial Zone, China). From the pump, substrate/nutrient mixture flowed into a push-to-connect manifold, where it was split into seven different flows, each directed to an individual bioreactor through ¼" OD nylon tubing that passed through the inside of the ½" or ¾" influent hose to the center of each bioreactor. The substrate/amendment mix passed through a controllable Dwyer flow meter (Dwyer Instrument Co., Michigan City, ID), before terminating inside the influent hose and mixing with the influent water, which was then dispersed through an H-shaped distribution system made from ½" heavy duty PVC hose (Fig. 4C).

**Composite effluent plenum details**. All bioreactor effluents were pumped to a common effluent standpipe, where they mixed to form a composite prior to the addition of chemical precipitants and delivery to the precipitation/settling tank. The effluent standpipe consisted of a vertical, open-topped, 4" ID X 6' long PVC pipe that received effluent lines from each bioreactor through seven ½" PVC Tee fittings inserted five feet below the water level. The remaining outlet on each Tee fitting held a ½" ID X 6' long PVC pipe that extended above the water line and was used as a port to sample individual effluent

flows. The composite effluent could be sampled directly through the open top of the standpipe or by a separate pipe fitted near the bottom of the standpipe.

A 12 VDC variable speed pump, connected to the base of the standpipe by a 1½" PVC hose, drew down the composite effluent volume and created negative pressure on the individual bioreactor effluent lines, which assisted the inflow of bioreactor effluent. The composite effluent was then pumped to top of the precipitation/settling tank, and mixed with chemicals intended to precipitate and remove sulfur species from solution (see below).

**Effluent treatment system design and operation details**. Several effluent treatment regimens were tested during the course of the experiments on Rafts A and B.[30] A 12 VDC diaphragm pump was used to transport chemical amendments (see below) from containers housed in or alongside the storage module to the well sides of 75 L Pentair Wellmate pressurized bladder tanks, which were suspended alongside the storage module. Bladder tank pressure was maintained by pressurized air from submerged 55-gallon drums, which were suspended beneath the rafts and held in place by rock ballast, either in the air supply drum itself (Raft B) or in a separate drum that was attached to the air supply drum (Raft A). The chemical amendments flowed from the bladder storage tanks through ⅜" HDPE tubing into the composite effluent line via a universal IV spike drip system, which could be adjusted by dial or thumbwheel flow control valves. The combined fluids either entered into the precipitation tanks directly, or passed through an inline mixing tube prior to flowing into the tank.

**Precipitation amendments**.

Raft A

Formic acid [pH control] - added into the composite plenum bottom outlet hose.

Hydrogen peroxide [hydrogen sulfide oxidation] - added immediately before the composite effluent enters the precipitation/settling tank. The hydrogen peroxide was dripped into the composite effluent line just upstream of a mixing tube that opened into the precipitation tank, which ensured complete mixing as the water enters the precipitation/settling tank.

Aluminum sulfate [sulfur coagulation and precipitation] – dripped into the effluent line between the first and second precipitation/settling tanks.

Raft B

Ferric chloride [sulfur coagulation and precipitation] – added in the effluent line just before entering a mixing tube leading into the single precipitation/settling tank.

As the treated bioreactor effluent flowed across the upper regions of the tank, the iron sulfide and other precipitates formed by the reaction between hydrogen sulfide and the chemical amendments settled to the bottom of the tank. The final effluent exited through an outlet bulkhead fitting located about 18" below the waterline on the opposite side of the tank, flowing either into a second settling tank or

[30] Although Raft C was fully prepared and inoculated with sulfate reducing bacteria, the limited time for establishing robust microbial growth and sulfate reduction capacity was considered insufficient for reliable testing, so Raft C's precipitation and settling tanks were used on Raft A, instead.

directly into the pit. A 2” PVC check valve attached to the discharge bulkhead fitting prevented backflow from the pit lake into the settling tank.

**Figure 1.** Bioreactor module materials, design, and construction.

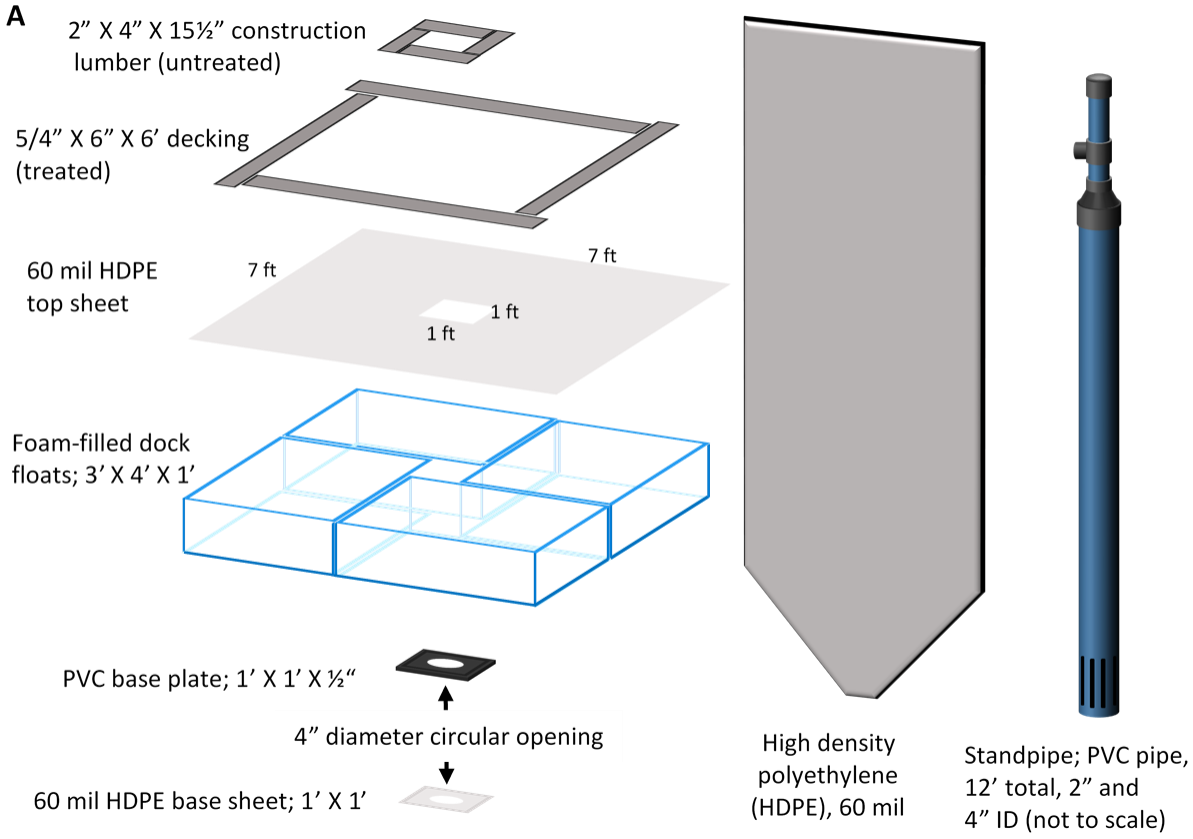

**Figure 1 (continued).**

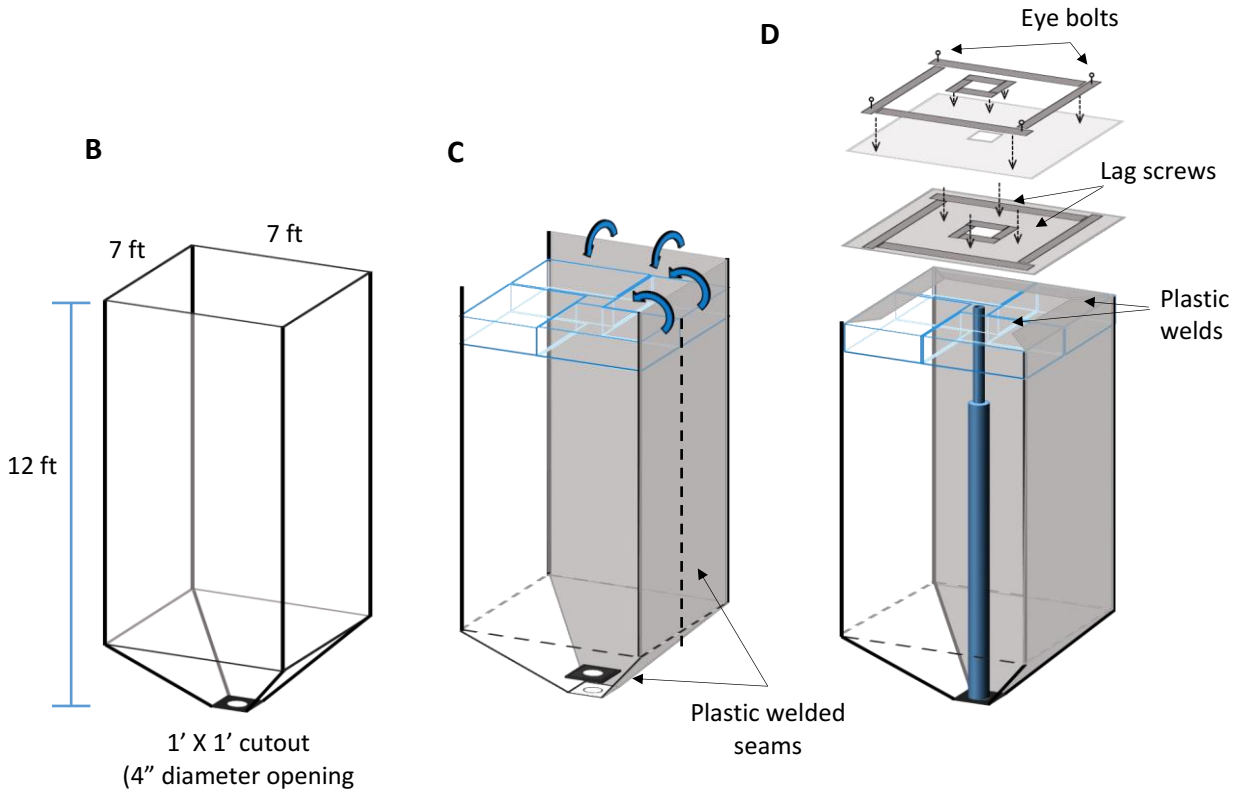


**Fig. 1.** Bioreactor general design and construction. **A**. Bioreactors were constructed using common, easily-obtainable materials, described in detail in the narrative. Note that individual wall-sized sheets are shown in this figure for clarity, but that the bioreactor skins were constructed from a single HDPE sheet, which was folded and sealed with a plastic weld at the middle of one wall (see Fig 1.C). All cutting, folding, and plastic welding was performed at the factory (Industrial & Environmental Concepts, Inc., Lakeville, MN). **B**. Overall skin dimensions were 7' X 7' X 12' (L X W X Total Depth). The bottom 24" of each HDPE membrane wall was cut at an angle, which, when bent inward and joined with the adjacent membranes, formed an inverted pyramid with a 1-$ft^2$ opening at the bottom. This open section was covered with a 1-$ft^2$ HDPE sheet that contained a 4" diameter circular cutout, and was reinforced with a 1-$ft^2$ PVC plate, containing a congruent 4" diameter opening. **C.** Plastic, foam filled dock floats formed a rigid top surface, which was attached by plastic welds to the flaps folded at the top of the bioreactor skin. **D.** A layer of HDPE membrane (Rafts A & B) or layers (bottom to top) of ½" marine plywood, smooth HDPE membrane, and rough HDPE membrane (Raft C), each containing a central 1-$ft^2$ cutout, were laid over the top of the dock floats. These layers were secured by 5/4" X 6" treated deck boards that were laid out and attached to the periphery of the floats with lag screws. A square of 2" X 4" construction lumber framing the central opening was joined together by connecting plates and attached to the dock floats with lag screws. Eye bolts inserted through the ends of the peripheral deck boards provided attachment points for lifting the empty bioreactors and for securing functioning bioreactors to each other to form rafts. The central PVC standpipe, which provided vertical rigidity to the bioreactor, was press-fitted to the bottom HDPE plate and attached by metal strapping to the inside of the 2" X 4" frame (Rafts A & B) or to the bottom surface of the marine plywood covering (Raft C).

**Figure 2.** Bioreactor modules and rafts; construction and final composition.

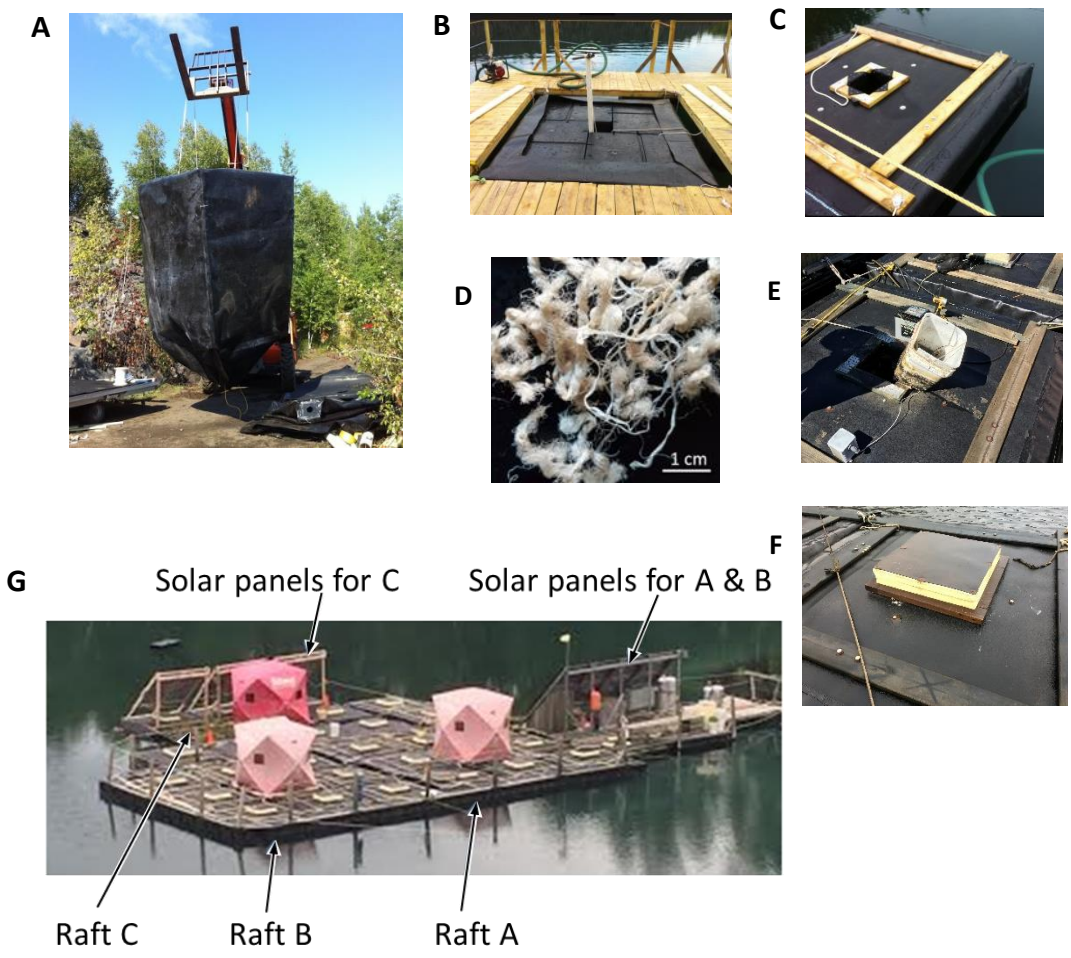


**Fig. 2.** Bioreactor modules and rafts; construction and final composition. (**A)** Bioreactors were partially constructed on land and lifted into a (**B**) floating construction dock, where (**C**) the top membrane, plywood, and structural wood pieces were added, the standpipe was inserted and fixed in place, and (**D**) the bioreactors were filled with shredded polypropylene fiber. Taconite ballast was added to the bottom of the bioreactor using a temporary standpipe inserted through the center opening (not shown). (**E**) On finished bioreactors, the center opening held square plastic bucket, which served to hold tubing outlets, flow meters, monitoring devices, and a standard 12V marine battery (shown partially hidden behind the bucket). (**F**) The central opening was covered by insulation panels and HPDE membrane. (**G**) Seven individual bioreactor units were coupled physically into rafts (**D**) which operated as independent units (Rafts A, B, and C), each with their own influent and effluent flows and modules dedicated to water pumps, material storage, and sulfur species precipitation and settling. The three rafts were attached to each other to form a single unit, which also housed solar panels, a supplemental generator, storage spaces, and work shelters.

**Figure 3.** Dock floats and attachment details.

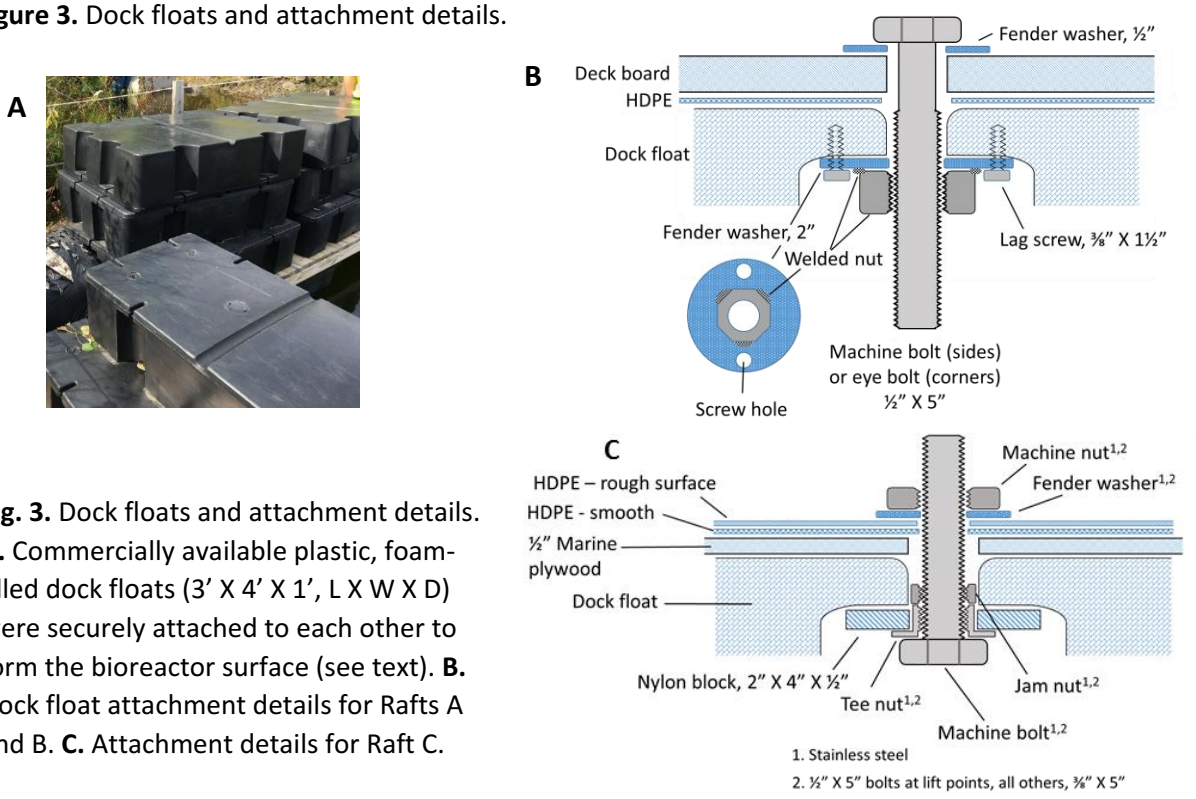


**Fig. 3.** Dock floats and attachment details. **A.** Commercially available plastic, foam-filled dock floats (3' X 4' X 1', L X W X D) were securely attached to each other to form the bioreactor surface (see text). **B.** Dock float attachment details for Rafts A and B. **C.** Attachment details for Raft C.

**Figure 4.** Standpipe detail and "H-shaped" influent water distribution system.

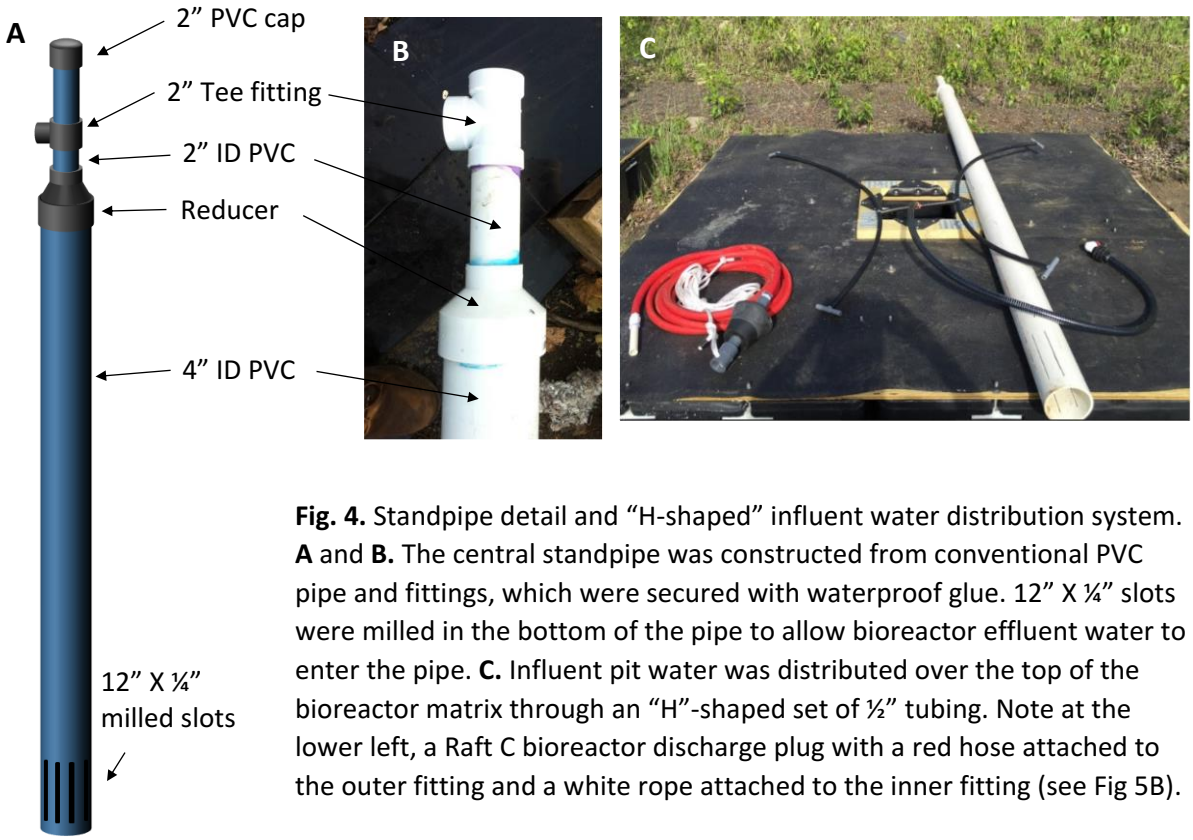


**Fig. 4.** Standpipe detail and "H-shaped" influent water distribution system. **A** and **B.** The central standpipe was constructed from conventional PVC pipe and fittings, which were secured with waterproof glue. 12" X ¼" slots were milled in the bottom of the pipe to allow bioreactor effluent water to enter the pipe. **C.** Influent pit water was distributed over the top of the bioreactor matrix through an "H"-shaped set of ½" tubing. Note at the lower left, a Raft C bioreactor discharge plug with a red hose attached to the outer fitting and a white rope attached to the inner fitting (see Fig 5B).

**Figure 6.** Discharge port plugs.

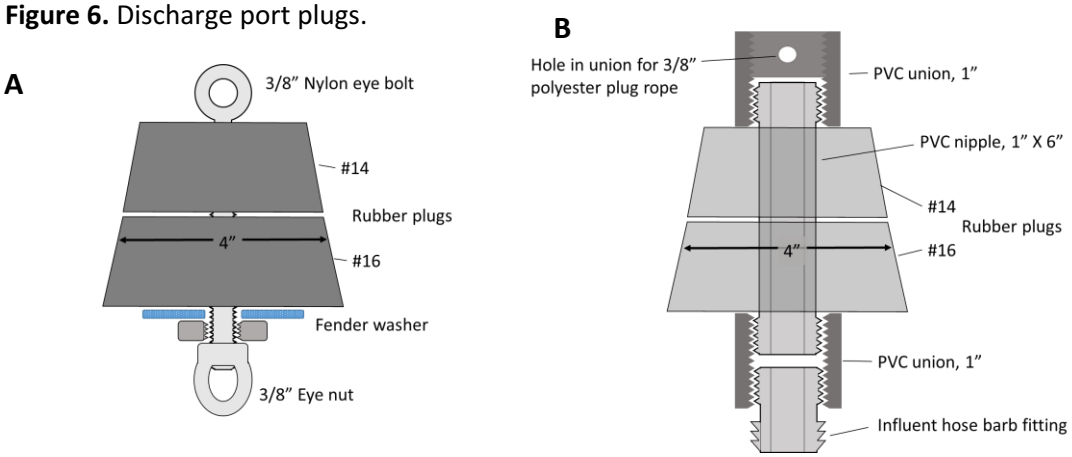


**Fig. 5.** Discharge port plugs. The bottom of each standpipe in Raft A and B (**A**) and Raft C (**B**) was sealed with a rubber plug that could be opened from the outside via a rope (Raft A and B) or a hose (Raft C) that was attached to the bottom of the plug and ran outside the bioreactor to the top, and re-sealed by pulling on a rope attached to the top of the plug and running to the top of the raft through the standpipe.

**Figure 5.** Raft configuration and flow paths.

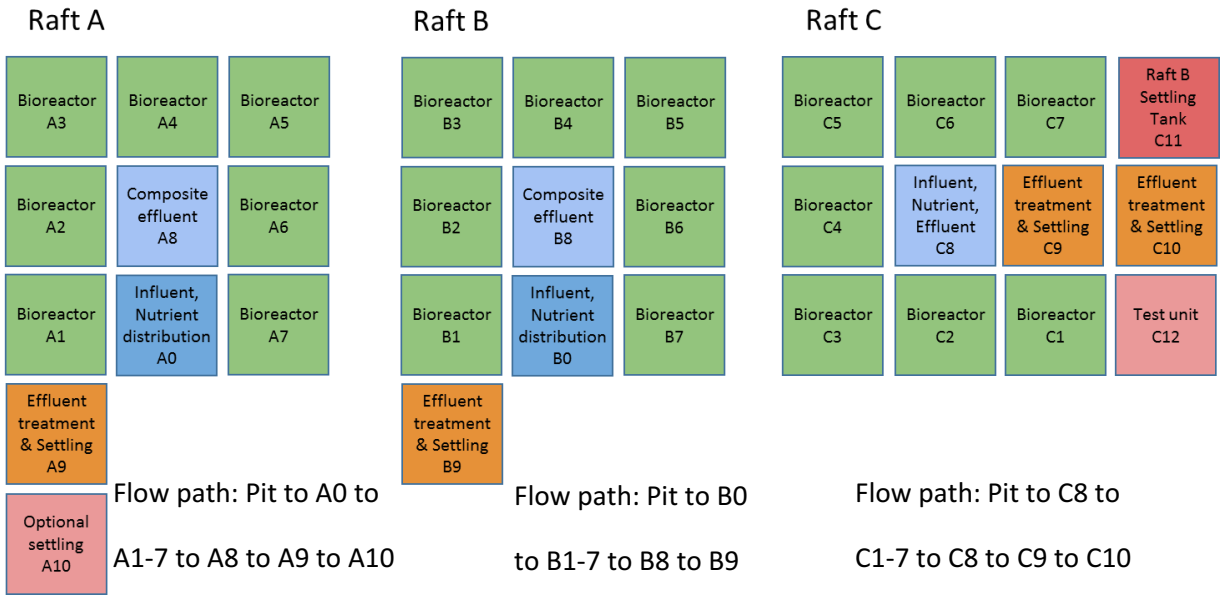


**Fig. 6.** Raft configuration and flow path. The bioreactors, precipitation tanks, and other modules (1-10) were configured similarly in Rafts A, B, and C. For Raft A, pit water was pumped into an influent manifold in the central module (A0), and distributed in parallel to each of the seven bioreactors (A1-A7). Effluent water from each bioreactor was combined in an effluent standpipe contained in module A8, and pumped into a settling and precipitation tank (A9) or two tanks in series (A9 & A10). Various chemical treatments designed to enhance precipitation were added to the combined effluent as it entered the precipitation/settling tank. Flow paths were similar for Rafts B and C. Raft C was designed for extended precipitation testing and included additional test modules, as well as the supplemental settling tank originally built for Raft B.

**Figure 7.** Raft A flow schematic.

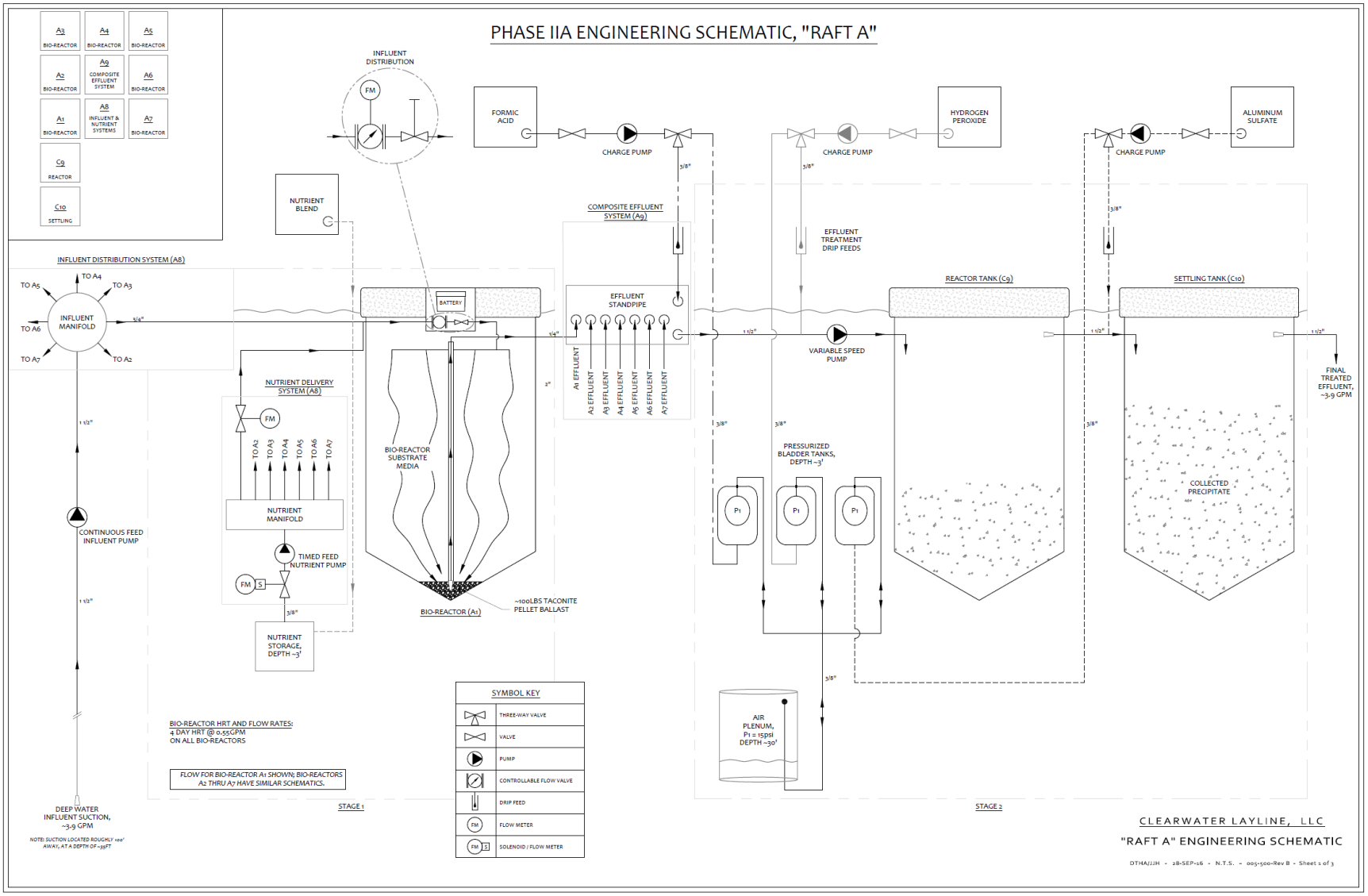

**Figure 8.** Raft B flow schematic.

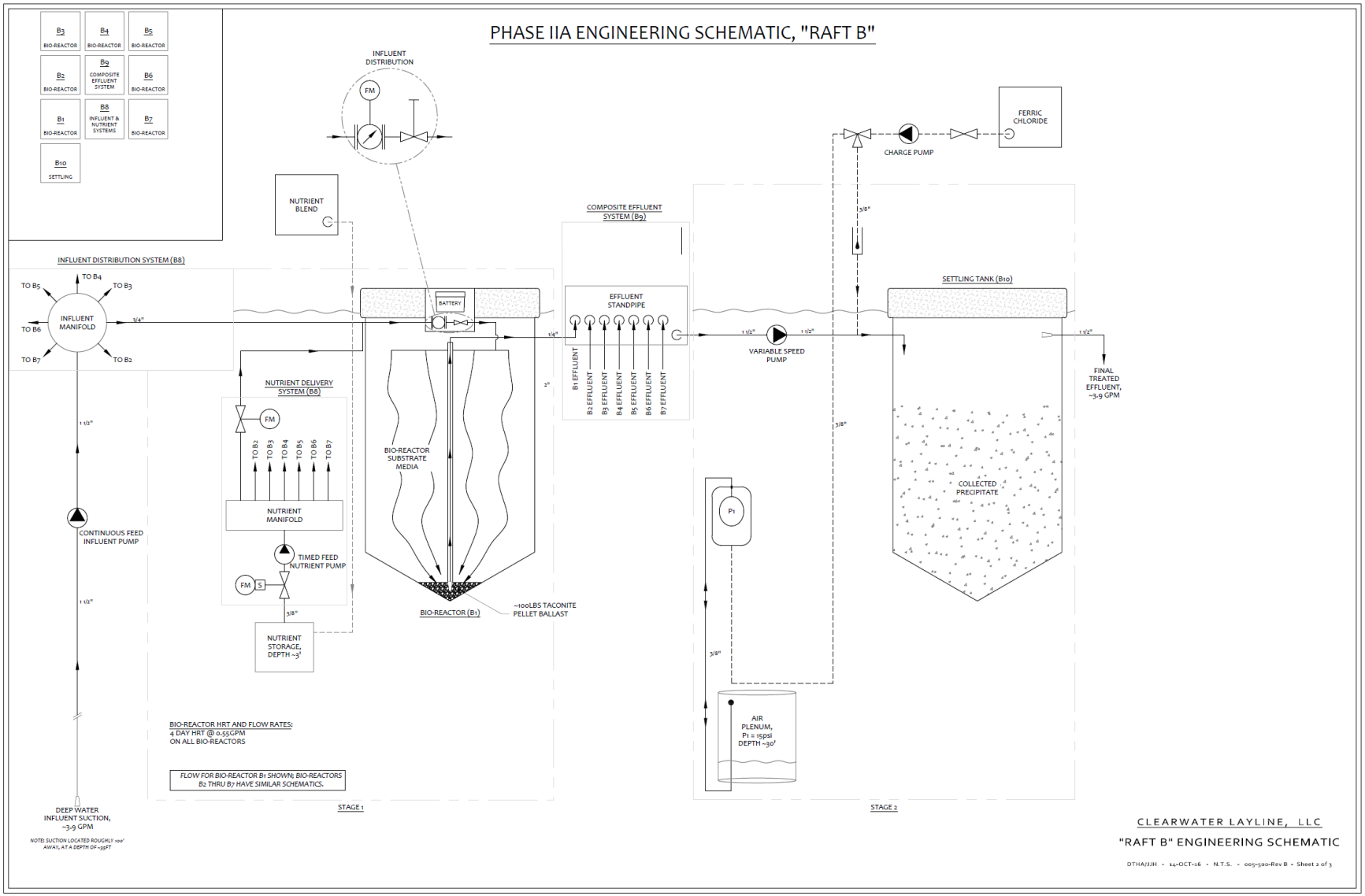

**Figure 9.** Raft C flow schematic.

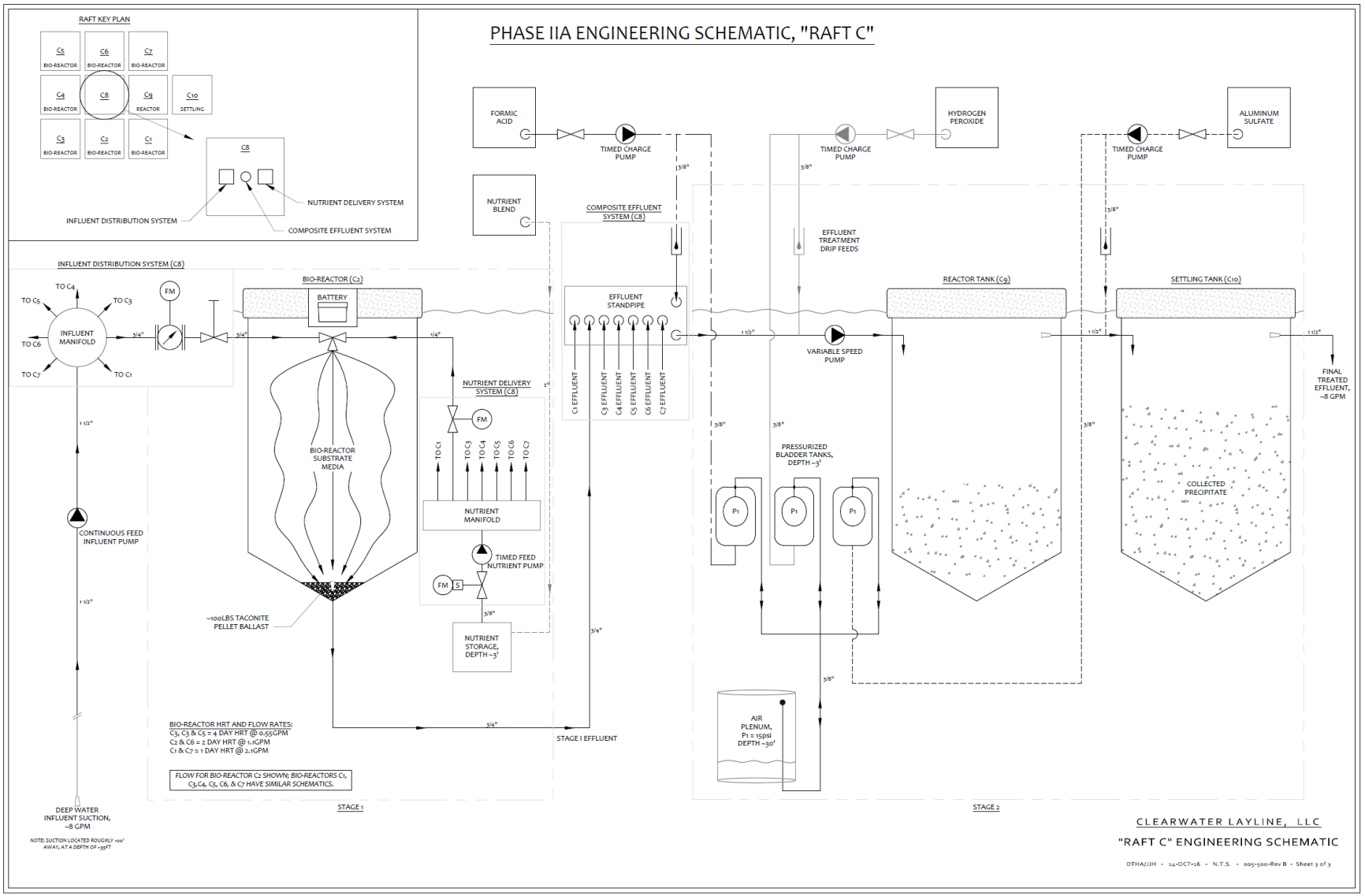

**Appendix 1A.** Influent and nutrient pumps and equipment.

**A. Intake screen**

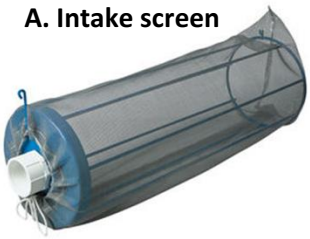

Deep pit water influent

**B. 12V Mini brushless DC pump**

Influent & effluent pumps; submersible

**C. Hall effect flow meter**

Influent flow meter; ½" ID

**D. Chem-flex pillow tanks**

Ethanol & lactic acid storage; 1000 gal (4 $m^3$) & 250 gal (1$m^3$)

**E. 12V DC gear pump**

Nutrient pump

**F. 12 DC programmable timer**

Nutrient feed

**G. Push-to-connect manifold**

Nutrient feed; 3/8" OD tube

**H. Dwyer flow meter**

Nutrient feed; adjustable

**I. Qwik-Loc™ Fittings**

Nutrient feed

**Appendix 1B.** Chemical additive storage and delivery.

**J. 12V DC Diaphragm pump**

Additive delivery;
2.2 GPM @ 70 PSI

**K. Pentair Wellmate pressurized bladder tanks**

Precipitation chemical storage

**L. Precipitation chemical pressurizing system**

Deep air plenum; constant air pressure for bladder tanks

**M. PVC Connectors and valves**

3-way push

3-way compression

Push connect elbow

Push connect MPT

PVC ball valve; ½”

Swing-Check valve

**N. IV spike, control valve, dripper**

Universal IV spike and control valve for chemical delivery

Dripper for aluminum sulfate

**Appendix 1C.** Assorted tubes, hoses, fittings, and other materials.

**O. Rollerflex™ 145 Heavy Duty PVC Hose**

**P. 1/2" ID x 13/16" OD POLYAIR® Blue Air & Water Hose**

**Q. Flexible Nylon Semi-Clear Tubing**

**R. Inline pipe mixing tube**

**S. Threaded rod eye nut**

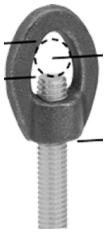

**T. Routing eyebolt (plastic)**

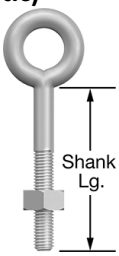


**U. Heavy duty polypropylene tank fitting**

**V. HDPE adapter**

**W. Backflow-prevention check valve**

**X. Tapered plugs**

**Appendix 1D.** Bioreactor materials, supplies, and equipment.

| Text Reference | # | Item | Primary use | Source | | Details/Description | Order number |
|---|---|---|---|---|---|---|---|
| Fig. 1, 2 | | HDPE pond liner | Module skins | Industrial & Environmental Concepts, Inc. | Lakeville, MN | 60 mil | Inquire |
| Fig. 3 | | Dock floats | Modules | Premier Materials Technology | Minneapolis, MN | Polyethylene shell, expanded polystyrene foam filled, 3'X4'X1' | 3648-12 |
| Fig. 3, 5 | | Washers, oversized | Plug assemblies | McMaster-Carr | Elmhurst, IL | 18-8 stainless steel washers | 98370A021 |
| Appendix A.1 | A | Kleen Flo Intake Screen | Pit water intake | Fleet Farm | Circle Pines, MN | | 87790 |
| " | B | 12V Mini Brushless DC pump | Influent & effluent pumps | ebay.com, various suppliers | China | 12VDC brushless, 50-1235A, 3000 LPH, submersible | |
| " | C | Hall Effect flow meter | Influent flow meter | ebay.com, various suppliers | China | 1-30 L/min, waterproof, | |
| " | D | Chem-flex pillow tanks: | Nutrients | Aero Tec Laboratories | Ramsey, NJ | | |
| " | D | 1000 gal (4 $m^3$) | | | | | 110730 |
| " | D | 250 gal (1 $m^3$) | | | | | 110717 |
| " | E | 12V DC Gear pump | Nutrient pump | Clark Solutions | Hudson, MA | 12VDC, 3300 rpm, 3.4A, 0-190 lph | MGC4 |
| " | F | Programmable timer | Nutrient feed | YANP (Yanpan Electric Science and Technology Co, Ltd.) | Yuequing City, China | 12VDC | YP109A |
| " | G | Push-to-connect manifold | Nutrient feed | McMaster-Carr | Elmhurst, IL | Nylon, 6 outlet, 3/8" inlet x 1/4" outlet | 5779K784 |
| " | H | Dwyer flow meter | Nutrient feed | Dwyer Instrument Co. | Michigan City, IN | | MMA-30 |
| " | I | Qwik-Loc™ Quick Connect fittings | Influent system | United States Plastic Corp | Lima, OH | Various types | |

| Text Reference | # | Item | Primary use | Source | | Details/Description | Order number |
|---|---|---|---|---|---|---|---|
| Appendix A.2 | J | 12V DC Diaphragm pump | Chemical additives | Northern Equipment | Burnsville, MN | NorthStar NS Series, 12V, 2.2 GPM@ 70 psi | 2682272 |
| “ | K | Wellmate® pressurized bladder tanks | Chemical additives | Pentair (Pro Source) | Minneapolis, MN | 75L, composite | PSC-20-6 |
| “ | M | 1/2" PVC Ball valve | Chemical additives | Menards | Virginia, MN | | |
| “ | M | Swing-Check valve | Chemical additives | Menards | Virginia, MN | | |
| “ | M | Push-to-Connect fittings: | Chemical additives | Menards | Virginia, MN | | |
| “ | | 3-way push-to-connect directional control valve | | United States Plastic Corp | Lima, OH | | |
| “ | | 3-way valve for compression fittings | | United States Plastic Corp | Lima, OH | | |
| “ | | MPT adapter | | United States Plastic Corp | Lima, OH | | |
| “ | | Elbow | | United States Plastic Corp | Lima, OH | | |
| “ | N | Hospiria IV Regulator Dial-a-Flow® | Chemical additives | Abcore Medical | Elmhurst, IL | 20-250 ml/hr | |
| “ | N | Administration IV LIne with injection site | Chemical additives | Abcore Medical | Elmhurst, IL | 76" | |
| Appendix A.3 | O | Heavy duty PVC Hose | Various | United States Plastic Corp | Lima, OH | 3/4" ID X 15/16" OD Rollerflex™ 145 | 54968 |
| “ | P | Kuri Tec® POLYAIR® PVC Air & Water Hose | Various | United States Plastic Corp | Lima, OH | I/2" ID X 313/16" OD | 60127 |
| “ | Q | Nylon tubing | Various | McMaster-Carr | Elmhurst, IL | 0.18" ID, 1/4" OD, 100 ft | 5112K63 |
| “ | R | Inline pipe mixing tube | Chemical additives | McMaster-Carr | Elmhurst, IL | PVC, 2" X 19" | 35385K27 |
| “ | S | Threaded rod eye nuts | Lifting bolts | McMaster-Carr | Elmhurst, IL | 3/8"-16 threaded rod size | 9436T041 |
| “ | T | Routing eyebolts (plastic) | Raft attachment | McMaster-Carr | Elmhurst, IL | 3/8" - 16 thread size, 4" shank | 9686T84 |
| “ | U | Polypropylene tank fittings | Various | United States Plastic Corp | Lima, OH | 1/2", fits 1-7/16" hole | 11800 |

| Text Reference | # | Item | Primary use | Source | | Details/Description | Order number |
|---|---|---|---|---|---|---|---|
| “ | V | HDPE barbed adapters | Various | United States Plastic Corp | Lima, OH | Various sizes | |
| “ | W | Backflow-prevention check valve | Final effluent outlet | McMaster-Carr | Elmhurst, IL | PVC, 2" X 6" | 45275K47 |
| “ | X | Tapered round plugs | Plug assemblies | McMaster-Carr | Elmhurst, IL | Various sizes | 954K138, etc. |
| | | | | | | | |
| Chemicals | | Ethanol, denatured with methanol | Nutrients & amendments | Chippewa Valley Ethanol Co. | Benson, MN | 95% ethanol, 5% methanol | |
| “ | | Lactic acid | Nutrients & amendments | Hawkins, Inc. | Roseville, MN | 50% | |
| “ | | Sodium lactate | Nutrients & amendments | Hawkins, Inc. | Roseville, MN | 60% | |
| “ | | Monoammonium phosphate (MAP) | Nutrients & amendments | Fertamix | Jordon, MN | Pure crystal form dissolved in well water on site | |
| “ | | Urea | Nutrients & amendments | Fertamix | Jordon, MN | Pure crystal form dissolved in well water on site | |
| “ | | Hydrogen peroxide | Precipitation | Hawkins, Inc. | Roseville, MN | 34%, Technical Grade | |
| “ | | Aluminum sulfate | Precipitation | Hawkins, Inc. | Roseville, MN | 48.5% | |
| “ | | Formic acid | Precipitation | Hawkins, Inc. | Roseville, MN | 30% | |
| “ | | Ferric chloride | Precipitation | Hawkins, Inc | Roseville, MN | 17.5% | |

## Bioreactor flow, monitoring, and sampling

Each raft contained seven independently operating bioreactors plus tanks or containers devoted to nutrient storage and distribution and bio-effluent treatment to promote precipitation and settling. Each raft was operated independently, with the individual bioreactors acting as within-raft replicates. Thus, several experiments were conducted over the course of the project, testing various nutrient additions, flow rates (hydraulic retention time), and sulfide precipitation schemes.

**Raft A** (Figures 10 and 11) operated continuously for over two years and was used primarily as a testing platform for sulfate-reducing bacterial growth and bioreactor performance using ethanol as a substrate.

**Figure 10.** Raft A Flow Diagram

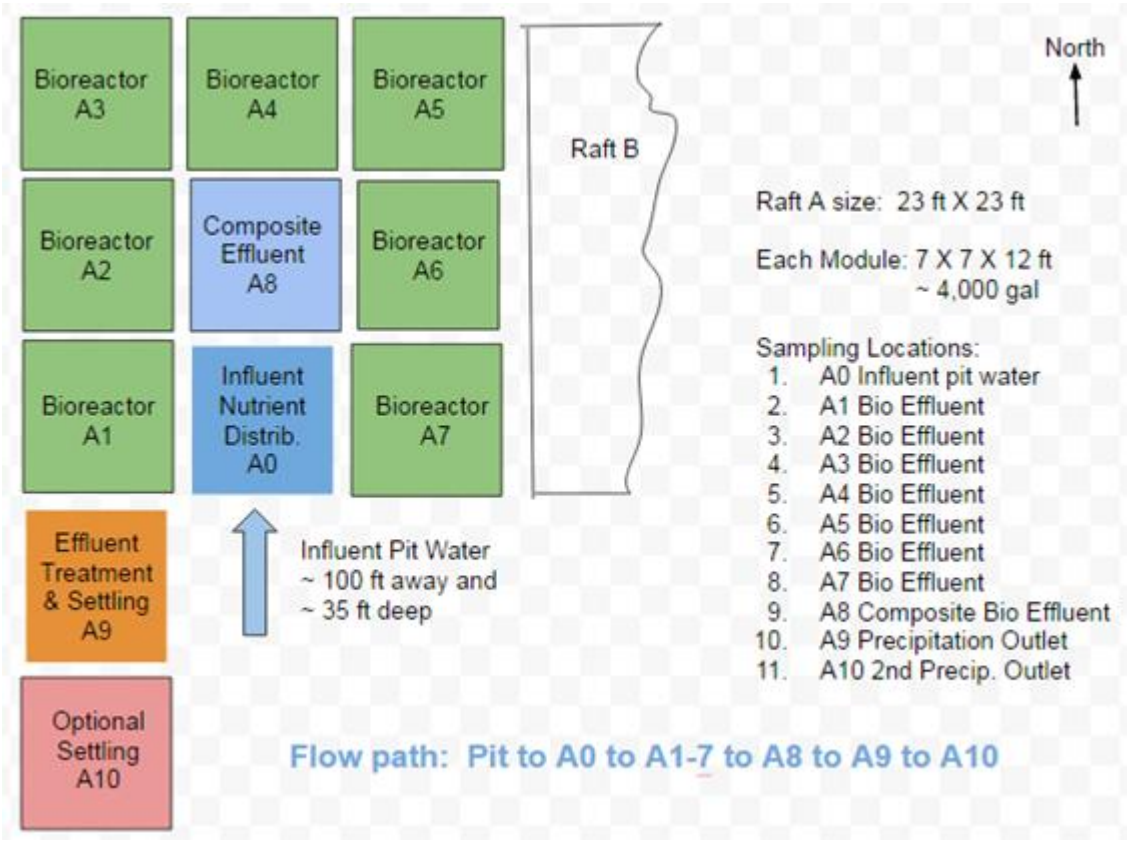


**Fig. 10.** Raft A layout and sampling locations. Pit water influent and nutrient amendments were distributed among each of the seven Raft A bioreactors. Bio-effluents were combined in a central unit (Composite Effluent A8) and pumped to a treatment and settling tank. Water samples were routinely collected at various sites and tested for sulfate, sulfide, and numerous physico-chemical characteristics.

**Figure 11.** Raft A Flow Diagram

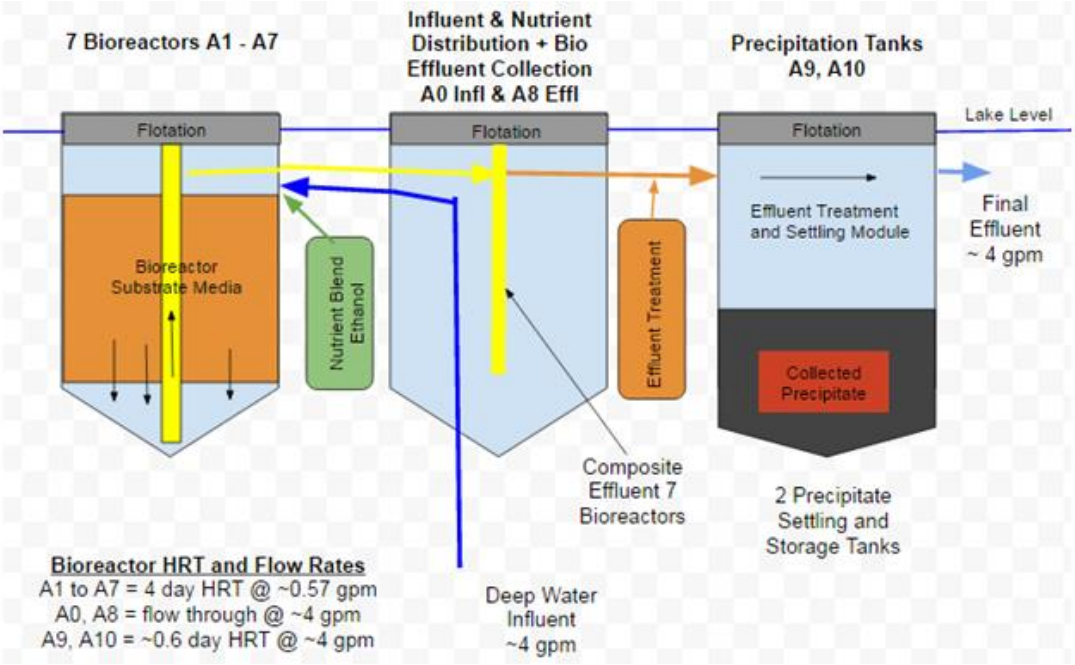


**Fig. 11.** Basic bioreactor and precipitation tank design and detailed flow diagram for Raft A. Each 4000 gallon bioreactor (left) was filled from a common pit water intake source, with flow rates controlled by a pump. Nutrient amendments, including phosphorus, nitrogen, and a carbon source, such as ethanol, are added. After passage through the bioreactors, bio-effluent water was combined and pumped into a settling/ precipitation tank (right), where it was chemically treated and solids were allowed to precipitate.

The overall flow rate for Raft A is approximately 15 liters per minute (lpm), with an average of 2.2 lpm for each bioreactor. No attempt was made to equalize flows for individual bioreactors, and each was allowed to develop a natural flow between 1.4 and 3.0 lpm. This variation allowed us to track performance of individual bioreactors as related to flow rate. Flows of individual bioreactors were monitored with flow meters placed at the inlet to each bioreactor prior to nutrient addition (Fig. 7). The pulse signal was transmitted wirelessly to remote internet based monitoring stations, allowing near real-time flow monitoring (see Sec. III. Energy and Control Systems).

Performance monitoring was done by sampling and analyzing water from the 11 different influent and effluent locations indicated in Figure 10. A comparison of these results provided a metric for the performance of each individual module within the system as well as for the overall system. In addition, sampling rods inserted into modules A2, A4, and A6 were used for periodic sampling of water and biological growth on the fiber substrate at three to six different depths (see section IV. Microbiology).

Raft A was supplied with ethanol as a carbon substrate, plus monoammonium phosphate (MAP) and urea, which provided phosphorus and nitrogen. The composite effluent treatment system for Raft A consisted of three parts; pH adjustment using an organic acid, oxidation with hydrogen peroxide, and flocculation and precipitation using aluminum sulfate (see Sec. V. Chemical treatments). Figure 11 illustrates a conceptual cross section view of these amendments and water flow for Raft A.

**Raft B** (Figures 12 and 13) was designed, constructed, and operated similarly to Raft A but was supplied with lactic acid, and later sodium lactate, as carbon substrates, along with MAP and urea nutrient amendments. In addition to testing alternate carbon substrates, Raft B was also used to test various sulfide precipitation regimes. The overall flow rate for Raft B was similar to Raft A at approximately 15 lpm, with an average of 2.2 lpm for each bioreactor, and individual bioreactor flow was approximately 15 lpm, with an average of 2.2 lpm for each bioreactor. Individual bioreactor flow, monitoring, and performance was treated as in Raft A. Raft B contained 10 water sampling locations (Fig. 12), and three bioreactors contained sampling rods to facilitate water and biological collections at different depths (see Sec. IV. Microbiology).

**Figure 12.** Raft B layout (aerial view)

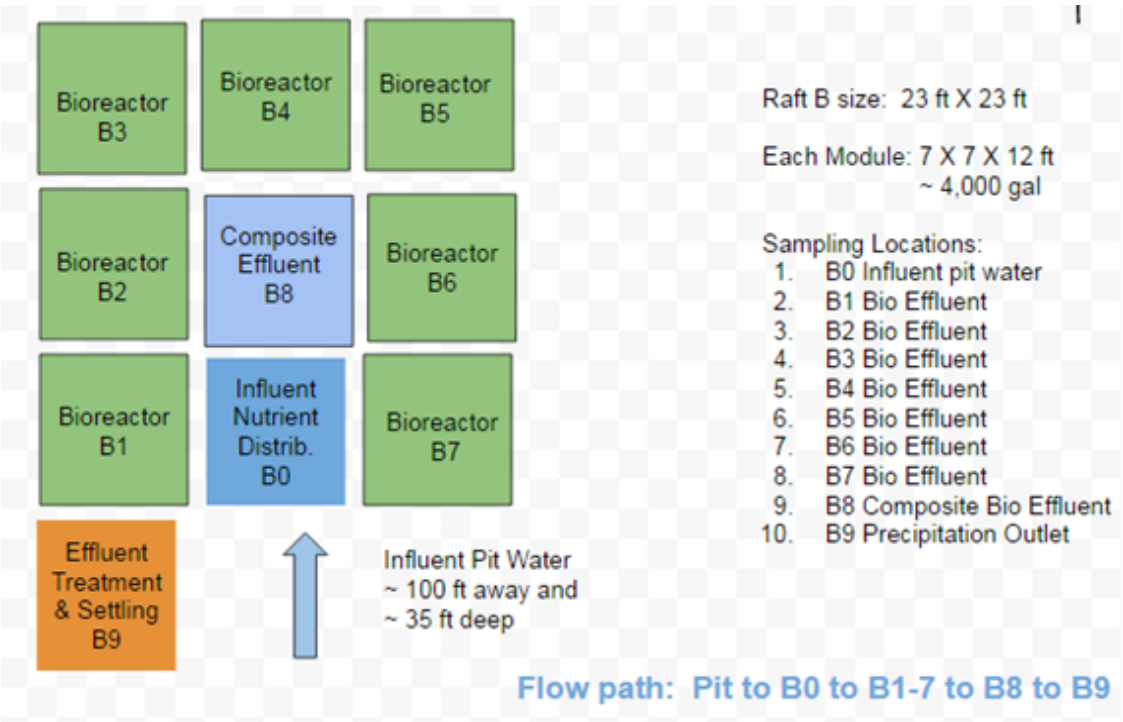


**Fig. 12.** Raft B layout and sampling locations. Pit water influent and nutrient amendments were distributed among each of the seven Raft B bioreactors. Bio-effluents were combined in a central unit (Composite Effluent) and pumped to a treatment and settling tank. Water samples were routinely collected at various sites and tested for sulfate, sulfide, and numerous physico-chemical characteristics.

**Figure 13.** Raft B Flow Diagram

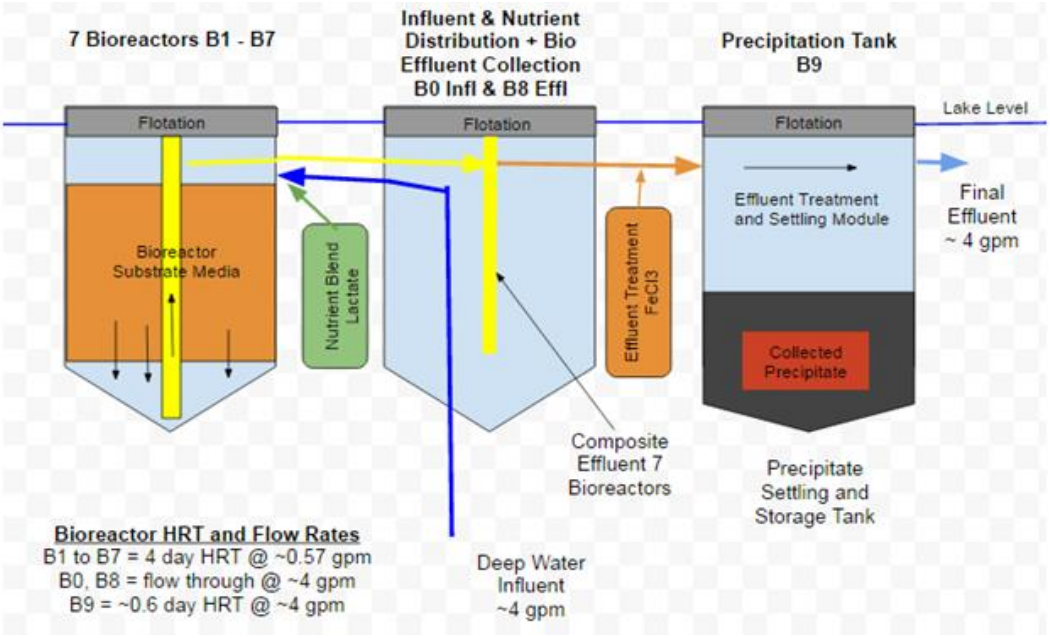


**Fig. 13.** Basic bioreactor and precipitation tank design and detailed flow diagram for Raft B. Each 4000 gallon bioreactor (left) is filled from a common pit water intake source, with flow rates controlled by a pump. Nutrient amendments, including phosphorus, nitrogen, and a carbon source, such as lactate, are added separately from a common source. After passage through the bioreactors, bio-effluent water is combined and pumped into a settling/precipitation tank (right), where it is chemically treated and solids are allowed to precipitate.

The composite effluent treatment system used ferric chloride to form iron sulfide and provide flocculation and precipitation. Figure 13 presents a conceptual cross-section view of the water and amendment flows for Raft B.

**Raft C** (Figures 14 – 16) was developed based on the experiences gained from operating Rafts A and B to provide a platform for testing specific MnDRIVE project objectives, including:

- Testing the effect of bioreactor flow rate and HRT (hydraulic retention time) on the production of hydrogen sulfide.
- Biological sampling of the biomass development over time on all bioreactors.
- Development of a totally solar photovoltaic power source that could fully and independently support raft operation throughout the summer and winter months.
- Provide more reliable flow monitoring, with sensors protected from the effects of moisture and corrosive gases.
- Develop a design that minimizes gassing-off of the generated hydrogen sulfide and avoids air locking.

**Figure 14.** Raft C layout (aerial view).

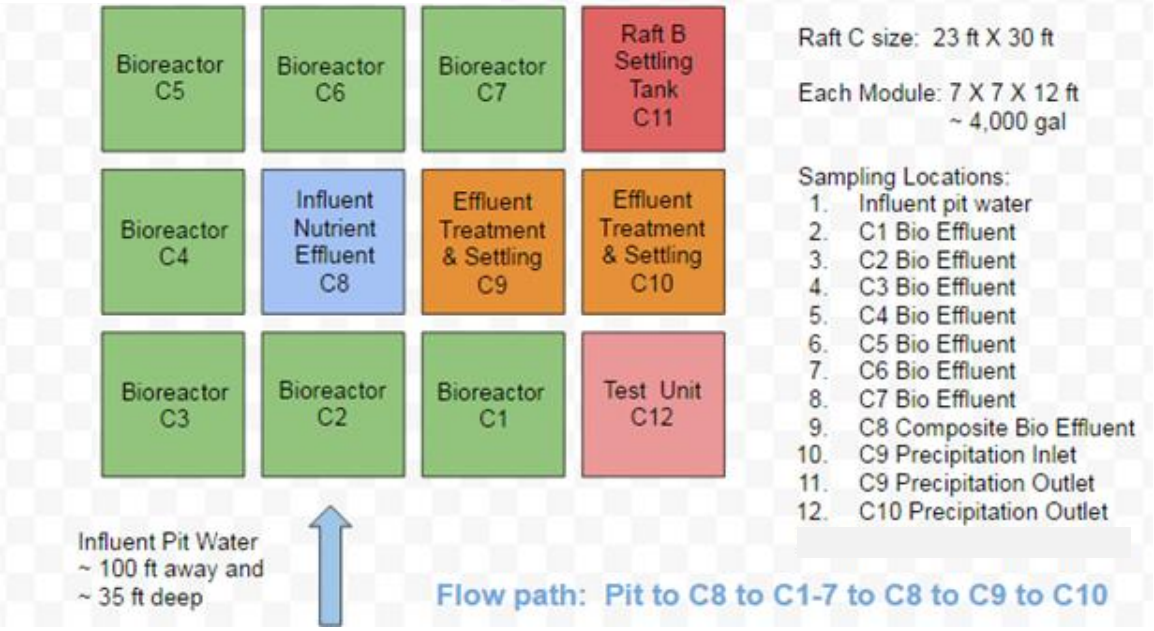


**Fig. 14.** Raft C layout and sampling locations. Pit water influent and nutrient amendments were distributed among each of the seven Raft C bioreactors. Bio-effluents were combined in a central unit and pumped to a treatment and settling tank. Water samples were routinely collected at various sites and tested for sulfate, sulfide, and numerous physico-chemical characteristics.

**Figure 15.** Raft C remote flow monitoring.


**Fig. 15.** Actual printout for Raft C flow monitoring; sent automatically to a remote server.

**Figure 16.** Raft C Flow Diagram.

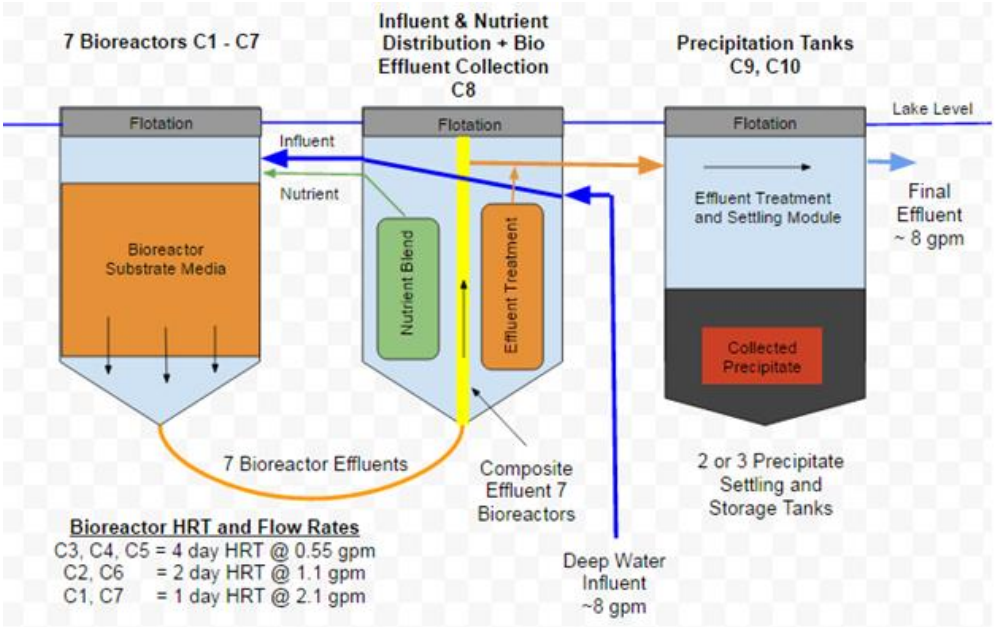


**Fig. 16.** Basic bioreactor and precipitation tank design and detailed flow diagram for Raft C. Each 4,000-gallon bioreactor (left) was filled from a common pit water intake source, with flow rates controlled by a pump. Nutrient amendments, including phosphorus, nitrogen, and a carbon source, such lactate, were added separately from a common source. After passage through the bioreactors, bio-effluent water was combined and pumped into a settling/precipitation tank (right), where it was chemically treated and solids were allowed to precipitate.

Raft C was designed with the standard seven bioreactor modules, but differed from Rafts A and B by using a central module to house the influent, nutrient feed, and effluent collection and flow monitoring mechanisms. Raft C also had a second precipitation/settling tank (Fig. 14, modules C9 and C10).

Raft C was designed to accommodate separate flow rates for different bioreactors and had a maximal flow rate of approximately 30 lpm. Three different target flow rates were regulated by separate pumps to replicate bioreactors; bioreactors C3, C4, and C5 were controlled to provide a four-day HRT, similar to the Raft A and B experiments, C2 and C6 doubled the standard flow, resulting in a two-day HRT, and C1 and C7 controlled to achieve a one-day HRT. This flow rate variation allowed us to track performance as related to hydraulic residence time. Flow to individual bioreactors was monitored with flow meters located in module C8 (Fig. 9 and 14). The pulse signal was transmitted wirelessly to remote internet based monitoring stations. This allowed for near real-time flow monitoring the functioning of the system (see Sec. III. Energy and Control Systems). Figure 15 shows a printout of the remote flow monitoring that demonstrates the different flow rates.

Performance monitoring was done by sampling and analyzing water from the nine effluent sampling locations indicated in Figure 14. Results from these measurements provided a comparison of performance for each individual module within the system as well as overall system performance. In addition, sampling rods inserted into all bioreactor modules allowed periodic sampling of water and

biomass on the fiber substrate at three to six different depths. This provided access for biological sampling for analysis of sulfate-reducing bacteria populations across the profile of these bioreactors. Raft C was initially supplied with lactic acid, then switched to sodium lactate.

The composite effluent treatment system designed for Raft C was a three-part treatment consisting of pH adjustment, oxidation using hydrogen peroxide, and flocculation/precipitation with aluminum sulfate (see Sec. V. Chemical treatment). A conceptual cross section view of these amendments and water flow for Experiment C is shown in Figure 16.

The system used for Raft C to draw the bioreactor effluent off from the modules kept the effluent flow deep in cold water with no place for gases to accumulate and thus avoided the potential for air locking of effluent lines. When effluent water with high levels of dissolved hydrogen sulfide was allowed to warm with reduced pressure, it tended to gas off and accumulate in the high points of the line. This design has proven to eliminate this problem.

The solar power system for Experiment C used six solar photovoltaic panels, nine 12VDC storage batteries, and a single controller to provide all power. The solar panels were mounted on top of bioreactor modules C1, C2, and C3 as shown in Figure 2G.

# Appendix 2. Chemical Analysis of Bioreactor Ballast Materials

## Lithogeochemical Analysis of Taconite Pellets Used For Bioreactor Raft Ballast

Taconite pellets were used as ballast in the SRB bioreactors and settling tanks located at the Pit 5NE field site. Since pit water being treated in the bioreactor and settling tank system comes in contact with these taconite pellets during treatment, knowledge of the chemical composition of the taconite pellets used for ballast is essential.

Taconite pellets from two sources were used as ballast in the original bioreactors and settling tanks[31] in Raft A and B (A8, B8). These pellets were produced at the former LTV Steel Mining Company taconite processing facility located approximately six miles north of Hoyt Lakes, Minnesota, which operated between 1957 and 2001. Taconite pellets were collected along former railroad lines, rinsed vigorously with water, and placed in the bioreactors and settling tanks.

Taconite pellets used for bioreactor ballast in Raft C were produced in 2015 at the Cliffs Natural Resources Northshore taconite processing plant, located in Silver Bay, Minnesota, and obtained directly from Cliffs Natural Resources immediately after production. These pellets were rinsed vigorously with water prior to their installation within the bioreactors associated with Raft C. Raft C does not contain settling tanks.

A five-gallon pail of LTV pellets utilized as ballast in Rafts A and B and a five-gallon pail of Northshore pellets utilized as ballast in Raft C were provided to NRRI scientists for analysis by Jeffrey Hanson of Clearwater Layline, LLC. Each pail contained approximately 25 kilograms of pellets. In preparation for lithogeochemical analysis, pellets from each pail were successively split using a sample splitter into two samples weighing approximately 500 grams each. The ~500 gram samples representing Raft A and Raft B ballast were labeled MN-15-AB1 and MN-15-AB2. The ~500 gram samples representing Raft C ballast were labeled MN-15-C1 and MN-15-C2. Samples were placed in Great Value$_{TM}$ slider-zipper quartz-size freezer bags which were labeled with the appropriate sample numbers.

The four ~500 gram samples contained in the freezer bags were shipped from the NRRI Duluth facility to Activation Laboratories Ltd. (ACTLABS; Ancaster, Ontario, Canada) for crushing/grinding and lithogeochemical analysis. Copies of sample request sheets are included in Appendix 2.1. In summary, ACTLABS performed the following sample preparation techniques and lithogeochemical analyses on the samples:

- *Crushing and pulverizing utilizing ACTLABS sample preparation method RX-1*, which includes crushing up to 90% passing 2mm, split (250g) and subsequent pulverization using mild steel to 95% 105 µm in size. Mild steel was utilized for sample pulverization, as it provides the least possible contamination to the sample (according to ACTLABS, iron (up to 0.2%) is the only contaminant added (http:// www.actlabs.com/page.aspx?menu=74&app=243&cat1=617&tp=2&lk=no).

[31]Note that updated versions of settling tanks for Rafts A and B did not contain taconite ballast.

- *Lithogeochemical analysis for major element oxides and select trace elements using ACTLABS analytical method WRA + Trace 4Lithores*, which utilizes a combination of lithium metaborate/tetraborate fusion inductively coupled plasma (ICP) analysis for major element oxides and ICP/MS (inductively coupled mass spectrometry) for trace element analysis. Tables A and B in Appendix 2.1 indicate elements analyzed by each method, as well as their detection limits.
- *Lithogeochemical analysis for selected trace elements using ACTLABS analytical method 4B1.* This four acid digestion method (hydrofluoric, nitric, perchloric, and hydrochloric) is utilized to obtain the low detection limit analyses for cadmium, copper, nickel, sulfur, and zinc. Table C in Appendix 2.1 indicates the elements analyzed by this method, as well as their detection limits.
- *Lithogeochemical analysis for selected trace elements using ACTLABS analytical method 4B INAA.* This instrumental neutron activation analysis method is utilized to obtain low detection limit analyses for arsenic, gold, bromine, chromium, iridium, scandium, selenium, and antimony. Table D in Appendix 2.1 indicates the elements analyzed by this method, as well as their detection limits.
- *Lithogeochemical analysis for carbon and sulfur using ACTLABS analytical method 5G (carbon & sulfur/metallurgical balance package).* This method is utilized to obtain low detection limit analyses for total carbon, graphitic carbon, organic carbon, carbon dioxide, total sulfur, and sulfate sulfur. Table E in Appendix 2.1 indicates the elements and compounds analyzed by this method, as well their detection limits.
- *Lithogeochemical analysis for mercury using ACTLABS analytical method 4F – Hg Cold Vapor FIMS (flow injection mercury system).* This method is utilized to obtain low detection limit (five parts per billion (ppb)) of mercury for samples containing up to 100,000 ppb Hg.

Analytical results for lithogeochemical analyses performed on LTV taconite pellets used as ballast in bioreactors and original settling tanks on rafts A and B (samples MN-15-AB1 and MN-15-AB2) are indicated in Table 1. Analytical results for lithogeochemical analyses performed on Northshore taconite pellets used as ballast in bioreactors on Raft C (samples MN-15-C1 and MN-15-C2) are also indicated in Table 1.

**Table 1.** Results of lithogeochemical analyses performed on taconite pellets used as ballast materials in the bioreactors and precipitation tanks located at Pit 5NE. Samples MN-15-AB1 and MN-15-AB2 represent LTV pellets utilized for ballast in rafts A and B. Samples MN-15-C1 and MN-15-C2 represent Northshore pellets utilized for ballast in Raft C. Lithogeochemical Analysis Summary.

**Table 1.**

| Analyte | Unit Symbol | Lower Limit | Method Code | MN-15-AB1 | MN-15-AB2 | MN-15-C1 | MN-15-C2 | Average AB Pellet | Average C Pellet |
|---|---|---|---|---|---|---|---|---|---|
| SiO2 | % | 0.01 | FUS-ICP | 8.36 | 8.39 | 4.87 | 4.84 | 8.38 | 4.86 |
| Al2O3 | % | 0.01 | FUS-ICP | 0.35 | 0.33 | 0.46 | 0.44 | 0.34 | 0.45 |
| Fe2O3 | % | 0.01 | FUS-ICP | 89.98 | 88.17 | 92.55 | 93.54 | 89.08 | 93.05 |
| MnO | % | 0.001 | FUS-ICP | 0.150 | 0.185 | 0.138 | 0.136 | 0.168 | 0.137 |
| MgO | % | 0.01 | FUS-ICP | 0.44 | 0.50 | 0.40 | 0.41 | 0.47 | 0.41 |
| CaO | % | 0.01 | FUS-ICP | 0.61 | 0.58 | 0.82 | 0.82 | 0.60 | 0.82 |
| Na2O | % | 0.01 | FUS-ICP | 0.04 | 0.04 | 0.07 | 0.06 | 0.04 | 0.07 |
| K2O | % | 0.01 | FUS-ICP | 0.04 | 0.03 | 0.02 | 0.02 | 0.04 | 0.02 |
| TiO2 | % | 0.001 | FUS-ICP | 0.037 | 0.036 | 0.086 | 0.086 | 0.037 | 0.086 |
| P2O5 | % | 0.01 | FUS-ICP | 0.05 | 0.05 | 0.06 | 0.06 | 0.05 | 0.06 |
| LOI | % | -- | FUS-ICP | 0.64 | 1.06 | 0.00 | -0.02 | 0.85 | -0.01 |
| Total | % | 0.01 | FUS-ICP | 100.70 | 99.38 | 99.47 | 100.40 | 100.04 | 99.935 |
| Ag | ppm | 0.3 | TD-ICP | 0.4 | <0.3 | 0.3 | 0.4 | 0.3 | 0.4 |
| As | ppm | 5 | FUS-MS | 13 | 11 | 6 | 7 | 12 | 7 |
| As | ppm | 0.5 | INAA | 9.5 | 10.6 | 6.6 | 7.1 | 10.1 | 6.9 |
| Au | ppb | 2 | INAA | <2 | <2 | <2 | <2 | <2 | <2 |
| Ba | ppm | 2 | FUS-ICP | 3 | <2 | 4 | 2 | 2 | 3 |
| Be | ppm | 1 | FUS-ICP | 2 | 2 | <1 | <1 | 2 | <1 |
| Bi | ppm | 0.1 | FUS-MS | <0.1 | <0.1 | <0.1 | <0.1 | <0.1 | <0.1 |
| Br | ppm | 0.5 | INAA | <0.5 | <0.5 | <0.5 | <0.5 | <0.5 | <0.5 |
| Cd | ppm | 0.5 | TD-ICP | 0.5 | 0.6 | 0.6 | <0.5 | 0.6 | 0.4 |
| Ce | ppm | 0.05 | FUS-MS | 5.26 | 5.44 | 5.84 | 5.93 | 5.35 | 5.89 |
| Co | ppm | 1 | FUS-MS | 4 | 4 | 8 | 8 | 4 | 8 |
| CO2 | % | 0.01 | CO2 | 0.53 | 0.93 | 0.04 | 0.04 | 0.73 | 0.04 |
| C-Graph | % | 0.05 | IR | <0.05 | <0.05 | <0.05 | <0.05 | <0.05 | <0.05 |
| C-Organic | % | 0.5 | IR | <0.5 | <0.5 | <0.5 | <0.5 | <0.5 | <0.5 |
| C-Total | % | 0.01 | CS | 0.15 | 0.28 | <0.01 | <0.01 | 0.22 | <0.01 |
| Cr | ppm | 20 | FUS-MS | 60 | 60 | 50 | 50 | 60 | 50 |
| Cr | ppm | 5 | INAA | 45 | 52 | 39 | 46 | 49 | 43 |
| Cs | ppm | 0.1 | FUS-MS | 0.7 | 0.5 | 0.4 | 0.3 | 0.6 | 0.4 |
| Cu | ppm | 1 | TD-ICP | 4 | 2 | 3 | 2 | 3 | 3 |
| Dy | ppm | 0.01 | FUS-MS | 0.43 | 0.42 | 0.4 | 0.41 | 0.43 | 0.41 |
| Er | ppm | 0.01 | FUS-MS | 0.28 | 0.27 | 0.26 | 0.28 | 0.28 | 0.27 |
| Eu | ppm | 0.005 | FUS-MS | 0.117 | 0.120 | 0.124 | 0.114 | 0.119 | 0.119 |
| Ga | ppm | 1 | FUS-MS | 2 | 2 | 4 | 4 | 2 | 4 |
| Gd | ppm | 0.01 | FUS-MS | 0.38 | 0.38 | 0.41 | 0.47 | 0.38 | 0.44 |
| Ge | ppm | 0.5 | FUS-MS | 28.5 | 27.0 | 17.1 | 17.1 | 27.8 | 17.1 |
| Hf | ppm | 0.1 | FUS-MS | 0.3 | 0.2 | 0.2 | 0.2 | 0.3 | 0.2 |
| Hg | ppb | 5 | 1G | <5 | <5 | <5 | <5 | <5 | <5 |
| Ho | ppm | 0.01 | FUS-MS | 0.09 | 0.10 | 0.09 | 0.09 | 0.10 | 0.09 |
| In | ppm | 0.1 | FUS-MS | <0.1 | <0.1 | <0.1 | <0.1 | <0.1 | <0.1 |
| Ir | ppb | 5 | INAA | <5 | <5 | <5 | <5 | <5 | <5 |
| La | ppm | 0.05 | FUS-MS | 2.60 | 2.62 | 2.82 | 2.79 | 2.61 | 2.81 |
| Lu | ppm | 0.002 | FUS-MS | 0.037 | 0.039 | 0.029 | 0.028 | 0.038 | 0.029 |
| Mo | ppm | 2 | FUS-MS | 4 | 4 | 2 | <2 | 4 | 2 |
| Nb | ppm | 0.2 | FUS-MS | 1.9 | 1.7 | 2.7 | 2.7 | 1.8 | 2.7 |
| Nd | ppm | 0.05 | FUS-MS | 2.22 | 2.25 | 2.33 | 2.45 | 2.24 | 2.39 |
| Ni | ppm | 1 | TD-ICP | 9 | 7 | 11 | 11 | 8 | 11 |
| Pb | ppm | 3 | TD-ICP | 5 | 7 | 5 | 8 | 6 | 7 |
| Pr | ppm | 0.01 | FUS-MS | 0.58 | 0.57 | 0.57 | 0.62 | 0.58 | 0.60 |
| Rb | ppm | 1 | FUS-MS | 2 | 1 | 1 | 1 | 2 | 1 |
| S | % | 0.001 | TD-ICP | 0.003 | 0.007 | 0.005 | 0.003 | 0.005 | 0.004 |
| S-Total | % | 0.01 | CS | <0.01 | <0.01 | <0.01 | <0.01 | <0.01 | <0.01 |
| SO4 | % | 0.3 | SO4 | <0.3 | <0.3 | <0.3 | <0.3 | <0.3 | <0.3 |
| Sb | ppm | 0.2 | FUS-MS | 0.9 | 0.8 | 0.7 | 0.8 | 0.9 | 0.8 |
| Sc | ppm | 1 | FUS-ICP | <1 | <1 | <1 | <1 | <1 | <1 |
| Sc | ppm | 0.1 | INAA | 0.7 | 0.6 | 0.7 | 0.7 | 0.7 | 0.7 |
| Se | ppm | 3 | INAA | <3 | <3 | <3 | <3 | <3 | <3 |
| Sm | ppm | 0.01 | FUS-MS | 0.43 | 0.42 | 0.51 | 0.50 | 0.43 | 0.51 |
| Sn | ppm | 1 | FUS-MS | <1 | <1 | <1 | <1 | <1 | <1 |
| Sr | ppm | 2 | FUS-ICP | 11 | 12 | 20 | 20 | 11.5 | 20 |
| Ta | ppm | 0.01 | FUS-MS | 0.24 | 0.27 | 0.29 | 0.3 | 0.26 | 0.30 |
| Tb | ppm | 0.01 | FUS-MS | 0.07 | 0.07 | 0.06 | 0.07 | 0.07 | 0.07 |
| Th | ppm | 0.05 | FUS-MS | 0.58 | 0.61 | 0.61 | 0.61 | 0.60 | 0.61 |
| Tl | ppm | 0.05 | FUS-MS | <0.05 | <0.05 | <0.05 | <0.05 | <0.05 | <0.05 |
| Tm | ppm | 0.005 | FUS-MS | 0.041 | 0.047 | 0.037 | 0.039 | 0.044 | 0.038 |
| U | ppm | 0.01 | FUS-MS | 0.18 | 0.19 | 0.22 | 0.23 | 0.185 | 0.225 |
| V | ppm | 5 | FUS-ICP | 45 | 42 | 62 | 64 | 43.5 | 63 |
| W | ppm | 0.5 | FUS-MS | 4.6 | 3.0 | 2.8 | 3.2 | 3.8 | 3.0 |
| Y | ppm | 0.5 | FUS-MS | 2.8 | 2.8 | 2.5 | 2.5 | 2.8 | 2.5 |
| Yb | ppm | 0.01 | FUS-MS | 0.25 | 0.31 | 0.22 | 0.21 | 0.28 | 0.22 |
| Zn | ppm | 1 | TD-ICP | 8 | 14 | 12 | 14 | 11 | 13 |
| Zr | ppm | 1 | FUS-ICP | 10 | 7 | 10 | 7 | 9 | 9 |
| Mass | g | -- | INAA | 48.8 | 48.8 | 49.8 | 44.8 | 48.8 | 47.3 |

Taconite pellets produced at the former LTV plant used as ballast on rafts A and B are primarily composed of $Fe_2O_3$ (88.17% – 89.98%), $SiO_2$ (8.36% – 8.39%), CaO (0.58% – 0.61%), MgO (0.44% – 0.50%), and $Al_20_3$ (0.33% – 0.35%). Sulfur content of the pellets as sulfate ($SO_4$) is below the detection limit of 0.3% for both samples. Loss on Ignition (LOI), which represents volatile components such as carbon dioxide ($CO_2$) and water ($H_2O$) tied up in mineral structures as well as attached to the pellets (for example, the moisture contents of the pellets), ranges from 0.64% to 1.06%. Carbon dioxide ($CO_2$) contents of the two samples ranges from 0.53% to 0.93%, suggesting that the $H_2O$ contents of the pellets ($H_2O \approx LOI - CO_2$) range from 0.11% to 0.13%. Such LOI contents are not surprising considering these pellets were exposed to atmospheric conditions for a minimum of 13 years prior to being collected and used as ballast. Of particular note is that mercury contents of the pellets for both samples is below the detection limit (<5 parts per billion) for both samples MN-15-AB1 and MN-15-AB2.

Taconite pellets produced in 2015 at the Northshore taconite processing plant utilized for ballast in Raft C bioreactors are primarily composed of $Fe_2O_3$ (92.55% – 93.54%), $SiO_2$ (4.84% – 4.87%), CaO (both samples 0.82%), $Al_2O_3$ (0.44% – 0.46%), and MgO (0.40% – 0.41%). Sulfur content of the pellets as sulfate ($SO_4$) is below the detection limit of 0.3% for both samples. Loss on Ignition (LOI) values are insignificant and are consistent with the pellets utilization as ballast shortly after production and before their opportunity for alteration by atmospheric conditions. It should also be noted that the mercury concentrations of the two pellet samples utilized as ballast in Raft C bioreactors (samples MN-15-C1 and MN-15-C2) are below detection limits (<5 parts per billion).

## Request for Analysis Forms and Method Detection Limit Information

**Lithogeochemical Analyses Performed by Activation Laboratories on Taconite Pellet Ballast in Rafts A, B, and C**

**MnDRIVE Sulfate Water Treatment System**

**Pit 5NE, Hoyt Lakes, Minnesota**

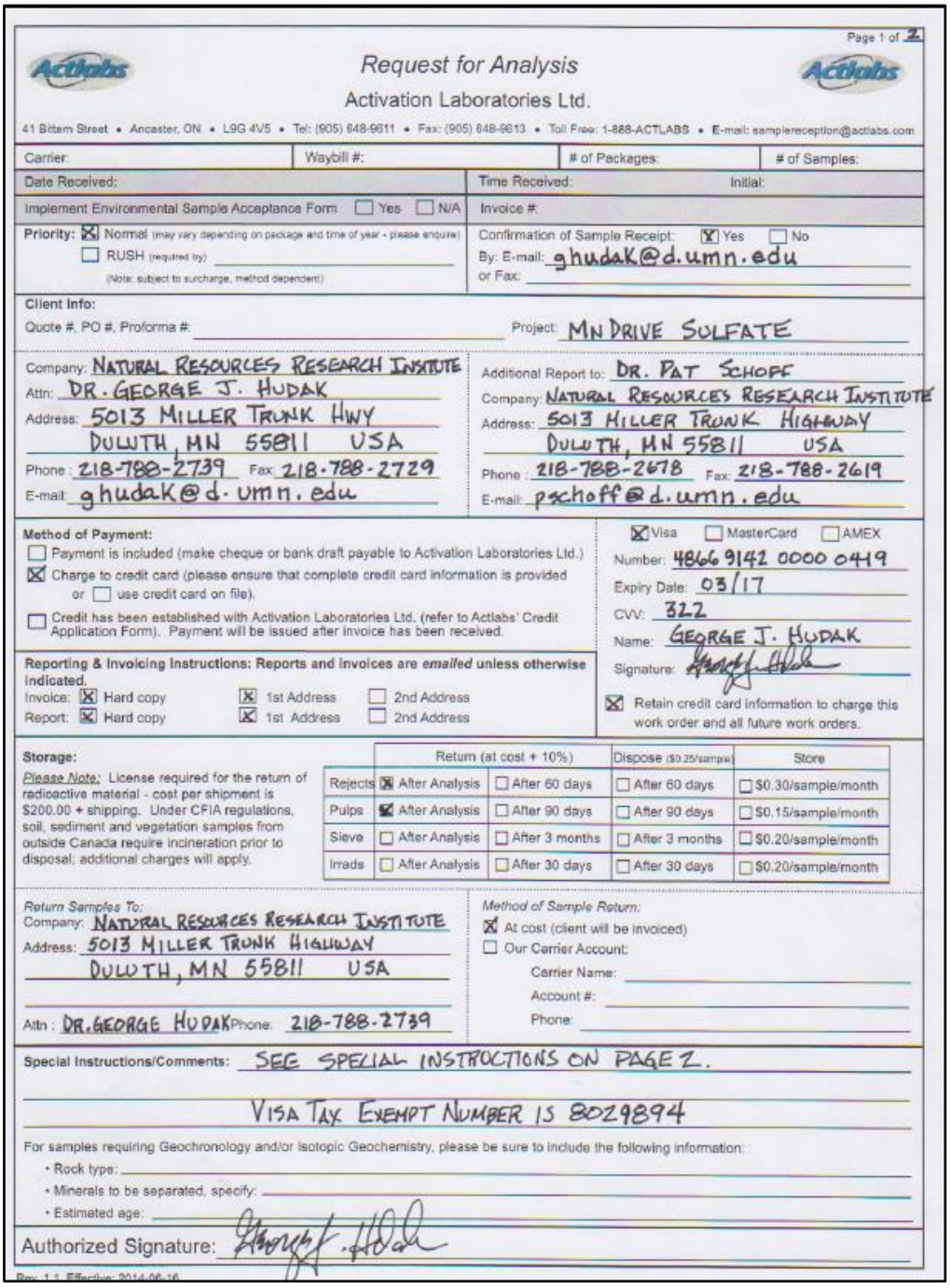

Page 1 of 2

Request for Analysis

Activation Laboratories Ltd.

41 Bittern Street • Ancaster, ON • L9G 4V5 • Tel: (905) 648-9611 • Fax: (905) 648-9613 • Toll Free: 1-888-ACTLABS • E-mail: samplereception@actlabs.com

| Carrier: | Waybill #: | # of Packages: | # of Samples: |
|---|---|---|---|
| Date Received: | Time Received: | Initial: | |
| Implement Environmental Sample Acceptance Form ☐ Yes ☐ N/A | Invoice #: | | |

Priority: ☒ Normal (may vary depending on package and time of year - please enquire) ☐ RUSH (required by) _____ (Note: subject to surcharge, method dependent)

Confirmation of Sample Receipt: ☒ Yes ☐ No
By: E-mail: ghudak@d.umn.edu
or Fax: _____

Client Info:
Quote #, PO #, Proforma #: _____ Project: MN DRIVE SULFATE

Company: NATURAL RESOURCES RESEARCH INSTITUTE
Attn: DR. GEORGE J. HUDAK
Address: 5013 MILLER TRUNK HWY
DULUTH, MN 55811 USA
Phone: 218-788-2739 Fax: 218-788-2729
E-mail: ghudak@d.umn.edu

Additional Report to: DR. PAT SCHOFF
Company: NATURAL RESOURCES RESEARCH INSTITUTE
Address: 5013 MILLER TRUNK HIGHWAY
DULUTH, MN 55811 USA
Phone: 218-788-2678 Fax: 218-788-2619
E-mail: pschoff@d.umn.edu

Method of Payment:
☐ Payment is included (make cheque or bank draft payable to Activation Laboratories Ltd.)
☒ Charge to credit card (please ensure that complete credit card information is provided or ☐ use credit card on file).
☐ Credit has been established with Activation Laboratories Ltd. (refer to Actlabs' Credit Application Form). Payment will be issued after invoice has been received.

☒ Visa ☐ MasterCard ☐ AMEX
Number: 4866 9142 0000 0419
Expiry Date: 03/17
CVV: 322
Name: GEORGE J. HUDAK
Signature: George J. Hudak

Reporting & Invoicing Instructions: Reports and invoices are *emailed* unless otherwise indicated.
Invoice: ☒ Hard copy ☒ 1st Address ☐ 2nd Address
Report: ☒ Hard copy ☒ 1st Address ☐ 2nd Address

☒ Retain credit card information to charge this work order and all future work orders.

Storage:
*Please Note:* License required for the return of radioactive material - cost per shipment is $200.00 + shipping. Under CFIA regulations, soil, sediment and vegetation samples from outside Canada require incineration prior to disposal; additional charges will apply.

| | Return (at cost + 10%) | | Dispose ($0.25/sample) | Store |
|---|---|---|---|---|
| Rejects | ☒ After Analysis | ☐ After 60 days | ☐ After 60 days | ☐ $0.30/sample/month |
| Pulps | ☒ After Analysis | ☐ After 90 days | ☐ After 90 days | ☐ $0.15/sample/month |
| Sieve | ☐ After Analysis | ☐ After 3 months | ☐ After 3 months | ☐ $0.20/sample/month |
| Irrads | ☐ After Analysis | ☐ After 30 days | ☐ After 30 days | ☐ $0.20/sample/month |

Return Samples To:
Company: NATURAL RESOURCES RESEARCH INSTITUTE
Address: 5013 MILLER TRUNK HIGHWAY
DULUTH, MN 55811 USA
Attn: DR. GEORGE HUDAK Phone: 218-788-2739

Method of Sample Return:
☒ At cost (client will be invoiced)
☐ Our Carrier Account:
Carrier Name: _____
Account #: _____
Phone: _____

Special Instructions/Comments: SEE SPECIAL INSTRUCTIONS ON PAGE 2.

VISA TAX EXEMPT NUMBER IS 8029894

For samples requiring Geochronology and/or Isotopic Geochemistry, please be sure to include the following information:
- Rock type: _____
- Minerals to be separated, specify: _____
- Estimated age: _____

Authorized Signature: George J. Hudak

Rev. 1.1 Effective: 2014-06-16

FOR FASTER TURNAROUND TIME, EMAIL A COPY OF YOUR SUBMITTAL FORM TO **samplereception@actlabs.com**

Client Name: NATURAL RESOURCES RESEARCH INSTITUTE, ATTN. GEORGE HUDAK

Sample Preparation Charges: ☐ Contact me if sample preparation is required. ☒ I authorize any required sample preparation charges.

| # of samples | Sample Numbers (list all or range) | Sample Code (see below) | Prep. Code (if required) | Pkg. Code / Elements |
|---|---|---|---|---|
| 1 | MN-15-AB1 | C | RX-1 | SEE BELOW |
| 1 | MN-15-AB2 | C | RX-1 | SEE BELOW |
| 1 | MN-15-C1 | C | RX-1 | SEE BELOW |
| 1 | MN-15-C2 | C | RX-1 | SEE BELOW |
| | | | | |
| | | | | |
| | FOR ALL SAMPLES, PLEASE PERFORM THE FOLLOWING ANALYSES: | | | |
| | - WRA + TRACE 4 LITHORESEARCH | | | |
| | - CODE 4B (Cd, Cu, Ni, S, Zn) | | | |
| | - CODE 4B INAA (As, Au, Br, Cr, Ir, Sc, Se) | | | |
| | - CODE 5G - CARBON / SULFUR METALLURGICAL BALANCE PACKAGE | | | |
| | - CODE 4F - Hg BY COLD VAPOR FINS | | | |
| | | | | |
| | - PLEASE RETURN UNUSED SAMPLES / PULPS TO GEORGE HUDAK AT THE ADRESS PROVIDED IN THE CLIENT INFO SECTION | | | |
| | | | | |
| | - THE TACONITE PELLETS THAT COMPRISE THE SAMPLES HAVE ROUGHLY THE FOLLOWING CHEMISTRY: | | | |
| | Fe 63-65%. | | | |
| | Si 2.2-2.5%. | | | |
| | Mg 0.1-0.4%. | | | |
| | Mn 0.1-0.2%. | | | |
| | Al 0.15-0.25%. | | | |
| | Ca 0.00-0.61%. | | | |
| | ⊛ IMMEDIATELY CONTACT GEORGE HUDAK AT 218-788-2739 IF PELET CHEMISTRIES ARE NOT COMPATIBLE WITH REQUESTED ANALYTICAL TECHNIQUES | | | |

Sample Codes: R – Rock; CR – Crushed Rock; HMC – Heavy Minerals; H – Humus; S – Soil; V – Vegetation; B – Brine; MW – Marine Water; W – Water; C – Ore Conc.; O – Other (specify); P – Pulp; LS – Lake Sediment; SS – Stream Sediment

Please copy page for additional sample lists.
Rev. 1-1, Effective: 2014-08-18

**Table A.** Detection limits for elements analyzed using ACTLABS lithium metaborate/tetraborate fusion ICP whole rock analysis associated with ACTLABS 4Lithores method (from http://www.actlabs.com/page.aspx?page=517&app=226&cat1=549&tp=12&lk=no&menu=64 ).

| Oxide | Detection Limit (%) | Oxide | Detection Limit (%) | Oxide | Detection Limit (%) |
|---|---|---|---|---|---|
| $SiO_2$ | 0.01 | MgO | 0.01 | $Na_2O$ | 0.01 |
| $Al_2O_3$ | 0.01 | MnO | 0.001 | $K_2O$ | 0.01 |
| $Cr_2O_3$ | 0.01 | CaO | 0.01 | $P_2O_5$ | 0.01 |
| $Fe_2O_3$ | 0.01 | $TiO_2$ | 0.001 | Loss on Ignition | 0.01 |

**Table B.** Detection limits for trace elements analyzed using ICP or ICP/MS associated with ACTLABS 4Lithores method (from http://www.actlabs.com/page.aspx?page=517&app=226&cat1= 549&tp= 12&lk=no&menu=64 ).

| Element | Detection Limit (mg/L) | Upper Limit (mg/L) | Reported By | Element | Detection Limit (mg/L) | Upper Limit (mg/L) | Reported By |
|---|---|---|---|---|---|---|---|
| Ag | 0.5 | 100 | ICP/MS | Nd | 0.05 | 2000 | ICP/MS |
| As | 5 | 2000 | ICP/MS | Ni | 20 | 10000 | ICP/MS |
| Ba | 3 | 500000 | ICP | Pb | 5 | 10000 | ICP/MS |
| Be | 1 | -- | ICP/MS | Pr | 0.01 | 1000 | ICP/MS |
| Bi | 0.1 | 2000 | ICP/MS | Rb | 1 | 1000 | ICP/MS |
| Ce | 0.05 | 3000 | ICP/MS | Sb | 0.2 | 200 | ICP/MS |
| Co | 1 | 1000 | ICP/MS | Sc | 1 | -- | ICP/MS |
| Cr | 20 | 10000 | ICP/MS | Sm | 0.01 | 1000 | ICP/MS |
| Cs | 0.1 | 1000 | ICP/MS | Sn | 1 | 1000 | ICP/MS |
| Cu | 10 | 10000 | ICP/MS | Sr | 2 | 10000 | ICP |
| Dy | 0.01 | 1000 | ICP/MS | Ta | 0.01 | 500 | ICP/MS |
| Er | 0.01 | 1000 | ICP/MS | Tb | 0.01 | 1000 | ICP/MS |
| Eu | 0.005 | 1000 | ICP/MS | Th | 0.05 | 2000 | ICP/MS |
| Ga | 1 | 500 | ICP/MS | Tl | 0.05 | 1000 | ICP/MS |
| Gd | 0.01 | 1000 | ICP/MS | Tm | 0.005 | 1000 | ICP/MS |
| Ge | 0.5 | 500 | ICP/MS | U | 0.01 | 1000 | ICP/MS |
| Hf | 0.1 | 1000 | ICP/MS | V | 5 | 10000 | ICP |
| Ho | 0.01 | 1000 | ICP/MS | W | 0.5 | 5000 | ICP/MS |
| In | 0.1 | 200 | ICP/MS | Y | 0.5 | 10000 | ICP/MS |
| La | 0.05 | 2000 | ICP/MS | Yb | 0.01 | 1000 | ICP/MS |
| Lu | 0.002 | 1000 | ICP/MS | Zn | 30 | 10000 | ICP/MS |
| Mo | 2 | 100 | ICP/MS | Zr | 1 | 10000 | ICP/MS |
| Nb | 0.2 | 1000 | ICP/MS | -- | -- | -- | -- |

**Table C.** Detection limits for trace elements analyzed using ACTLABS analytical method 4B1 (from http://www.actlabs.com/page.aspx? page=517&app=226&cat1=549&tp=12&lk=no&menu=64).

| Element | Detection Limit (mg/L) | Upper Limit (mg/L) | Element | Detection Limit (mg/L) | Upper Limit (mg/L) |
|---|---|---|---|---|---|
| Cd | 0.5 | 5000 | S | 0.001% | 20% |
| Cu | 1 | 10000 | Zn | 1 | 10000 |
| Ni | 1 | 10000 | -- | -- | -- |

**Table D.** Detection limits for trace elements analyzed using ACTLABS analytical method 4B INAA (from http://www.actlabs.com/page.aspx? page=517&app=226&cat1=549&tp=12&lk=no&menu=64).

| Element | Detection Limit (mg/L) | Upper Limit (mg/L) | Element | Detection Limit (mg/L) | Upper Limit (mg/L) |
|---|---|---|---|---|---|
| As | 0.5 | 10000 | Ir | 5 ppb | 10000 |
| Au | 2 ppb | 30000 ppb | Sc | 0.1 | 1000 |
| Br | 0.5 | 5000 | Se | 3 | 10000 |
| Cr | 5 | 100000 | Sb | 0.2 | 10000 |

**Table E.** Detection limits for trace elements analyzed using ACTLABS analytical method 5G (from http://www.actlabs.com/page.aspx?page=736&app=226&cat1=549&tp=12&lk=no&menu=64).

| Element/Compound | Detection Limit (%) | Element/Compound | Detection Limit (%) |
|---|---|---|---|
| C – Total | 0.01 | $CO_2$ | 0.01 |
| C – Graphitic | 0.05 | S – Total | 0.01 |
| C - Organic | 0.5 | $SO_4$ | 0.3 |

# Appendix 3. Chemical treatments for sulfide precipitation - details.

## Treatment methods for removal of $H_2S$ from bio-effluents.

Several chemical methods designed to remove $H_2S$ from water have been tested in lab and field trials and are summarized here and in Table 1. Experimental details are described in the next section.

## Reaction mechanisms

**1. Iron salts** (Table 1, Reactions 1 & 2)
Iron salts of chloride, sulfate, or nitrate can be added to sulfide-containing water either in ferric (Fe(III)) or ferrous (Fe(II)) forms. Fe(II) can remove sulfide by precipitation as ferrous sulfide (FeS). Fe(III) can remove sulfide by two different mechanisms; 1) by oxidizing it chemically to elemental sulfur while being reduced to Fe(II), which can subsequently produce FeS; or 2) by reacting with sulfide to form intermediate $Fe_2S_3$, which undergoes thermal decomposition to produce FeS and S.

**Mechanism 1**

$$2Fe^{3+} + HS^- \rightarrow 2Fe^{2+} + S^o + H^+$$

$$Fe^{2+} + HS^- \rightarrow FeS + H^+$$

**Mechanism 2**

$$3S^{2-} + 2FeCl_3 \rightarrow Fe_2S_3 + 6Cl^- \rightarrow (FeS + FeS_2 + S) + 6Cl^-$$

Since mining affected pit water at the field site commonly contained sulfate anion concentrations around 1200 mg/L, we expected sulfide ($S^{2-}$) concentrations up to 333 mg/L to be generated (Section V. Table V-1). This treatment method, which effectively reduced aqueous sulfide concentrations in both lab and field trials, also offers several challenges. The most notable of these is that addition of Fe(II) or Fe(III) to water increased counter ion concentrations. For example, addition of $FeCl_2$ or $FeCl_3$ for treatment of 300 mg/L of $S^{2-}$ will introduce up to 665 mg/L of $Cl^-$ (Table 1), an effect that was evident in field trials (data not shown). The major disadvantage of this treatment method is that it results in unacceptably high chloride concentrations into the discharged water.

**2. Granulated ferric hydroxide $Fe(OH)_3$)** (Table 1, Reaction 3)

Chloride addition can be avoided by using ferric hydroxide ($Fe(OH)_3$) as a precipitating agent. The interaction of sulfide with granulated ferric hydroxide is a surface reaction, which can result in chemisorption of $S^{2-}$. The reaction will happen according this equation:

$$Fe(OH)_3 + H_2S \rightarrow FeS + FeS_2 + S + (FeO)_2S + \text{etc.}$$

Since this is a surface reaction, the major portion of the added granulated ferric hydroxide will not react with $S^{2-}$ and will be waste. Therefore, while this treatment system was also effective in both lab and field trials, it has a distinct disadvantage in that the reaction is highly inefficient and it produces large quantities of sludge (Table 1), introducing prohibitively high operational, maintenance, and disposal costs (not shown).

**Table 1.** Calculated material balance and anion concentrations resulting from chemical precipitation treatments. Ppt. = precipitate; MW = molecular weight.

| Reaction | S (%) | $S^{2-}$ (mg/L) | Ppt. [expected] (mg/L) | Volume treated water (gal/min) | Sludge (Kg/day) | $C(Cl^-)$ (mg/L) |
|---|---|---|---|---|---|---|
| **1. $3S^{2-} + 2FeCl_3 \Rightarrow Fe_2S_3 + 6Cl^- \Rightarrow (FeS + FeS_2 + S) + 6Cl^-$** | | | | | | |
| Reagent: $FeCl_3$ (162.2 MW) | 0.462 | 150 | 325.00 | 10 | 17.71 | 332.81 |
| Intermediate: $Fe_2S_3$ (208 MW) | 0.462 | 200 | 433.33 | 10 | 23.62 | 443.75 |
| | 0.462 | 250 | 541.67 | 10 | 29.52 | 554.69 |
| | 0.462 | 300 | 650.00 | 10 | 35.43 | 665.63 |
| | 0.462 | 330 | 715.00 | 10 | 38.97 | 732.19 |
| **2. $S^{2-} + FeCl_2 \Rightarrow FeS + 2Cl^-$** | | | | | | |
| Reagent: $FeCl_2$ (126.8 MW) | 0.364 | 150 | 412.03 | 10 | 22.46 | 332.81 |
| Intermediate: FeS (87.9 MW) | 0.364 | 200 | 549.38 | 10 | 29.94 | 443.75 |
| | 0.364 | 250 | 686.72 | 10 | 37.43 | 554.69 |
| | 0.364 | 300 | 824.06 | 10 | 44.91 | 665.63 |
| | 0.364 | 330 | 906.47 | 10 | 49.41 | 732.19 |
| **3. $S^{2-} + Fe(OH)_3 \Rightarrow Fe_2S_3 + FeOOH + OH^- \Rightarrow FeS + FeS_2 + S + (FeO)_2S$** | | | | | | |
| Reagent: $Fe(OH)_3$ (106.9 MW) | 0.462 | 150 | 325.00 | 10 | 17.71 | 0.00 |
| [unstable] | 0.462 | 200 | 433.33 | 10 | 23.62 | 0.00 |
| Intermediate: $Fe_2S_3$ (208 MW) | 0.462 | 250 | 541.67 | 10 | 29.52 | 0.00 |
| | 0.462 | 300 | 650.00 | 10 | 35.43 | 0.00 |
| | 0.462 | 330 | 715.00 | 10 | 38.97 | 0.00 |
| **4. $S^{2-} + H_2O_2 + H^+ \Rightarrow S + H_2O$ (byproducts $S_2O_3^{2-}$ & $SO_4^{2-}$)** | | | | | | |
| Reagent: $H_2O_2$ (34 MW) | 1.000 | 150 | 150.00 | 10 | 8.18 | 0.00 |
| Intermediate: S (32 MW) | 1.000 | 200 | 200.00 | 10 | 10.90 | 0.00 |
| | 1.000 | 250 | 250.00 | 10 | 13.63 | 0.00 |
| | 1.000 | 300 | 300.00 | 10 | 16.35 | 0.00 |
| | 1.000 | 330 | 330.00 | 10 | 17.99 | 0.00 |

**3. Chemical oxidation** (Table 1, Reaction 4)

a) Chlorine will oxidize sulfide to sulfate or to elemental sulfur, depending on the pH. The effectiveness of this reaction is frequently low because of reactions with other components. Chlorine may be added as an aqueous solution (NaClO or $Ca(ClO)_2$) at a $Cl^-$:$H_2S$ ratio of 1.8 – 2.0:1 (w/w) or directly as a gas at a ratio of 9.0 – 15.0:1 (w/w). The disadvantage of this treatment is that with high sulfide anion concentrations it will produce high levels of chloride anion into discharged water.

b) Potassium permanganate ($KMnO_4$) is a strong oxidizing agent that can convert sulfide to sulfate. It is normally supplied in a dry state during sewage water treatments to decrease $H_2S$

concentrations. Disadvantages to this method include high cost, high manganese concentrations in the final effluent, and the potential for oxidation of sulfide back to sulfate.

c) Hydrogen peroxide ($H_2O_2$) oxidizes dissolved sulfide in bio-effluents and decomposes to water and oxygen, thus keeping conditions aerobic. The proper ratio of $H_2O_2$:$H_2S$ is 1.3 – 4.0:1 (w/w), resulting in an average sulfide oxidation of 85 – 100%. The reaction is pH dependent and can be controlled by adjusting pH:

$$S^{2-} + H_2O_2 + 2H^+ \rightarrow S^0 + 2H_2O$$

The primary advantages of this method are that under controlled pH conditions the final product will be mostly elemental sulfur and the process does not introduce unwanted byproducts. Disadvantages include chemical costs, particularly hydrogen peroxide and formic acid (see Section V.B. Table V-2).

## Materials and methods

Formic acid (88%, ACS grade), glacial acetic acid (ACS grade), aluminum sulfate, and sodium thiosulfate (0.1N) were purchased from Fisher Scientific and used without further purification. Potassium iodine (ACS grade), hydrogen peroxide (30% aqueous solution, ACS grade), and hydrochloric acid (0.1 N and 6 N) were purchased from RICCA Chemical Company and used without further purification.

An Oakton PC700 pH meter was used for pH analysis, and sulfate and chloride anion concentrations were measured using a Metrohm 881 Compact ion Chromatograph Pro equipped with a pump, injector, eluent degasser, MSM, MCS, IC Conductivity Detector, Column and 858 Professional Sample Processor, and sample Rack # 6.2041.440. All samples were filtered using a 0.45 µm syringe filter and diluted using Type I deionized water as needed.

## Experiments

### 1. Ferric chloride ($FeCl_3$) treatment of $S^{2-}$ in bio-effluent water.

As discussed above, ferric chloride can remove sulfide by oxidation to elemental sulfur while being reduced to Fe(II), which can subsequently produce (FeS), or form the intermediate compound $Fe_2S_3$, which undergoes thermal decomposition to S° and FeS. Because the initial temperature for addition of $FeCl_3$ was 0 – 5°C, the second reaction mechanism seemed more feasible (Table 1, Reaction 2), and we implemented this treatment procedure using conditions similar to those found in the test pit:

$$3S^{2-} + 2FeCl_3 \rightarrow Fe_2S_3 + 6Cl^- \rightarrow (FeS + FeS_2 + S) + 6Cl^-$$

Fig. 1. Reaction vessel containing

1.2 ml of a 35% solution of ferric chloride was added to 1L of bio-effluent water (SRB reactor) at -5°C and extensive mixing, producing a black precipitate, followed by a second, white-gray precipitate. The two precipitates, which separated in the reactor (Figure 1) were harvested in separation funnel and were each filtered and dried in a vacuum desiccator at room temperature for 72 hours over sulfuric acid. Dried solids were sent for elemental analysis to Atlantic Microlab, Inc. (Table 2, Figure 2).

**Table 2.** Elemental analysis of precipitates.

| Material | Found concentration of S, % | Calculated concentration of S, % |
|---|---|---|
| Black precipitate | 34.34 | 36.47 (FeS)<br>53.45 ($FeS_2$)<br>100 (S) |
| White-gray precipitate | 79.175 | |

**Figure 2.** Elemental analysis of black and white-gray precipitates.

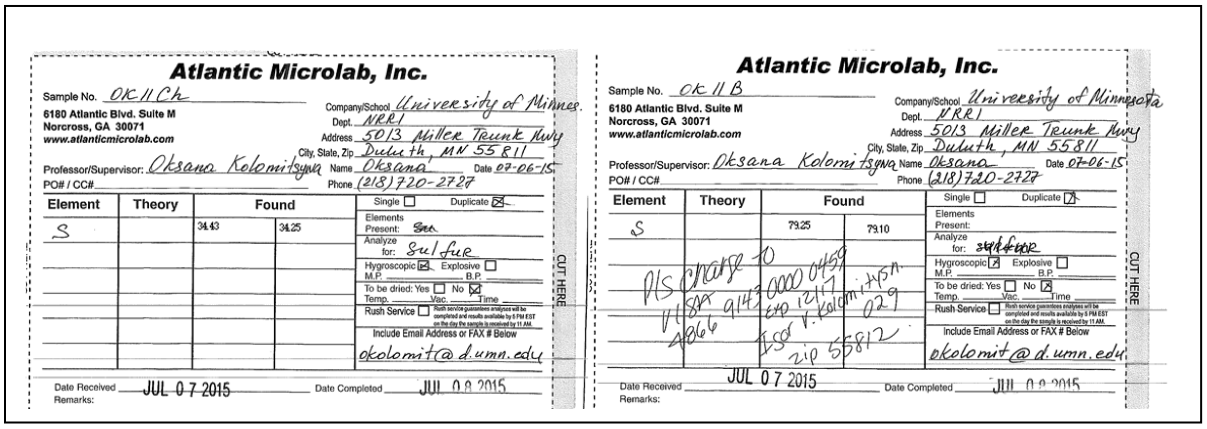


Figure 2. Report from Atlantic Microlab, Inc. for elemental analysis of the precipitates. A) Elemental analysis confirmed that the black precipitate is a mostly FeS, with a minor S component, and B) that the white-gray precipitate was mostly elemental S.

After filtration, the aqueous filtrate was tested for sulfide using the EPA-3764 protocol, and chloride using ion chromatography, as described above. Result showed that only trace amounts of sulfide anion were present after treatment, however, around 400 mg/L of chloride anion were detected. Thus, the addition of ferric or ferrous chlorides into bio-effluent effectively reduces sulfide concentrations, but the disadvantage of this method is that, in bio-effluents containing high sulfate concentrations, it will also introduce unacceptably high concentrations of chloride anions into the discharge water.

## 2. Granulated ferric hydroxide $Fe(OH)_3$ treatment of $S^{2-}$ in bio-effluent water.

Our goals in this experiment were to compare the sorption capacity and activity of commercially available granulated ferric hydroxide (GFH) to sorb $S^{2-}$ from bio effluent water, and to measure the capacity and activity of GFH in tests of bioreactor hydraulic retention time (i.e., flow rate). We calculated the cost of using GFH for sulfide treatment, assuming that all GFH will be used to react with $S^{2-}$. But since the interaction between $S^{2-}$ and GFH is a surface reaction, which can result in chemisorption of $S^{2-}$, the calculated cost for bio-effluent treatment should be considered a “best case scenario” only.

The reaction:

$$Fe(OH)_3 + H_2S \rightarrow FeS + FeS_2 + S + (FeO)_2S + \text{other compounds}$$

By stoichiometric calculations (Table 1) using a flow rate of 10 gal/minute or 14,400 gal/day, a minimum of 18 kg of GFH $Fe(OH)_3$ should be loaded daily. After obtaining quotes from several manufacturers (Omega Waters, READE, Evoqua price for GFH $Fe(OH)_3$) we estimated that daily spending will be $250, or $91,500/year for GFH alone. These numbers are accurate if 100% chemisorption capacity of GFH is assumed. However, since the company claims that GFH can absorb up to 20% of its theoretical chemisorption capacity, the yearly cost of $Fe(OH)_3$ may be $457,115.00 with a 10 gal/minute flow rate.

The advantage of this process is that it does not add chloride anions into discharged water, as in case of treatment with $FeCl_3$, but disadvantages include the production of large amounts of sludge (Table 1), as well as excessively high operational costs.

## 3. $H_2O_2$ treatment of $S^{2-}$ in bioreactor effluent water.

Oxidation of $H_2S$ by $H_2O_2$ can proceed to elemental sulfur in neutral or acidic solutions, and may provide a convenient and economical method for the final step of sulfate removal. Oxidation of sulfide may produce or consume protons ($H^+$), depending on the final products, as illustrated in these reactions:

$$HS^- + H_2O_2 + H^+ \rightarrow 1/8S_8 + 2H_2O \quad \text{with pH} < 7$$

$$HS^- + 4H_2O_2 \rightarrow SO_4^{2-} + 4H_2O + H^+ \quad \text{with pH} > 7$$

The stoichiometry for the reaction of $H_2S$ and $H_2O_2$ in a neutral or acidic solution is normally written as

$$H_2S + H_2O_2 \rightarrow 2H_2O + S,$$

where zero valent sulfur is formed in the colloidal state. Since colloidal sulfur is a complex mixture of cyclohexasulfur, cyclooctasulfur, polycatenasulfur, and higher-molecular weight sulfanes, the chemical equation should be written emphasizing the complexity of this reaction:

$$H_2S + H_2O_2 \rightarrow 1/xS_x + H_2O$$

Our goals were to find reaction conditions that selectively oxidized sulfide anions to elemental sulfur and prevented oxidation of sulfide anions back to sulfates, and to develop a protocol to precipitate elemental sulfur from the water solution.

These goals was pursued in the following phases:

**Phase 1:** Development of a means to control pH of treated water by finding a suitable pH adjuster, and establishing the influence of temperature, reaction time, and concentration of $H_2O_2$ on the reactions.

**Phase 2**: Development of flocculation reagent and flocculation parameters to precipitate colloidal sulfur.

**Optimizing reaction conditions for sulfide oxidation using hydrogen peroxide** (see Figure 3). One ml of a 30% formic acid solution was added to 1L of bioreactor effluent water at 11°C and extensively mixed for 1 – 5 minutes to achieve a pH of 6.5, after which 1.4 ml of a 34% hydrogen peroxide solution was

added, and the reaction mixture was stirred for an additional 1 – 5 minutes. After 30 minutes, a white colloidal sulfur precipitate formed, and 0.06 ml of 48.5% a solution of aluminum sulfate (flocculent) in water was added. The reaction mixture was incubated at 11°C for 8 – 12 hours to achieve total sulfur sedimentation. The solution was filtered using 0.45 µm syringe filters, and the aqueous portion was tested for alkalinity, sulfate, sulfide, and chloride anion concentration.

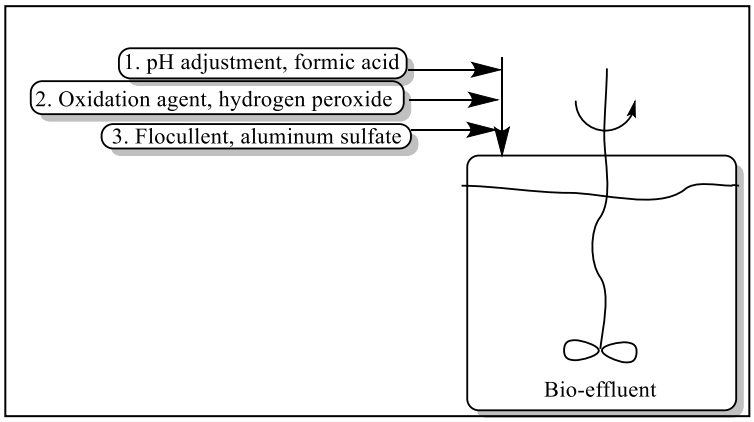


**Figure 3.** Schematic of the laboratory experimental protocol.

**Measurement of alkalinity in the water samples.** Alkalinity was analyzed using ASTM D1067-11 "Standard Test Methods for Acidity or Alkalinity of Water," and $HCO_3^-$ concentration was measured by titration with a 0.1N HCl water solution using 1 drop of a 0.1% methyl orange solution as an indicator. 100 ml of water was placed in a 0.5L flask using a volumetric pipette, then a few drops of 0.1% methyl orange indicator solution were added and the solution was titrated with a 0.1N solution of HCl in water until the orange color changed to magenta. Alkalinity was calculated and reported in terms of $CaCO_3$ (mg/L).

**Measurement of sulfide concentration in the water samples.** Sulfide concentrations were analyzed using EPA 3761 "Sulfide (Titrimetric, Iodine)." The concentration of a solution of $I_2$ was measured by titration with a solution of $Na_2S_2O_3$ in water using a starch solution as an indicator. A volume of iodine solution, estimated to be in excess of the sulfide concentration, was placed in a 0.5L flask, and 1ml of 6N HCl was added. A set amount of sample was pipetted into a flask, discharged under the solution surface. The resulting mixture was back-titrated with a solution of $Na_2S_2O_3$ in water, with a few drops of starch solution added at the end of titration as the end point was approached, and titration was continued until the blue color disappeared.

**Test for presence of hydrogen peroxide in water.** Two ml of Type I deionized water was placed in 4 ml glass vial, to which three drops of a 20% solution of KI and three drops of a 20% solution of acetic acid in water were added. The vial was capped and the reagents were mixed by shaking. Five drops of a water sample solution were added into the reagent and allowed to react for 6 minutes. Hydrogen peroxide was indicated by a yellow color.

**Flocculation reagent and flocculation parameters.** A variety of primary coagulants, including $ZnCl_2$, $FeCl_2$, $FeCl_3$, and $Al_2(SO_4)_3$, were screened as flocculating reagents in bio-effluents. These tests showed that aluminum sulfate ($Al_2(SO_4)_3$, alum) effectively coagulating colloidal sulfur at pH = 6.0 – 7.3. Alum,

which is extensively used as a flocculent in water treatment plants, reacts with water to produce positively charged aluminum hydroxide particles, which promote a flocculent that attaches and removes colloidal particles from water by precipitation within 30 to 45 minutes. The coagulation/flocculation process is affected by pH, salts, alkalinity, turbidity, temperature, mixing, and coagulant chemicals.

**Measuring amount of reagents that were required to oxidize sulfide to sulfur.** Reagents were added in the following sequence (see Table 3):

1) A 30% solution of acetic acid was added to 1 L of bio-effluent to adjust pH to 6.5 or lower.
2) After 10 min, a 10% solution of hydrogen peroxide in water was added at 5°C and stirred for 30 minutes, forming a cloudy white precipitate.
3) A 1% solution of $Al_2(SO_4)_3$ in water was added at 11°C and kept for 6 – 12 hours to complete the coagulation and precipitation of colloidal sulfur.

All water samples were filtered using a 0.45 µm syringe filter. Aqueous alkalinity, sulfide, and sulfate anion concentrations were measured using the procedure described above. Reagent volumes and other data are presented in Table 3.

**Table 3.** Amount of reagents and resulting concentration of $S^{2-}$ and $SO_4^{2-}$. Raft A bio-effluent water was used. Bio-effluent was collected on 11/3/2015.

| Exp. # | V 30% Acetic Acid, ml | V 10% $H_2O_2$, ml/L | V 1% $Al_2(SO_4)_3$, ml/L | Effluent $S^{2-}$ Mg/L | Final $S^{2-}$ mg/L | Effluent pH | pH after adjust. | Effluent alkalinity | Final alkalinity | Effluent $SO_4^{2-}$ mg/L | Final $SO_4^{2-}$ mg/L |
|---|---|---|---|---|---|---|---|---|---|---|---|
| OK-81 | 2 | 3 | 1 | 252 | 18 | 7.23 | 6.38 | 1250 | 1125 | 41.25 | 66.2 |
| **OK-75** | **2** | **4** | **1** | **252** | **0** | **7.23** | **6.38** | **1250** | **1125** | **41.25** | **81** |
| OK-78 | 2 | 5 | 1 | 252 | 0 | 7.23 | 6.38 | 1250 | 1100 | 41.25 | 81.4 |
| OK-80 | 2.5 | 3 | 1 | 252 | 12 | 7.23 | 6.17 | 1250 | 1075 | 41.25 | 76.2 |
| OK-74 | 2.5 | 4 | 1 | 252 | 0 | 7.23 | 6.17 | 1250 | 1050 | 41.25 | 85.3 |
| OK-77 | 2.5 | 5 | 1 | 252 | 0 | 7.23 | 6.17 | 1250 | 1050 | 41.25 | 86 |
| OK-79 | 3 | 3 | 1 | 252 | 6 | 7.23 | 6.04 | 1250 | 1050 | 41.25 | 84.4 |
| OK-73 | 3 | 4 | 1 | 252 | 0 | 7.23 | 6.04 | 1250 | 1050 | 41.25 | 104.7 |
| OK76 | 3 | 5 | 1 | 252 | 0 | 7.23 | 6.04 | 1250 | 1050 | 41.25 | 105.6 |

These experiments indicated that at least 4 ml of a 10% solution of hydrogen peroxide should be added to 1 L of bio-effluent from raft A to complete oxidation of sulfide anions. To minimize oxidation of sulfide to sulfate, pH should be adjusted to 6.38. Lowering pH below 6.34 does not help minimize oxidation sulfide to sulfate. The optimum conditions for this experiment are marked in bold in Table 3.

**Testing the reaction of sulfide oxidation by hydrogen peroxide at pH level above 6.38.** Reagents were added in the following sequence (see Table 4):

1) A 30% solution of acetic acid was added to 1 L of bio-effluent to adjust pH to 7.24 – 6.32.
2) After 10 minutes, a 10% solution of hydrogen peroxide in water was added at $5^0$ C and stirred for 30 minutes, forming a cloudy white precipitate.
3) A 1% solution of $Al_2(SO_4)_3$ in water was added at $11^0$ C and kept for 6 – 12 hours to complete the coagulation and precipitation of colloidal sulfur.

All water samples were filtered using a 0.45 µm syringe filter. Aqueous alkalinity, sulfide, and sulfate anion concentrations were measured using the procedure described above. Reagent volumes and other data are presented in Table 4.

This set of experiments indicated that at least 4 ml of 10% hydrogen peroxide added to 1 L of Raft A bio-effluent was required for complete oxidation of sulfide anions, with pH ≤ 6.52 to minimize oxidation to sulfate. At least 2.5 ml of a 1% solution of $Al_2(SO_4)_3$ was needed to fully coagulate and precipitate colloidal sulfur. The optimum conditions for this experiment are marked in bold in Table 4.

**Table 4.** Amount of acetic acid, hydrogen peroxide, and aluminum sulfate vs pH and concentration of sulfate in the final effluent. Raft A bio-effluent water was used. Bio-effluent was collected 11/3/2015.

| Exp. # | V 30% Acetic acid ml | V10% $H_2O_2$ ml/L | V1% $Al_2(SO_4)_3$, ml/L | Effluent $S^{2-}$ mg/L | Final $S^{2-}$ mg/L | pH after adjustment | Effluent alkalinity | Final alkalinity | Effluent $SO_4^{2-}$, mg/L | Final $SO_4^{2-}$, mg/L |
|---|---|---|---|---|---|---|---|---|---|---|
| OK-82 | 0 | 5 | 2.5 | 272 | 0 | 7.24 | 1070 | 925 | 110 | 336.5 |
| OK-83 | 0.5 | 4.5 | 1.8 | 272 | 0 | 6.95 | 1070 | 975 | 110 | 187.5 |
| OK-84 | 0.5 | 5 | 1.8 | 272 | 0 | 6.99 | 1070 | 975 | 110 | 183.5 |
| OK-85 | 0.5 | 4.5 | 2 | 272 | 0 | 6.99 | 1070 | 950 | 110 | 248.6 |
| OK-86 | 0.5 | 5 | 2 | 272 | 0 | 7 | 1070 | 1000 | 110 | 200.3 |
| OK-87 | 1 | 3.5 | 1.8 | 272 | 0 | 6.75 | 1070 | 1000 | 110 | 156.1 |
| OK-88 | 1 | 3.5 | 2 | 272 | 0 | 6.77 | 1070 | 1000 | 110 | 161.8 |
| OK-89 | 1 | 4 | 2.3 | 272 | 0 | 6.76 | 1070 | 1025 | 110 | 161.2 |
| OK-90 | 1 | 4 | 2.5 | 272 | 0 | 6.84 | 1070 | 1000 | 110 | 147.3 |
| OK-91 | 1.5 | 3.5 | 2.3 | 272 | 0 | 6.51 | 1070 | 1000 | 110 | 149.2 |
| OK-92 | 1.5 | 3.5 | 2.5 | 272 | 0 | 6.55 | 1070 | 1000 | 110 | 151.3 |
| OK-93 | 1.5 | 4 | 2.3 | 272 | 0 | 6.56 | 1070 | 1000 | 110 | 138.1 |
| **OK-94** | **1.5** | **4** | **2.5** | **272** | **0** | **6.52** | **1070** | **1025** | **110** | **130.35** |
| OK-95 | 1.5 | 3.5 | 1.8 | 272 | 0 | 6.3 | 1070 | 975 | 110 | 155.65 |
| OK-96 | 2 | 3.5 | 2 | 272 | 0 | 6.29 | 1070 | 975 | 110 | 162.2 |
| OK-97 | 2 | 4 | 1.8 | 272 | 0 | 6.37 | 1070 | 1000 | 110 | 142.2 |
| OK-97 | 2 | 4 | 1.5 | 272 | 0 | 6.32 | 1070 | 1000 | 110 | 166.45 |

**<u>Testing the sequence of reagent addition</u>.** Reagents were added in the following sequence (see Table 5):

A 30% solution of acetic acid was added to 1 L of bio-effluent to adjust the pH to 7.4 – 6.4 in order to obtain elemental sulfur as a final product.

A 1% solution of $Al_2(SO_4)_3$ in water was added at 11°C and kept for 3 minutes to complete coagulation and precipitation of colloidal sulfur.

1) After 10 minutes, a 10% solution of hydrogen peroxide in water was added at 5°C and stirred for 6 – 12 hours, forming a cloudy white precipitate.

All water samples were filtered using a 0.45 µm syringe filter. Aqueous alkalinity, sulfide, and sulfate anion concentrations were measured using the procedure described above. Reagent volumes and other data are presented in Table 5.

At least 4 ml of a 10% solution of hydrogen peroxide should be added to 1 L of Raft A bio-effluent for complete oxidation of sulfide anions, with pH ≤ 6.49 to minimize oxidation to sulfate. At least 2 ml of a 1% $Al_2(SO_4)_3$ solution was needed to fully coagulate and precipitate colloidal sulfur. The order of hydrogen peroxide and aluminum sulfate addition can be reversed, as long as the solution is allowed 3 - 5 minutes after the first addition. The optimum conditions for this set of experiments are marked in bold in the Table 5.

**Table 5.** Analytical data after sequence to add reagents was changed. Raft A bio-effluent water was used. Bio effluent was collected 11/18/2015.

| Exp. # | V 30% Acetic Acid, ml | V1% $Al_2(SO_4)_3$, ml/L | V10% $H_2O_2$, ml/L | Effluent $S^{2-}$ mg/L | Final $S^{2-}$ mg/L | pH after adjustment | Effluent alkalinity | Final alkalinity | Effluent $SO_4^{2-}$ mg/L | Final $SO_4^{2-}$ mg/L |
|---|---|---|---|---|---|---|---|---|---|---|
| OK-105 | 0 | 2.5 | 5 | 196 | 0 | 7.38 | 900 | 700 | 304 | 385.45 |
| OK-107 | 0 | 3 | 5 | 196 | 0 | 7.36 | 900 | 700 | 304 | 449.3 |
| OK-104 | 0 | 3 | 5 | 196 | 0 | 7.36 | 900 | 720 | 304 | 411.7 |
| OK-106 | 0 | 3.5 | 5 | 196 | 0 | 7.32 | 900 | 700 | 304 | 442.6 |
| OK-120 | 0 | 4 | 5 | 196 | 0 | 7.31 | 900 | 675 | 304 | 479.8 |
| OK-103 | 0 | 5 | 5 | 196 | 0 | 7.3 | 900 | 725 | 304 | 395.5 |
| OK-108 | 0.5 | 2.5 | 4 | 196 | 0 | 7.26 | 900 | 800 | 304 | 374.3 |
| OK-109 | 0.5 | 3 | 4 | 196 | 0 | 7.20 | 900 | 750 | 304 | 383.8 |
| OK-118 | 0.5 | 3.5 | 4 | 196 | 0 | 7.16 | 900 | 775 | 304 | 386.5 |
| OK-110 | 1 | 2.5 | 4 | 196 | 0 | 6.98 | 900 | 730 | 304 | 346.2 |
| OK-111 | 1 | 3 | 4 | 196 | 0 | 6.80 | 900 | 720 | 304 | 348.1 |
| OK-117 | 1 | 3.5 | 4 | 196 | 0 | 6.78 | 900 | 800 | 304 | 350.55 |
| OK-112 | 1.5 | 2.5 | 4 | 196 | 0 | 6.76 | 900 | 700 | 304 | 342.75 |
| OK-113 | 1.5 | 3 | 4 | 196 | 0 | 6.69 | 900 | 690 | 304 | 335.35 |
| OK-116 | 1.5 | 3.5 | 4 | 196 | 0 | 6.60 | 900 | 775 | 304 | 354.35 |
| **OK-115** | **2** | **2** | **4** | **196** | **0** | **6.49** | **900** | **775** | **304** | **331.5** |
| OK-114 | 2 | 2.5 | 4 | 196 | 0 | 6.44 | 900 | 725 | 304 | 354.75 |
| OK-119 | 2 | 3 | 4 | 196 | 0 | 6.4 | 900 | 700 | 304 | 342.2 |

**Testing the sequence of reagent addition as well as influence the addition a mixture of hydrogen peroxide and a solution of aluminum sulfate on the oxidation of sulfide anion**
Reagents were added following this sequence (see Table 6):

An acidified effluent solution was prepared by adding a 1.25 ml or a 1.5 ml of a 30% solution of acetic acid to 1 L of bio-effluent, and three scenarios were executed:

Scenario 1. A 10% solution of hydrogen peroxide was added to 1 L of acidified bio-effluent; a solution was stirred for 30 minutes at $11^0$ C, then a 1% solution of aluminum sulfate was added. The reaction mixture was kept at $5^0$ C for 12 hours. (Table 6, OK-124 and OK-127).

Scenario 2. A 1% solution of aluminum sulfate was added at $11^0$C, kept for 10 minutes and then a 10% solution of hydrogen peroxide was added. The reaction mixture was mixed, and kept for 12 hours at $5^0$ C (Table 6, OK-125 and OK-128).

Scenario 3. A 1% solution of aluminum sulfate was added to a 10% solution of hydrogen peroxide at $11^0$ C. The resulted mixture was added to a 1 L of acidified bio-effluent at $11^0$C, mixed by shaking for 1 minutes and kept at $5^0$ C for 12 hours. (Table 6, OK-126 and OK-129).

All water samples were filtered using a 0.45 µm syringe filter. Aqueous alkalinity, sulfide, and sulfate anion concentrations were measured using the procedure described above. Reagent volumes and other data are presented in Table 6.

**Table 6.** Volume of reagents and water parameters for 3 different scenarios of reagent addition. Raft A bio-effluent water was used. Bio effluent was collected 12/10/2015.

| Exp. # | V 30% Acetic Acid, ml | V 10% $H_2O_2$ ml/L | V 1% $Al_2(SO_4)_3$ ml/L | Effluent $S^{2-}$ mg/L | Final $S^{2-}$ mg/L | Effluent pH | pH after adjustment | Effluent alkalinity | Final alkalinity | Effluent $SO_4^{2-}$ mg/L | Final $SO_4^{2-}$ mg/L |
|---|---|---|---|---|---|---|---|---|---|---|---|
| OK-124 | 1.5 | 3.5(1) | 2.5(2) | 208 | 0 | 6.83 | 6.12 | 955 | 750 | 259.35 | 284.58 |
| OK-125 | 1.5 | 3.5(2) | 2.5(1) | 208 | 0 | 6.83 | 6.08 | 955 | 750 | 259.35 | 315.53 |
| OK-126 | 1.5 | 3.5(mix) | 2.5(mix) | 208 | 0 | 6.83 | 6.06 | 955 | 720 | 259.35 | 329.78 |
| OK-127 | 1.25 | 3.5(1) | 2.5(2) | 208 | 0 | 6.83 | 6.19 | 955 | 740 | 259.35 | 318.2 |
| OK-128 | 1.25 | 3.5(2) | 2.5(1) | 208 | 0 | 6.83 | 6.19 | 955 | 750 | 259.35 | 317.93 |
| OK-129 | 1.25 | 3.5(mix) | 2.5(mix) | 208 | 0 | 6.83 | 6.19 | 955 | 750 | 259.35 | 272.05 |

Note that there were no substantial differences found in the resulted water chemistry after adding reagents using the three different scenarios.

**Testing a potential of using formic acid instead of acetic acid to adjust a pH of bio-effluent**
Reagents were added following this sequence (Table 8):

1) A 10% solution of acetic acid or a 8.8% solution of formic acid was added to 1 L of bio-effluent to adjust the pH to 6.15 – 6.74.
2) A 10% solution of hydrogen peroxide in water was added at $5^0$C and stirred for 30 minutes. A formation of cloudy white precipitation was observed.
3) A 1% solution of $Al_2(SO_4)_3$ in water was added at $11^0$C and kept for 12 hours to complete coagulation and precipitation of colloidal sulfur.

All water samples were filtered using 0.45 µm syringe filter. Aqueous alkalinity, sulfide, and sulfate anion concentrations were measured using the procedure described above. Reagent volumes and other data are presented in Table 8.

**Table 8.** Comparison of formic and acetic acids as pH adjusters and alkalinity reducers. Raft A bio-effluent water was used. Bio-effluent was collected 03/01/2016.

| Exp. # | V 8.8% Formic Acid ml | V 10% $H_2O_2$ ml/L | V 1% $Al_2(SO_4)_3$ ml/L | Effluent $S^{2-}$ mg/L | Final $S^{2-}$ mg/L | Effluent pH | pH after adjustment | Effluent alkalinity | Final alkalinity | Effluent $SO_4^{2-}$ mg/L | Final $SO_4^{2-}$ mg/L |
|---|---|---|---|---|---|---|---|---|---|---|---|
| OK-131b | 1 | 4.5 | 4 | 200 | 0 | 7.03 | 6.74 | 850 | 550 | 300 | 486 |
| OK-132b | 2 | 4.5 | 4 | 200 | 0 | 7.03 | 6.53 | 850 | 550 | 300 | 486.9 |
| OK-133 | 2.5 | 4.5 | 4 | 200 | 0 | 7.03 | 6.48 | 850 | 525 | 300 | 456.4 |
| OK-134 | 3 | 4.5 | 4 | 200 | 0 | 7.03 | 6.29 | 850 | 510 | 300 | 471.1 |
| OK-135 | 4 | 4.5 | 4 | 200 | 0 | 7.03 | 6.15 | 850 | 500 | 300 | 485.4 |

| Exp. # | V 10% Acetic Acid ml | V 10% $H_2O_2$ ml/L | V 1% $Al_2(SO_4)_3$ ml/L | Effluent $S^{2-}$ mg/L | Final $S^{2-}$ mg/L | Effluent pH | pH after adjustment | Effluent alkalinity | Final alkalinity | Effluent $SO_4^{2-}$ mg/L | Final $SO_4^{2-}$ mg/L |
|---|---|---|---|---|---|---|---|---|---|---|---|
| OK-136 | 1.5 | 4.5 | 4 | 200 | 0 | 7.03 | 6.72 | 850 | 740 | 300 | 469.6 |
| OK-137 | 2 | 4.5 | 4 | 200 | 0 | 7.03 | 6.68 | 850 | 800 | 300 | 483 |
| OK-138 | 2.5 | 4.5 | 4 | 200 | 0 | 7.03 | 6.57 | 850 | 600 | 300 | 451.5 |
| OK-139 | 3 | 4.5 | 4 | 200 | 0 | 7.03 | 6.60 | 850 | 675 | 300 | 486.5 |
| OK-140 | 4 | 4.5 | 4 | 200 | 0 | 7.03 | 6.38 | 850 | 700 | 300 | 474 |

Oxidation of sulfide to sulfur occurred in all experiments, but these experiments indicated that formic acid was preferred to adjust pH. Lower quantities of formic acid were needed to achieve the target pH level, and formic acid produced lower alkalinity in the final water.

# Appendix 4. MnDRIVE Project Accountability – Year 1

**Task 1. Description and Participants: Increase the number of bioreactor modules by 10 units to create MnDRIVE demonstration system.**

Work Completed to Date: The remaining three of the ten modules were built and installed at the pit lake study site in Hoyt Lakes, MN. The new raft system contains seven bioreactor modules, one nutrient dosing module and two effluent treatment modules. The installed modules currently operating are the bioreactor units, where the first step of aqueous sulfate removal takes place utilizing the metabolic process of ambient sulfate reducing bacteria (SRB). The nutrient feeding began in November 2015. The effluent treatment modules were relocated to treat Raft A effluent because Raft C had not yet produced high levels of hydrogen sulfide. The effluent treatment system is operating as planned on Raft A. Nutrient feed to Raft C has been suspended due to project budget constraints and therefore is not generating hydrogen sulfide.

Percent Complete: 100%

Remaining Work: The effluent treatment will continue on Raft A with hydrogen peroxide and on Raft B with ferric chloride through August 2016. Continuing the microbiological sampling and analysis through the coming summer months will allow completion of a full year of sampling for this particular portion of the experiment and will significantly enhance the value of the work.

PI(s)/PI Team(s) Responsible: Hanson

**Task 2. Embed personal computer modules to provide control and system optimization.**

Work Completed to Date: The original objective was to install on-board autonomous control system; however, the scope and timing of the objective were revised. The task scope was changed from *installation of systems* to *specification of systems*. Initiation of work on Original Tasks 2 and 3 (below) were dependent on finalizing raft monitoring and control needs and algorithms, which were still under development. Adequate time does not remain in the project schedule to either finalize these needs or design and construct a control system for meeting the requirements. Some general control and monitoring functions and capabilities are desirable in the future. By developing a general specification for a control system, details can be added to the specification in the future when specific control algorithms involving the bioremediation process have been established.

A general specification is now complete and serves as a template for development of future systems when specific knowledge is available on raft biology, flows, and process oversight. The specification structure includes the raft power and energy system requirements, raft control system (that encompasses alarms, control points, autonomous functions and communications), human-machine interface at a distant monitoring location, software, spare parts, documentation, and training. The specification was developed with the philosophy that a single central monitoring and control site can be connected with multiple sulfate reduction sites anywhere in the world.

Some analysis work however resulted in the installation of equipment on Raft C, and this subset of raft control system work is part of the revised Task 2 Objective to: Analyze the electromagnetic environment of wireless sensors that will be employed and provide recommendations for minimizing interference issues that may degrade performance. The use of wireless communications between sensors on the raft eliminates issues associated with wired connections but can also create new problems. By modeling the various antenna designs contemplated, proper installation and

operation are better assured. Although the specific orientation and application of these sensor antennas may be unique, the modeling and prediction of fields from arrays are not. The antenna arrangement is now in operation and working without issue; therefore, this revised objective is complete.

Percent Complete: 100% based on revised scope.

Remaining Work: The task is complete.

PI(s)/PI Team(s) Responsible: Ferguson

### Task 3. Provide additional smart sensors and controls to advance remote control in remote locations.

Work Completed to Date: The scope and timing of the objective were modified. The scope was revised from *installation of systems* to *specification of systems*. Initiation of work on Original Tasks 2 and 3 was dependent on finalization of raft monitoring and control needs and algorithms which, however, were still evolving. Thus, adequate time to finalize these needs no longer remains in the project schedule to design and construct a control system. The revised Task 3 objective, of which Task 2 is also associated, is to**:** Develop a functional and design specification for both autonomous and remote control of the bioremediation system to serve as a template for future operations.

Production-scale systems (e.g., systems used by mining operations to comply with requirements) will require real-time monitoring of parameters such as flow rates, temperatures, electrical load behavior, weather, and solar system performance. The ability to remotely monitor and control the system improves the chances of optimal operation by alerting experts off-site that certain valid operating ranges have been violated and minimizes the cost of operations and maintenance. In these instances, the off-site facility may issue a control signal to the system to perhaps override any actions taken by the local controls. Or, the data may indicate that a technician must be dispatched to the site. Remote monitoring and control will also provide operational transparency, enable accumulation of historical operating data, capture of steps to remedy certain operating issues to modify or embody in control system logic and operational transparency.

Percent Complete: 100% based on revised scope. Refer to the description of work in Task 2 above.

Remaining Work: The task is complete.

PI(s)/PI Team(s) Responsible: Ferguson

### Task 4. Improve solar panel technology to deliver needed current to change on-board battery packs.

Work Completed to Date: During this reporting period, the scope of this objective expanded significantly. Reliant on the solar panel manufacturing industry to improve panel technology, the project team was required to integrate existing retail offerings of such products into the design. Thus Task 4 Objective was revised to encompass: a) review of available National Oceanographic and Atmospheric Administration (NOAA) solar insolation data sets, and selection of the most useful set for this project; b) development of solar insolation data specific to the Aurora mine site; c) identification of a month on record during which solar insolation is at its nadir to establish a “worst-case” test month for the design analysis; d) identification of the loads on Raft C in terms of power

consumption, voltage rating, duty cycle, and criticality to reliability of the overall bioremediation process; and e) development of a custom model for predicting solar panel array solar energy and electrical energy output based on conversion efficiency for predicting daily electrical energy produced by the array in the worst-case month and behavior of battery plant terminal voltage as a function of charging input and load supply. Finally, the scope was then expanded to include new data from UMD's Malosky Stadium solar panel array as a form of corroborating the behavior predicted by modeling for Aurora. The panel and battery count were finalized, and equipment was purchased and installed to complete the solar system on Raft C.

A comparison of Malosky Stadium data with Aurora modeling results is complete. While the model tracks generally well with the real-world behavior exhibited by the Malosky solar panel system, several factors limit the analysis. First, the model is very course relative to actual solar insolation. For example, the model might assume that a particular day is partly cloudy for the entire day, whereas actual sunshine during a "partly cloudy" day could include hours of clear sky, followed by hours of mostly cloudy skies. This suggests a future enhancement to the model that uses a probability engine behind each type of day (clear, partly cloudy, mostly cloudy or overcast). Randomizing solar insolation around some nominal day-type value would facilitate a more granular model output, which in turn may improve the model's correlation with actual insolation behavior.

Another factor limiting the comparison was discovered in the engineering design of the Malosky photovoltaic system. The charge controller (which is responsible for managing energy coming from the PV panels to the loads) has a much higher "cut in" voltage than the charge controller at the Aurora site. This essentially wastes energy from the PV panels at low light conditions and creates deviation from the model predictions. Furthermore, the Malosky controller has a maximum rating that is less than the rated output of the PV array, so energy is also wasted when the sun is at its zenith. Here again, the Malosky data differs at these times of day from the model predictions, as the model correctly assumes that the rating of the charge controller on the Aurora system EXCEEDS the rating of the associated PV array.

A third factor that may skew the Aurora modeling from the Duluth-based Malosky system is simply geography. The sky conditions and weather generally differ to some unknown degree due to the 50-70 mile separation and each site's distance from the fog-generating Lake Superior.

The agreement between Malosky and the model is encouraging, however, as the general correlation suggests that the model is representing the solar and electrical behavior well enough to be used in initial system design. During the worst-case month (for solar insolation) of December 2014 (which was used for all system design calculations), the model-predicated electrical energy production was 29% greater than that produced by the Malosky system. The factors mentioned above very likely contribute to this difference.

Percent Complete: 100%

Remaining Work: The task is complete.

PI(s)/PI Team(s) Responsible: Ferguson

**Task 5. Sample input and output water weekly for chemical analysis at NRRI's CMRL.**

Work Completed to Date: Procedures were completed for on-site water analysis at the Hoyt Lakes, Minnesota, study site. Chemical analysis of all rafts and individual bioreactors continue, with the results posted for the project participants to review. Biological/microbial physical and chemical parameters (e.g., including sulfate, sulfide, pH, temperature, Red/Ox potential, dissolved oxygen concentration) for the bioreactor system influent and effluent continue to be collected approximately monthly or bi-monthly. New recommendations for nutrient dosing were implemented and tested and dissolved phosphate is being monitored on site as an additional measure for real-time nutrient evaluation and dosing modification. The biological sampling within the bioreactors began in early December with the first six months of sampling completed on schedule.

Percent Complete: 75%

Remaining work: Continue to analyze bioreactor influent and effluent analysis in monitoring the efficiency of the bioreactors and precipitation modules in removing sulfate and sulfide from the pit lake water. Microbiological collection and analysis will continue. A synthesis of microbial data in the context of nutrient feeding and sulfur geochemistry will result in a recommendation for optimal nutrient feed composition and microbial community composition (both in terms of SRB biomass and different SRB groups) to achieve the highest sulfate reduction rate. Based on the experience of several microbial community sampling events, procedures will be revised to provide for a faster collection process while improving reliability. Procedures for all chemical, physical and microbiological parameter sampling and analysis will be included in the final report.

PI(s)/PI Team(s) Responsible: Hanson, Hicks, Sadowsky, Kolomitsyna

**Task 6. Measure sulfate reducing bacterial abundance in bioreactors utilizing the dsrA gene qPCR method to help optimize bioreactors.**

Work Completed to Date: Measured dsrA gene abundance in influent, effluent, and depth profiles in bioreactors A3 and A4 from October 2014 to August 2015. Results were used to help design the 2015-2016 rafts A, B, and C bioreactors experiment and sampling regime.

Percent Compete: 100%

Remaining Work: The task is complete.

PI(s)/PI Team(s) Responsible: Hicks

**Task 7. Identify SRB populations in bioreactors to help optimize sulfate reduction.**

Work Completed to Date:

Researched, developed, and tested methods for appropriate collection, handling, and analysis of water samples for sulfide, sulfate, and certain intermediate sulfur species. Total sulfur (sum of sulfide and sulfate) remains constant, within the error of the sample test. No significant loss of total sulfur was noted, except following iron dosing.

Researched and developed methods for sample collection, processing, DNA extraction, and 16S rRNA gene sequencing to identify sulfate-reducing bacterial populations in bioreactors. Major findings include:

The reactors are populated by a complex microbial community containing microbial populations associated with sulfate reduction, fermentation, and methanogenesis. At shallow depths (within a few cm of the surface), the reactors are dominated by sulfide-oxidizing bacteria. Microbial communities in the pit lake are very different from those in the bioreactors.

Planktonic and fiber-attached communities are distinct, based on DNA extraction and analysis of water and fiber bag samples.

Major genera of sulfate reducers in the reactors include *Desulfovibrio*, *Desulfobacter* and *Desulfobulbus*. Other abundant taxa include *Alkalibacter*, *Pseudomonas* and *Acetobacterium* (likely fermenters), and *Methanomethylovorans* and *Methanosarcina* (likely methanogens). Note that culturing work indicates that some of the *Pseudomonas* spp. might be novel sulfate-reducing bacteria. Major groups of sulfide-oxidizing bacteria near the reactor surface include *Arcobacter*, *Sulfuricurvum*, *Sulfurospirillum* and *Sulfurimonas.*

Based on available data, methanogens, sulfate reducers, and fermenters co-occur below 0.5 m depth, and the relative abundance of methanogens and sulfate reducers are correlated. Methanogens typically represent between 0 and 8% of total rRNA gene sequences, and sulfate reducers typically represent between 0 and 30%. The most abundant operational taxonomic unit ("species") represent potentially novel populations of *Alkalibacter* spp. And *Pelosinus* spp (in some cases, >50% of rRNA gene sequences).

Percent Complete: 100%

Remaining Work: none

PI(s)/PI Team(s) Responsible: Sadowsky

## Task 8. Evaluate microbial production of elemental sulfur from hydrogen sulfide as another method of removing sulfate from water column vs. precipitation as iron sulfide.

Work Completed to Date: Determined that sulfur oxidizing bacteria (largely the genus of *Arcobacter*) were predominant in the surface (few centimeters from the top) of the bioreactor. Isolation of sulfur oxidizing bacteria is currently conducted in the lab.

Percent Complete: This portion of the MnDRIVE project was discontinued.

Remaining Work: While biological sulfur production holds promise, the preliminary evaluation is that, at this time, it may not be suitable or straightforward to adapt for this system. This component of the work has been discontinued in favor of elemental sulfur production by chemical means.

PI(s)/PI Team(s) Responsible: Sadowsky

## Task 9. Improve biological activity in bioreactor modules by selecting the best SRB assemblages and finding optimum growth conditions (temperature, substrates, nutrients).

Work Completed to Date: Isolated strains of sulfate reducing bacteria including *Desulfovibrio* and *Pseudomonas extremaustralis* from the bioreactors. Improved nutrient feeding by switching to a lactate-based blend, and started new phosphate monitoring procedures to avoid excess nutrients in the outflow.

New chemical testing procedures on the rafts, combined with microbiological data in the context of nutrient feeding and sulfur geochemistry, resulted in recommendations for the nutrient feed and microbial community composition (both in terms of SRB biomass and different SRB groups) that achieved the highest sulfate reduction rates.

Two continuous-flow bench-scale bioreactors were assembled using fiber material from the pit lake bioreactors as inoculum. Results show that a continuously fed sodium lactate blend (pH 7.5 – 8) can achieve >90% sulfate reduction in 36 hours residence time, and experimentally manipulating residence time showed that even shorter residence times of 18 hours lead to enhanced sulfate reduction (up to 1.5x higher sulfate reduced per unit time). Microbial communities in bench-scale bioreactors were similar to those found in the floating bioreactors.

Percent Complete: 100%

Remaining Work: none

PI(s)/PI Team(s) Responsible: Sadowsky

## Task 10. Optimize precipitation of hydrogen sulfide to form iron sulfide.

Work Completed to Date: Evaluation of results obtained from the five methods presented during the previous reporting period indicated those methods were either economically and/or ecologically inapplicable to remove hydrogen sulfide from the bioreactor module effluent. Thus, evaluation of a new method was initiated: addition hydrogen peroxide to remove sulfides and form insoluble elemental sulfur.

During this period, the process of oxidation of sulfides to elemental sulfur and not back to sulfates was fully investigated and optimized. The following parameters were evaluated and optimized:

- starting pH should be in range 6.3 to 6.5;
- formic acid, which adjust pH to required level, lower bio-effluent alkalinity, but not add any additional undesirable anions ($Cl^-$, $Br^-$, $I^-$, $SO_4^{2-}$, $PO_4^{3-}$, $CO_3^{2-}$, $NO_3^-$) to discharge water;
- hydrogen peroxide as an appropriate oxidative agent, which completely oxidizes sulfides to elemental sulfur;
- aluminum sulfate as an appropriate flocculent, which provides excellent sedimentation of colloidal sulfur, but add only 5-10 mg/L of additional sulfate anion in to discharge water;
- sequence of reagents loading;
- loading ratio and concentration of reagents;
- reaction of oxidation temperature and time;
- colloidal sulfur precipitation time.

A bench-scale model of sulfides oxidation and sulfur precipitation treatment process was developed.

Percent Complete: 100%

Remaining Work: Once oxidative and precipitation of elemental sulfur processes are installed and operational on Raft A, it will be necessary to monitor it to do bench-scale process optimization. The bench-scale reactors will be used to test parameters that may have an effect on sulfides-oxidation activity, such as pH, flow rate and accumulation of sulfur.

PI(s)/PI Team(s) Responsible: Kolomitsyna

# Appendix 5. MnDRIVE Project Accountability – Year 2

**Task 1. Compare summer with winter operations and make appropriate equipment and operation changes to optimize bioreactor operation throughout year.**

Work Completed to Date: Raft C solar panels and batteries were installed and operational to ascertain the design goal of 100% renewable energy availability during remaining winter months. Recommendations for winter operation and microbial community sampling were made according to the first 12 months of operation data. The nutrient feed was adjusted to avoid excess of nutrients in the bioreactor effluent and subsequent eutrophication of the pit lake water, especially during winter months which characteristically have lower microbial activity. Raft A consistently achieved high sulfate reduction over the winter months, indicating that high rates of biological sulfate reduction can be achieved year round.

Percent Complete: 80%

Remaining Work: Electrical/solar operating data from December 2015 to April 2016 were to be compared with theoretical modeling. However, delays in the start-up of Raft C rendered the completion of this task as impracticable. No data were available from Raft C to use in a comparison with model results.

The engineering and design work for the sulfate bioreactor and associated water treatment system was completed. Monitoring of the physical, chemical and microbial analysis data parameters will continue through August with adjustments to nutrient feed if necessary.

PI(s)/PI Team(s) Responsible: ALL PIs/PI Teams.

**Task 2. a.) Increase number of bioreactor modules by 10 units, and b.) Install additional onboard computers for smart control.**

Work Completed to Date: Ten modules were built and installed at the pit lake study site in Hoyt Lakes, MN. The new raft system (Raft C) contains seven bioreactor modules, one nutrient dosing module and two effluent treatment modules. The installed modules currently operating are the bioreactor units, where the first step of aqueous sulfate removal takes place utilizing the metabolic process of ambient sulfate reducing bacteria (SRB). The nutrient feeding was initiated during in November 2015.

Additional and revised flow sensors, transmitters, and nutrient feed flow monitors were installed on Raft C and are operating. The flow controls and monitoring are fully operational and performing as planned on Raft C.

The effluent treatment system is operating as planned on Raft A, and sampling will continue through August 2016. Changes related to bioreactor nutrients and water treatment methods required approval from the Minnesota Pollution Control Agency. These approvals took longer than anticipated, and neither enough time nor budget remains in the project to continue work on Raft C. Thus, nutrient feed to Raft C was suspended and therefore is not generating hydrogen sulfide. Plans to move the effluent treatment to Raft C were suspended when the nutrient feed to C was suspended. Raft C is flowing still, but not producing hydrogen sulfide.

Percent Complete: 100%

Remaining Work: Although operations were defined as planned for Raft C, operations will only continue on Raft A for the duration of the project.

PI(s)/PI Team(s) Responsible: Hanson

### Task 3. Optimize smart control of new modules and operate them in a continuous mode to prove ability to locate and operate these systems in remote wild rice growth areas.

Work Completed to Date: The scope and timing of this objective were revised. The scope has changed from *installation of systems* to *specification of systems*. The new objective for Task 3 is to *Develop a functional and design specification for both autonomous and remote control of the bioremediation system to serve as a template for future operations.* By developing a general specification for a control system, details can be added to the specification at a later date once specific control algorithms involving the bioremediation process are established. A general outline was created for a controls system specification. Knowledge of control subsystem needs will exist prior to subsequent installation of equipment on Raft C in December 2015.

A general specification is complete and serves as a template for development of future systems when specific knowledge is available about raft biology, flows, and process oversight. The specification structure includes the raft power and energy system requirements, raft control system (that encompasses alarms, control points, autonomous functions and communications), human-machine interface at a distant monitoring location, software, spare parts, documentation and training. The specification was developed with the philosophy that a single central monitoring and control site can be connected with multiple sulfate reduction sites anywhere in the world.

Percent Complete: 100%

Remaining Work: The task is complete.

PI(s)/PI Team(s) Responsible: Ferguson

### Task 4. Sample input and output water weekly for chemical analysis at NRRI's CMRL plus SOPs (procedures).

Work Completed to Date: Year 2, Task 4 is a continuation of Year I, Task 5: Input, output and profile water sampling is now fully operational per the established schedule. Chemical analysis is preformed on-site regularly.

Percent Complete: 90%

Remaining Work: Bioreactor influent and effluent will continue for monitoring the efficiency of the bioreactors and precipitation modules in removing sulfate and sulfide from the pit lake water. Procedures for on-site chemical analysis and biological sampling are complete, unless modifications are required, and will be incorporated into the final report.

PI(s)/PI Team(s) Responsible: PI(s)/PI Team(s) Responsible: Hanson, Hicks, Sadowsky, Kolomitsyna

## Task 5. a.) Conduct statistical analysis on all operating data, and b.) Optimize sulfate reducing bacterial community growth rate and sulfide production.

Work Completed to date: Recommendations on flow rate and reactor design were provided to optimize sulfate-reducing bacterial communities and sulfide production.

Water and fiber samples from specific bioreactors in every bioreactor raft were sampled from December 2015 through September 2016 based on the experimental design agreed to by the project participants. Water and fiber samples were immediately processed prior to DNA extraction. DNA was extracted from all water and fiber samples. Multivariate analyses indicate that, when reactors were performing best in terms of total sulfate reduction, they were populated by diverse communities that contained specific sulfate reducers, methanogens and fermenters. The prevalence of the fermentative and methanogenic populations indicates that sulfate reduction is not optimized in the system, and that shortening residence time or adjusting feed ratios might better select for sulfate reducers and/or more sulfate reducer biomass. It is noteworthy that the sulfate-reducing populations that were specifically associated with optimal reactor performance were often members of the *Desulfobulbaceae*, which was also consistent with laboratory reactors, although additional work in the future would be required to confirm this association.

Geochemical and microbial data do not suggest that shorter residence times are detrimental to performance, and shortening residence times could substantially increase the amount of sulfate reduced per unit time. When reactors are operating most efficiently, most sulfate reduction occurs in the top 1m, so future operating parameters and designs might consider options to better make use of the entire reactor volume. Feed ratios might be better to select for sulfate reducers over fermentative and methanogenic populations and increase sulfate reducer biomass. Moreover, the use of fiber material in sulfate-reducing bioreactors is recommended to provide attachment sites for sulfate-reducing bacteria.

Percent Complete: 100%

Remaining work: none

PI(s)/PI Team(s) Responsible: Hicks, Sadowsky

## Task 6. Conduct on-site demonstrations of the bioremediation technology with the mining industry and public/private sectors.

Work Completed to Date: No demonstrations of the bioreactors have been conducted, as the system is still being optimized.

Percent Compete: 0%

Remaining Work: Due to the limited time remaining in the project to provide on-site demonstrations of a fully optimized treatment system, it is unlikely this task will be completed.

PI(s)/PI Team(s) Responsible: Hanson, Ferguson, Hicks, Sadowsky, Kolomitsyna

**Task 7. Present technical papers to industrial partners and scientific peers for project review and evaluation, publish results in peer-reviewed.**

Work Completed to Date: Continue to collect data and optimize system performance.

Percent Complete: 0%

Remaining Work: Scientific results from this project will be submitted to peer-reviewed journals for publication.

PI(s)/PI Team(s) Responsible: ALL PIs/PI Teams

**Task 8. Analyze the potential economic implications for northeast Minnesota from the failure to adequately address the sulfate/sulfide issue.**

Work Completed to Date: Attended project and task-specific meetings with MnDRIVE team to clarify project scope and deliverables as the project has evolved. Collected data on northeast Minnesota's iron ore industry for use in economic modeling. Performed economic contribution sensitivity analysis on iron ore industry (normal and reduced production levels) that addresses the direct, indirect and induced economic impacts of the industry. Prepared draft report for review and finalized for submittal.

Percent Complete: 100%

Remaining Work: The task is complete.

PI(s)/PI Team(s) Responsible: Haynes